Oviduct-on-a-chip

Creating an *in vitro* oviduct to study bovine gamete interaction and early embryo development

ISBN: 978-90-393-6916-6

Layout and cover design: Eduardo de Melo Ferraz Jr. and Marcia Cristina de Almeida Monteiro

The thesis printing was sponsored by the Department of Farm Animal Health of the Faculty of Veterinary Sciences, Utrecht University.

Oviduct-on-a-chip

Creating an *in vitro* oviduct to study bovine gamete interaction and early embryo development

Eileider-op-een-chip

De ontwikkeling van een *in vitro* eileider voor de bestudering van de interactie tussen gameten en de vroege embryonale ontwikkeling bij het rund

(met een samenvatting in het Nederlands)

Proefschrift

ter verkrijging van de graad van doctor aan de Universiteit Utrecht
op gezag van de rector magnificus, prof.dr. G.J. van der Zwaan,
ingevolge het besluit van het college voor promoties in het openbaar te verdedigen
op donderdag 25 januari 2018 des middag te 12.45 uur

door

Marcia de Almeida Monteiro Melo Ferraz
geboren op 11 februari 1986 te Poa, Brazilië

Promotor:
Prof.dr. T.A.E. Stout

Copromotoren:
Dr. B.M. Gadella
Dr. P.L.A.M. Vos

Table of contents

Chapter 1
Introduction

Adapted from:

FERRAZ, M.A.M.M.; HENNING, H.H.W.; STOUT, T.A.E.; VOS, P.L.A.M., GADELLA, B.M. Designing 3-dimensional *in vitro* oviduct culture systems to study mammalian fertilization and embryo production**.** Ann Biomed Eng (2016). doi:10.1007/s10439-016- 1760-x

Abstract

The oviduct was long considered a largely passive conduit for gametes and embryos. However, an increasing number of studies into oviduct physiology have demonstrated that it specifically and significantly influences gamete interaction, fertilization and early embryo development. While oviduct epithelial cell (OEC) function has been examined during maintenance in conventional tissue culture dishes, cells seeded into these two-dimensional (2-D) conditions suffer a rapid loss of differentiated OEC characteristics, such as ciliation and secretory activity. Recently, three-dimensional (3-D) cell culture systems have been developed that make use of cell inserts to create basolateral and apical medium compartments with a confluent epithelial cell layer at the interface. Using such 3-D culture systems, OECs can be triggered to redevelop typical differentiated cell properties and levels of tissue organization can be developed that are not possible in a 2-D culture. 3-D culture systems can be further refined using new micro-engineering techniques (including microfluidics and 3-D printing) which can be used to produce 'organs-on-chips', i.e. live 3-D cultures that bio-mimic the oviduct. In this review, concepts for designing bio-mimic 3-D oviduct cultures are presented. The increased possibilities and concomitant challenges when trying to more closely investigate oviduct physiology, gamete activation, fertilization and embryo production are discussed.

The oviduct

The oviduct, or fallopian tube, was first described by Fallopius in 1561 as a presumably passive channel to hold or transport gametes and early embryos in mammals[1]. The oviduct is a convoluted tube consisting of longitudinal and circular muscular, and a stromal layer lined by a simple cuboidal to columnar epithelium containing both ciliated and secretory cells[2–4]. The ciliated cells are important for gamete transport and sperm interaction, in particular helping to create a 'sperm reservoir'; while the secretory cells are responsible for producing oviduct fluid; a mixture of specific cell secretions and serum transudate[5–9]. In adult mammals (including the woman), four anatomical segments can be distinguished along the length of the oviduct; the infundibulum, ampulla, isthmus and utero-tubal junction, respectively[10,11] (Figure 1C). The fimbriae of the infundibulum are responsible for capturing the cumulus oocyte complex (COC) and ensuring its transport from the ovary into the oviductal tube. The epithelium of the ampulla is highly folded, has the largest diameter of any oviductal segment and is the specific site where fertilization takes place[5] (Figure 1B). The ampulla connects to the much narrower isthmic tube (Figure 1A). Prior to fertilization, sperm entering the oviductal isthmus from the uterus bind to isthmic epithelial cells which help to prolong sperm viability (the formation of a so called "sperm reservoir")[12–15]. A limited number of these bound sperm will be released at around the time of ovulation, undergoing the final changes required to achieve fertilizing capacity as they do so, and migrate into the ampullary region[16] where they will encounter the mature oocyte (Figure 1C). After fertilization, the developing embryo will migrate along the isthmic tube towards the utero-tubal junction. At the morula (16 cell) stage, the embryo will exit

the oviduct and enter the uterine lumen (Figure 1C), where it will develop further and undergo a series of complicated interactions with the endometrium in preparation for implantation. The oviductal vasculature is composed of branches of the uterine and ovarian arteries and veins, allowing local exchange of metabolites, hormones and signaling molecules between the oviduct, uterus and ovary[1].

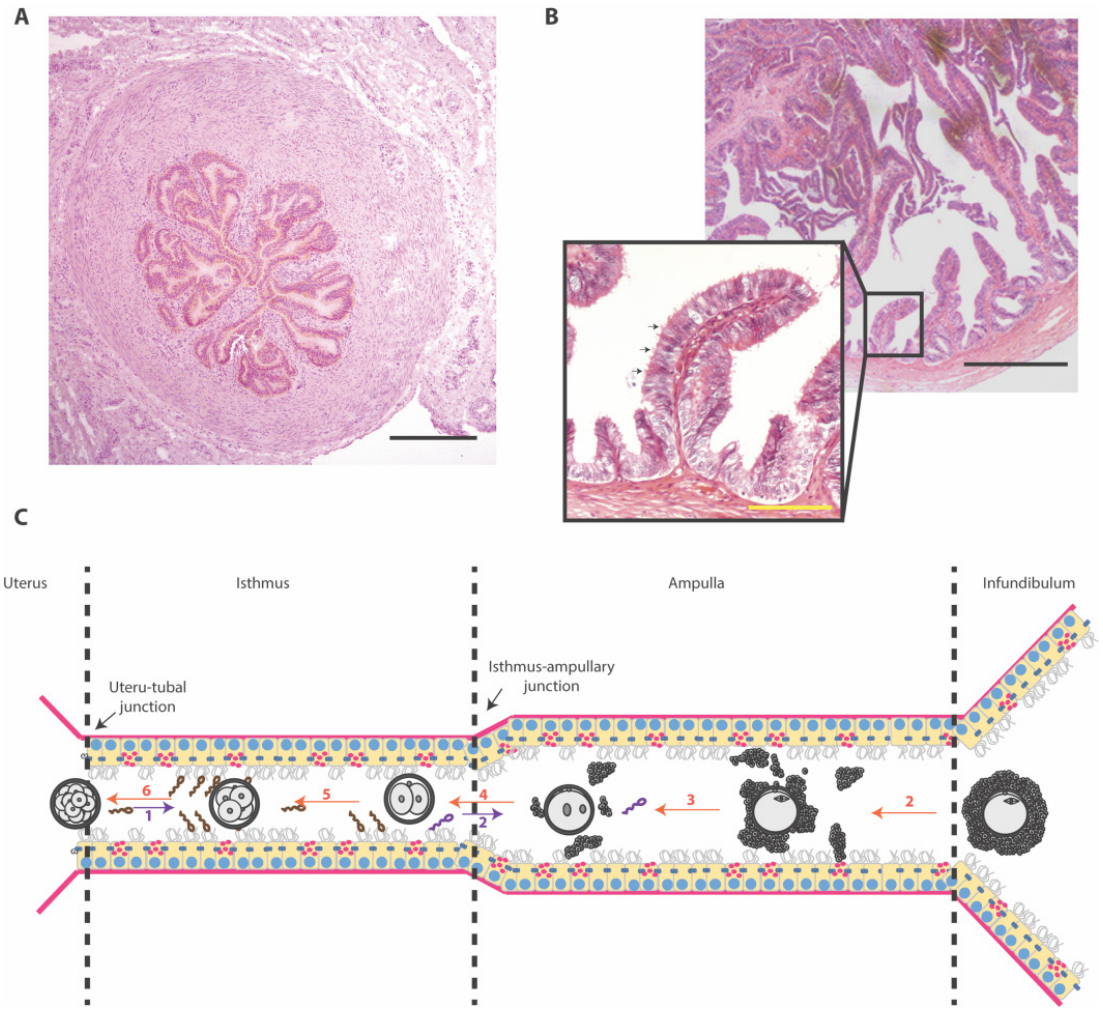

Figure 1. Histological images from bovine oviduct sections of (A) the isthmus (B) the ampulla (with an enlargement of a folded area to show the organization of the cuboid to columnar epithelial cells; black arrows indicate ciliated cells). Note the thicker stroma and muscular wall, and smaller lumen, of the isthmus (A) compared to the ampulla (B), and the higher degree of folding of the ampulla. (C) A schematic view of the entire length of the oviduct including the different segments: the utero-tubal junction, the isthmus, the isthmus-ampullary junction, the ampulla and the infundibulum, respectively. In this schematic view, the various reproductive processes are listed in chronological and spatial order: (1) entry of sperm from the uterine lumen and establishment of a sperm reservoir in the isthmus; (2) at the time of ovulation, the released COC will be captured by the infundibulum, and biochemical changes in the oviduct milieu will stimulate sperm release form the reservoir, and migration to the site of fertilization; (3) the COC will be transported through the ampulla and fertilized by one of the capacitated spermatozoa while, during transport, the COC will gradually lose its cumulus mass; (4) the fertilized oocyte (zygote) will continue its development until the first cell cleavage event; (5) the 2-cell embryo, and after successive cleavages 4, 8 and 16 cell stages are formed (the latter is termed a morula); (6) the morula stage leaves the oviduct via the UTJ and will develop further and implant within the uterus.

Black bars = 50 µm, yellow bar = 10 µm.

The oviduct is an active organ that orchestrates dynamic changes in its luminal fluid composition to provide optimal microenvironments for gamete maturation/activation, fertilization and early embryo development[17]. It is the first environment to which an embryo is exposed, and contributes vital factors that affect embryonic development and help atune it to predicted external environmental circumstances during the first 2-6 days post-fertilization, depending on the species[18,19] (Table 1). The successful development of conditions for *in vitro* production (IVP) of embryos for various species has in part been the reason for the relative neglect of the importance of the oviductal microenvironment in early development[20]. That the oviduct could be successfully by-passed supported the supposition that it was little more than a passive tube for temporarily hosting gametes and embryos[20]. Nevertheless, it has become clear that not only are fertilization and embryo development less efficient *in vitro* than *in vivo*, but the embryos produced are qualitatively different; a number of studies have now demonstrated the importance of the oviduct for sperm storage and activation [19,21–32], oocyte modification [33–36], fertilization and early embryo development [34,37–44] (Figure 2A).

Table 1. Embryo development within the oviduct of different species (timing is recorded as days after fertilization).

SPECIES	2-CELLS	4-CELLS	8-CELLS	MORULA
WOMAN	1.5 days	2 days	3 days	4 days
COW	1.5 days	2 days	2.5 days	3.5 days
SOW	0.75 days	1.5 days	2 days	4.5 days
MARE	1 day	1.5 days	3 days	5.5 days
EWE	1 day	1.5 days	2 days	3 days
MOUSE	1.5 days	2 days	2.5 days	3 days

Studying oviduct function

Due to its intra-abdominal location, it is difficult to access the delicate interior of the oviduct for experimental studies *in situ*. It is possible to ligate and excise the oviduct from experimental animals and given reproductive stages and to fix the tissues for histological or other microscopic investigation[45,46]. It is also possible to harvest epithelial cells from recovered oviducts. Methods to culture these oviduct epithelial cells (OEC) can differ with respect to cell isolation techniques, culture conditions and duration, medium used and supplements included[18]. The aim of the present review is to describe how 3-D culture systems can be designed and modified such that contained OECs mimic their *in vivo* physiology as closely as possible. In this respect, the OECs should at least have a similar morphological appearance and differentiation characteristics and be connected to neighboring cells by tight junctions to form a confluent epithelial cell monolayer. The OECs should also resemble *in vivo* oviduct epithelial cells with respect to protein expression, ciliary and secretory activity, and responses to physiological stimuli[18].

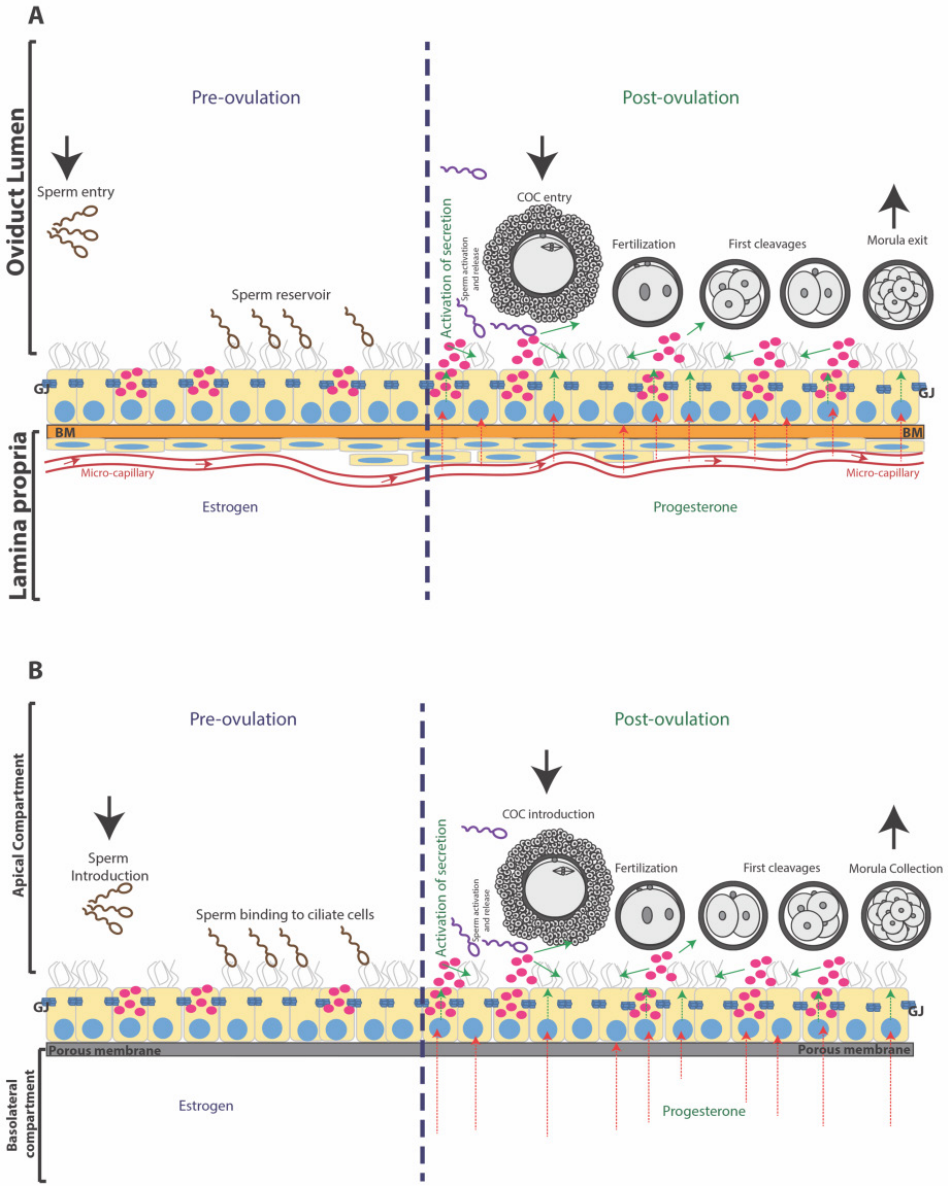

Figure 2. Schematic representation of the oviduct, including its microenvironment before and after ovulation, and of the ideal *in vitro* model of the oviduct. (A): the oviduct epithelium consists of ciliated and non-ciliated (secretory) cells held together in a confluent monolayer of communicating cells by gap junctions (GJ). This epithelium is attached to the luminal side of the basal membrane (BM) which is, in turn, connected to the stroma (containing fibroblast cells and endothelial blood supply) at its peripheral side. Sperm can enter the oviduct and bind to the ciliated cells. This results in the formation of a sperm reservoir during the pre-ovulatory period, under the influence of elevated circulating estrogen concentrations. Ovulation coincides with a switch in endocrine environment in the capillary blood flow of the oviduct. This change stimulates secretory activity in the oviduct epithelium which triggers the release of bound sperm from the isthmus, aids capture of the cumulus-oocyte-complex (COC) and migration of sperm into the ampulla of the oviduct. In the post-ovulatory period, the oviduct is under the influence of progesterone which should promote fertilization and embryo development to the morula stage, when the embryo is ready to leave the oviduct and enter the uterus for further development and implantation. (B) A separation of two compartments with a porous filter, apical reservoir (medium inside the insert) and basolateral reservoir (medium in petri dish), is necessary to mimic the oviduct lumen and lamina propria of the *in vivo* oviduct, respectively (conform (A)). The double perfusion system can be used to simulate peri-ovulatory changes in the blood supply (in the basolateral compartment) and introduce gametes and collect embryos, as would take place in the oviduct *in vivo* (A).

An ideal *in vitro* oviduct model should at least allow the possibility to mimic the hormonal changes that occur in the afferent vasculature in the lead up to, and following, ovulation. Moreover, the system should allow the addition and removal of fluids and gametes into the luminal compartment, promote fertilization and allow the culture of embryos to at least the compact morula stage of development (Figure 2B). These conditions cannot be met when oviduct epithelial cells are simply plated into a petri dish or a cell culture flask. When oviduct epithelial cells are grown in such 2-D cultures they rapidly dedifferentiate into flattened cells without cilia or secretory activity, and also almost completely lose the ability to bind sperm[47] or to promote fertilization *in vitro*[48]. Interestingly, with the aid of cell inserts separate compartments (conform Figure 3) can be created since the medium in the culture dish is separated from the medium in the cell insert, resulting in a basolateral (petri dish) and an apical (cell insert) compartment. OECs can be cultured to confluence on the cell insert and by removing the medium in the insert an air-liquid interface is created that induces the OECs to establish polarity comparable to that seen *in situ* in the oviduct and to differentiate into active secretory and ciliated cells[46,49–54].

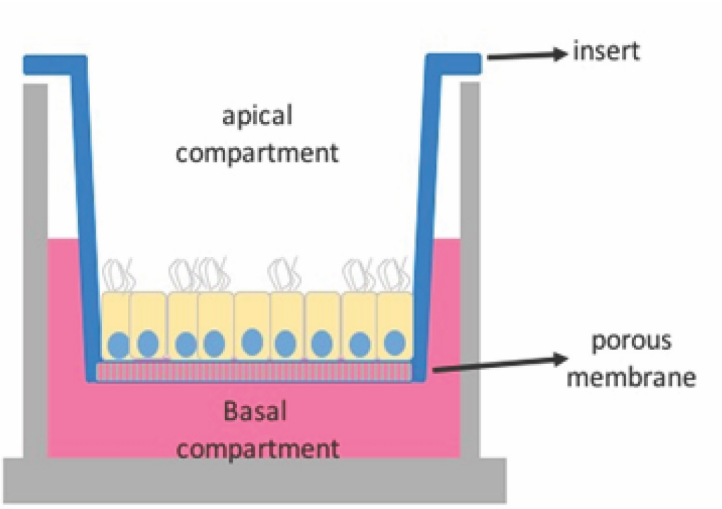

Figure 3. Porous membrane cell culture inserts. In this culture system two compartments are formed (apical and basolateral) that are separated by a porous membrane and a confluent layer of oviduct epithelial cells. This cell culture insert only allows static fluid culture.

Interestingly, there are no reports of embryo production in these 3-D cell insert-based OEC systems, presumably at least in part because in the insert filters, on which the epithelial cells grow, neither the medium in the petri dish nor that in the cell insert can be perfused to mimic the endocrine changes that will in turn influence OEC function during the peri-ovulatory period. A number of recently introduced technologies may help overcome these short comings: (1) advances in three-dimensional (3-D) printing within biomedical engineering have allowed the creation of scaffolds for live cells, microfluidic devices, and tools for medical imaging [55]. Since the technology allows rapid printing of prototypes directly from computer-based designs, it is possible to quickly (hours or days) produce novel devices on demand[55]. The typical folding of the oviduct epithelium (Figure 1) could be mimicked using these modern 3-D printing ap-

proaches. (2) More accurate and miniaturized cell perfusion systems are being developed using microfluidic circuits. When micro-perfusion of both the basolateral (petri dish) and apical (insert) compartments can be achieved, this will mimick the peri-ovulatory hormone changes while simultaneously permitting introduction and collection of gametes and embryos, and sampling of cell secretions. Combining these technologies could result in the creation of a reliable *in vitro* oviduct model to study gamete activation, gamete interaction, fertilization, early embryo development and *in vitro* embryo production. Ultimately, it would be hoped that the embryos produced would be more similar to *in vivo* embryos than IVP embryos produced using current systems. In the following sections, the differences between current OEC culture systems are described in more detail. The type of information that can be gathered from each approach, and their shortcomings, are dealt with. These are further discussed with respect to the anticipated requirements when designing new 3-D culture systems for enhanced gamete maturation, fertilization and early embryo production.

Approaches to study oviduct function

In vivo and ex vivo

In situ research of oviduct function is difficult due to its intra-abdominal location and tortuous morphology. A single study has reported *in vivo* imaging of pre-labeled sperm cells in the oviduct, using fibered fluorescent confocal microscopy (FCM) in the ewe[56]. FCM allowed individual spermatozoa to be observed with high resolution *in situ* in the female genital tract, and moreover to quantitatively track their transit through the uterus and entrance into the oviduct[56].

Most investigations of oviduct function described as "*in vivo*" are actually *ex vivo* experiments, because the organ was first removed from the animal. These studies are also not entirely *in vitro* because the organ, or at least a part of it, is intact[57]. Usually, such *ex vivo* intact organ experiments are hampered by a rapid loss of cell viability, which significantly limits the duration of any experiments (several minutes to a few hours). Nevertheless, *ex vivo* organ incubations have been widely used to study sperm migration through the oviduct by video microscopy[14,58–62] and epifluorescence microscopy[28]. These techniques are especially applicable to species, like the hamster and the mouse, with a transparent wall to the ampullary region or entire oviduct[58].However, *ex vivo* approaches are further limited in that they allow only the imaging of physically detectable changes, such as cilia beating and gamete/embryo movement within the oviduct. In addition, the imaging must be done after collecting the oviducts post-mortem or after surgical removal or by using laparoscopy under general anesthesia, all of which are laborious and invasive procedures.

In vitro

The most commonly reported method for investigating oviduct function *in vitro* oviduct is the monolayer culture (2-D culture; Figure 4A). 2-D culture of OECs is hampered by a rapid loss of typical differentiated OEC properties, such as ciliation, columnar cell morphology, cell polarity, secretory granules and bulbous protrusions [18,45,47,50,63–66]. The use of 2-D culture was nevertheless a useful first step in trying to understand the roles of the oviduct during gamete interaction and early embryo development. Even though OEC morphology is not preserved during 2-D culture, several studies demonstrated interactions between the OECs and spermatozoa, indicating that OECs and/or their secretions could influence sperm function[15,26,67,68]. Additionally, there is evidence of beneficial effects of OECs in 2-D culture on the early embryo via OEC-derived embryotrophic growth factors[69], a decreased oxygen tension and avoidance of the block to embryonic genome activation[70–72].

Another *in vitro* model used to study gamete interaction and embryo development is the oviduct explants (Figure 4B). Oviduct explants are aggregates of epithelial and stromal cells that organize to form motile, everted vesicles with active cilia on the outer surface[45,73,74]. OECs in oviduct explants are able to maintain their differentiated morphology as characterized by secondary cilia, numerous mitochondria and rough endoplasmic reticulum[74], and expression of oviductal epithelial cell markers such as oviductal glycoprotein 1 (OVGP1), glutathione peroxidase 4 (GPX4) and forkhead box protein 1 (FOXJ1)[75]. One drawback is the limited viability of the explants that, within hours to days, lose their differentiated state with the epithelial cells becoming flat and non-ciliated. Another disadvantage is the fact that the system doesn't mimick the air-liquid interface as it happens *in vivo* needing a large volume of medium during culture, therefore not mimicking oviductal conditions properly.

Three-dimensional culture using inserts with porous membranes and air-liquid interfaces (Figures 3C and 3D) have been developed in recent years. This technique allows cultured OECs to retain their polarized columnar epithelial cell characteristics, and has been applied successfully to OECs from various mammalian species[29,45,52–54,76,77]. Within the inserts, seeded OECs first form a confluent layer on the porous membrane. Subsequently, the medium from the apical aspect is removed to establish an air-liquid interface. As a result, the cells receive metabolites only from the basal surface, a trick that induces apical-basolateral polarity. Moreover, the OECs start to re-differentiate and begin to express secondary cilia on their apical surface from 2-3 weeks post-confluence and are able to maintain the polarized state during long term culture (for at least 6 more weeks). The resulting polarized OECs are able to bind introduced sperm[29,45,46] and secrete factors into medium film of the insert that triggers the release of previously bound sperm[45]. Moreover, the OECs are responsive to endocrine stimulation, as demonstrated by an increase in the expression of prostaglandin receptor (PGR), estrogen receptor 1 (ESR1) and epithelial markers such as mucin 16 (MUC16), OVGP1 and heat shock protein 90 beta member 1 (HSB90B1), when exposed to estrogens, and a decrease in the same markers when stimulated by progesterone[46]. Despite all the potential advantages of 3-D

OEC cultures, current well inserts do not permit live imaging or perfusion studies. Moreover, theses 3-D OEC systems lack the tubular folded architecture of the oviduct. These shortcomings are likely to limit their use to study gamete interactions and early embryo development in any detail.

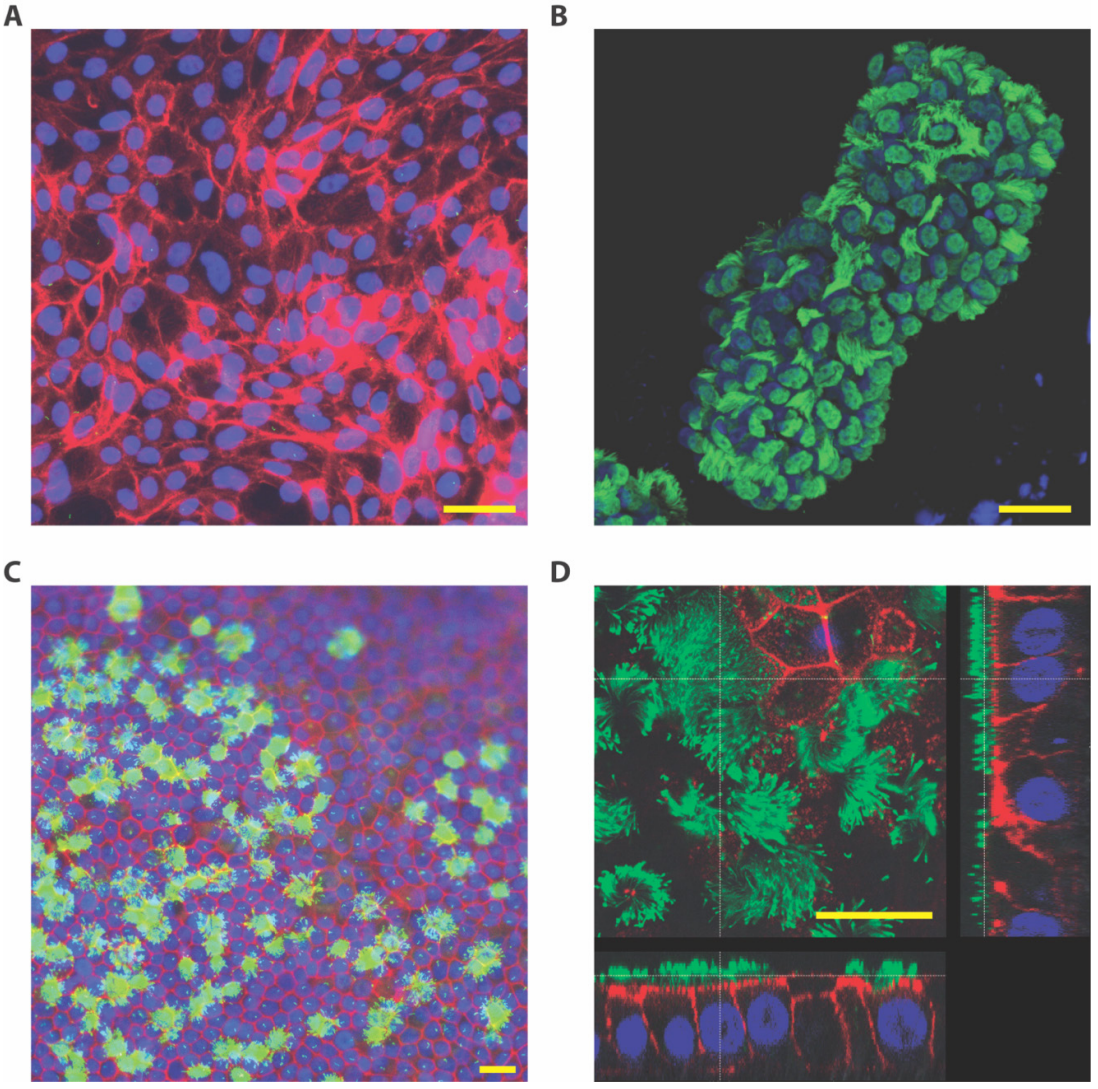

Figure 4. Fluorescent staining for nuclei (blue, Hoechst33342), actin filaments (red, phalloidin) and cilia (green, indirect immunofluorescent labeling of acetylated alpha tubulin) in different *in vitro* oviduct epithelial cell (OEC) culture techniques. (A) An equine 2-D OEC culture without secondary cilia. (B) A bovine OEC explant vesicle showing ciliated and non-ciliated cells (note; we did not stain this specimen for phalloidin as confluent contact between the cells in this epithelial vesicle is known to remain intact). (C) and (D) Equine OECs cultured on porous membranes for 6 weeks at an air-liquid interface; note the presence of ciliated and non-ciliated cells in C and D, and the columnar shape of the cells with nuclei at the base and cilia at the apical aspect of the cells in D. Equine images were provided by H.H.W.H (data unpublished) and bovine image by M.A.M.M.F. (data unpublished). Bars = 25 µm.

Organoid models

Two different methods for developing oviduct organoids have been described[78–80] and, in both, it was possible to maintain differentiated OECs within a folded tubular structure reminiscent of the *in vivo* oviduct: (1) In the first method, small pieces of oviduct were cultured inside an alginate matrix. These organoids were maintained in culture for 7 days and expressed normal oviductal epithelial cell markers, such as OVGP1, paired box 8 (PAX8), E-cadherin and cytokeratin; they also preserved a columnar epithelium with a mix of ciliated and non-ciliated cells[80]. (2) The second method for organoid culture was based on the existence of adult stem cells in the distal part of the oviduct[78,81–83]. Kessler and collaborators[78] isolated these adult stem cells and cultured them in a Matrigel matrix supplemented with a cocktail of growth factors, including epidermal growth factor (EGF), fibroblast growth factor 10 (FGF-10) and transforming growth factor beta (TGF-β). The cells were able to proliferate and form spheroids, with folds appearing during the second week of culture. The resulting organoids also presented highly polarized columnar epithelial cells orientated with the apical side into the sphere's lumen. The mature organoids presented both PAX-8 positive secretory cells and PAX-8 negative, but acetylated tubulin positive, ciliated cells and were able to maintain this morphology during long term culture (up to 8 months). Demonstrating a fully differentiated epithelium, with both ciliated and secretory cells, that can communicate directly (by the interaction between the sperm cell and the cilia, the sperm reservoir) or indirectly (by secreting factors into its lumen) with gametes and embryos. Although organoid culture can preserve oviduct morphology and OEC polarization, it has limitations in that the luminal compartment of the organoid is only accessible for gametes or embryos via micro-puncturing. Thus, expensive micromanipulators are required and technical expertise must be developed to further study gamete activation, fertilization and embryo development.

Microfluidics

Research into microfluidics and reproductive events have increased in the past years, and relatively new papers on microfluidics and gamete development have been published[84–99]. In most cases, these papers relate to sperm migration, and none have included OECs in the model. Interestingly, microfluidics devices have been designed to study sperm rheotaxis, movement, thermotaxis and chemotaxis, thereby mimicking physical and chemical factors that sperm encounter during their passage through the female tract (for a detailed description see Suarez and Wu, 2016[100]). Zhang and collaborators[98] included oviductal fluid to help select sperm cells via a microfluidics system. Using this combination, they were able to observe sperm migration and select sperm with better motility and DNA integrity, concluding that it was a useful tool for selecting sperm for IVF procedures. It was also demonstrated that sperm rely more on the channel geometry than chemotaxis (i.e. sperm cells preferentially swim along boundaries and, when two boundaries intersect, the cells will follow the corner, swimming

along one-dimensional folds[99]). Although the folding of the oviduct is more complex than the walls of a fabricated microchannel, these results suggest that the 3-D architecture of the compartment in which sperm migrate is important and that the topography of the oviduct wall may help guide the spermatozoa to the oocyte *in vivo*[99].

Angione and collaborators[85] engineered a microfluidic device that allows precise and flexible handling of individual oocytes and embryos. Their system allowed perfusion and live imaging of the introduced oocytes or developing embryos that could be used for both clinical and research IVF purposes. Nevertheless, most current embryo culture systems are static[92], although interest in microfluidic devices for embryo culture systems has increased in recent years. Potential benefits of a dynamic (microfluidic) embryo culture system are continuous removal of harmful products and replenishment of substrates, disruption of unwanted environmental gradients, physical stimulation and activation of signaling pathways[92]. Mechanical stimulation of bovine embryos in a microfluidic device increased the proportion of 2-cell embryos developing into 8-cell embryos, when a constrictive channel was used (increasing from 23.9 to 56.7%)[93]. Mechanical shear stresses imposed should not however be too harsh because embryos degenerate at values above 1.2dyn/cm^2 [96]. A “womb-on-a-chip” was designed to establish a dynamic co-culture between endometrial cells and the embryo[97]. This system allows investigation of the interaction between the embryo and secretions from the endometrial cells, moreover the co-culture resulted in improved murine blastocyst rates[97]. Nevertheless, a similar approach using microfluidics combined with OECs to enhance embryo production has not yet been reported.

3-D printing

Micro-engineered 3-D cell cultures, in which cells are maintained in micro-3-D fabricated devices that mimic tissue- and organ-specific micro-architecture[101], have recently attracted attention. These approaches promote levels of cell differentiation and polarization that are not readily achieved by normal 2-D cultures. Nowadays, 3-D printing offers a fast prototyping process technology, such that researchers can design and print devices in a short period of time[55]. Combined with microfluidics, these techniques can lead to rapid creation and refinement of organs-on-a-chip to study human and animal organ-specific physiology and may, thereby, offer better *in vitro* organ models for research into aspects of physiology, disease and toxicology[101].

3-D printing has been used to fabricate various tissues including bone, cartilage, skin, heart tissue, and vascular tubes[102]. To our surprise, we were the first to use 3-D printing technology in combination with microfluidics for assisted reproduction, when developing an *oviduct-on-a-chip* model[48]. We designed and 3-D printed, using the stereolithography technique, a tubular like insert in which OECs could be cultured at an air-liquid interface and acquire and maintain epithelial polarization and differentiated cell state during long-term culture. The 3-D culture

and polarization of OECs in our 3-D printed inserts resembles that of the cell insert approach with porous membranes (Figure 3). However, with the new 3-D OEC system, live imaging is possible, sperm can bind to the apical side of the OEC and be released. Furthermore, the system promotes normal fertilization and is easy to manipulate (i.e. for adding or removing gametes, embryos and cell secretions). The system also allows independent double perfusion (i.e. of the apical and basolateral medium compartments independently; Figure 5) while maintaining a tubular morphology that could be made more complex to better mimic the oviduct. Furthermore, the cells can keep a polarized state for long term cultures (at least six weeks), without losing ciliation and ability to promote sperm activation[103].

Therefore, the *oviduct-on-a-chip* is a step forward for mimicking the interaction between gametes and embryos and the maternal oviductal environment. This will yield a better and more accessible bio-mimicking tool to study oviduct physiology and improve understanding of reproductive health and disease, as well as for screening toxicological compounds and novel drugs.

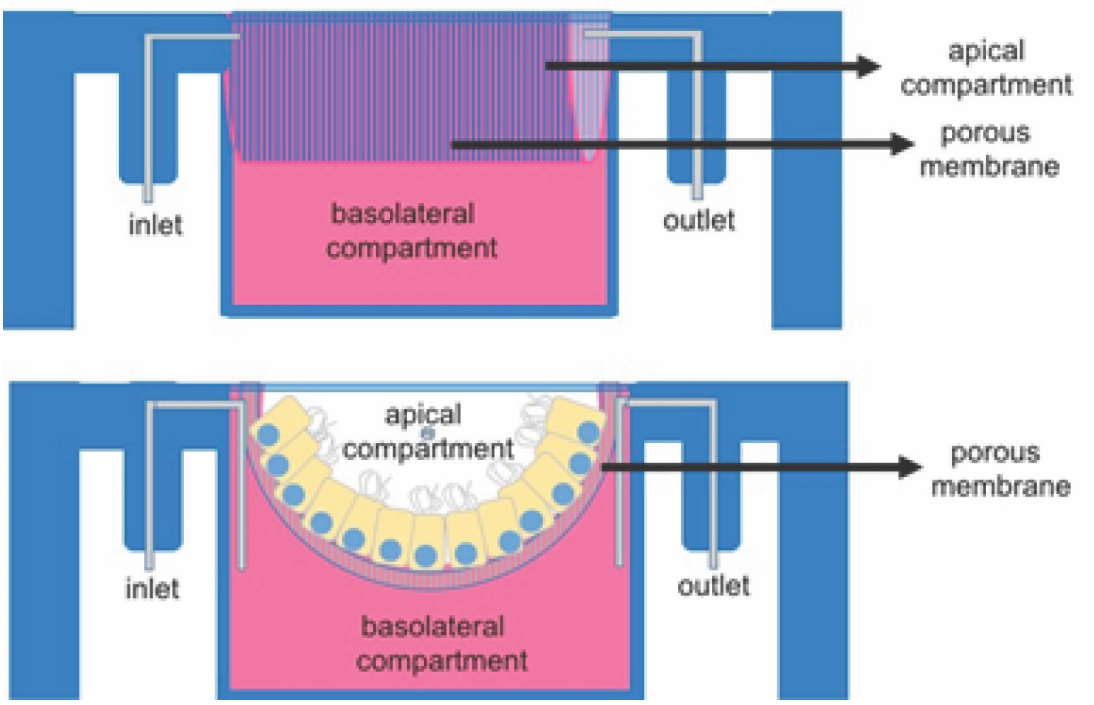

Figure 5. The 3-D printed oviduct-on-a-chip cultures. Also in this culture systems two compartments are formed (apical and basolateral) that are separated by a porous membrane and a confluent layer of oviduct epithelial cells. Note the inlets and outlets for independent perfusion of the apical and basolateral compartments, and the folded U-shape structure, that are introduced into the 3-D printed oviduct-on-a-chip.

Improvements in oviduct modelling via bioengineering

Better 3-D cell culture systems to bio-mimic the oviduct can help to improve our understanding of *in vivo* processes that take place in this organ, and should help to improve the efficacy of assisted reproductive technologies (ARTs). The oviduct has an essential function in guiding and regulating sperm activation, oocyte maturation, fertilization and early embryo development[22,34,40,69,72,104]. A better understanding of how the oviduct orchestrates these processes could aid in the development of better sperm storage and cryopreservation techniques[105,106]. Moreover, improved oocyte maturation and IVP results, including a reduction in polyspermic fertilization and parthenogenetic activation, can also be achieved[33,35,40,107,108]. Another aspect of improved IVP embryo quality could be survival after cryopreservation, reduced lipid content and avoidance of epigenetic changes that can impair embryo development or offspring health[44,109–119]. Conventional *in vitro* fertilization (IVF) and embryo production has species specific problems. For instance, equine oocytes cannot be fertilized *in vitro* unless intracytoplasmic sperm injection (ICSI) is used, which requires expensive and dedicated technology and is labour intensive[120–122]. For cattle, it is known that *IVP* embryos are of lower quality and have reduced cryosurvival compared to embryos flushed from the uterus[123–125]. Both examples, clearly indicate that the oviductal environment is more conducive to producing good quality embryos than any *in vitro* system tested to date. Future studies will reveal whether or not the oviduct-on-a-chip approach will offer a superior oviduct-like environment for improved embryo production. A working oviduct-on-a-chip system would also offer a novel approach to reproductive toxicology testing or pharmaceutical agent screening, and for male and female infertility testing.

As we move from 2-D cultures to micro-engineered organs-on-a-chip, new challenges will undoubtedly arise. For instance, optimizing biological (cell) and non-biological (materials) culture requirements, optimizing/allowing cell polarization, differentiation and preventing possible toxic effects of the materials used. A multidisciplinary approach will be necessary to solve the likely challenges and maximally exploit the new opportunities the organ-on-a-chip technique will offer. In the more distant future, more complex bioengineered tissues (such as multilayered oviduct, follicles and endometrial cell cultures) could be combined to create a female-reproductive-tract-on-a-chip. However, at present we believe that the oviduct-on-a-chip technology is closer to being ready, and has more obvious immediate applications in the field of ART.

General aim and scope of the thesis

The underlying theme of this thesis is the combination of new technologies, such as 3D-printing and microfluidics, to create a more *in vivo*-like oviduct epithelial cell culture system. The primary goal is to improve our understanding of the molecular and cellular mechanisms underlying the interaction between the gametes and the early embryo with the oviduct; this should enable the development of novel approaches to infertility, and the production of 'more physiological' *in vitro* embryo production systems that improve the likelihood of producing embryos, improve the quality of those embryos and, most importantly, reduce the risk of introducing epigenetic changes that could affect the lifelong health of the resulting offspring. In **chapter 2**, the differences in the time course and extent of epigenetic reprogramming between *in vitro* and *in vivo* produced zygotes is investigated. Correct reprogramming of epigenetic marks during preimplantation embryo development is essential, first to the establishment of a transcriptionally active totipotent zygote, and subsequently to appropriate regulation of gene silencing during embryo development and cell differentiation[126–128]. During the preimplantation period, however, epigenetic reprogramming is exquisitely vulnerable to disturbance in response to adverse environmental conditions. *In vitro* fertilization (IVF) can impose such disturbances because the gametes are recovered from the male and female genital tracts, washed and exposed to culture media, light, temperature and non-physiological oxygen tensions[129–131]. The results from **chapter 2** illustrate the need for a better bio-mimicking system for *in vitro* embryo production.

To this end, in **chapter 3** an attempt to create an oviduct-on-a-chip using 3D-printing technologies is described. Micro-engineered 3D cell cultures that mimic tissue and organ-specific micro-architecture are a recent development. Micro 3D fabricated devices are used to engineer levels of cell organization, differentiation and interaction that are not readily achieved in conventional 2D culture[101]. By using 3D-printing and microfluidics technologies, it is possible to rapidly create and refine organs-on-a-chip to study mammalian organ-specific physiology and, thereby, create better *in vitro* models to examine aspects of organ physiology, disease and toxicology[101,102,132,133]. The use of 3D-printing technologies to create a u-shaped chamber to culture bovine oviductal epithelial cells in a more *in vivo*-like environment is described in **chapter 3**. This first 3D-printed oviduct-on-a-chip design supported oocyte penetration in the absence of artificial sperm capacitation factors, while also preventing polyspermy and parthenogenic activation, both of which occur in classical *in vitro* fertilization systems.

Although the prototype oviduct-on-a-chip improved early aspects of bovine *in vitro* fertilization in **chapter 3**, in **chapter 4** we show that the chip inhibited further embryo development, i.e. beyond the 2-4 cell stage. The possibility that the material used had adverse effects on embryo development was tested further; to this end, in **chapter 4,** five different materials were tested for possible adverse effects on embryo development. The objective was to select the best material for producing the second generation oviduct-on-a-chip. We found that the tested polymers leaked toxic compounds into solution (polyethylene glycol and diethyl-phthalate); these toxins are known to adversely influence biological activities, for instance by binding

to and either stimulating or blocking hormone receptors. Taken together, our results reveal that the fertilized bovine oocyte is extremely sensitive to components leaking from 3D-printed polymers, which do not affect oviduct cell survival but do inhibit early embryogenesis. This demonstrates that only after a dedicated set of toxicity screening tests, would one be able to make a reliable prediction of the biocompatibility of a 3D-printed bioengineered polymer for general biological application.

The non-toxic plastic material identified in **chapter 4** was used to create the microfluidics based oviduct-on-a-chip platform described in **chapter 5.** This chapter shows that the new 3D oviduct epithelial cell culture system supported more physiological embryo development up to the blastocyst stage (i.e. no blockage at the 2 or 4 cell stages).

Finally, in **chapter 6**, the findings of these studies are discussed and put into context, including future perspectives for the use of the oviduct-on-a-chip for embryo production and in artificial reproductive technologies, but also in the context of 3D cell culture approaches in general.

References

1. Menezo, Y. & Guerin, P. The mammalian oviduct: Biochemistry and physiology. *Eur. J. Obstet. Gynecol. Reprod. Biol.* **73,** 99–104 (1997).
2. Steinhauer, N., Boos, A. & Günzel-Apel, A. R. Morphological changes and proliferative activity in the oviductal epithelium during hormonally defined stages of the oestrous cycle in the bitch. *Reprod. Domest. Anim.* **39,** 110–119 (2004).
3. Murray, M. K. Epithelial lining of the sheep ampulla oviduct undergoes pregnancy-associated morphological changes in secretory status and cell height. *Biol. Reprod.* **53,** 653–63 (1995).
4. Yaniz, J. L., Lopez-Gatius, F. & Hunter, R. H. F. Scanning electron microscopic study of the functional anatomy of the porcine oviductal mucosa. *Anat. Histol. Embryol.* **35,** 28–34 (2006).
5. Abe, H. The mammalian oviductal epithelium: Regional variations in cytological and functional aspects of the oviductal secretory cells. *Histol. Histopathol.* **11,** 743–768 (1996).
6. Lamy, J. *et al.* Regulation of the bovine oviductal fluid proteome. *Reproduction* **152,** 629–644 (2016).
7. Buhi, W. C., Alvarez, I. M. & Kouba, a J. Secreted proteins of the oviduct. *Cells. Tissues. Organs* **166,** 165–179 (2000).
8. Abe, H. Immunocytochemical evidence that a specialised region of the rat oviduct secretes an oviductal glycoprotein. *J. Anat.* **188 (Pt 2,** 333–9 (1996).
9. Verhage, H. G. *et al.* The baboon oviduct: Characteristics of an oestradiol-dependent oviduct-specific glycoprotein. *Hum. Reprod. Update* **3,** 541–552 (1997).
10. Yamanouchi, H., Umezu, T. & Tomooka, Y. Reconstruction of Oviduct and Demonstration of Epithelial Fate Determination in Mice. *Biol. Reprod.* **82,** 528–33 (2010).
11. Burkitt, M., Romano, D. M., Walker, D. C. & Fazeli, A. 3D modelling of complex biological structures: the oviduct. *Theory Pract. Comput. Graph.* 255–262 (2010). doi:10.2312/LocalChapterEvents/TPCG/TPCG10/255-262
12. Coy, P., García-Vázquez, F. a., Visconti, P. E. & Avilés, M. Roles of the oviduct in mammalian fertilization. *Reproduction* **144,** 649–660 (2012).
13. Rodriguez-Martinez, H. Role of the oviduct in sperm capacitation. *Theriogenology* **68,**

138–146 (2007).
14. Suarez, S. S. Mammalian sperm interactions with the female reproductive tract. *Cell Tissue Res.* **363,** 185–194 (2016).
15. Talevi, R. & Gualtieri, R. Molecules involved in sperm-oviduct adhesion and release. *Theriogenology* **73,** 796–801 (2010).
16. Burkitt, M., Walker, D., Romano, D. M. & Fazeli, A. Computational modelling of maternal interactions with spermatozoa: Potentials and prospects. *Reprod. Fertil. Dev.* **23,** 976–989 (2011).
17. Lamy, J. *et al.* Steroid hormones in bovine oviductal fluid during the estrous cycle. *Theriogenology* **86,** 1409–1420 (2015).
18. Ulbrich, S. E., Zitta, K., Hiendleder, S. & Wolf, E. In vitro systems for intercepting early embryo-maternal cross-talk in the bovine oviduct. *Theriogenology* **73,** 802–816 (2010).
19. Killian, G. J. Evidence for the role of oviduct secretions in sperm function, fertilization and embryo development. *Anim. Reprod. Sci.* **82–83,** 141–153 (2004).
20. Ménézo, Y., Guérin, P. & Elder, K. The oviduct: A neglected organ due for re-assessment in IVF. *Reprod. Biomed. Online* **30,** 233–240 (2015).
21. Rodríguez, C., Killian, G., Rodríguez, C. & Killian, G. Identification of ampullary and isthmic oviductal fluid proteins that associate with the bovine sperm membrane. *Anim. Reprod. Sci.* **54,** 1–12 (1998).
22. Parrish, J. J., Susko-Parrish, J. L., Handrow, R. R., Sims, M. M. & First, N. L. Capacitation of bovine spermatozoa by oviduct fluid. *Biol. Reprod.* **40,** 1020–1025 (1989).
23. Hung, P. & Suarez, S. S. Alterations to the bull sperm surface proteins that bind sperm to oviductal epithelium. *Biol. Reprod.* **87,** 88 (2012).
24. Kumaresan, A., Ansari, M. R. & Garg, A. Modulation of post-thaw sperm functions with oviductal proteins in buffaloes. *Anim. Reprod. Sci.* **90,** 73–84 (2016).
25. Mcnutt, T. & Killian, G. Influence of Bovine Follicular and Oviduct Fluids on sperm Capacitation In Vitro. *J. Androl.* **12,** 244–252 (1991).
26. Morales, P., Palma, V., Salgado, a M. & Villalon, M. Sperm interaction with human oviductal cells in vitro. *Hum. Reprod.* **11,** 1504–1509 (1996).
27. Dejonge, C. J. *et al.* The Acrosome Reaction-Inducing Effect of Human Follicular and Oviductal Fluid. *J. Androl.* **141,** 359–365 (1993).
28. Spina, F. A. La *et al.* Mouse sperm begin to undergo acrosomal exocytosis in the upper isthmus of the oviduct. *Dev. Biol.* 1–11 (2016). doi:10.1016/j.ydbio.2016.02.006
29. Pollard, J. W. *et al.* Fertilizing capacity of bovine sperm may be maintained by binding of oviductal epithelial cells. *Biol. Reprod.* **44,** 102–107 (1991).
30. King, R. S., Anderson, S. H. & Killian, G. J. Effect of Bovine Oviductal Estrus-Associated Protein on the Ability of Sperm to Capacitate and Fertilize Oocytes. *J. Androl.* **15,** 468–478 (1994).
31. McNutt, T., Rogowski, L., Vasilatos-Younken, R. & Killian, G. Adsorption of oviductal fluid proteins by the bovine sperm membrane during in vitro capacitation. *Mol. Reprod. Dev.* **33,** 313–323 (1992).
32. Erikson, D. W., Way, A. L., Bertolla, R. P., Chapman, D. A. & Killian, G. J. Influence of osteopontin , casein and oviductal fluid on bovine sperm capacitation. *Anim. Reprod.* **4,** 103–112 (2007).
33. Mondéjar, I., Martínez-Martínez, I., Avilés, M. & Coy, P. Identification of potential oviductal factors responsible for zona pellucida hardening and monospermy during fertilization in mammals. *Biol. Reprod.* **89,** 67 (2013).
34. Gonçalves, R. F., Staros, A. L. & Killian, G. J. Oviductal fluid proteins associated with the bovine zona pellucida and the effect on in vitro sperm-egg binding, fertilization and embryo development. *Reprod. Domest. Anim.* **43,** 720–729 (2008).

35. Coy, P. & Avilés, M. What controls polyspermy in mammals, the oviduct or the oocyte? *Biol. Rev.* **85,** 593–605 (2010).
36. Gabler, C. *et al.* Exploring cumulus-oocyte-complex-oviductal cell interactions: Gene profiling in the bovine oviduct. *J. Physiol. Pharmacol.* **59,** 29–42 (2008).
37. Besenfelder, U., Havlicek, V. & Brem, G. Role of the oviduct in early embryo development. *Reprod. Domest. Anim.* **47,** 156–163 (2012).
38. Maillo, V. *et al.* Oviduct-Embryo Interactions in Cattle: Two-Way Traffic or a One-Way Street? *Biol. Reprod.* **92,** 144–144 (2015).
39. Monaco, E. *et al.* Effect of osteopontin (OPN) on in vitro embryo development in cattle. *Theriogenology* **71,** 450–457 (2009).
40. Lloyd, R. E. *et al.* Effects of oviductal fluid on the development, quality, and gene expression of porcine blastocysts produced in vitro. *Reproduction* **137,** 679–687 (2009).
41. Ventura-Juncá, P. *et al.* In vitro fertilization (IVF) in mammals: epigenetic and developmental alterations. Scientific and bioethical implications for IVF in humans. *Biol. Res.* **48,** 68 (2015).
42. Eyestone, W. H. & First, N. L. Co-culture of early cattle embryos to the blastocyst stage with oviducal tissue or in conditioned medium. *J. Reprod. Fertil.* **85,** 715–20 (1989).
43. Gad, a. *et al.* Molecular Mechanisms and Pathways Involved in Bovine Embryonic Genome Activation and Their Regulation by Alternative In Vivo and In Vitro Culture Conditions. *Biol. Reprod.* **87,** 100–100 (2012).
44. Salilew-Wondim, D. *et al.* Genome-wide DNA methylation patterns of bovine blastocysts developed in vivo from embryos completed different stages of development in vitro. *PLoS One* **10,** 1–31 (2015).
45. Gualtieri, R. *et al.* Bovine oviductal monolayers cultured under three-dimension conditions secrete factors able to release spermatozoa adhering to the tubal reservoir in vitro. *Theriogenology* **79,** 429–435 (2013).
46. Chen, S., Einspanier, R. & Schoen, J. In vitro mimicking of estrous cycle stages in porcine oviduct epithelium cells: estradiol and progesterone regulate differentiation, gene expression, and cellular function. *Biol. Reprod.* **89,** 54 (2013).
47. Sostaric, E. *et al.* Sperm binding properties and secretory activity of the bovine oviduct immediately before and after ovulation. *Mol. Reprod. Dev.* **75,** 60–74 (2008).
48. M. A. M. M. Ferraz, H. H. W. Henning, K. M. A. Van Dorenmalen, P. L. A. M. Vos, T. A. E. Stout, P. F. Costa, J. Malda, and B. M. G. & J. Malda, and B. M. G. M. A. M. M. F. H. H. W. H. K. M. A. V. D. P. L. A. M. V. T. A. E. S. P. F. C. 52 Use of transwell cell culture and 3-dimensional printing technology to develop an in vitro bovine oviduct. *Reprod. Fertil. Dev.* **28,** 130 (2016).
49. Pampaloni, F., Reynaud, E. G. & Stelzer, E. H. K. The third dimension bridges the gap between cell culture and live tissue. *Nat. Rev. Mol. Cell Biol.* **8,** 839–845 (2007).
50. Gualtieri, R. *et al.* Long-term viability and differentiation of bovine oviductal monolayers: Bidimensional versus three-dimensional culture. *Theriogenology* **78,** 1456–1464 (2012).
51. Miessen, K., Sharbati, S., Einspanier, R. & Schoen, J. Modelling the porcine oviduct epithelium: A polarized in vitro system suitable for long-term cultivation. *Theriogenology* **76,** 900–910 (2011).
52. Chen, S., Einspanier, R. & Schoen, J. Long-term culture of primary porcine oviduct epithelial cells: Validation of a comprehensive invitro model for reproductive science. *Theriogenology* **80,** 862–869 (2013).
53. Rajagopal, M., Tollner, T. L., Finkbeiner, W. E., Cherr, G. N. & Widdicombe, J. H. Differentiated structure and function of primary cultures of monkey oviductal epithelium. *Vitr. cell. Dev. Biol.* **42,** 248–254 (2006).

54. Fotheringham, S., Levanon, K. & Drapkin, R. Ex vivo Culture of Primary Human Fallopian Tube Epithelial Cells. *J. Vis. Exp.* 3–7 (2011). doi:10.3791/2728
55. Macdonald, N. P. *et al.* Assessment of biocompatibility of 3D printed photopolymers using zebrafish embryo toxicity assays. *Lab Chip* **16,** 291–7 (2016).
56. Druart, X. *et al.* In vivo imaging of in situ motility of fresh and liquid stored ram spermatozoa in the ewe genital tract. *Reproduction* **138,** 45–53 (2009).
57. Van Soom, A., Vandaele, L., Peelman, L. J., Goossens, K. & Fazeli, A. Modeling the interaction of gametes and embryos with the maternal genital tract: From in vivo to in silico. *Theriogenology* **73,** 828–837 (2010).
58. Suarez, S. S. Sperm transport and motility in the mouse oviduct: observations in situ. *Biol. Reprod.* **36,** 203–210 (1987).
59. Kölle, S. Live cell imaging of the oviduct. *Methods Enzymol.* **506,** 415–423 (2012).
60. Kölle, S. *et al.* Ciliary transport, gamete interaction, and effects of the early embryo in the oviduct: ex vivo analyses using a new digital videomicroscopic system in the cow. *Biol. Reprod.* **81,** 267–274 (2009).
61. Kölle, S., Reese, S. & Kummer, W. New aspects of gamete transport, fertilization, and embryonic development in the oviduct gained by means of live cell imaging. *Theriogenology* **73,** 786–795 (2010).
62. Shalgi, R. & Phillips, D. M. Motility of rat spermatozoa at the site of fertilization. *Biol. Reprod.* **39,** 1207–1213 (1988).
63. Betsha, S. *et al.* Sperm binding properties and secretory activity of the bovine oviduct immediately before and after ovulation. *Mol. Reprod. Dev.* **80,** 315–333 (2013).
64. Joshi, M. S. Isolation, cell culture, and characterization of oviduct epithelial cells of the cow. *Microsc. Res. Tech.* **31,** 507–518 (1995).
65. Schoen, J., Bondzio, a., Topp, K. & Einspanier, R. Establishment and characterization of an adherent pure epithelial cell line derived from the bovine oviduct. *Theriogenology* **69,** 536–545 (2008).
66. Karst, A. M. & Drapkin, R. Primary culture and immortalization of human fallopian tube secretory epithelial cells. *Nat. Protoc.* **7,** 1755–1764 (2012).
67. Ellington, J. E. *et al.* Higher-quality human sperm in a sample selectively attach to oviduct (fallopian tube) epithelial cells in vitro. *Fertil. Steril.* **71,** 924–929 (1999).
68. Ellington, J. E. *et al.* Coculture of human sperm with bovine oviduct epithelial cells decreases sperm chromatin structural changes seen during culture in media alone. *Fertil. Steril.* **69,** 643–9 (1998).
69. Tse, P. K. *et al.* Preimplantation embryos cooperate with oviductal cells to produce embryotrophic inactivated complement-3b. *Endocrinology* **149,** 1268–1276 (2008).
70. Nancarrow, C. D. & Hill, J. L. Co-culture, oviduct secretion and the function of oviduct-specific glycoproteins. *Cell Biol. Int.* **18,** 1105–1114 (1994).
71. Gandolfi, F. & Moor, R. M. Stimulation of early embryonic development in the sheep by co-culture with oviduct epithelial cells. *J. Reprod. Fertil.* **81,** 23–28 (1987).
72. Ellington, J. A., Carney, E. W., Farrell, P. B., Simkin, M. E. & Foote, R. H. Bovine 1-2-cell embryo development using a simple medium in three oviduct epithelial cell coculture systems. *Biol. Reprod.* **43,** 97–104 (1990).
73. Leemans, B. *et al.* Combined albumin and bicarbonate adversely affects equine sperm-oviduct binding. *Reproduction* **151,** 313–330 (2016).
74. Nelis, H. *et al.* Equine oviduct explant culture: a basic model to decipher embryo–maternal communication. *Reproduction, Fertility and Development* **26,** 954–966 (2014).
75. Maillo, V. *et al.* Maternal-embryo interaction in the bovine oviduct: evidence from in vivo and in vitro studies. *Theriogenology* **86,** 443–450 (2016).
76. Reischl, J. *et al.* Factors affecting proliferation and dedifferentiation of primary bovine oviduct epithelial cells in vitro. *Cell Tissue Res.* **296,** 371–383 (1999).

77. Comer, M. T., Leese, H. J. & Southgate, J. Induction of a differentiated ciliated cell phenotype in primary cultures of Fallopian tube epithelium. *Hum. Reprod.* **13,** 3114–3120 (1998).
78. Kessler, M. *et al.* The Notch and Wnt pathways regulate stemness and differentiation in human fallopian tube organoids. *Nat. Commun.* **6,** 8989 (2015).
79. King, S. M., Quartuccio, S., Hilliard, T. S., Inoue, K. & Burdette, J. E. Alginate hydrogels for three-dimensional organ culture of ovaries and oviducts. *J. Vis. Exp.* e2804 (2011). doi:10.3791/2804
80. King, S. M. *et al.* The impact of ovulation on fallopian tube epithelial cells: Evaluating three hypotheses connecting ovulation and serous ovarian cancer. *Endocr. Relat. Cancer* **18,** 627–642 (2011).
81. Wang, Y. *et al.* Identification of Quiescent, Stem-Like Cells in the Distal Female Reproductive Tract. *PLoS One* **7,** e40691 (2012).
82. Ng, A. *et al.* Lgr5 marks stem/progenitor cells in ovary and tubal epithelia. *Nat. Cell Biol.* **16,** 745–57 (2014).
83. Paik, D. Y. *et al.* Stem-like epithelial cells are concentrated in the distal end of the fallopian tube: A site for injury and serous cancer initiation. *Stem Cells* **30,** 2487–2497 (2012).
84. Scherr, T. *et al.* Microfluidics and numerical simulation as methods for standardization of zebrafish sperm cell activation. *Biomed. Microdevices* **17,** 1–10 (2015).
85. Angione, S. L., Oulhen, N., Brayboy, L. M., Tripathi, A. & Wessel, G. M. Simple perfusion apparatus for manipulation, tracking, and study of oocytes and embryos. *Fertil. Steril.* **103,** 281–290 (2015).
86. Knowlton, S. M., Sadasivam, M. & Tasoglu, S. Microfluidics for sperm research. *Trends Biotechnol.* **33,** 221–229 (2016).
87. El-Sherry, T. M., Elsayed, M., Abdelhafez, H. K. & Abdelgawad, M. Characterization of rheotaxis of bull sperm using microfluidics. *Integr. Biol.* **6,** 1111–1121 (2014).
88. Huang, H. *et al.* Motile Human Sperm Sorting by an Integrated Microfluidic System. *J. Nanomed. Nanotechnol.* **5,** (2014).
89. Cheng, S.-Y. *et al.* A hydrogel-based microfluidic device for the studies of directed cell migration. *Lab Chip* **7,** 763–769 (2007).
90. de Wagenaar, B. *et al.* Towards microfluidic sperm refinement: impedance-based analysis and sorting of sperm cells. *Lab Chip* **16,** 1514–1522 (2016).
91. de Wagenaar, B. *et al.* Microfluidic single sperm entrapment and analysis. *Lab Chip* **15,** 1294–1301 (2015).
92. Swain, J. E. & Smith, G. D. Advances in embryo culture platforms: Novel approaches to improve preimplantation embryo development through modifications of the microenvironment. *Hum. Reprod. Update* **17,** 541–557 (2011).
93. Kim, M. S., Bae, C. Y., Wee, G., Han, Y. M. & Park, J. K. A microfluidic in vitro cultivation system for mechanical stimulation of bovine embryos. *Electrophoresis* **30,** 3276–3282 (2009).
94. Huang, H. Y. *et al.* Digital microfluidic dynamic culture of mammalian embryos on an Electrowetting on Dielectric (EWOD) chip. *PLoS One* **10,** 1–15 (2015).
95. Lai, D., Takayama, S. & Smith, G. D. Recent microfluidic devices for studying gamete and embryo biomechanics. *J. Biomech.* **48,** 1671–1678 (2015).
96. Y, X. *et al.* Shear Stress Induces Preimplantation Embryo Death That Is Delayed by the Zona Pellucida and Associated with Stress-Activated Protein Kinase-Mediated Apoptosis. *Biol. Reprod.* **75,** 45–55 (2006).
97. Mizuno, J. *et al.* Human ART on chip: improved human blastocyst development and quality with IVF-chip. *Fertil. Steril.* **88,** S101 (2007).
98. Zhang, B., Yin, T. L. & Yang, J. A novel microfluidic device for selecting human sperm

to increase the proportion of morphologically normal, motile sperm with uncompromised DNA integrity. *Anal. Methods* **7,** 5981–5988 (2015).
99. Denissenko, P., Kantsler, V., Smith, D. J. & Kirkman-Brown, J. Human spermatozoa migration in microchannels reveals boundary-following navigation. *Proc Natl Acad Sci* **109,** 8007–8010 (2012).
100. Suarez, S. S. & Wu, M. Microfluidic devices for the study of sperm migration. *Mol. Hum. Reprod.* (2016). doi:10.1093/molehr/gaw039
101. Huh, D., Hamilton, G. A. & Ingber, D. E. From 3D cell culture to organs-on-chips. *Trends Cell Biol.* **21,** 745–754 (2011).
102. Murphy, S. V & Atala, A. 3D bioprinting of tissues and organs. *Nat Biotech* **32,** 773–785 (2014).
103. Ferraz, M. A. M. M. *et al.* Improved bovine embryo production in an oviduct-on-a-chip system: Prevention of poly-spermic fertilization and parthenogenic activation. *Lab Chip* (2017). doi:10.1039/C6LC01566B
104. Killian, G. Physiology and endocrinology symposium: Evidence that oviduct secretions influence sperm function: A retrospective view for livestock. *J. Anim. Sci.* **89,** 1315–1322 (2011).
105. Di Santo, M., Tarozzi, N., Nadalini, M. & Borini, A. Human sperm cryopreservation: Update on techniques, effect on DNA integrity, and implications for ART. *Adv. Urol.* **2012,** (2012).
106. Squires, E. L. Semen cryopreservation - challenges and perspectives. *Rev. Bras. Reprod. Anim.* **37,** 136–139 (2013).
107. Hunter, R. H. Oviduct function in pigs, with particular reference to the pathological condition of polyspermy. *Mol. Reprod. Dev.* **29,** 385–91 (1991).
108. Coy, P. *et al.* Oviduct-specific glycoprotein and heparin modulate sperm-zona pellucida interaction during fertilization and contribute to the control of polyspermy. *Proc. Natl. Acad. Sci. U. S. A.* **105,** 15809–15814 (2008).
109. Brezina, P. R. *et al.* Fertility preservation in the age of assisted reproductive technologies. *Obstet. Gynecol. Clin. North Am.* **42,** 39–54 (2015).
110. Schnorr, J. A., Muasher, S. J. & Jones, H. W. Evaluation of the clinical efficacy of embryo cryopreservation. *Mol.Cell Endocrinol.* **169,** 85–89 (2000).
111. El Hajj, N. & Haaf, T. Epigenetic disturbances in in vitro cultured gametes and embryos: Implications for human assisted reproduction. *Fertil. Steril.* **99,** 632–641 (2013).
112. Nelissen, E. C. M. *et al.* Altered gene expression in human placentas after IVF/ICSI. *Hum. Reprod.* **29,** 2821–31 (2014).
113. Arnaud, P. & Feil, R. Epigenetic deregulation of genomic imprinting in human disorders and following assisted reproduction. *Birth Defects Res. Part C - Embryo Today Rev.* **75,** 81–97 (2005).
114. DeBaun, M. R., Niemitz, E. L. & Feinberg, A. P. Association of in vitro fertilization with Beckwith-Wiedemann syndrome and epigenetic alterations of LIT1 and H19. *Am. J. Hum. Genet.* **72,** 156–60 (2003).
115. Thompson, J. G., Kind, K. L., Roberts, C. T., Robertson, S. A. & Al, E. Epigenetic risks related to assisted reproductive technologies: Short-and long-term consequences for the health of children conceived through assisted reproduction. *Hum. Reprod.* **17,** 2783–2786 (2002).
116. Huntriss, J. D. & Picton, H. M. Epigenetic consequences of assisted reproduction and infertility on the human preimplantation embryo. *Hum. Fertil. (Camb).* **11,** 85–94 (2008).
117. Li, T. *et al.* IVF results in de novo DNA methylation and histone methylation at an Igf2-H19 imprinting epigenetic switch. *Mol. Hum. Reprod.* **11,** 631–640 (2005).
118. Santos, F. *et al.* Evaluation of epigenetic marks in human embryos derived from IVF

and ICSI. *Hum. Reprod.* **25,** 2387–2395 (2010).
119. Betsha, S. *et al.* Transcriptome profile of bovine elongated conceptus obtained from SCNT and IVP pregnancies. *Mol. Reprod. Dev.* **80,** 315–333 (2013).
120. Sessions-Bresnahan, D. R., Graham, J. K. & Carnevale, E. M. Validation of a heterologous fertilization assay and comparison of fertilization rates of equine oocytes using invitro fertilization, perivitelline, and intracytoplasmic sperm injections. *Theriogenology* **82,** 274–282 (2014).
121. Alonso, A. *et al.* In vitro equine embryo production using air-dried spermatozoa, with different activation protocols and culture systems. *Andrologia* **47,** 387–394 (2015).
122. Leemans, B. *et al.* Procaine Induces Cytokinesis in Horse Oocytes via a pH-Dependent Mechanism. *Biol. Reprod.* **93,** 23 (2015).
123. Villamil, P. R., Lozano, D., Oviedo, J. M., Ongaratto, F. L. & Bo, G. A. Developmental rates of in vivo and in vitro produced bovine embryos cryopreserved in EG based solutions by slow freezing or solid surface vitrification. *Anim. Reprod.* **9,** 86–92 (2012).
124. Nedambale, T. L. *et al.* Comparison on in vitro fertilized bovine embryos cultured in KSOM or SOF and cryopreserved by slow freezing or vitrification. *Theriogenology* **62,** 437–449 (2004).
125. Sudano, M. J. *et al.* Lipid content and apoptosis of in vitro-produced bovine embryos as determinants of susceptibility to vitrification. *Theriogenology* **75,** 1211–1220 (2011).
126. Fulka, H., Mrazek, M., Tepla, O. & Fulka, J. DNA methylation pattern in human zygotes and developing embryos. *Reproduction* **128,** 703–708 (2004).
127. Messerschmidt, D. M., Knowles, B. B. & Solter, D. DNA methylation dynamics during epigenetic reprogramming in the germline and preimplantation embryos. *Genes Dev.* **28,** 812–828 (2014).
128. Guibert, S. & Weber, M. *Functions of DNA Methylation and Hydroxymethylation in Mammalian Development*. *Current Topics in Developmental Biology* **104,** (Copyright © 2013 Elsevier Inc. All rights reserved., 2013).
129. Menezo, Y. Oxidative Stress (OS) and DNA Methylation Errors in Reproduction . A Place for a Support of the One Carbon Cycle (1-C Cycle) before Conception Women ' s Health & Gynecology Oxidative Stress (OS) and DNA Methylation Errors in Reproduction . A Place f. (2016).
130. Canovas, S. *et al.* DNA methylation and gene expression changes derived from assisted reproductive technologies can be decreased by reproductive fluids. *Elife* **6,** 1–24 (2017).
131. Deshmukh, R. S. *et al.* DNA methylation in porcine preimplantation embryos developed in vivo and produced by in vitro fertilization, parthenogenetic activation and somatic cell nuclear transfer. *Epigenetics* **6,** 177–187 (2011).
132. Huh, D. *et al.* Microfabrication of human organs-on-chips. *Nat. Protoc.* **8,** 2135–57 (2013).
133. Bhattacharjee, N., Urrios, A., Kang, S. & Folch, A. The upcoming 3D-printing revolution in microfluidics. *Lab Chip* **16,** 1720–1742 (2016).

Chapter 2

In vitro produced bovine zygotes exhibit aberrant global methylation dynamics

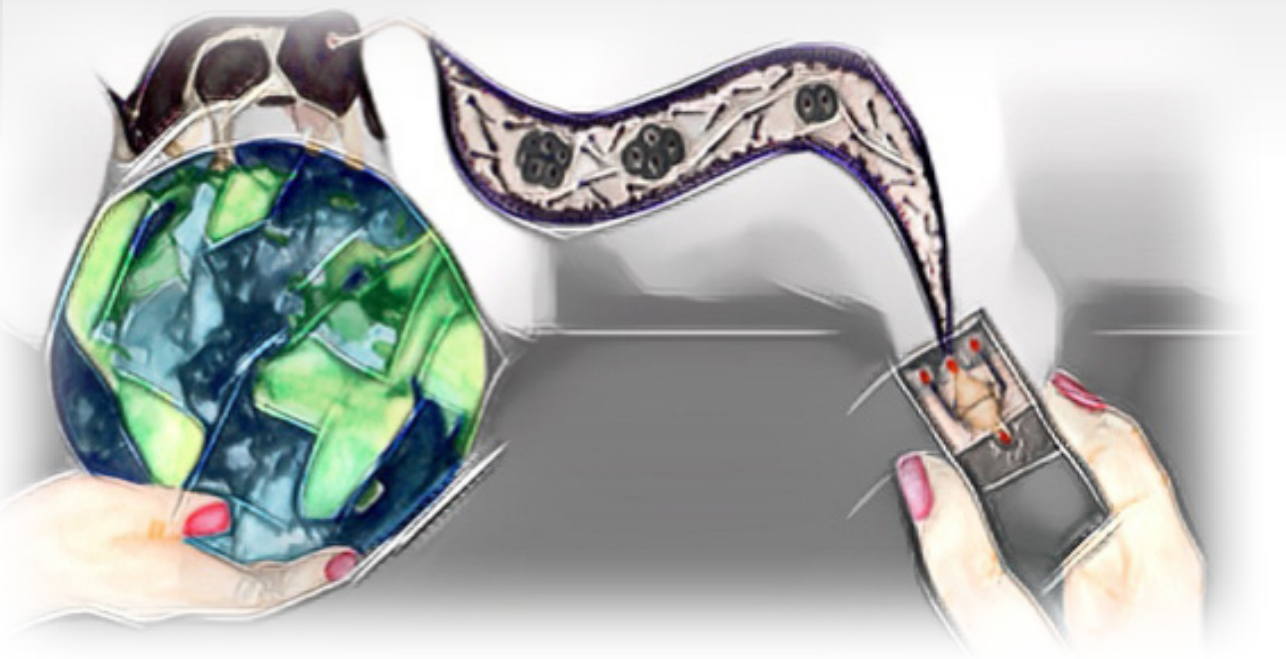

Adapted from:

FERRAZ, M.A.M.M.; HÖLKER, M.; HENNING, H.H.W.; van TOL, H.T.A.; VOS, P.L.A.M., STOUT, T.A.E.; HAVLICEK, H.; BESENFELDER, U.; GADELLA, B.M. *In vitro* produced bovine zygotes exhibit aberrant global (de)methylation dynamics. Submitted.

Abstract

Preimplantation epigenetic reprogramming is sensitive to the environment of the embryo. The possibility that the *in vitro* fertilization (IVF) environment can distort this process is tested by determining whether the global DNA methylation pattern (measured by immunofluorescent labelling of 5-methylcytosine, 5mC) in bovine zygotes produced *in vitro* differed to that of *in vivo* zygotes. In addition, differences in gene expression of enzymes (DNMT1, 3a and 3b; TET1, 2 and 3) involved in the regulation of DNA methylation and, single zygote RNA sequencing (Cell-seq) was performed. Pronuculei of *in vitro* produced zygotes had a higher 5mC immunofluorescent intensity compared to *in vivo* zygotes. In *in vitro* zygotes the cytosine methylating enzyme DNMT1 was the most abundantly transcribed DNMT whereas DNMT3b was most prominent in *in vivo* zygotes. Similarly, while the predominant 5mC translocating enzyme transcribed in *in vitro* zygotes was TET3, TET1 was most abundantly transcribed in *in vivo* zygotes. These results were validated and confirmed by global transcriptomic analysis of the zygotes and predicted differences in gene expression in pathways related to chromatin (de)methylation and (de)acetylation were found. We have demonstrated that *in vitro* oocyte maturation and fertilization alter the dynamics of DNA (de)methylation and the transcription of 5mC regulating genes in bovine zygotes. In particular, *in vitro* produced zygotes exhibit reduced 5mC demethylation, which may compromise both the establishment of pluripotency and early embryonic development. Moreover, if the embryo survives aberrant epigenetic reprogramming could affect the health of the resulting offspring.

Introduction

In mammals, epigenetic silencing has been described to play an important role in ensuring the stability of gene expression during germ-line differentiation, leading to genome-wide silencing of gene expression in sperm cells and oocytes [1]. After fertilization, the early embryo undergoes complete reprogramming of its epigenome in preparation for the reacquisition of epigenetic marks as differentiation proceeds [2]. In this reprogramming period, the mammalian zygote undergoes partially erasure of its epigenetic marks to re-establish the totipotent state, prior to regulated reacquisition of epigenetic marks, indicative of the cell differentiation decisions that are made [2]. The most extensively studied type of epigenetic modification is DNA methylation, in which cytosine (C) nucleotides in the DNA are methylated to 5-methylcytosine (5mC), a process that is associated with silencing of gene transcription [3,4]. The formation of 5mC is executed by DNA methyltransferases (DNMTs), where DNMT1 is a maintenance DNA methyltransferase primarily involved in methylating newly formed DNA strands [1,5], whereas DNMT 3a and b promote *de novo* DNA methylation during gametogenesis and early embryonic development [1,5]. DNA methylation is associated with cell differentiation and occurs in mature sperm and oocytes, as well as in the embryonic stages during which cell differentiation processes are initiated. However, in the recently fertilized oocyte, a rapid and almost complete DNA demethylation takes place which will last until around the

morula to blastocyst transition, when methylation of DNA starts anew [7]. DNA demethylation is achieved by the action of ten-eleven translocation proteins (TETs), which catalyze the iterative oxidation of 5mC to 5hmC (5-hydroxymethylcytosine) and further to 5-formylcytosine (5fC) and 5-carboxycytosine (5aC). The oxidated forms (5fC and 5aC) are subsequently regenerated into cytosine (C) by a deformylation or decarboxylation reaction, respectively. The resulting demethylated C residues in the DNA are permissive to the re-initiation of gene transcription [1,6].

After the DNA demethylation period, correct DNA methylation reprogramming (DMR) must occur during preimplantation embryo development to ensure that new cell lineages develop appropriately. It is essential in this period that proper timing of regulated gene silencing takes place. This ensures the formation of a transcriptionally active, totipotent zygote [4,7,8]. Furthermore, DMR plays an import role in X-chromosome inactivation, parent-of-origin specific regulation of the expression of imprinted genes, and in the control of (retro)transposon activity [1]. During early embryogenesis, the gamete-specific methylation (5mC) pattern is erased by active demethylation of the paternal pronucleus (PN), followed by a slower demethylation of the female PN [9–11]. The female PN, formed after the second meiotic division has been triggered by fertilization, remains in close proximity to the second polar body that is extruded at completion of the second meiotic division. Later, this female PN migrates towards the more centrally located male PN [4]. Subsequently, the two pronuclei are drawn together by microtubular activity, and fuse to form a diploid cell (syngamy). Syngamy is followed shortly by the first (mitotic) cleavage division, from which a two cell embryo is formed [4]. Previous studies have demonstrated that in the mouse, rat and man the paternal PN undergoes DNA demethylation immediately after sperm DNA decondensation, whereas only partial male PN demethylation is observed in the goat and the cow, and paternal DNA methylation appears to be maintained during syngamy in the pig, rabbit, horse and sheep [3,7,12].

The period of epigenetic reprogramming in fertilized oocytes is considered to be extremely sensitive to changes in environmental conditions that have an impact on the female genital tract; compromised maternal health, unhealthy diets, medication etc. are all reported to influence DMR in embryos [13]. More relevant for the current study, are the effects on DMR imposed by *in vitro* oocyte maturation (IVM), IVF and *in vitro* embryo production (IVP). During *IVP*, gametes are washed, incubated in culture media and exposed to light, temperature and oxidative stress [2,14]. Previous studies have indicated that the dynamics of DNA methylation during early embryo development are altered by *IVM* and embryo culture in various species, including the mouse, pig and man [3,9,15–20]. Likewise, it has been shown that *in vivo* derived porcine zygotes have lower global methylation levels than zygotes produced by IVF, by parthenogenetic activation (PA) or by somatic cell nuclear transfer (SCNT) [5]. Nevertheless, to our knowledge there are no reports on whether IVF alters the de- and re-methylation dynamics of *in vitro* produced bovine zygotes compared to *in vivo* zygotes. To date, the preimplantation dynamics of 5mC (global methylation) in bovine embryos have been monitored in IVF embryos only, and there are no reports of 5mC patterns differ to those in *in vivo*

derived zygotes and early embryos [7,9,21–23]. The preferential use of IVF embryos to study developmental processes in cows can be explained by the difficulty and expense of collecting zygotes *in vivo.* By contrast, it is easy to source ovaries from slaughtered cows for *in vitro* embryo production, and the oocytes can be used efficiently for producing bovine embryos in research laboratories.

The main objectives of the present study were to compare global levels of DNA methylation in bovine zygotes produced *in vitro* and *in vivo*, and to investigate whether any variations in cytosine nucleotide methylation were associated with differential transcription of specific genes (DNMT1, DNMT3a, DNMT3b, TET1, TET2 and TET3) which code for enzymes involved in regulating the methylation and demethylation of cytosine nucleotides. The differences found were compared and validated with a global transcriptome analysis of individual *in vivo* versus *in vitro* zygotes.

Materials and Methods

Chemicals

Unless stated otherwise, all chemicals used were obtained from Sigma Chemical Co. (St. Louis, MO) and were of the highest available purity.

Oocyte collection and in vitro oocyte maturation (IVM)

Bovine ovaries were collected from a local abattoir and transported to the laboratory within 2 hours. The ovaries were washed in physiological saline (0.9 % w/v NaCl) and held in physiological saline containing 100 U/mL penicillin and 100 µg/mL streptomycin at a temperature of 30°C. Follicular fluid and cumulus oocyte complexes (COCs) were aspirated from follicles with a diameter ranging from 2 to 8 mm and collected into 50ml conical tubes using a 19-gauge needle and a vacuum pump [24]. COCs with a minimum of three layers of intact cumulus cells were selected and washed first in HEPES-buffered M199 (Gibco BRL, Paisley, U.K.), before being washed and cultured in maturation medium (M199 supplemented with 0.02 IU/mL follicle-stimulating hormone [Sioux Biochemical Inc., Sioux Center, IA]), 10% FCS, fatty acid-free bovine serum albumin (BSA) and 100 U/mL penicillin and 100 µg/mL streptomycin) in four-well culture plates (Nunc A/S, Roskilde, Denmark). The oocytes were matured in groups of 50 COCs in 500 µl maturation medium and incubated in a humidified atmosphere of 5% CO_2-in-air for 24 hours at 38.5°C.

Sperm preparation and in vitro fertilization (IVF)

Frozen semen was thawed and processed as described before [24]. After the final washing step,

the remaining sperm pellet was resuspended in fertilization medium (modified Tyrode's medium supplemented with 25mM sodium bicarbonate, 22 mM lactate, 1 mM pyruvate, 6 mg/mL fatty acid–free BSA) containing 100 U/mL penicillin and 100 µg/mL streptomycin. Following maturation, COCs were distributed into groups of 35-50 in four-well culture plates (Nunc A/S, Roskilde, Denmark) in 500 µL of fertilization medium which was supplemented with sperm activation factors (10 µg/ml heparin, 20 µM d-penicillamine, 10 µM hypotaurine, and 1 µM epinephrine). Sperm were then added at a final concentration of $1x10^6$ sperm cells/mL. After 14-24 h of co-incubation under a humidified atmosphere of 5% CO_2-in-air at 38.5°C, cumulus cells were removed by pipetting and the presumptive zygotes (*in vitro* zygotes) were either fixed (at time points: 16, 18, 20, 22 and 24 hpi) in 4% paraformaldehyde for 30 min at room temperature; or snap frozen (at 20-22 hpi) for subsequent RNA extraction.

Animal preparation for embryo collection

All experimental animals were handled according to the animal protection law of Germany. Care and use for all experimental animals within this study was done following the guidelines of the Society for the Study of Reproduction and was approved by the Ethical Commission on Animal Experiments of the University of Bonn. Eight Simmental heifers aged between 15 and 20 months and weighing between 380 and 500 kg were used in this study. All animals were kept under identical farm conditions within the same herd. Pre-synchronization of animals was performed by i.m. administration of 500 µg of cloprostenol (PGF2α, Estrumate ®; Essex Tierarznei, Munich, Germany) twice within 11 days. Two days after each of the PGF2α treatments animals received 20 µg of GnRH (Receptal ®; Intervet, Boxmeer, the Netherlands). Twelve days after the last GnRH injection, heifers received the first of eight consecutive FSH-injections over 4 days in decreasing doses (in total 400 mg of FSH equivalent according to body weight; Stimufol ®, University of Liege, Belgium). Two PGF2α treatments were performed 60 and 72 h after the initial FSH injection. The first of a total of three artificial inseminations within a 12-h interval was conducted 48h after the first PGF2α application. Finally, 60 h after the first PGF2α application, at the time of the second insemination, ovulation was induced by a single administration of 10 mg GnRH.

Collection of embryos at the zygote stage

Embryos at the zygote stage were collected 19-23.5 h after expected ovulation. Flushing was accomplished as described previously[25]. Briefly, after restraining the recipients, administering 5 ml of a 2% lidocaine solution (Xylanest ®, Richter Pharma, Wels, Austria) for epidural anesthesia and disinfecting the vulva (Octenisept, Schülke/Mayer, Vienna, Austria), a trocar set consisting of a universal metal tube (12.5 mm x 52 cm, Storz, Vienna, Austria) and an

atraumatic mandrin was placed caudodorsal to the vaginal fornix. The mandrin was replaced by a sharp trocar, and the trocar set was inserted through the vaginal wall into the peritoneal cavity. The trocar was replaced by a shaft bearing the endoscope (5.5 mm forward Hopkins endoscope; Storz) and the transfer system. The site was illuminated by a fiberoptic cold light (250W, Storz) and visualized with a camera (Telecam PAL-Endovision, Storz) connected to a monitor. The flushing system consisted of a 20-ml syringe connected to a perfusor tube (No. 08272514; Braun, Melsungen, Germany) and a metal tube (14 cm × 2.5 mm) with numerous lateral holes covered by a silicon tube. Thus, after the metal tube was inserted via the infundibulum into the ampulla, careful management of the flushing pressure allowed the balanced adjustment of tubal sealing to avoid medium reflux. Oviducts were flushed with 50 ml flushing medium (phosphate-buffered saline supplemented with 1% fetal calf serum). Flushing medium (50 ml) was forced through the uterotubal junction into the uterine horn and from there collected via a uterus flushing catheter (CH15, Wörrlein, Ansbach, Germany) into an embryo filter (Emcon filter, No. 04135; Immuno Systems Inc., Spring Valley, WI, USA).

RNA extraction and cDNA synthesis

Total RNA was isolated from single zygotes using the RNEasy Micro RNA extraction kit (Qiagen GmbH, Hilden, Germany), and treated with RNAse-free DNAse I (Qiagen GmbH, Hilden, Germany) to remove genomic DNA, following the manufacturer's instructions. cDNA synthesis was performed using Superscript III Reverse Transcriptase with random hexamer priming (Thermo Fishes Scientific, Langenselbold, Germany), according to the manufacturer's instructions.

Quantitative real-time RT-PCR

Real-time RT-PCR was performed using a CFX Connect™ Real-Time PCR detection system (Bio-Rad Laboratories B.V., Veenendal, Netherlands). The PCR reaction was performed in a final volume of 20 µL, consisting of 17.6 µL of SybrGreen mix (Bio-Rad Laboratories B.V., Veenendal, Netherlands), 0.2 µL of each forward and reverse primer, and 2 µL of cDNA template. The program started with 10 min at 95 °C followed by 40 cycles each of 10 s at 95 °C and 60 s at 60 °C. Melting curves were plotted after each cycle series. A standard curve of cDNA, with a 3-fold dilution series was obtained by plotting the log of the starting amount against the cycle threshold value of the dilution series. GAPDH was used as a reference gene for normalization of expression levels [24]. A total of 12 zygotes per group (*in vitro* and *in vivo*) were individually evaluated. The primers for TET1, TET2, TET3, DNMT1, DNMT3a and DNMT3b are listed in Table I.

Table I. Primer sequences.

Gene		Primer sequence (5' - 3')	Accession number
DNMT1	*F*	TATCGGCTGTTCGGCAACAT	NM_182651.2
	R	GGCACCCTCCTCCTTGATTT	
DNMT3a	*F*	CGATGAACCGGAGTACGAGG	NM_001206502.1
	R	CCACTGAGAACTTGCCGTCT	
DNMT3b	*F*	GGACATCTCTCGGTTTTTGGAG	NM_181813.2
	R	AGTGCACAGGAAAGCCGAAG	
TET1	*F*	AGCAGCGATGATGACAGAGG	XM_015469834
	R	CGGGGTTGGTGAGTAGCTTT	
TET2	*F*	ACTTGCCTTTGCTCCTGGTT	XM_015465318,1
	R	TGAATGAATTCAGCAGCTCTGTC	
TET3	*F*	AACTCATGGAGGAGCGGTACG	XM_015465318,1
	R	GCAGCTTCTCTTCTAGCGTGT	
GAPDH	*F*	AGGCATCACCATCTTCCAG	AJ000039
	R	GGCGTGGACAGTGGTCATAA	

F, forward primer; R, reverse primer.

Cel-seq II primer design

The reverse transcription primer was designed with an anchored polyT, a 6 bp unique barcode, a 6 bp UMI (unique molecular identifier), the 5' Illumina adapter and a T7 promoter. The barcodes were designed such that each pair is different by at least two nucleotides, so that a single sequencing error will not produce the wrong barcode (adapted from [26]).

Linear mRNA amplification

Single zygote extracted RNA was precipitated with isopropanol and the pellet was used for the reverse-transcription (RT) reaction. RT was performed with 5 ng of primer per reaction. A total of 0.2 µL of the primer mixed with 1 µL of water or 1 µL of a 1:1,000,000 dilution of the ERCC spike-in kit (a total of 1.2 µL) was added directly to the Eppendorf tube where the RNA was precipitated, and incubated at 65^{o}C for 5 min (with the lid of the thermal cycler heated to 65^{o}C). The sample was spun to the bottom of the tube mid incubation. After the second-strand synthesis, samples were pooled and cleaned on a single column before proceeding to the *in vitro* transcription (Ambion AM1334, Invitrogen) reaction for 13 hr. Solution was treated with EXO-SAP to remove primers and RNA was fragmented (one-fifth volume

of 200 mM Tris-acetate [pH 8.1], 500 mM KOAc, 150 mM MgOAc added) for 3 min at 94 C, and the reaction was stopped by placing on ice and the addition of one-tenth volume of 0.5 M EDTA, followed by RNA cleanup. The RNA quality and yield were analyzed using a Bioanalyzer (Agilent).

Library construction and Cel-seq II

RT reaction was performed using SuperScript II, following manufacturers protocol (Invitrogen, CA, USA). A total of 14 cycles of PCR was performed using Phusion® High-Fidelity PCR Master Mix with HF Buffer (NEB, MA, USA) and an elongation time of 30 s. PCR products were cleaned two times with an AMPure XP beads (Beckman Coulter, Woerden, the Netherlands). Libraries were sequenced on the Illumina Nextseq500 platform, a high output paired end run of 2x 75bp was performed.

Cel-seq II data analysis

Genes differentially expressed were identified using Deseq2 (v1.10.1) package[27]. Genes with low counts (whose sum of all counts across samples included in the analysis was < 10) were removed. The p-value was determined by Wald statistics. An adjusted p-value to correct for multiple testing was calculated using the Benjamini-Hochberg method. Differential expressed genes (DEGs) were filtered by fold change (lfcThreshold=1) and false discovery rate (FDR) less than 1% (alpha = 0.1).

Functional GO Clustering

The Cytoscape 3.5.1 plugin ClueGO[28] was used to functionally group the up- and down-regulated genes by GO terms “biological processes” from *Bos taurus* genome. The evidence was set to “Inferred by Curator (IC),” and the statistical test was set to a right-sided hypergeometrical test with a Bonferroni (step down) and a κ score of 0.7-0.9. The GO term restriction levels were set to 3–8, with a minimum of three genes or 5% genes in each GO term and the function “GO Term fusion” was selected.

Immunofluorescent staining for global methylation

Immunofluorescent staining for 5-methylcyotsine (5mC) was performed on pronucleus stage zygotes as previously described [21]. Briefly, zygotes were fixed in 4% paraformaldehyde for 30 min. Fixed zygotes were permeabilized by incubation for 30 min in 1% Triton-X100 in

PBS, followed by denaturation with 3M HCl for 30 min, which was then neutralized using 100 mM Tris-HCl buffer (pH 8.5) for 15 min. Non-specific binding was blocked by incubating the permeabilized zygotes for 1 hour in PBS containing 5 % normal goat serum (NGS). The zygotes were then incubated overnight at 4°C with a mouse anti-5mC primary antibody (1:100 dilution with PBS + 5% NGS + 0.1% Triton-X100; Eurogentec, BI-MECY-0100). Next, the zygotes were washed three times in PBS-polyvinylpirrolydone (PVP, 3mg/mL; 10 min each) and incubated with an Alexa 488 conjugated goat anti-mouse antibody (1:100, Santa Cruz Biotechnology, Santa Cruz, CA) for 1 hour. Zygotes were then incubated with propidium iodide (PI; 25 µg/mL) for 30 min to counterstain the DNA. Negative controls were produced by omitting incubation with the primary antibody. Analysis was performed by laser scanning confocal microscopy using a TCS SPE-II system (Leica Microsystems GmbH, Wetzlar, Germany) attached to an inverted semi-automated DMI4000 microscope (Leica) with a 40 x magnification objective (with NA 1.25). Z-stacks of 1 µm of both pronuclei were obtained. Images were analyzed by evaluating the fluorescence intensity for 5mC and DNA in each pronucleus using ImageJ software (National Institutes of Health, Bethesda, MD, USA). After maximum projection reconstruction of Z-stacks, the fluorescence intensity of each channel was measured by manually outlining each pronucleus, and adjusted for cytoplasmic background. The average intensity of fluorescence for 5mC and PI was then adjusted by multiplying by the PN area, and 5mC intensity was divided by PI fluorescence to normalize 5mC fluorescence. Zygotes were classified into 3 distinct stages: (i) prior to syngamy (corresponding to PN stages 2-5; 1C-PN), (ii) during syngamy (1C-Sy), and (iii) immediately after syngamy but before the first cleavage division (pre-2C).

Data analysis

The data were analyzed using IBM SPSS Statistics (version 24). A Shapiro-Wilk test was performed and, all data were found to be normally distributed. Mean and standard deviation are depicted in graphs. Differences between groups were examined using independent t-tests ($p<0.05$).

Results

In vivo embryos were collected between 31 and 35.5 h after induction of ovulation with exogenous GnRH. Since not all ovulations would be exactly synchronous while fertilization and early stages of embryonic/zygote development may also proceed at subtly different speeds, we chose to divide the collected zygotes into 3 distinct stages: (i) prior to syngamy (corresponding to PN stages 2-5; 1C-PN), (ii) during syngamy (1C-Sy), and (iii) immediately after syngamy but before the first cleavage division (pre-2C). In all experiments, we compared *in*

vitro (n = 262) produced with *in vivo (n = 48)* recovered 1 cell (1C) embryos. The distribution of *in vitro* and *in vivo* zygotes among the different developmental stages (1C-PN, 1C-Sy and pre-2C), is depicted in figure 1. Considerable variation in the developmental stage at any given time point was observed, which demonstrates that fertilization and the progress of pronucleus formation was indeed not synchronous for all oocytes either *in vitro* or *in vivo*. In all cases, only a small proportion of zygotes were in the process of syngamy (1C-Sy) at any given time point of development, suggesting that the actual process of syngamy is rapid, both *in vitro* and *in vivo*.

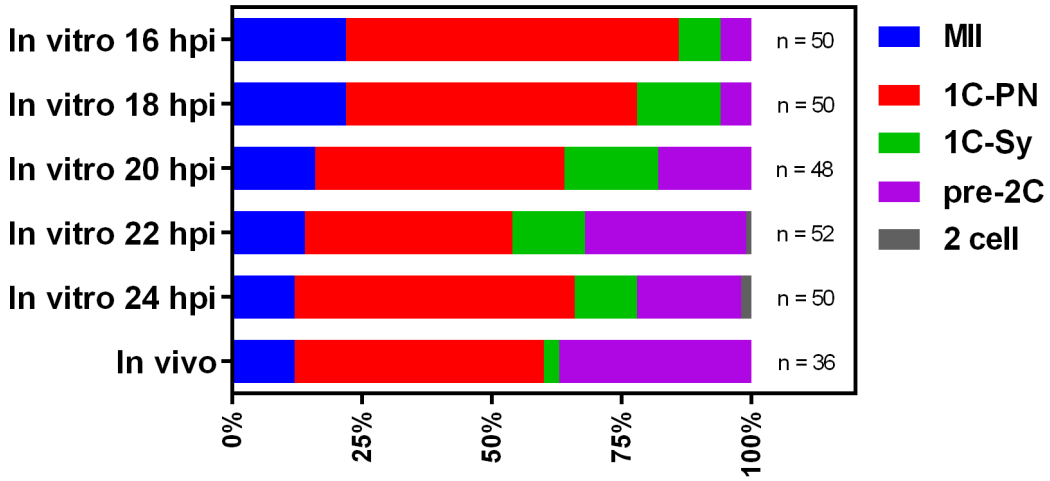

Figure 1. Distribution of *in vitro* and *in vivo* bovine zygotes over different developmental stages at each collection time point for *in vitro* zygotes, and 43-47.5 hpi for *in vivo* zygotes (19-23.5 h post presumed ovulation). Collection time points were measured as hours post introduction of sperm into the incubation medium, i.e. fertilization (hpi) *in vitro*, and 50 hours post ovulation inductin *in vivo*. The total number of presumptive zygotes is indicated on the right. MII: metaphase II oocytes; 1C-PN: before syngamy (PN stages 2-5); 1C-Sy: during syngamy (fused PN), pre-2C: after syngamy but before first cleavage; and 2 cell: 2 cell stage.

Global DNA methylation is increased in in vitro zygotes

We analyzed the global methylation patterns of 250 *in vitro* zygotes and 36 *in vivo* zygotes using fluorescent 5mC staining intensity normalized to the intensity of a general DNA stain (propidium iodide: PI); zygotes were then analyzed depending on their developmental stage (1C-PN, 1C-Sy and pre-2C; figure 2). We found that *in vitro* 1C-PN zygotes had 3.2-times as much global methylation as *in vivo* 1C-PN. In both *in vitro* and *in vivo* zygotes the levels of 5mC decreased during the 1C-Sy and pre-2C stages, albeit that *in vitro* zygotes showed a much reduced degree of demethylation. Indeed, 5mC staining in 1C-Sy and pre-2C *in vitro* zygotes was 11.5- and 4.9-fold higher than in their *in vivo* equivalents, respectively. This indicated that demethylation was barely or not detectable in *in vitro* zygotes.

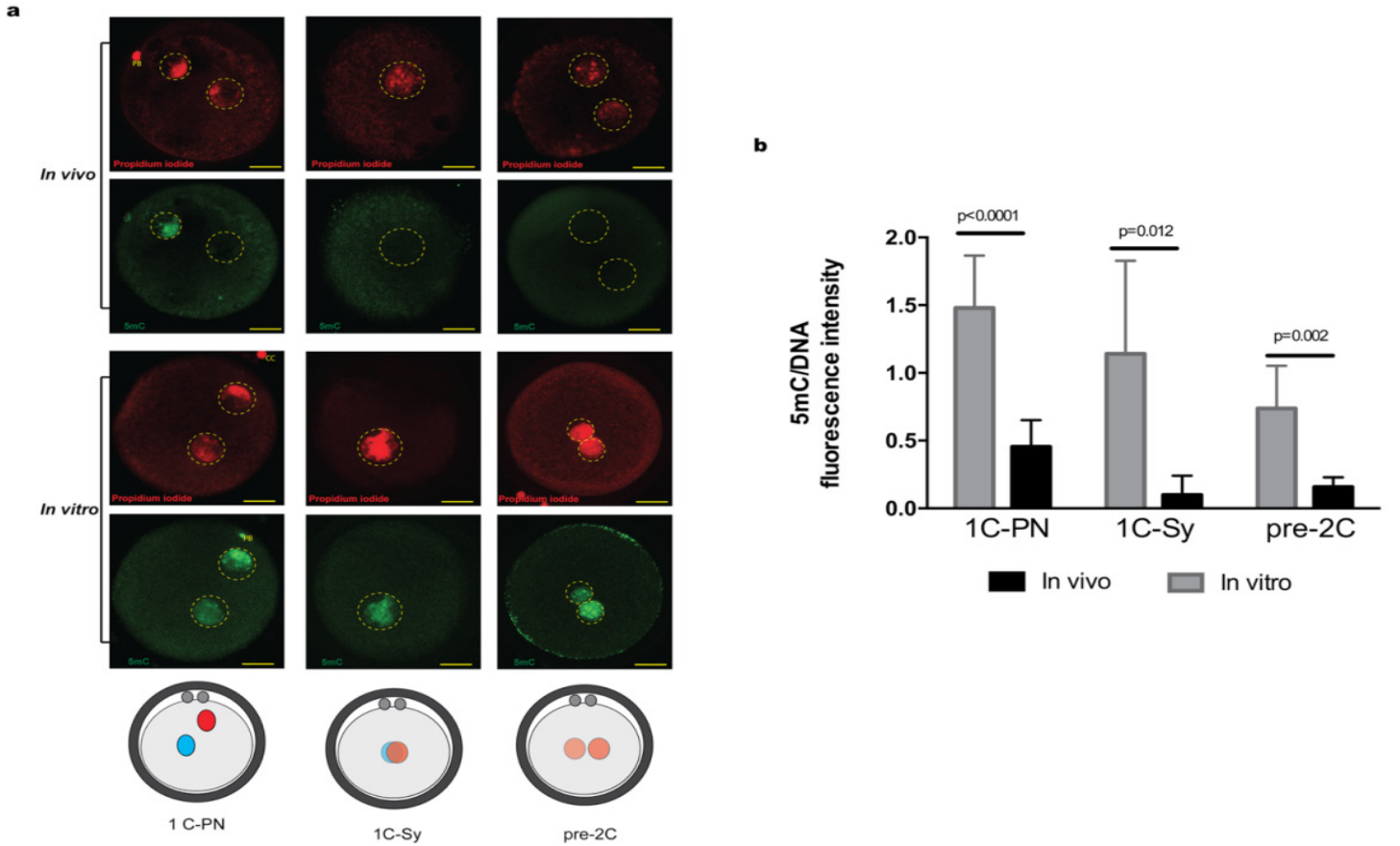

Figure 2. 5-Methylcytosine (5mC) and DNA (propidium iodide) staining patterns in *in vivo* and *in vitro* derived zygotes. Zygotes were divided into three groups, depending on their developmental stage: before syngamy (1C-PN), during syngamy (1C-Sy), and after syngamy but before first cleavage (pre-2C). (A) 5mC (green) was clearly present in both PN of all three developmental stages *in vitro*. *In vivo*, 5mC was most prominent at the 1C-PN stage and in only one parental PN. (B) Quantification of 5mC staining adjusted to DNA staining in *in vivo* and *in vitro* zygotes. No significant differences were observed in the 5mC:DNA fluorescence ratio of the three stages for *in vitro* zygotes. By contrast, for *in vivo* zygotes 1C-PN zygote had higher fluorescence intensity than 1C-Sy and pre-2C (p-values of 0.0445 and 0.036, respectively). PB: Polar Body, CC: cumulus cell Scale bar = 25 µm.

Relative mRNA levels coding for enzymes involved in (de)methylation differs in in vitro compared to in vivo bovine zygotes

We investigated the amount of mRNA for three DNA methyltransferases (DNMT1, DNMT3a and DNMT3b), involved in different aspects of DNA methylation. Levels of mRNA coding for DNMT1 was the most abundant in *in vitro* zygotes, whereas DNMT3b was the most abundant in *in vivo* zygotes. Expression of DNMT1 and DNMT3b differed significantly between *in vivo* and *in vitro* zygotes (Figure 3).

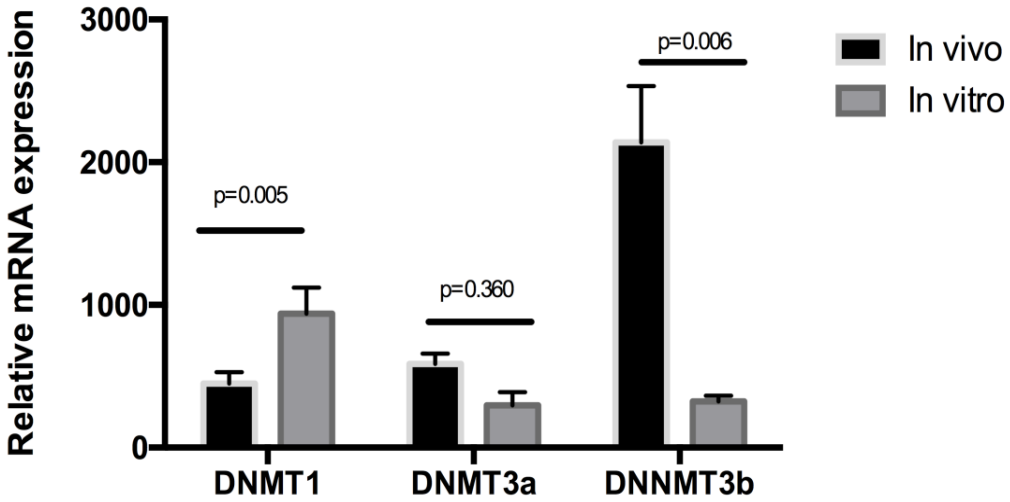

Figure 3. Relative expression of mRNA for DNMTs in *in vitro* and *in vivo* individual bovine zygotes (n=12 zygotes for each group). GAPDH was used as the reference gene for normalizing mRNA expression.

Since TET enzymes play an integral role in DNA demethylation, we also compared mRNA expression for the 3 TETs described to be active in gametes and embryos (TET1, TET2 and TET3) between *in vitro* and *in vivo* zygotes (figure 4). Levels of mRNA coding for TET1 were by far most abundant in *in vivo* zygotes (317 times higher levels). Levels of mRNA for TET2 tended (p=0.095) to be higher in *in vivo* than *in vitro* zygotes. By contrast, mRNA levels for TET3 were higher in *in vitro* than *in vivo* zygotes. In general, therefore, *in vivo* zygotes expressed higher levels of mRNA that could be translated into TET enzymes involved in the 5mC demethylation machinery.

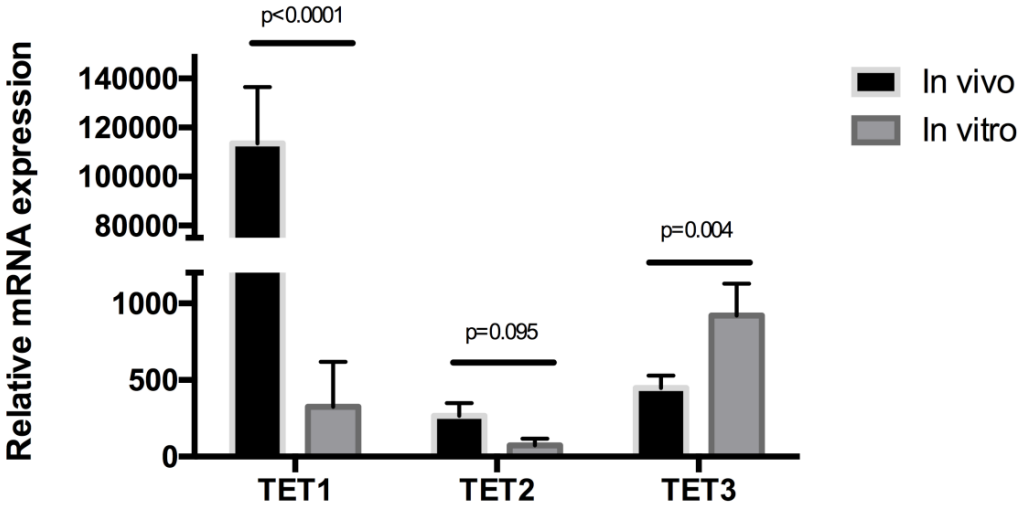

Figure 4. Relative expression of mRNA for TETs in *in vitro* and *in vivo* individual bovine zygotes (n=12 zygotes for each group). mRNA expression was normalized using GAPDH as the reference gene.

Single zygote Cel-seq II demonstrated changes on pathways related to (de)methylation and (de)acethylation *in in vitro compared to in vivo zygotes*

Here we used Cel-seq II to investigate the transcriptome of individual bovine zygotes produced under different conditions: *in vivo and in vitro* (n = 10 zygotes for each group). A total of 18,258 transcripts were detected; from which, 14,042 genes were common to *in vivo* and *in vitro* zygotes. Important GO pathways related to (de)methylation and (de)acetylation were up- or down-regulate *in vitro* when compared to *in vivo* zygotes (Figure 5). Most importantly, the up-regulation of TET1 and DNMT3b, and down regulation of TET3 and DNMT1 in *in vivo* zygotes (Table II) confirmed our RT-PCR results. In line with the RT-PCR results, TET2 and DNMT3a were also detected by Cell-Seq, but no significant differences between *in vivo* and *in vitro* zygotes were observed. On top of this other up- and down-regulation of genes related to methylation and histone modifications were observed (Figure 5 and Table II). The differential *in vivo* expression of all these genes together -when compared to in vitro zygotes- culminated into the noted vastly higher DNA methylation in *in vivo* zygotes. In contrast the *in vitro* zygotes had higher expression of genes related to DNA methylation, histone modification and meiosis (Figure 5).

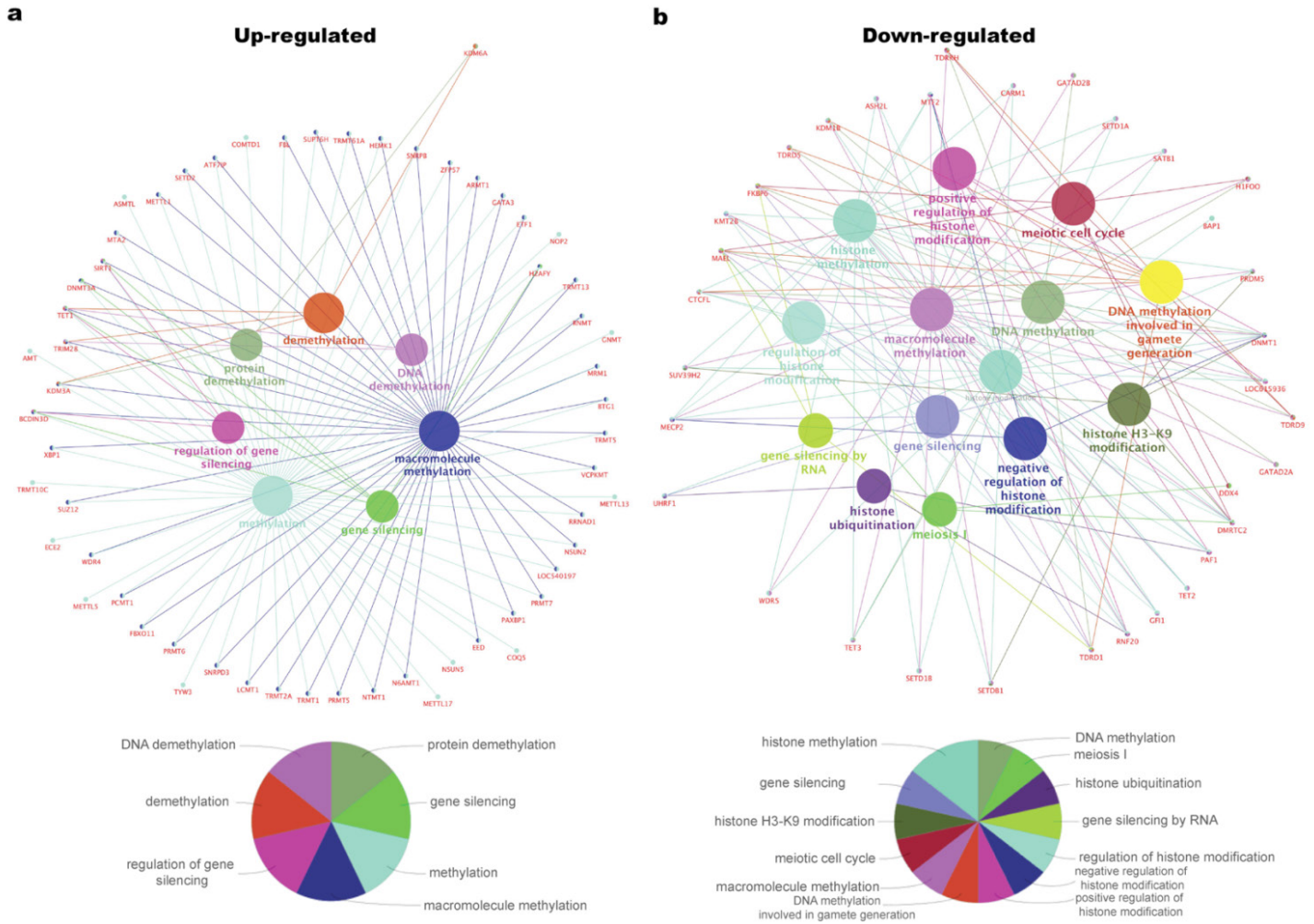

Figure 5. Functional grouped gene ontology (GO) terms for genes up- and down-regulated in *in vivo* vs *in vitro* zygotes. The CytoScape plugin ClueGO was used to group the genes into functional GO terms of "biological processes" using genes related to (de)methylation and (de)acethylation. In (a) up-regulated GO pathways; in (b) down-regulated GO pathways.

Table II. Highly up- (red) and down- (green) regulated genes related to (de)methylation and (de)acetylation processes between *in vitro* and *in vivo* zygotes.

Gene	Fold Change	P-value
TET1	222.89	1.60E-48
IDH1	21.11	1.55E-102
HDAC6	12.91	3.66E-14
HDAC8	11.63	5.98E-28
DNMT3b	11.16	2.31E-20
TDG	10.27	2.94E-12
HDAC5	9.78	3.41E-11
IDH2	9.45	5.97E-10
HDAC7	0.31	5.81E-06
MBD4	0.15	1.10E-16
DNMT1	0.12	1.24E-26
TET3	0.11	5.54E-07
HDAC9	0.06	0.0085
AMPD3	0.04	1.55E-10
HDAC11	0.02	1.73E-08

Discussion

In this study we compared global methylation and expression of genes involved in (de) methylation in *in vitro* and *in vivo* produced bovine zygotes. Since collecting *in vivo* zygotes from the oviduct is an invasive and difficult procedure, most previous epigenetic studies on early bovine embryos have been performed using *in vitro* produced zygotes. Using an endoscopic transvaginal approach it is, however, possible to collect ovulated oocytes and/or very early embryos directly from the oviduct relatively non-traumatically [25]. In the current study, we used transvaginal endoscope-guided oviduct flushing to collect bovine zygotes approximately 43-47.5 hpi (which equals 19-23.5 h post presumed ovulation). For *in vitro* zygote production, a routine IVP protocol was used with zygotes collected at different time points (ranging between 16 to 24 hpi) to ensure collection of different 1C developmental stages. We divided the zygotes into three morphologically distinct stages for fluorescent staining; prior to syngamy (corresponding to PN stages 2-5; 1C-PN), during syngamy (1C-Sy), and after syngamy but before the first cleavage division (pre-2C). Considerable asynchrony in PN development was observed both *in vivo* and *in vitro*. This asynchrony is not surprising given that oocyte penetration by a spermatozoon, oocyte activation and initiation of pronucleus formation would also be imperfectly synchronized during fertilization of multiple oocytes both *in vivo* and *in vitro*. Indeed, similar asynchrony was observed in equine embryos produced by intracytoplasmic sperm injection (ICSI) [3], even though time of sperm introduction would be known precisely.

To examine the overall extent of DNA (de)methylation and the progress of the anticipated demethylation, we used immunofluorescent 5mC staining of individual zygotes. Immunofluorescent labelling provides an indirect index of DNA methylation status that depends on the specificity and affinity of the antibodies used. 5mC immunostaining has been widely used to detect global methylation in embryos from various species, including the mouse, rabbit, cow, sheep, horse, pig and man [3,10,15,21,29–33]. We demonstrated that *in vitro* oocyte maturation and fertilization alters the dynamics of DNA methylation of bovine zygotes. The resulting more intense 5mC staining of *in vitro* compared to *in vivo* zygotes has also been observed in the pig, where the effect was most marked after conventional IVF and slightly less pronounced after parthenogenic activation or somatic cell nuclear transfer [5]. We also noted differences in 5mC abundance between the PNs of *in vivo* 1C-PN, with one PN being highly methylated while the other PN had 50-70% less 5mC. This difference between the PNs was less pronounced at the pre-2C stage, accompanied by a general reduction in methylation of both PNs such that 5mC abundance was both very low and not different between the PNs right after the time of fusion. The dynamics of global methylation were very different in *in vitro* produced zygotes, where the difference in 5mC staining intensity between the partner PNs was less marked, ranging from 3 to 52%, and independent of the developmental stage of the zygote. Notably, all 3 stages showed abundant 5mC staining.

Genome-wide reprogramming of DNA methylation (5mC) is accepted as an essential epigenomic process during early embryo development. In mammalian zygotes, the demethylation of the paternal PN is thought to be a more rapid process that must precede DNA replication, whereas demethylation of the maternal PN is more gradual. Thus, the maternal PN exhibits more constant 5mC levels [7,22]. However, the asymmetry in the loss of 5mC between the maternal and paternal PN differs between species, and can be divided into three types: Type 1 is characterized by an active DNA demethylation of the male PN (rodents, lagomorphs); type 2 is characterized by a maintenance of the paternal 5mC level (pig and sheep); and type 3 is characterized by a paternal PN 5mC demethylation followed by *de novo* methylation in a short period of time (cow, man and goat) [7,11]. Note that type 1 is reported for *in vivo* produced and flushed zygotes (rabbit, rat and mouse) and types 2 and 3 were reported for zygotes obtained *in vivo* from sheep while for other mammalian species only zygotes after IVF were studied [7,11,12]. In analogy, it is therefore likely that a similar reduced demethylation of 5mC in the male pronucleus is taken place during IVF in these other mammals including in human zygotes when compared to *in vivo* developing zygotes. However, data on DNA methylation measurements of *in vivo* flushed zygotes are lacking for many mammalian species and studying *in vivo* zygotes from women is difficult by ethically restrains. Nevertheless, in bovine material we observed type 1 pronucleus reprogramming (active DNA demethylation of one PN) in *in vivo* zygotes, and a reduced DNA demethylation pattern (type 3) in *in vitro* produced zygotes.

In an attempt to understand why these differences in global methylation pattern existed between zygotes produced in different environments, we performed Cell-seq II and quantitative

reverse transcription PCR (qRT-PCR) for genes implicated in DNA (de)methylation on single zygotes produced *in vivo* and *in vitro*. Improvements on low throughput RNA-sequence techniques allowed the analysis of the transcriptome of embryos at single-cell resolution [26,34]. The transcriptome is important to determine cell behavior and identity, and is regulated by genetic and epigenetic mechanisms[34]. Note that, due to the much darker cytoplasm in the bovine zygote when compared to the mouse zygote, it was not possible to differentiate between developmental stages without staining the bovine zygote. Consequently, we selected zygotes for gene expression studies by the presence of two extruded polar bodies, and did not consider different PN stages. With regard to the expression of methylation factors, *DNMT1* was significantly highly expressed in *in vitro* zygotes whereas *DNMT3b* was significantly more abundant in *in vivo* zygotes and *DNMT3a* did not differ. These results suggest that, even at these early stages, *in vivo* zygotes are preparing for *de novo* methylation, the primary function of DNMT3a and b, whereas *in vitro* zygotes are more primed for maintenance of their existing methylation, the primary function of DNMT1. RT-PCR revealed the same directional trends in gene expression as Cell-Seq, with lower magnitude of fold change after analysis by Cell-Seq, similarly to the *ratio compression phenomena* described by others for microarrays data [35,36].

The most obvious potential explanation for the reduced global methylation in *in vivo* compared to *in vitro* embryos, and to the asymmetry of partner PN 5mC staining in 1C-PN *in vivo* zygotes is the difference in TET activity: When comparing *in vitro* and *in vivo* zygotes *TET1* and *TET2* were highly expressed in *in vivo* zygotes whereas *TET3* expression was higher in *in vitro* than *in vivo* zygotes. In general, *TET* expression levels in *in vitro* zygotes were lower, which may explain the inhibited/delayed demethylation of 5mC. The *in vitro* results agree with previous reports of the expression of these genes in mouse and bovine zygotes and 2-cell embryos [10,21,22]. Moreover, the results suggest that the dynamics of global DNA methylation in *in vivo* bovine zygotes is similar to that in rodents, but must involve different mechanisms, since TET1 seems to be the most abundant TET in bovine, whereas, TET3 is the most abundant in mouse. Most strikingly, the *in vitro* environment clearly modifies both TET expression and the dynamics of demethylation.

In addition to DNA methylation, changes of nucleosomal histones, such as acetylation, methylation, phosphorylation and ubiquitination, also play critical roles in regulation of gene expression and are involved in the processes of epigenetic reprogramming [37]. Interestingly, *in vitro* zygotes had higher expression of genes that are responsible for such histone modifications. Modifications in specific histone variants, such as H3.3 have been described to impair embryo development [38]. From these results it becomes apparent that histone modifications are altered during IVM and/or IVF. Future studies should focus on the relation of such histone modifications and reduced IVP and pregnancy rates of *in vitro* produced embryos. Note that mRNA data are only partially informative and proteins expression levels as well as enzyme activities and substrate product levels should be determined to better understand the mechanisms of DNA methylation and histone modifications in bovine zygotes. Never-

theless, the amount of embryos required to perform a reliable protein analysis, such as in Western blotting or in reliable enzyme assays, makes it difficult to use *in vivo* embryos, while mRNA can be extracted from single zygotes.

Our results indicate that the oviduct environment provides an optimized environment to support proper epigenetic reprogramming during fertilization and early embryo development *in vivo*. The *in vitro* production of bovine embryos falls short in providing this optimal environment and results in delayed DNA demethylation and into enhanced expression of transcripts encoding for DNA and histone modification enzymes. Note also that *in vivo* zygotes maternal (oocyte) transcripts are of upmost importance and that embryonic gene transcription is initiated between the 4-8 cells stages in bovine *in vivo* embryos [39] while it is delayed to the 8-16 cells stages in bovine *in vitro* embryos [40]. Moreover, a minor embryonic genome transcription activity is already manifest in the 2 cell stage [39]. Related to this induction of transcription and genome-wide DNA methylation was observed when 4-cell and zygotes produced by IVF were transferred into the oviduct of cows and the blastocysts were recovered for analysis [41,42].

On the basis of the differences observed between *in vitro* and *in vivo* cattle zygotes, we propose a model for the dynamics of DNA demethylation in bovine zygotes (Figure 6). In this model, 5mC is demethylated more rapidly in *in vivo* zygotes than *in vitro* zygotes. One of the two PN (probably the paternal PN) is demethylated more rapidly than the other, both *in vitro* and *in vivo*. Further studies will investigate what happens between the first cleavage division and blastocyst formation *in vivo*, during an anticipated re-establishment of epigenetic marks.

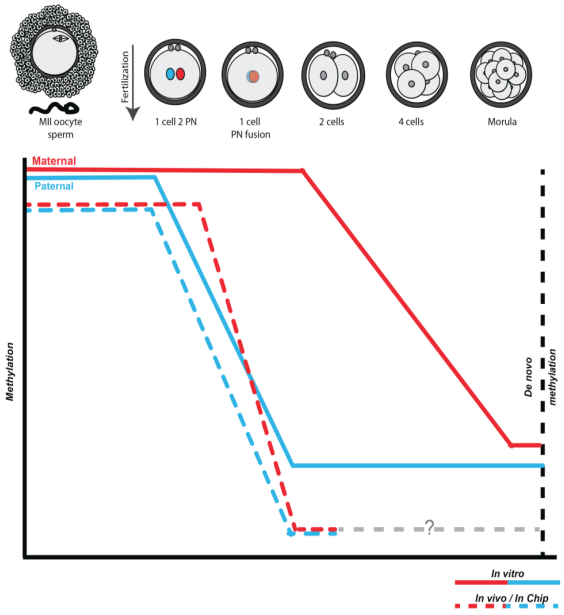

Figure 6. Proposed model for (de)methylation dynamics of *in vitro* (continuous lines) and *in vivo* (dashed lines) derived bovine embryos. *In vitro* data adapted from Yang et al.[43]. Blue: paternal PN; Red: maternal PN; Grey: unknown.

In conclusion, we have demonstrated that conventional *in vitro* oocyte maturation and IVF markedly alter the dynamics of DNA (de)methylation and the expression of genes related to (de)methylation in 1C bovine embryos. This implies that the *in vitro* processes and/or handling induce profound epigenetic disturbances in the gametes and developing zygotes. The fact that *in vivo* zygotes had a more profound demethylation suggests a more effective reestablishment of the totipotent state enabling enhanced potential for widespread genome activation. The perturbed demethylation of *in vitro* produced bovine zygotes may contribute to reduced embryo development and embryo quality following *in vitro* production of bovine embryos. We are currently testing whether a bovine oviduct-on-a-chip system can be employed to avoid the aberrant epigenetic effects introduced by *in vitro* production of zygotes.

References

1. Messerschmidt, D. M., Knowles, B. B. & Solter, D. DNA methylation dynamics during epigenetic reprogramming in the germline and preimplantation embryos. *Genes Dev.* **28,** 812–828 (2014).
2. Ventura-Juncá, P. *et al.* In vitro fertilization (IVF) in mammals: epigenetic and developmental alterations. Scientific and bioethical implications for IVF in humans. *Biol. Res.* **48,** 68 (2015).
3. Heras, S., Smits, K., De Schauwer, C. & Van Soom, A. Dynamics of 5-methylcytosine and 5-hydroxymethylcytosine during pronuclear development in equine zygotes produced by ICSI. *Epigenetics Chromatin* **10,** 13 (2017).
4. Fraser, R. & Lin, C. J. Epigenetic reprogramming of the zygote in mice and men: On your marks, get set, go! *Reproduction* **152,** R211–R222 (2016).
5. Deshmukh, R. S. *et al.* DNA methylation in porcine preimplantation embryos developed in vivo and produced by in vitro fertilization, parthenogenetic activation and somatic cell nuclear transfer. *Epigenetics* **6,** 177–187 (2011).
6. Rasmussen, K. D. & Helin, K. Role of TET enzymes in DNA methylation, development, and cancer. *Genes Dev.* **30,** 733–750 (2016).
7. Jung, S. P., Young, S. J., Sang, T. S., Lee, K. K. & Kang, Y. K. Dynamic DNA methylation reprogramming: Active demethylation and immediate remethylation in the male pronucleus of bovine zygotes. *Dev. Dyn.* **236,** 2523–2533 (2007).
8. Feil, R. Epigenetic asymmetry in the zygote and mammalian development. *Int. J. Dev. Biol.* **53,** 191–201 (2009).
9. Abdalla, H., Hirabayashi, M. & Hochi, S. Demethylation dynamics of the paternal genome in pronuclear-stage bovine zygotes produced by in vitro fertilization and ooplasmic injection of freeze-thawed or freeze-dried spermatozoa. *J. Reprod. Dev.* **55,** 433–439 (2009).
10. Iqbal, K., Jin, S.-G., Pfeifer, G. P. & Szabó, P. E. Reprogramming of the paternal genome upon fertilization involves genome-wide oxidation of 5-methylcytosine. *Proc. Natl. Acad. Sci. U. S. A.* **108,** 3642–7 (2011).
11. Fulka, H., Mrazek, M., Tepla, O. & Fulka, J. DNA methylation pattern in human zygotes and developing embryos. *Reproduction* **128,** 703–708 (2004).
12. Beaujean, N. *et al.* Non-conservation of mammalian preimplantation methylation dynamics [2]. *Curr. Biol.* **14,** 266–267 (2004).
13. El Hajj, N. & Haaf, T. Epigenetic disturbances in in vitro cultured gametes and embryos: Implications for human assisted reproduction. *Fertil. Steril.* **99,** 632–641 (2013).
14. Ménézo, Y., Guérin, P. & Elder, K. The oviduct: A neglected organ due for re-assessment in IVF. *Reprod. Biomed. Online* **30,** 233–240 (2015).

15. Cao, Z. *et al.* Dynamic reprogramming of 5-hydroxymethylcytosine during early porcine embryogenesis. *Theriogenology* **81,** 496–508 (2014).
16. Lee, K. *et al.* Dynamics of TET family expression in porcine preimplantation embryos is related to zygotic genome activation and required for the maintenance of NANOG. *Dev. Biol.* **386,** 86–95 (2014).
17. Nelissen, E. C. M. *et al.* Altered gene expression in human placentas after IVF/ICSI. *Hum. Reprod.* **29,** 2821–31 (2014).
18. Santos, F. *et al.* Evaluation of epigenetic marks in human embryos derived from IVF and ICSI. *Hum. Reprod.* **25,** 2387–2395 (2010).
19. Maalouf, W. E., Alberio, R. & Campbell, K. H. S. Differential acetylation of histone H4 lysine during development of in vitro fertilized, cloned and parthenogenetically activated bovine embryos. *Epigenetics* **3,** 199–209 (2008).
20. Salvaing, J. *et al.* 5-Methylcytosine and 5-Hydroxymethylcytosine Spatiotemporal Profiles in the Mouse Zygote. *PLoS One* **7,** 20–23 (2012).
21. Bakhtari, A. & Ross, P. J. DPPA3 prevents cytosine hydroxymethylation of the maternal pronucleus and is required for normal development in bovine embryos. *Epigenetics* **9,** 1271–1279 (2014).
22. Wossidlo, M. *et al.* 5-Hydroxymethylcytosine in the mammalian zygote is linked with epigenetic reprogramming. *Nat. Commun.* **2,** 241 (2011).
23. Lepikhov, K. *et al.* Evidence for conserved DNA and histone H3 methylation reprogramming in mouse, bovine and rabbit zygotes. *Epigenetics Chromatin* **1,** 8 (2008).
24. Van Tol, H. T. A. A., Van Eerdenburg, F. J. C. M. C. M., Colenbrander, B. & Roelen, B. A. J. J. Enhancement of Bovine oocyte maturation by leptin is accompanied by an upregulation in mRNA expression of leptin receptor isoforms in cumulus cells. *Mol. Reprod. Dev.* **75,** 578–587 (2008).
25. Besenfelder, U., Havlicek, V., Mösslacher, G. & Brem, G. Collection of tubal stage bovine embryos by means of endoscopy a technique report. *Theriogenology* **55,** 837–845 (2001).
26. Hashimshony, T., Wagner, F., Sher, N. & Yanai, I. CEL-Seq: Single-Cell RNA-Seq by Multiplexed Linear Amplification. *Cell Rep.* **2,** 666–673 (2012).
27. Love, M. I., Huber, W. & Anders, S. Moderated estimation of fold change and dispersion for RNA-seq data with DESeq2. *Genome Biol.* **15,** 550 (2014).
28. Bindea, G. *et al.* ClueGO: a Cytoscape plug-in to decipher functionally grouped gene ontology and pathway annotation networks. *Bioinformatics* **25,** 1091–3 (2009).
29. Petrussa, L., Van de Velde, H. & De Rycke, M. Similar kinetics for 5-methylcytosine and 5-hydroxymethylcytosine during human preimplantation development in vitro. *Mol. Reprod. Dev.* **83,** 594–605 (2016).
30. Heras, S., Smits, K., Leemans, B. & Van Soom, A. Asymmetric histone 3 methylation pattern between paternal and maternal pronuclei in equine zygotes. *Anal. Biochem.* **471,** 67–69 (2015).
31. Kang, J. *et al.* Simultaneous deletion of the methylcytosine oxidases Tet1 and Tet3 increases transcriptome variability in early embryogenesis. *Proc. Natl. Acad. Sci. U. S. A.* **112,** E4236-45 (2015).
32. Lan, J., Lepikhov, K., Giehr, P. & Walter, J. Histone and DNA methylation control by H3 serine 10/threonine 11 phosphorylation in the mouse zygote. *Epigenetics Chromatin* **10,** 5 (2017).
33. Reis e Silva, A. R. *et al.* Alteration of DNA demethylation dynamics by in vitro culture conditions in rabbit pre-implantation embryos. *Epigenetics* **7,** 440–446 (2012).
34. Yan, L. *et al.* Single-cell RNA-Seq profiling of human preimplantation embryos and embryonic stem cells. *Nat. Struct. Mol. Biol.* **20,** 1131–1139 (2013).
35. Cerny, K. L., Garrett, E., Walton, A. J., Anderson, L. H. & Bridges, P. J. A transcriptomal analysis of bovine oviductal epithelial cells collected during the follicular phase versus the luteal phase of the estrous cycle. *Reprod. Biol. Endocrinol.* **13,** 84 (2015).

36. Wang, Y. *et al.* Large scale real-time PCR validation on gene expression measurements from two commercial long-oligonucleotide microarrays. **16,** 1–16 (2006).
37. Hou, J. *et al.* Epigenetic modification of histone 3 at lysine 9 in sheep zygotes and its relationship with DNA methylation. *BMC Dev. Biol.* **8,** 60 (2008).
38. Lin, C.-J., Conti, M. & Ramalho-Santos, M. Histone variant H3.3 maintains a decondensed chromatin state essential for mouse preimplantation development. *Development* **140,** 3624–3634 (2013).
39. Jiang, Z. *et al.* Transcriptional profiles of bovine in vivo pre-implantation development. *BMC Genomics* **15,** 756 (2014).
40. Graf, A. *et al.* Fine mapping of genome activation in bovine embryos by RNA sequencing. *Proc. Natl. Acad. Sci. U. S. A.* **111,** 4139–4144 (2014).
41. Gad, a. *et al.* Molecular Mechanisms and Pathways Involved in Bovine Embryonic Genome Activation and Their Regulation by Alternative In Vivo and In Vitro Culture Conditions. *Biol. Reprod.* **87,** 100–100 (2012).
42. Salilew-Wondim, D. *et al.* Genome-wide DNA methylation patterns of bovine blastocysts developed in vivo from embryos completed different stages of development in vitro. *PLoS One* **10,** 1–31 (2015).
43. Yang, X. *et al.* Nuclear reprogramming of cloned embryos and its implications for therapeutic cloning. *Nat. Genet.* **39,** 295–302 (2007).

Chapter 3

Improved bovine embryo production in an oviduct-on-a-chip system: Prevention of poly-spermic fertilization and parthenogenic activation.

Adapted from:

FERRAZ, M.A.M.M.; HENNING, H.H.W.; COSTA, P.F.; MALDA, J.; VOS, P.L.A.M., STOUT, T.A.E.; GADELLA, B.M. Improved bovine embryo production in an oviduct-on-a-chip system: Prevention of poly-spermic fertilization and parthenogenic activation. Lab on a chip. 2017, 17, 905 – 916.

Abstract

The oviduct provides the natural micro-environment for gamete interaction, fertilization and early embryo development in mammals, such as the cow. In conventional culture systems, bovine oviduct epithelial cells (BOEC) undergo a rapid loss of essential differentiated cell properties; we aimed to develop a more physiological *in vitro* oviduct culture system capable of supporting fertilization. U-shaped chambers were produced using stereo-lithography and mounted with polycarbonate membranes, which were used as culture inserts for primary BOECs. Cells were grown to confluence and cultured at an air-liquid interface for 4 to 6 weeks and subsequently either fixed for immune staining, incubated with sperm cells for live-cell imaging, or used in an oocyte penetration study. Confluent BOEC cultures maintained polarization and differentiation status for at least 6 weeks. When sperm and oocytes were introduced into the system, the BOECs supported oocyte penetration in the absence of artificial sperm capacitation factors while also preventing polyspermy and parthenogenic activation, both of which occur in classical *in vitro* fertilization systems. Moreover, this "oviduct-on-a-chip" allowed live imaging of sperm-oviduct epithelium binding and release. Taken together, we describe for the first time the use of 3D-printing as a step further on bio-mimicking the oviduct, with polarized and differentiated BOECs in a tubular shape that can be perfused or manipulated, which is suitable for live imaging and supports *in vitro* fertilization.

Introduction

In mammals, the oviducts are paired organs that connect the uterus to the respective ovaries. The oviduct also forms the specific niche in which mammalian fertilization takes place. Its lumen provides the physiological microenvironment required for gamete interaction and early embryo development [1–5]. Sperm enter the oviduct from the isthmic end, which is connected to the uterus by the utero-tubal junction. Close contact of sperm with the epithelium of the oviductal isthmus has been proven to be important for extending sperm survival, in a so-called 'sperm reservoir'. It also serves to trigger subsequent activation (*i.e.* capacitation) around the time of ovulation. This allows sperm to detach from the isthmus and to ascend into the ampulla where fertilization will take place [5–9]. The ampulla of the oviduct is connected to the funnel-shaped infundibulum, which catches the freshly ovulated cumulus oocyte complex (COC) and directs it further into the ampulla. Final modifications of the COC takes place in the ampulla which will ensure that the oocyte is ready to become fertilized by a sperm cell [10,11]. After fertilization, the first embryonic divisions and further development take place in the oviduct and, once the morula stage is achieved, the bovine embryo will leave the isthmic part of the oviduct to enter the uterus.

Conditions for supporting fertilization and early embryo development *in vitro* have been developed for a wide range of species. However, despite advances in reproductive biotech-

nology and embryo culture media, it is clear that *in vitro* produced embryos differ markedly from those that develop *in vivo* [12–15]. Despite common belief that the oviduct is more than a simple tube allowing the transport of gametes and early stage embryos, the findings that *in vitro* embryos are of reduced developmental competence convincingly demonstrates the importance of the oviduct environment for optimal embryo development. Both the gametes and the early embryo are in close contact with the epithelial lining the oviduct. This epithelium is composed of a mixture of ciliated and non-ciliated, *i.e.* secretory, cells. The oviduct tubular morphology with its intricately folded morphology[16] influences the flux of fluids. Fluid movements are created with muscular contractions and ciliary beating which both actively support the transport of the sperm and oocyte to the ampulla, where fertilization takes place. In this respect, the critical contribution of the oviduct to the complex regulated processes of fertilization of the oocyte and optimal early embryo development remains to be elucidated in detail [17].

Oviduct physiology and function has poorly been studied due to the location of the organ being deep within the abdominal cavity. This makes it difficult to perform *in vivo* observational studies in mammals. Consequently, various *in vitro* models have been designed to study the role of oviduct epithelial cells in gamete interaction and fertilization. The most commonly used models are based on monolayer cultures of oviduct epithelial cells[7,8,18,19], or on explant cultures of oviduct tissue that forms cellular vesicles with ciliary beating activity [20–22]. Standard *in vitro* oviduct monolayer cultures (OMs, 2D culture) are typically hampered by a rapid transformation of the differentiated, cuboidal - columnar oviduct epithelial cells (OECs) into flattened cells with a complete loss of cilia and with a reduced secretory ability [18,23–25]. Recently, the use of porous membrane inserts to allow oviduct epithelial cells to be cultured at an air-liquid interface, has been shown to allow the formation of epithelial monolayers that preserve their epithelial secretory and ciliary beating activity [8,23,26–28]. Although, this has been a break-through in terms of cell culture, commercial insert systems do have a number of limitations for some experimental purposes. For example, it is not possible to perform live cell imaging within most inserts, and perfusion is difficult because the inserts are flat circular discs rather than mimicking the tubular structure of the oviduct.

Ideally, an *in vitro* model of the oviduct would be compartmentalized with a basolateral perfusion compartment mimicking the blood circulation, and an independently apical perfusion compartment mimicking the luminal fluid movements of the oviduct. Such a system would allow mimicking the endocrine changes that do occur during a natural estrous cycle at the basal side and facilitate the apical addition and removal of gametes, embryos, and medium or cell secretions. Indeed, it was recently demonstrated that specific tissue morphology and functions can be preserved better in customized three-dimensional (3D) culture systems than in conventional 2D systems [24,29–33].

Three-dimensional (3D) printing technology can generate prototypes rapidly, allowing researchers to design and print devices within a short period of time [34]. Combined with micro-

fluidic technology, 3D printing has led to the creation of “organs-on-a-chip” to study human and animal physiology in an organ-specific context and, thereby, create models for researching specific aspects of health, disease and toxicology [31]. The advances of 3D printing and cell insert culture systems andthe lack of a physiological *in vitro* model to study oviduct function, led us to design and print a tube-like chamber in which BOECs can be cultured at an air-liquid interface that supports further epithelial polarization and differentiation during long-term culture period. We tested the designed chamber for its suitability for live imaging the interaction between sperm and oviduct cells. Furthermore, the functionality of the epithelial cells cultured in a 3D chamber for supporting fertilization is demonstrated in an oocyte penetration approach. Using this oviduct-on-a-chip design, we aim to better understand the interactive role of the oviduct environment supporting gamete interaction, early embryonic development, and ultimately to be able to produce *in vitro* embryos more similar to *in vivo* embryos than is currently possible.

Materials and Methods

Chemicals

Unless stated otherwise, all chemicals used were obtained from Sigma Chemical Co. (St. Louis, MO) and were of the highest purity available.

Three-dimensional chamber design and printing

The prototype design of the oviduct–on-a-chip was created using Tinkercad (Autodesk Inc., San Francisco, CA, USA). The design included flat upper and lower surfaces to allow attachment to a glass slide for future perfusion and imaging. A curved inner chamber was created to better mimic the tubular surface of the oviduct, while remaining shallow enough not to interfere with imaging. Inlets and outlets in both the apical and basolateral compartments were included, with the size and shape of the inlets designed to permit easy attachment of tubing and to allow adequate fluid flow. An outer cuboid chamber shape was used to facilitate later up-scaling by printing multiple conjoined parallel chambers. The design was exported from Tinkercad as an STL file, and then imported into Mimics software (Materialise NV, Leuven, Belgium) to verify and repair any mesh errors and generate printing support structures. The screenshot of the prototype including its inlets and outlets is shown in Figure 1.

Three-dimensional printing of the device was performed using a photo-cured resin, PIC100 (Envisiontec GmbH, Gladbeck, Germany), via a Perfactory 3 Mini 3D printer (Envisiontec GmbH, Gladbeck, Germany) at a resolution of 50 µm, which exploits the photo-polymerization technique for 3D printing.

Post-curing, mounting a porous membrane and sterilization of the 3D chamber

To avoid the leakage of compounds from the printed material that might interfere with cell viability, removal of excess resin was performed by a 15 minute immersion in ethanol. After complete air drying, the chambers were immersed 3 times for 2 hours each in isopropanol solution. After repeated air drying, the chambers were light-cured using 4000 flashes in an Otoflash G171 (Envisiontec GmbH, Gladbeck, Germany).

The polycarbonate membrane (0.4 µm pores; SABEU GmbH & Co. KG, Germany) was attached to the chamber using the silicone elastomer Kwik-Sil (World Precision Instruments Inc., Florida, USA) and cured for 5 minutes at room temperature. Before incubation with cells, the chambers were sterilized by immersion for 1 hour in 70% ethanol, washed three-times for 30 minutes each in phosphate-buffered saline solution (PBS; 163.9 mM Na^+, 140.3 mM CL^-, 8.7 mM HPO_4^{3-}, 1.8 mM $H_2PO_4^-$, pH 7.4; Braun, Melsungen, Germany) and washed for 1 hour in HEPES buffered Medium 199 (Gibco BRL, Paisley, U.K.) supplemented with 100 U/mL penicillin and 100 µg/mL streptomycin (Gibco BRL, Paisley, U.K.).

Isolation of oviduct cells and long term oviduct cell culture

Cow oviducts were collected from a local abattoir immediately after slaughter and transported to the laboratory on ice, within two hours. The oviducts were dissected free of surrounding tissue and washed three times in cold PBS supplemented with 100 U/mL of penicillin and 100 µg/mL of streptomycin. BOECs were isolated by squeezing the total oviduct contents out of the ampullary end of the oviducts, and collected in HEPES buffered Medium 199 supplemented with 100 U/mL penicillin and 100 µg/mL streptomycin. The cells were washed twice by centrifuging for 500 x g for 10 minutes at 25°C in HEPES buffered Medium 199 supplemented with 100 U/mL of penicillin and 100 µg/mL of streptomycin. The cells were then cultured for 24 hours in HEPES buffered Medium 199 supplemented with 100 U/mL penicillin, 100 µg/mL streptomycin and 10% fetal calf serum (FCS; Bovogen Biologicals, Melbourne, Australia). During these 24 hours, the cells arranged themselves into floating vesicles with outward facing actively beating cilia; these vesicles were collected, centrifuged at 500 x g for 10 minutes at 25 °C, resuspended in DMEM/Ham's F12 medium (DMEM/F-12 Glutamax I, Gibco BRL, Paisley, U.K.) supplemented with 1.4 mM hydrocortisone, 5 mg/mL insulin, 10 mg/mL transferrin, 2.7 mM epinephrine, 9.7 nM tri-iodothyronine, 0.5 ng/mL epidermal growth factor, 50 nM trans-retinoic acid, 2 % bovine pituitary extract (containing 14 mg/mL protein), 1.5 mg/mL BSA, 100 mg/mL gentamycin, and 2.5 mg/mL amphotericin B (3D culture medium, adapted from [24]), and pipetted up and down several times to mechanically separate the cells. Next, cells were seeded either into: (i) the oviduct-on-a-chip (3D culture; 0.6 x 10^6 cells/cm^2) or (ii) into 24 well culture dishes with glass coverslips in the bot-

tom of the wells (2D culture; 0.3 x 10^6 cells/cm^2). Cells in both systems were cultured in 3D culture medium in a humidified atmosphere of 5 % CO_2-in-air at 38.5 °C until they reached confluence (5-7 days). Once the cells had reached confluence, an air-liquid interface was established in the 3D culture by removing the medium in the apical compartment. Cells in the 3D chambers were cultured at an air-liquid interface for up to 42 days in a humidified atmosphere of 5 % CO_2-in-air at 38.5 °C. The culture medium was completely refreshed twice a week in both systems.

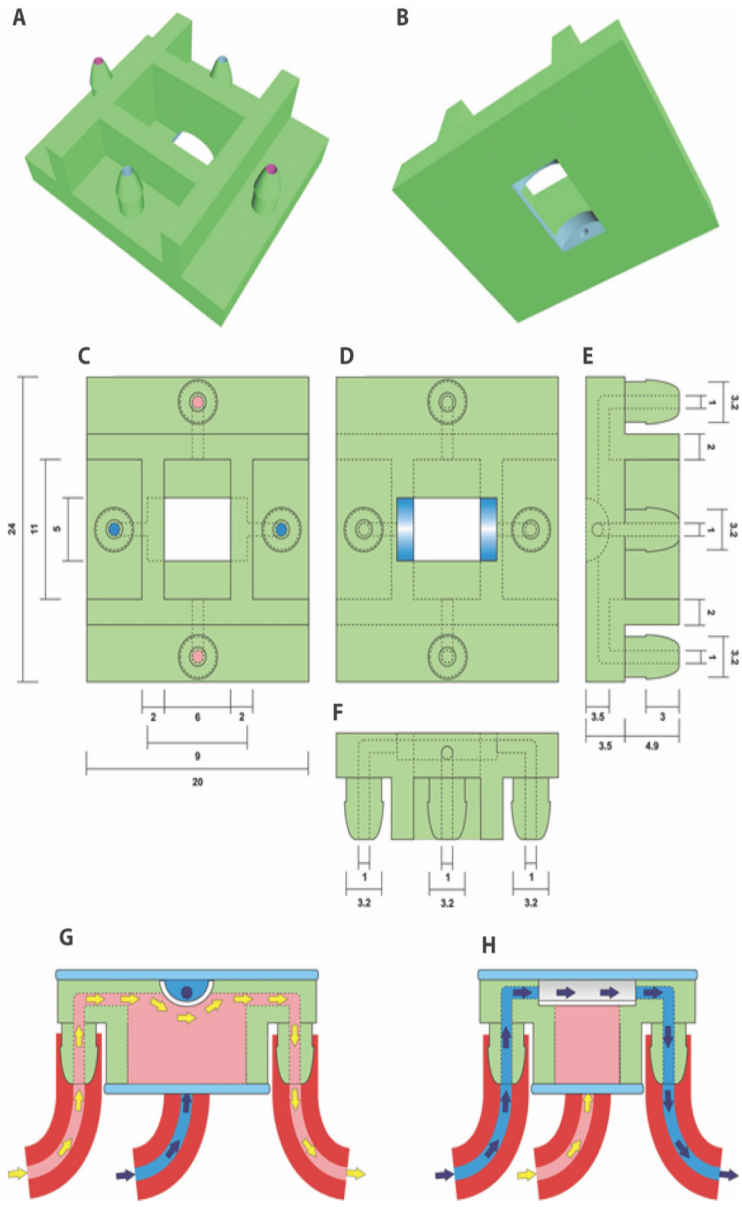

Figure 1. Perspective visualization of the open device's 3D printable model from above (A) and below (B). Schematic top (C), bottom (D), right (E) and front (F) view of the open device. Schematic right (G) and front (H) cross section of the closed device while being separately perfused with two (pink and blue) different types of media/cells. Dimensions are represented in millimeters.

Oocyte collection and in vitro maturation

Oocyte collection and maturation was performed as described somewhere else[35]. Briefly, bovine ovaries were collected from a local abattoir and transported to the laboratory within 2 hours after dissection. The ovaries were washed in physiological saline (0.9 % w/v NaCl) and held in physiological saline containing 100 U/mL penicillin and 100 µg/mL streptomycin at a temperature of 30°C. The fluid and cumulus oocyte complexes (COCs) were aspirated from follicles with a diameter ranging from 2 to 8 mm and were collected into a 50ml conical tube using a 19-gauge needle and a vacuum pump. COCs with a minimum of three layers of intact cumulus cells were selected and first washed in HEPES-buffered M199 (Gibco BRL, Paisley, U.K.) before being washed and cultured in maturation medium (M199 supplemented with 0.02 IU/mL follicle-stimulating hormone [Sioux Biochemical Inc., Sioux Center, IA]), 0.02 IU/mL luteinizing hormone (Sioux Biochemical Inc.), 7.71 µg/mL cysteamine, 10 ng/mL epidermal growth factor in 0.1 % w/v fatty acid-free bovine serum albumin (BSA) and 100 U/mL penicillin and 100 µg/mL streptomycin. Selected COCs were cultured in four-well culture plates (Nunc A/S, Roskilde, Denmark) containing maturation medium. The oocytes were matured in groups of 50 COCs in 500 µl maturation medium and incubated in a humidified atmosphere of 5 % CO_2-in-air for 24 hours at 38.5 °C.

Sperm washing and staining with mitotracker

Frozen sperm, from 3 different bulls, were thawed at 37 °C for 30 seconds and washed by centrifugation at 100 x g for 10 minutes through a BoviPure discontinuous gradient, following manufacture instructions (Nidacon International AB, Gothenburg, Sweden) at room temperature. The supernatant was removed, the pellet resuspended in 3 mL of BoviPure wash solution, and centrifuged again at 100 x g for 5 minutes. Spermatozoa from the 3 pellets were pooled and then incubated for 30 minutes with 200 nM mitotracker green FM® or mitotracker red FM®(MTG and MTR respectively; Molecular Probes Inc., Eugene, USA) in fertilization medium (modified Tyrode's medium supplemented with 25 mM sodium bicarbonate, 22 mM lactate, 1 mM pyruvate, 6 mg/mL fatty acid–free BSA) containing 100 U/mL penicillin and 100 µg/mL streptomycin instead of gentamycin and without glucose or activation factors (heparin, d-penicillamine, hypotaurine and epinephrine). The mitotracker stained spermatozoa were then washed three times in fertilization medium without activation factors by centrifuging at 100 x g for 5 minutes and used for *in vitro* fertilization.

In vitro fertilization

MTG stained sperm were added to the fertilization medium at a final concentration of 1 x 10^6 sperm cells/mL in the presence (control IVF, 500 µL volume) or absence (3D culture, 2D

culture and no activation factors control IVF; 80, 500 and 500 µL volume, respectively) of 10 µg/ml heparin, 20 µM d-penicillamine, 10 µM hypotaurine, and 1 µM epinephrine (activation factors). For the 3D culture IVF, the sperm suspension (80 µL) was manually perfused to the apical compartment and-after 2 hours- unattached sperm were perfused out of the system by flushing 240 µL of PBS over the apical side of the BOEC and immediately thereafter, a total of 25 COCs were perfused to the apical compartment in 80 µL of fertilization medium without activation factors of each of the 3D culture chambers (n=8 chambers; 25 COCs per chamber). In 2D cultures 50 COCs were added in 500 µL of fertilization medium without activating factors. A standard IVF protocol[35], with or without activation factors, was performed as a control on 300 COCs. After 24 h of co-incubation under a humidified atmosphere of 5% CO_2-in-air at 38.5°C, cumulus cells were removed by pipetting and the presumptive zygotes were fixed and stained with the membrane permeable DNA stain Hoechst 33342 (5 µg/mL in PBS) to distinguish parthenotes and poly-spermic from mono-spermic fertilized oocytes. All experiments were performed in 4 replicates, using 2 different animals per replicate for the 2D and 3D cultures groups.

The sperm cells perfused out of the 3D culture chambers were centrifuged at 100 x g for 5 minutes, resuspended in 50 µL of fertilization medium, and the number of recovered sperm cells was calculated in order to determine the number of spermatozoa that remained bound to the epithelial cells. A routine IVF with the same number of sperm cells as the ones that remained attached to the epithelial cells in the 3D culture (69 x 10^3 sperm cells/well) and a routine IVF with same proportion of sperm cells that remained attached to the 3D culture were performed (0.431 x 10^6 sperm cells/well, 86.25 % of sperm cells used for control IVF). After 24 hours of co-incubation under a humidified atmosphere of 5 % CO_2-in-air at 38.5 °C, presumptive zygotes were fixed and stained as described above.

Ciliation of cells and cell morphology

At weeks 3, 4, 5 and 6 of air-liquid interface culture, two oviduct-on-a-chip chambers and 1 coverslip from the 2D culture was sacrificed per animal (n = 4) for assessment of cilia formation on epithelial cells. The membranes were dismounted from the chamber for immune fluorescent staining. The membranes or cover slips were washed in PBS, fixed in 4 % paraformaldehyde dissolved in PBS, and permeabilized for 30 minutes using 0.5 % Triton-X100 in PBS. Non-specific binding was blocked by incubation for 1 hour in PBS containing 5 % normal goat serum, at room temperature. The cells were then incubated overnight at 4°C with a mouse anti-acetylated α-tubulin primary antibody (1 : 100 dilution with PBS Santa Cruz Biotechnology, Santa Cruz, CA). The next morning the cells were washed three times in PBS (5 minutes per wash) and incubated with an Alexa 488 conjugated goat anti-mouse antibody (1:100 dilution with PBS, Santa Cruz Biotechnology, Santa Cruz, CA) at room temperature for 1 hour. Hoechst 33342 (5 µg/mL) was used to stain cell nuclei and phalloidin

conjugated to Alexa 568 (1:100 dilution with PBS) was used to stain actin filaments. Negative controls were performed by omitting incubation with the primary antibody. Analysis was performed by laser scanning confocal microscopy using a TCS SPE-II system (Leica Microsystems GmbH, Wetzlar, Germany) attached to an inverted semi-automated DMI4000 microscope (Leica) with a 40 x NA 1.25 magnification objective. Five random field of views in the center of the membrane and coverslip were imaged for each animal and group and, at least, 350 cells per animal and per group were classified; the percentage of ciliated cells was determined. Moreover, Z-stacks of 0.2 µm were obtained by laser scanning confocal microscopy at 100 x NA 1.40 magnification objective. 3D constructs of the cells were performed using ImageJ software (National Institutes of Health, Bethesda, MD, USA) to demonstrate cell morphology.

Pieces of 5 mm from ampullary and isthmic regions of the oviduct ipsilateral to the ovary with an active corpus luteum were fixed for 24 hours in 4 % w/v paraformaldehyde, paraffin embedded and sections of 4 µm were stained as described above.

Live cell imaging

After one week of the air-liquid interface culture, the oviduct-on-a-chip was incubated with MTR labeled sperm and stained with Hoechst 33342 (5 µg/mL) in the 3D culture medium for 30 minutes. Live cell imaging was done on a Nikon Eclipse TE2000 equipped with the Perfect Focus System with a two-channel simultaneous imaging system by exciting with the lasers Vortran 405 nm and Cobolt Jive 561 nm, using the filters ET-DAPI (490/00) and ET-DSRed (490/05). Images from both channels were detected with a 20 x magnification long distance objective (Plan Apo 20x/NA 0.75 dry) with a speed of 60 frames per second.

Detection of oocyte penetration

Fixed presumptive zygotes were stained with Hoechst 33342 (5 µg/mL in PBS) for 30 min, washed three times in PBS containing 3 mg/mL polyvinyl pyrrolidone (PVP) and then mounted into a 0.12 mm eight-well Secure-Seal Spacer (Molecular Probes) on a glass slide (Superfrost Plus; Menzel, Braunschweig, Germany), covered with Vectashield antifade (Vector Laboratories, Burlingame, CA), and sealed with a coverslip. Slides were analyzed by Laser scanning confocal microscopy using a TCS SPE-II system (Leica Microsystems GmbH, Wetzlar, Germany) attached to an inverted semi-automated DMI4000 microscope (Leica) with a 40 x NA 1.25 magnification objective. The number of oocytes with the presence of labeled sperm mid-piece(s) within the ooplasm was determined (i.e. sperm-penetrated oocytes). Poly-spermy was identified by the detection of 2 or more sperm mid-pieces within the ooplasm, while parthenotes were identified in the case when 2 or more nuclei were detected

without the presence of a sperm mid-piece.

Data analysis

The data were analyzed using IBM SPSS Statistics (version 24). A Shapiro-Wilk test was performed and all groups were normally distributed. Mean ± standard deviation is provided and differences between groups were examined by one-way ANOVA, followed by a Tukey's post hoc analysis ($p<0.05$).

Results and Discussion

In this study, we designed and successfully 3D printed an oviduct-on-a-chip model using a stereo-lithographic technique (Figure 1). The chamber was designed such that its dimensions were compatible with live-cell imaging. Nowadays, 3D printing generates fast prototyping process technology, allowing researchers to design and print devices in a short period of time [34]. On the other hand, research employing technologies, such as 3D printing and microfluidics, to bio-mimic 3D cultures for reproductive events is scarce and only a handful of papers on 3D microfluidics and gamete research have been published [36–40].

The oviductal lumen has a complex morphology due to folding of the mucosa of the oviduct wall. This folding varies in the different anatomical parts of the oviduct[41]. Exactly mimicking those folding *in vitro* is difficult and does not allow accurate live imaging. Therefore, we had to compromise our bio-mimicked model and decided to create an U-shape topology as this construct, at least, would allow live imaging and perfusion of the system, also providing a niche where more cell contact area is offered for introduced COCs. The oviduct-on-a-chip was designed in such a way that the distance between cells adhered to the porous filter and the glass coverslip was less than 2 mm, to meet the working distance of objectives available and permit live-cell imaging using an inverted epifluorescence microscope after incubation of the cells with MTR pre-labeled sperm (Supplementary movie 1). To our knowledge, this is the first published 3D printed device with a half-pipe shaped porous filter for BOEC culture. The potential benefits of this system for BOEC culture extend beyond the accessibility for live-cell imaging, since both the apical and basolateral compartments can be independently perfused or otherwise manipulated. The possibility of live imaging within the device is a significant advantage over currently available commercial porous membrane systems, and should allow a greater range of *in vitro* experiments, in particular those focusing on the changes within sperm cells during their incubation with oviduct epithelial cells just prior to fertilization and further embryonic development under different conditions.

When BOECs were cultured under 2D conditions the cells did not become ciliated but lost

their columnar epithelium shape instead and became flat. This is in line with previous reports that describe this process known as de-differentiation [25,27,42–44]. In contrast, BOECs cultured in the 3D printed device regained and maintained their ciliated and cuboidal to columnar pseudostratified epithelium for a period of at least 6 weeks, with a mixed population of ciliated and non-ciliated secretory cells (Figure 2A to C). This morphology was comparable to the *in vivo* oviduct epithelium (Figure 2D and E). It was also possible to observe the formation of actin rich protrusions in non-ciliated cells, the secretory bulbs. Cilia emerged at the air-liquid interface side of the cells (apical) within about 2 weeks of culture, was complete within 3 weeks and remained stable during weeks 3-6 of culture ($P<0.05$; Figure 3). Similar results have been described, previously, using porous membranes cultured at an air-liquid interface system for OECs derived from different species including mouse, cow, pig, monkey and man [8,24,26–28,42,45]. However, such systems do not allow live-cell analysis and monitoring in contrast to the BOEC system described in our current study.

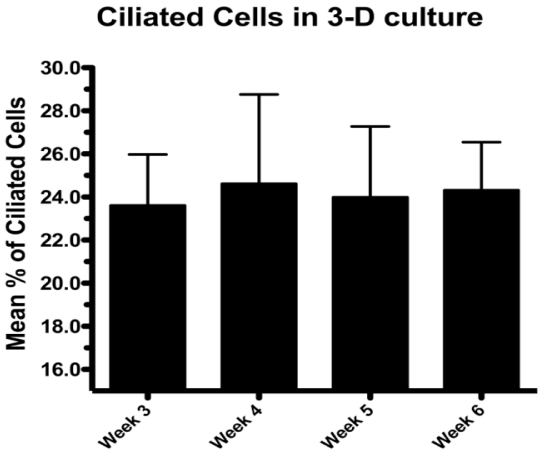

Figure 3. Average percentage of ciliated BOECs in 3D culture during weeks 3, 4, 5 and 6 of air-liquid interface culture (n=4 animals). No difference was observed in the percentages of ciliated cells across the period studied ($p>0.05$).

The functionality of our oviduct-on-a-chip system was tested using a bio-monitoring assay in which sperm penetration of the oocyte was scored (this is indicative for fertilization). Although a lower percentage of oocytes was penetrated, compared to a standard bovine IVF system (Figure 4), the oviduct-on-a-chip system resulted in a similar proportion of oocytes that were mono-spermic fertilized (Figures 4 and 5). Remarkably, and in contrast to standard IVF, no parthenogenic oocyte activation nor poly-spermic fertilization was observed in our developed oviduct-on-a-chip fertilization system (Figures 4 and 6). In contrast, parthenogenesis and poly-spermy both occurred with an incidence of approximately 10 % in the routine IVF system (Figure 4). Thus the developed oviduct-on-a-chip allowed similar normal fertilization of oocytes and completely reduced the incidence of abnormal fertilization/activation of oocytes when compared to routine IVF. Further to this, it should be noted that in

our developed oviduct-on-a-chip system we have not added factors to the incubation media to stimulate sperm activation and capacitation in the model, in contrast to conventional bovine IVF where such additions are a routine requirement. Thus the apical fluid compartment must have been conditioned by the secretions of the polarized BOECs allowing similar mono-spermic fertilization rates to those achieved via conventional IVF.

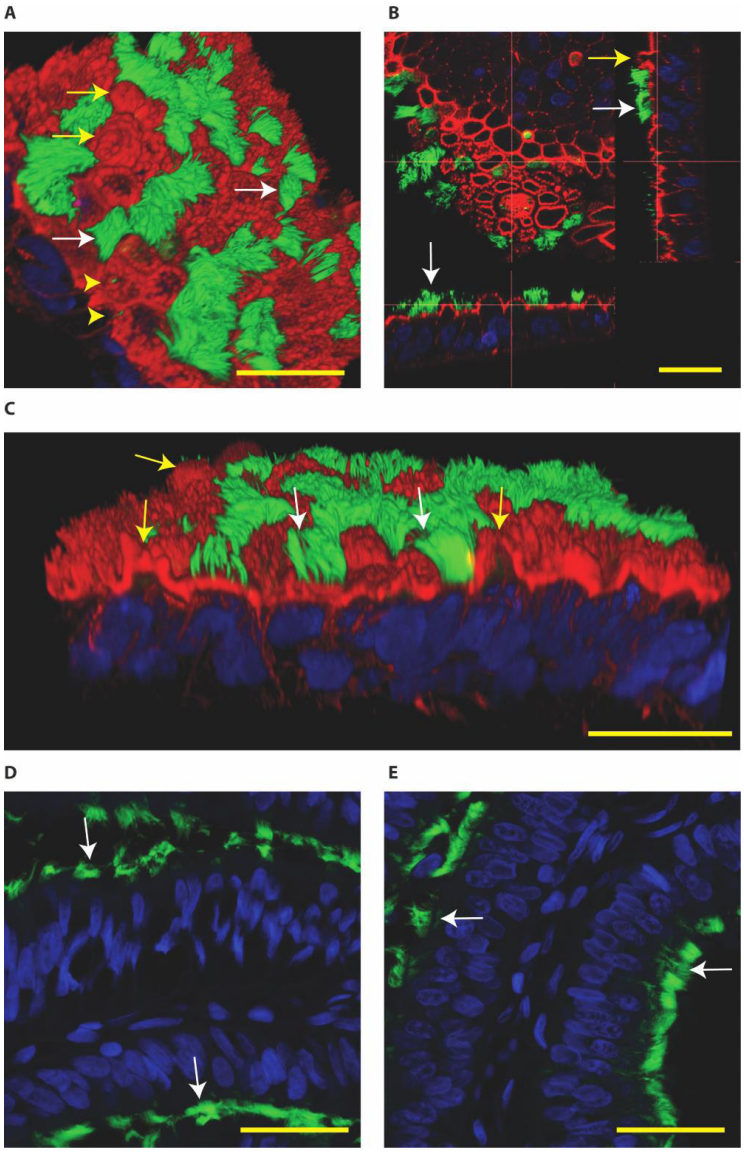

Figure 2. Confocal immune fluorescent images of bovine oviduct epithelial cells (BOECs) in 3D culture at an air-liquid interface for 28 days (A, B and C) and from paraffin sections of oviductal isthmus and ampulla (D and E, respectively). Acetylated α-tubulin was used to stain secondary cilia (green), phalloidin to label actin filaments (red in A, B and C) and Hoechst 33342 to stain nuclei (blue). A, B and C: Note the presence of ciliated cells (green, white arrows), actin rich secretory protrusions (red, yellow arrows) and primary cilia (yellow arrow heads). In B, note the cuboid to columnar pseudostratified epithelium. D and E: Note columnar pseudostratified morphology of oviduct paraffin sections, similar to the one encountered in the 3D cultured BOEC. In paraffin embedded sections the phalloidin staining was not observed. The Z-stacks from top to bottom of the cells cultured on the 3D system can also be observed in the supplementary movie 2. Bars = 25 µm.

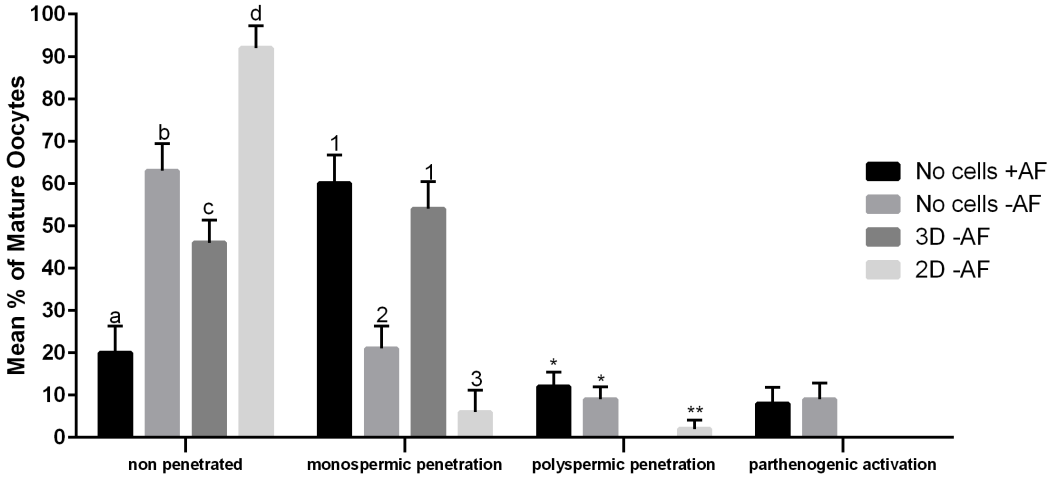

Figure 4. Mean percentage of COCs placed in maturation medium that were penetrated by sperm. *In vitro* fertilization was performed in four replicates using different systems: 3D culture (n=200 COCs), 2D culture (n=200 COCs) and in the absence of oviductal epithelial cells (with or without activation factors; n=300 COCs for each group). Total penetrated: different letters indicate values that differ statistically ($p<0.05$); Polyspermy: different numbers indicate values that differ statistically ($p<0.05$); Parthenogenesis: no differences were observed ($p>0.05$). Activation factors: heparin, penicillamine and hypothaurine.

The reduced rates in poly-spermy and parthenogenic activation of oocytes in the 3D BOEC system was not due to a reduction of the amount sperm (non-bound sperm were perfused away) when compared to conventional IVF: the majority of sperm (86.3 ± 2.9 %) remained attached to the 3D BOEC (representing 69,000 ± 2,300 sperm per 3D-BOEC). When a similar proportional reduction of sperm was used in conventional IVF (i.e. only 0.43 x 10^6 instead of 0.5 x 10^6 sperm per well) no differences on mono-spermic penetration, poly-spermic penetration and parthenogenic activation was observed (for control 60.1%, 12.4% and 8.9%; for reduced number of sperm 55.63%, 12.23% and 10.11%, respectively; $p > 0.05$). In another control we compared the fertilization results using 69,000 cells (the same number of sperm that remained bound in the 3D-BOEC) with 500,000 cells (normally used in conventional IVF).

The large reduction of sperm resulted in severely reduced mono-spermic fertilization (20.5 % versus 60.1 %; $p <0.05$) and a concomitant reduction of poly-spermic fertilization (5.1 % versus 12.5 %; $p<0.05$) while the parthenogenic activation rates remained the same (10.3% and 8.9%, $p > 0.05$). Note that both poly-spermic fertilization and parthenogenic activation of oocytes was not observed in the 3D-BOEC system: (i) The binding and activation of sperm to the 3D-BOEC and the absence of the activation factors are required to achieve high mono-spermic fertilization rates in combination with complete abolishment of poly-spermic fertilization and parthenogenic activation. (ii) In the 3D-BOEC system a strong reduction of

number of sperm (13.8 %) leads to similar mono-spermic fertilization rates when compared to conventional IVF while such a reduction of sperm in conventional IVF leads to a severe reduction of mono-spermic fertilization rates. (iii) Reducing the amount of sperm in conventional IVF, in presence of activation factors, does not reduce poly-spermic fertilization/mono-spermic fertilization ratio (both are reduced to >60%) and does not reduce the incidence of parthenogenic activation. Altogether these data confirm that the higher efficiency of mono-spermic fertilization (at low sperm dose) and the abolition of poly-spermic fertilization as well as parthenogenic activation in the 3D BOEC culture IVF is due to an interaction between the sperm and/or the oocyte with the oviduct cells and/or secretions rather than to the severe reduction in number of sperm when compared to conventional IVF.

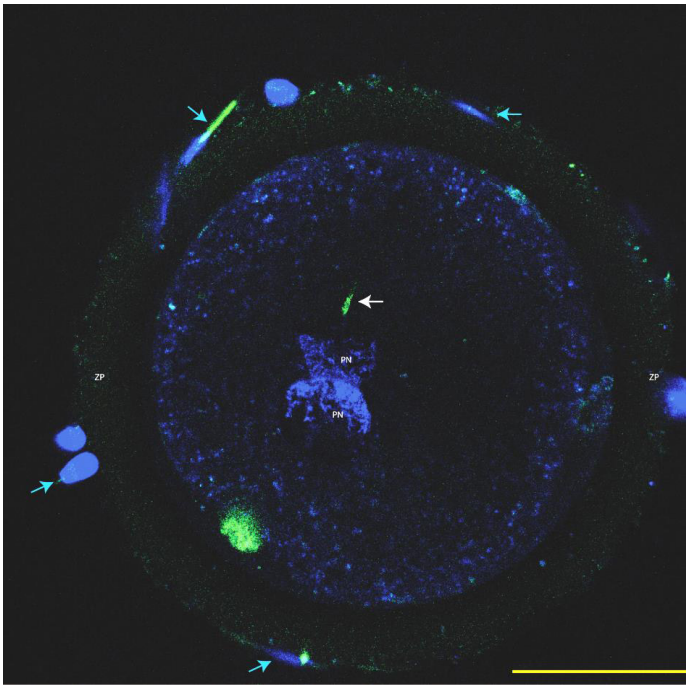

Figure 5. Monospermic oocyte penetration; Hoechst 33342 used to stain DNA (blue) and MTG used to label sperm mid pieces (green). Note the presence of maternal and paternal pronuclei (PN), the mid piece (white arrow) of the spermatozoa that penetrated the zona pellucida (ZP) and fertilized the oocyte, and spermatozoa attached to the zona pellucida (blue arrows). Bar = 50 µm.

Our results may indicate that routine IVF misses the optimal conditioning factors that are secreted by the oviduct epithelium and this absence caused the noted increase in rates of oocytes that are abnormally parthenogenic activated or poly-spermic fertilized. Note that the activating factors used in conventional IVF are not responsible for the incidence of poly-spermic fertilization and/or parthenogenic activation of the oocytes (Figure 4). They only served to increase the mono-spermic fertililization rate to similar levels when compared to the 3D-BOEC, albeit approximately 7.2 times more sperm were needed in the conventional IVF when compared to the 3D-BOEC. This result further supports the notion that the ovi-

duct-on-a-chip have conditioned and optimized the apical environment for mono-spermic fertilization. Altogether our data indicate that when OECs are cultured into a polarized and differentiated state within a 3D topology, they appear to condition apical medium as they exclusively support mono-spermic fertilization. In the 2D culture system, where the majority of OECs were flat and non-ciliated, the conditioning of the apical medium was insufficient and did not inhibit poly-spermic fertilization (even though the total penetration rate was reduced).

A reduction of poly-spermy with even higher (74-84%) fertilization rates was demonstrated previously in an IVF system using BOECs cultured on porous membrane inserts [8]. The major difference of that study and our approach is that we did not add any sperm activating components to the 3D BOEC culture medium. Moreover, in our oviduct-on-a-chip system we not only showed reduced rates but even a complete absence of both poly-spermic fertilization and parthenogenic activation. With regards to the higher fertilization rates in the former BOEC study[8], the addition of estrous cow serum may have stimulated changes in the BOECs secretory activity. Studies to examine the influence of factors such as endocrine stimulation, as well to investigate the influence of different segments of the oviduct (ampulla vs isthmus) on sperm activation and embryo development are planned for the oviduct-on-a-chip system.

The concept that conditioning of the apical medium by the BOECs in the 3D system is responsible for preventing poly-spermy, is in line with previously described, inhibitory, effects of oviduct fluid on poly-spermic fertilization in cows and pigs [46,47]. Moreover, studies have also reported beneficial effects of oviduct fluid and/or oviduct proteins on sperm motility, acrosome reaction, bull fertility [3,8,48–54] and on oocyte and embryo development and quality [1,47,55–61]. Despite of this, the oviduct has remained a largely neglected organ when designing IVF procedures in man and domestic animals[17].

Note that epigenetic modulation of the maturing oocyte and the early developing embryo can also be of concern while producing embryos *in vitro*. *In vivo* these epigenetic events take place in the oviduct and are thought to allow reprogramming of the embryonic genome. For instance, the methylation of sperm DNA is erased in the paternal pronucleus after fertilization. Amongst other functions this process allows specific pluripotency genes to be expressed. Failure of, or disturbances to, this process leads to impaired embryo development [62]. Interestingly, bovine blastocysts developed after culturing embryos partially *in vitro* and partially *in vivo* have been shown to differ in DNA methylation patterns when compared to blastocysts developed completely *in vivo* and to those completely developed *in vitro* [13].

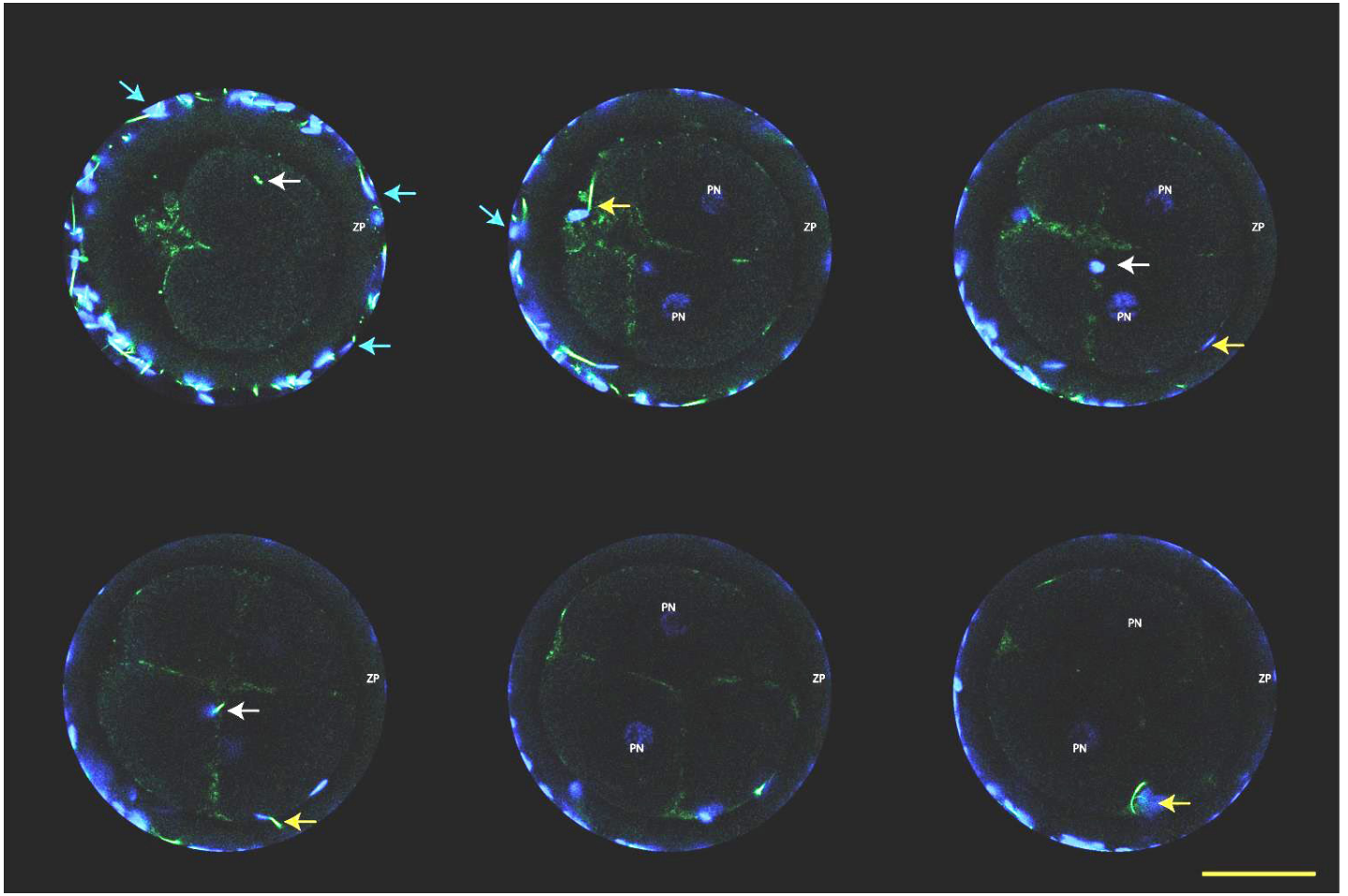

Figure 6. Confocal Z-stacks of a polyspermic penetrated oocyte, stained with Hoechst 33342 for DNA (blue) and MTG for sperm mid piece (green). Note the presence of multiple pronuclei (PN), the mid piece (white arrows) of two sperm cells that penetrated the zona pellucida (ZP) and fertilized the oocyte; a sperm cell that penetrated the ZP, but not the oolema (yellow arrow), and spermatozoa attached to the zona pellucida (blue arrows). Bar = 75 µm.

A classic example of the possible epigenetic effects of *in vitro* embryo production conditions on embryo development is the Large Offspring Syndrome (LOS), which is characterized by increased size and weight at birth, breathing difficulties, reluctance to suckle, and perinatal death of the born calves [63]. The LOS was described in cattle and sheep derived from *in vitro* cultured embryos in the presence of elevated serum concentrations[63]. The pathogenesis of the syndrome is not completely clear, but there is evidence that a loss of gene-imprinting and overexpression of insulin growth factor 2 (IGF2) receptor may be an important contributor [64,65]. The epigenetic changes that may be induced during embryo culture emphasize the need for improved *in vitro* embryo production systems. Not only the quantitative production of blastocysts, but also the quality and genetic normality of such embryos produced are highly relevant. We believe that the oviduct-on-a-chip approach will be an ideal starting point to better mimic the physiological environment for mammalian fertilization and embryo production. This more physiological environment likely serves to reduce metabolic and genetic programming abnormalities caused by *in vitro* embryo production conditions.

Conclusions

In conclusion, a 3D oviduct-on-a-chip model with a U-shaped porous membrane allowed BOEC polarization that could be maintained during long-term culture (over 6 weeks). In this system the oviduct cells under culture must have conditioned the apical medium, as this allowed proper sperm and oocyte interactions, fertilization and completely abolished poly-spermic fertilization and parthenogenic activation of oocytes in the absence of added sperm activating factors. The oviduct-on-a-chip system is easy to manipulate, can be used for introduction, manipulation and live microscopic visualization of sperm cells, oocytes and early embryos and study their cellular processes around fertilization. The fact that fertilization is exclusively mono-spermic may become relevant for assisted reproductive technologies for both bovine and other mammalian species.

Acknowledgements

This research is part of the research focus theme Life Sciences of Utrecht University, experiments were performed in the research group Fertility and Reproduction and confocal imaging was performed at the Centre for Cell Imaging, both on the Faculty of Veterinary Medicine of the same university.

Supplementary information

Supplementary videos 1 and 2 can be accessed at: http://pubs.rsc.org/en/content/article-landing/2017/lc/c6lc01566b#!divAbstract.

References

1. Lloyd, R. E. *et al.* Effects of oviductal fluid on the development, quality, and gene expression of porcine blastocysts produced in vitro. *Reproduction* **137,** 679–687 (2009).
2. Coy, P., García-Vázquez, F. a., Visconti, P. E. & Avilés, M. Roles of the oviduct in mammalian fertilization. *Reproduction* **144,** 649–660 (2012).
3. Killian, G. Physiology and endocrinology symposium: Evidence that oviduct secretions influence sperm function: A retrospective view for livestock. *J. Anim. Sci.* **89,** 1315–1322 (2011).
4. Zhang, B. R., Larsson, B., Lundeheim, N. & Rodriguez-Martinez, H. Sperm characteristics and zona pellucida binding in relation to field fertility of frozen-thawed semen from dairy AI bulls. *Int. J. Androl.* **21,** 207–16 (1998).
5. Suarez, S. S. Mammalian sperm interactions with the female reproductive tract. *Cell Tissue Res.* **363,** 185–194 (2016).
6. Talevi, R. & Gualtieri, R. Molecules involved in sperm-oviduct adhesion and release. *Theriogenology* **73,** 796–801 (2010).
7. Gualtieri, R., Mollo, V., Barbato, V. & Talevi, R. Ability of sulfated glycoconjugates and disulfide-reductants to release bovine epididymal sperm bound to the oviductal epithelium in vitro. *Theriogenology* **73,** 1037–1043 (2010).
8. Pollard, J. W. *et al.* Fertilizing capacity of bovine sperm may be maintained by binding of oviductal epithelial cells. *Biol. Reprod.* **44,** 102–107 (1991).
9. Mcnutt, T. & Killian, G. Influence of Bovine Follicular and Oviduct Fluids on sperm Capacitation In Vitro. *J. Androl.* **12,** 244–252 (1991).
10. Gabler, C. *et al.* Exploring cumulus-oocyte-complex-oviductal cell interactions: Gene profiling in the bovine oviduct. *J. Physiol. Pharmacol.* **59,** 29–42 (2008).
11. Gonçalves, R. F., Staros, A. L. & Killian, G. J. Oviductal fluid proteins associated with the bovine zona pellucida and the effect on in vitro sperm-egg binding, fertilization and embryo development. *Reprod. Domest. Anim.* **43,** 720–729 (2008).
12. Gad, a. *et al.* Molecular Mechanisms and Pathways Involved in Bovine Embryonic Genome Activation and Their Regulation by Alternative In Vivo and In Vitro Culture Conditions. *Biol. Reprod.* **87,** 100–100 (2012).
13. Salilew-Wondim, D. *et al.* Genome-wide DNA methylation patterns of bovine blastocysts developed in vivo from embryos completed different stages of development in vitro. *PLoS One* **10,** 1–31 (2015).
14. Betsha, S. *et al.* Transcriptome profile of bovine elongated conceptus obtained from SCNT and IVP pregnancies. *Mol. Reprod. Dev.* **80,** 315–333 (2013).
15. Barrera, D. *et al.* Expression of DNA methyltransferase genes in four-cell bovine embryos cultured in the presence of oviductal fluid. *J. Vet. Med. Ser. C Anat. Histol. Embryol.* **42,** 312–315 (2013).
16. Miki, K. & Clapham, D. E. Rheotaxis Guides Mammalian Sperm. *Curr. Biol.* **23,** 443–452 (2013).
17. Ménézo, Y., Guérin, P. & Elder, K. The oviduct: A neglected organ due for re-assessment in IVF. *Reprod. Biomed. Online* **30,** 233–240 (2015).
18. Ulbrich, S. E., Zitta, K., Hiendleder, S. & Wolf, E. In vitro systems for intercepting early embryo-maternal cross-talk in the bovine oviduct. *Theriogenology* **73,** 802–816

(2010).
19. Morales, P., Palma, V., Salgado, a M. & Villalon, M. Sperm interaction with human oviductal cells in vitro. *Hum. Reprod.* **11,** 1504–1509 (1996).
20. Nelis, H. *et al.* Equine oviduct explant culture: a basic model to decipher embryo–maternal communication. *Reproduction, Fertility and Development* **26,** 954–966 (2014).
21. Leemans, B. *et al.* Combined albumin and bicarbonate adversely affects equine sperm-oviduct binding. *Reproduction* **151,** 313–330 (2016).
22. Maillo, V. *et al.* Maternal-embryo interaction in the bovine oviduct: evidence from in vivo and in vitro studies. *Theriogenology* **86,** 443–450 (2016).
23. Gualtieri, R. *et al.* Bovine oviductal monolayers cultured under three-dimension conditions secrete factors able to release spermatozoa adhering to the tubal reservoir in vitro. *Theriogenology* **79,** 429–435 (2013).
24. Gualtieri, R. *et al.* Long-term viability and differentiation of bovine oviductal monolayers: Bidimensional versus three-dimensional culture. *Theriogenology* **78,** 1456–1464 (2012).
25. Sostaric, E. *et al.* Sperm binding properties and secretory activity of the bovine oviduct immediately before and after ovulation. *Mol. Reprod. Dev.* **75,** 60–74 (2008).
26. Chen, S., Einspanier, R. & Schoen, J. Long-term culture of primary porcine oviduct epithelial cells: Validation of a comprehensive invitro model for reproductive science. *Theriogenology* **80,** 862–869 (2013).
27. Rajagopal, M., Tollner, T. L., Finkbeiner, W. E., Cherr, G. N. & Widdicombe, J. H. Differentiated structure and function of primary cultures of monkey oviductal epithelium. *Vitr. cell. Dev. Biol.* **42,** 248–254 (2006).
28. Fotheringham, S., Levanon, K. & Drapkin, R. Ex vivo Culture of Primary Human Fallopian Tube Epithelial Cells. *J. Vis. Exp.* 3–7 (2011). doi:10.3791/2728
29. Pampaloni, F., Reynaud, E. G. & Stelzer, E. H. K. The third dimension bridges the gap between cell culture and live tissue. *Nat. Rev. Mol. Cell Biol.* **8,** 839–845 (2007).
30. Yu, J., Peng, S., Luo, D. & March, J. C. In vitro 3D human small intestinal villous model for drug permeability determination. *Biotechnol. Bioeng.* **109,** 2173–2178 (2012).
31. Huh, D., Hamilton, G. A. & Ingber, D. E. From 3D cell culture to organs-on-chips. *Trends Cell Biol.* **21,** 745–754 (2011).
32. Kessler, M. *et al.* The Notch and Wnt pathways regulate stemness and differentiation in human fallopian tube organoids. *Nat. Commun.* **6,** 8989 (2015).
33. Costello, C. M. *et al.* Synthetic small intestinal scaffolds for improved studies of intestinal differentiation. *Biotechnol. Bioeng.* **111,** 1222–1232 (2014).
34. Macdonald, N. P. *et al.* Assessment of biocompatibility of 3D printed photopolymers using zebrafish embryo toxicity assays. *Lab Chip* **16,** 291–7 (2016).
35. Van Tol, H. T. A. A., Van Eerdenburg, F. J. C. M. C. M., Colenbrander, B. & Roelen, B. A. J. J. Enhancement of Bovine oocyte maturation by leptin is accompanied by an upregulation in mRNA expression of leptin receptor isoforms in cumulus cells. *Mol. Reprod. Dev.* **75,** 578–587 (2008).
36. Scherr, T. *et al.* Microfluidics and numerical simulation as methods for standardization of zebrafish sperm cell activation. *Biomed. Microdevices* **17,** 1–10 (2015).
37. Angione, S. L., Oulhen, N., Brayboy, L. M., Tripathi, A. & Wessel, G. M. Simple perfusion apparatus for manipulation, tracking, and study of oocytes and embryos. *Fertil. Steril.* **103,** 281–290 (2015).
38. Knowlton, S. M., Sadasivam, M. & Tasoglu, S. Microfluidics for sperm research. *Trends Biotechnol.* **33,** 221–229 (2016).
39. El-Sherry, T. M., Elsayed, M., Abdelhafez, H. K. & Abdelgawad, M. Characterization of rheotaxis of bull sperm using microfluidics. *Integr. Biol.* **6,** 1111–1121 (2014).
40. Kim, M. S., Bae, C. Y., Wee, G., Han, Y. M. & Park, J. K. A microfluidic in vitro cultivation system for mechanical stimulation of bovine embryos. *Electrophoresis* **30,**

3276–3282 (2009).
41. Abe, H. The mammalian oviductal epithelium: Regional variations in cytological and functional aspects of the oviductal secretory cells. *Histol. Histopathol.* **11,** 743–768 (1996).
42. Reischl, J. *et al.* Factors affecting proliferation and dedifferentiation of primary bovine oviduct epithelial cells in vitro. *Cell Tissue Res.* **296,** 371–383 (1999).
43. Joshi, M. S. Isolation, cell culture, and characterization of oviduct epithelial cells of the cow. *Microsc. Res. Tech.* **31,** 507–518 (1995).
44. Karst, A. M. & Drapkin, R. Primary culture and immortalization of human fallopian tube secretory epithelial cells. *Nat. Protoc.* **7,** 1755–1764 (2012).
45. Comer, M. T., Leese, H. J. & Southgate, J. Induction of a differentiated ciliated cell phenotype in primary cultures of Fallopian tube epithelium. *Hum. Reprod.* **13,** 3114–3120 (1998).
46. Coy, P. & Avilés, M. What controls polyspermy in mammals, the oviduct or the oocyte? *Biol. Rev.* **85,** 593–605 (2010).
47. Mondéjar, I., Martínez-Martínez, I., Avilés, M. & Coy, P. Identification of potential oviductal factors responsible for zona pellucida hardening and monospermy during fertilization in mammals. *Biol. Reprod.* **89,** 67 (2013).
48. Topper, E. K., Killian, G. J., Way, a, Engel, B. & Woelders, H. Influence of capacitation and fluids from the male and female genital tract on the zona binding ability of bull spermatozoa. *J. Reprod. Fertil.* **115,** 175–183 (1999).
49. Rodríguez, C., Killian, G., Rodríguez, C. & Killian, G. Identification of ampullary and isthmic oviductal fluid proteins that associate with the bovine sperm membrane. *Anim. Reprod. Sci.* **54,** 1–12 (1998).
50. Killian, G. J. Evidence for the role of oviduct secretions in sperm function, fertilization and embryo development. *Anim. Reprod. Sci.* **82–83,** 141–153 (2004).
51. Erikson, D. W., Way, A. L., Bertolla, R. P., Chapman, D. A. & Killian, G. J. Influence of osteopontin , casein and oviductal fluid on bovine sperm capacitation. *Anim. Reprod.* **4,** 103–112 (2007).
52. Taitzoglou, I. a., Kokoli, A. N. & Killian, G. J. Modifications of surface carbohydrates on bovine spermatozoa mediated by oviductal fluid: A flow cytometric study using lectins. *Int. J. Androl.* **30,** 108–114 (2007).
53. Dejonge, C. J. *et al.* The Acrosome Reaction-Inducing Effect of Human Follicular and Oviductal Fluid. *J. Androl.* **141,** 359–365 (1993).
54. King, R. S., Anderson, S. H. & Killian, G. J. Effect of Bovine Oviductal Estrus-Associated Protein on the Ability of Sperm to Capacitate and Fertilize Oocytes. *J. Androl.* **15,** 468–478 (1994).
55. Besenfelder, U., Havlicek, V. & Brem, G. Role of the oviduct in early embryo development. *Reprod. Domest. Anim.* **47,** 156–163 (2012).
56. Monaco, E. *et al.* Effect of osteopontin (OPN) on in vitro embryo development in cattle. *Theriogenology* **71,** 450–457 (2009).
57. Kölle, S., Reese, S. & Kummer, W. New aspects of gamete transport, fertilization, and embryonic development in the oviduct gained by means of live cell imaging. *Theriogenology* **73,** 786–795 (2010).
58. Zaccagnini, G., Maione, B., Lorenzini, R. & Spadafora, C. Increased production of mouse embryos in in vitro fertilization by preincubating sperm cells with the nuclease inhibitor aurintricarboxylic acid. *Biol. Reprod.* **59,** 1549–53 (1998).
59. Lopera-Vásquez, R. *et al.* Extracellular Vesicles from BOEC in In Vitro Embryo Development and Quality. *PLoS One* **11,** e0148083 (2016).
60. Maillo, V. *et al.* Oviduct-Embryo Interactions in Cattle: Two-Way Traffic or a One-Way Street? *Biol. Reprod.* **92,** 144–144 (2015).
61. Sanches, B. V. *et al.* Comparison of Synthetic Oviductal Fluid and G1/G2 Medium under Low-1 Oxygen Atmosphere on Embryo Production and Pregnancy Rates in

Nelore (Bos indicus) Cattle. *Reprod. Domest. Anim.* **48,** 7–9 (2013).
62. Bakhtari, A. & Ross, P. J. DPPA3 prevents cytosine hydroxymethylation of the maternal pronucleus and is required for normal development in bovine embryos. *Epigenetics* **9,** 1271–1279 (2014).
63. Young, L. E., Sinclair, K. D. & Wilmut, I. Large offspring syndrome in cattle and sheep. *Rev. Reprod.* **3,** 155–163 (1998).
64. Young, L. E. *et al.* Epigenetic change in IGF2R is associated with fetal overgrowth after sheep embryo culture. *Nat. Genet.* **27,** 153–154 (2001).
65. Young, L. E. *et al.* Conservation of IGF2-H19 and IGF2R imprinting in sheep: effects of somatic cell nuclear transfer. *Mech. Dev.* **120,** 1433–1442 (2003).

Chapter 4

Functional biocompatibility tests of bioengineered polymers on in vitro bovine embryo production

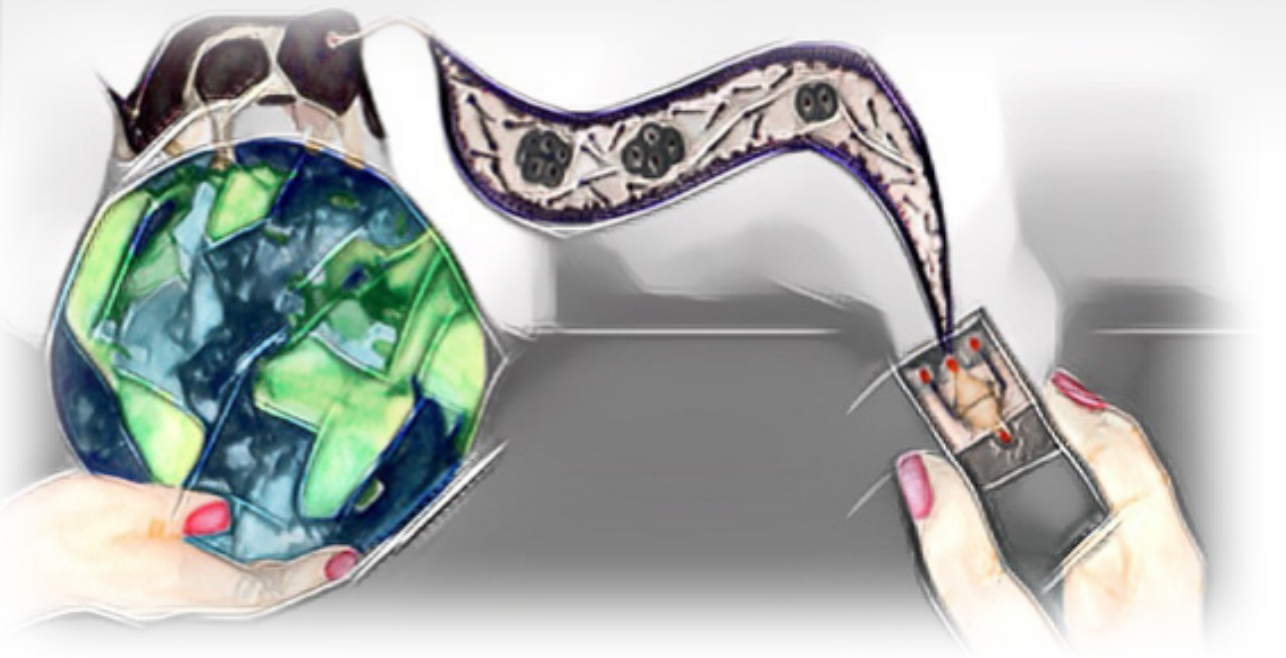

Marcia A. M. M. Ferraz, Heiko H. W. Henning, Pedro F. Costa, Jos Malda, Séverine Le Gac, Fabrice Bray, Majorie B. M. van Duursen, Jos F. Brouwers, Chris. H.A. van de Lest, Peter L. A. M. Vos, Tom A. E. Stout and Bart M. Gadella. Functional biocompatibility tests of bioengineered polymers on *in vitro* bovine embryo production. Submitted.

Abstract

The early embryo is sensitive to its surrounding environment, which should be taken into consideration when choosing materials for bioengineering. Previously, we showed that a PIC100 3D-printed oviduct-on-a-chip system improved fertilization with exclusive mono-spermic fertilization in bovine. Here, a follow-up on the embryo development further than 2-cell stage turned out to be inhibited by PIC100. In analogy, four other materials (E-Shell200, E-Shell300, polystyrene (PS) and polydimethylsiloxane (PDMS)) were tested for their biocompatibility towards bovine embryo development. PS and PDMS were found non-toxic for embryo development while PIC100 was most toxic. The degree of toxicity directly related to the amount of released diethyl-phthalate and polyethylene glycol, as revealed by mass spectrometry analysis. PS and PDMS only had minimal release and did not inhibit the two-cell stage to blastocyst development. Furthermore, only PS did not affect estrogen receptor (ER) transactivation in a human ovarian cell line. These findings imply that the first cleavages of bovine embryos are much more sensitive to components released from 3D-printed polymers than previously described for oviduct epithelial cells and that PS and PDMS are materials of choice for creating organs-on-a-chip, especially considering systems for optimized embryo production.

Introduction

The combination of recent innovations in three-dimensional (3D) cell culture such as 3D-printing and microfluidics allowed the creation of organ-on-a-chips systems that better mimic the *in vivo* morphology, physiology and pathophysiology of tissues and organs[1]. For instance, organ-on-a-chip models have been produced for various tissues including liver[2–4], lung[5,6], kidney[7,8], gut[9–11], bone[12], breast[13,14], eye[15], brain [6] and the female reproductive tract[17–19]. Nowadays, 3D-printing supports fast prototyping allowing researchers to design and fabricate devices in a short period of time[20]. The use of 3D-printed parts in life sciences and the medical fields has increased in the past decades; however, the effects of the 3D-printed materials to either the body or a bioengineered culture system need to be further investigated[21].

Bioengineered culture systems have also been used to study the physiology of gametes and embryo development[22–29]. Importantly, the developing embryos have been reported to be extremely sensitive to their *in vivo* as well as *in vitro* environments[30]. The current study focuses on polymer materials that are used for the fabrication of 3D casts and their potential adverse effects on biological models. To this end, biocompatibility assays have been performed using a variety of plastic materials that were tested on a routine procedure for bovine embryo production. The rationale to test these plastics on bovine embryo production originates from two recent studies. First, MacDonald et al. observed that four commercially available 3D-printing photo-polymers were highly toxic to zebrafish embryos (100% embryo loss within 90 hours of culture), one of these materials being still listed as being biocompatible for medical devices by its manufacturer [0]. This finding clearly confirms that early developmental stages of embryos are extremely sensitive to their environment. In another study, Oskui et al. demonstrated that

3D-printed parts leaked three different chemical components after five days of incubation with water[21]. These studies suggest that the deterioration of embryos cultured in presence of 3D-printed polymers could be due to the leakage of components from those materials.

To improve *in vitro* embryo production, we developed a 3D-printed oviduct-on-a-chip system, which was fabricated by stereolithography using PIC100 (mixture of acrylate and methacrylate monomers). This system was tested for bovine fertilization and early embryo development[17]. Using this system we reliably cultured a differentiated 3D confluent bovine oviductal epithelial cell (BOEC) layer[17]. At the apical side of the BOEC, sperm binding was observed on the 3D monolayer, resulting in both sperm activation as well as fertilization of the oocyte. In fact, the oviduct-on-a-chip system supported fertilization by self-conditioning of the apical fluid compartment, which excluded the incidence of polyspermic fertilization and parthenogenesis. Instead, in classical IVF, hormonal conditioning of the fertilization medium is required and this does not allow exclusive monospermic fertilization. Thus the oviduct-on-a-chip approach better mimics the *in vivo* situation[17]. Nevertheless, also based on previous reports, we were concerned about the possible leakage of components from the 3D-printed materials and their likely effects on the early embryos. Therefore, in the current study we have followed the developmental fate of zygotes in time (up to day eight) when in contact with PIC100, the material our oviduct-on-a-chip system was made of[17]. We compared PIC100 with a number of other polymer materials (E-Sell200, E-Shell300, PDMS and PS) also used in 3D cell culture applications regarding potential adverse effects during the first eight days of bovine embryo development. Based on our results, we finally propose a better and more stringent definition of biocompatibility when using polymers for 3D cell culturing and also discuss the importance of proper bio functionality assays when using 3D cell culture approaches for tissues and/or organs engineering.

Experimental

Chemicals

Unless stated otherwise, all chemicals were obtained from Sigma Chemical Co. (St. Louis, MO) and were of the highest purity available.

Polystyrene (PS) and polydimethylsiloxane (PDMS) polymer structures

A two-component kit (Sylgard 184, Dow Corning, Farnell, Maarssen, The Netherlands) consisting of pre-polymer and curing agent was used to fabricate PDMS structures. These two components were mixed in a 10:1 weight ratio. This mixture was degassed, poured onto a silicon wafer, and degassed again to remove any air bubble. Curing was performed at 60^{o}C overnight. After curing, the PDMS layer was released from the silicon wafer and cut into pieces

of 1 cm diameter and 0.2 cm thickness. For PS, CELLSTAR petri dishes (Greiner, Bio-One GmbH, Alphen aan de Rijn, The Netherlands) were cut into structures of 1cm diameter and 0.2 cm thickness.

Production, pre-washing and sterilization of three-dimensional printed PIC 100, E-Shell200 and E-Shell300 polymer structures

The prototype design of the polymer structures (discs of 1 cm diameter and 0.2 cm thickness) was created using Tinkercad (Autodesk Inc., CA, USA). The design was exported from Tinkercad as an STL file, into Mimics software (Materialise NV, Leuven, Belgium) to correct for any mesh error and generate printing support structures. Devices were 3D-printed using a photo-polymerization process and a Perfactory 3 Mini 3D printer (Envisiontec GmbH, Gladbeck, Germany) at a resolution of 50 µm, in various materials: PIC100, E-Shell200 and E-Shell300 (Envisiontec GmbH, Gladbeck, Germany).

To limit leakage of compounds from the PIC100 3D-printed material that could interfere with embryo viability, the excess resin was removed by 15 min immersion in ethanol at room temperature. After complete air drying, the structures were immersed 3 times for 2 h in isopropanol at room temperature. After air drying again, the structures were light-cured using 4000 flashes using an Otoflash G171 (Envisiontec GmbH, Gladbeck, Germany).

All polymer structures were next sterilized by immersion for 1 h in 70% ethanol, washed three times for 30 min in phosphate buffer saline solution (PBS) and then washed for 1 h in HEPES buffered Medium 199 supplemented with 100 U/mL penicillin and 100 µg/mL streptomycin at room temperature.

Isolation of oviduct cells and long-term oviduct cell culture

Cow oviducts were collected from a local abattoir immediately after slaughter and transported to the laboratory on ice. The oviducts were dissected free of surrounding tissue and washed three times in cold PBS supplemented with 100 U/mL of penicillin and 100 µg/mL of streptomycin. BOECs were isolated by squeezing the total oviduct content out of the ampullary end of the oviducts, and collected in HEPES buffered Medium 199 supplemented with 100 U/mL penicillin and 100 µg/mL streptomycin. Cells were washed twice by centrifuging at 500 x g for 10 min at 25°C in HEPES buffered Medium 199 supplemented with 100 U/mL of penicillin and 100 µg/mL of streptomycin. Next, cells were cultured for 24 h in HEPES buffered Medium 199 supplemented with 100 U/mL penicillin, 100 µg/mL streptomycin and 10% fetal calf serum (FCS; Bovogen Biologicals, Melbourne, Australia). During these 24 h, the cells arranged themselves into floating vesicles with outward facing actively beating cilia; these vesicles were collected, centrifuged at 500 x g for 10 min at 25°C, resuspended in DMEM/Ham's F12 medium (DMEM/F-12 Glutamax I, Gibco BRL, Paisley, U.K.) supplemented with 1.4 mM hydrocortisone, 5 mg/mL insulin, 10 mg/mL transferrin, 2.7 mM epinephrine, 9.7 nM

tri-iodothyronine, 0.5 ng/mL epidermal growth factor, 50 nM trans-retinoic acid, 2% bovine pituitary extract (containing 14 mg/mL protein), 1.5 mg/mL fatty acid free bovine serum albumin (BSA, a6003, Sigma Chemical Co., St. Louis, MO), 100 mg/mL gentamycin, and 2.5 mg/mL amphotericin B (3D culture medium), and pipetted up and down several times to mechanically separate the cells. Next, cells were seeded into a transwell device (Corning Inc, NY, USA; 3D culture; 0.6 x 10^6 cells/cm^2). Cells were cultured in 3D culture medium in a humidified atmosphere of 5% CO_2-in-air at 38.5°C until they reached confluence (5-7 days). Thereafter, an air-liquid interface was established by removing the medium in the apical compartment for up to 42 days in a humidified atmosphere of 5% CO_2-in-air at 38.5°C. The basolateral medium was completely refreshed with 3D culture medium twice a week. A total of six animals and 8 transwells for each animal were used for 3D culture.

Morphological and functional characterization of 3D cultures

Cell differentiation

At week 4 of air-liquid interface culture, in one transwell per animal (n = 6), cilia formation on the epithelial cells was assessed. The membranes were dismounted from the transwell chamber for immunofluorescent staining. The membranes were washed in PBS, fixed in 4% (w/v) paraformaldehyde dissolved in PBS, and permeabilized for 30 min using 0.5% (v/v) Triton-X100 in PBS. Non-specific binding was blocked by incubation for 1 h in PBS containing 5% (w/v) normal goat serum, at room temperature. Cells were then incubated overnight at 4°C with a mouse anti-acetylated α-tubulin primary antibody (1:100 dilution, Santa Cruz Biotechnology, Santa Cruz, CA). The next morning the cells were washed three times in PBS (5 min per wash) and incubated with an Alexa 488-conjugated goat anti-mouse antibody (1:100, Santa Cruz Biotechnology, Santa Cruz, CA) at room temperature for 1 h. Hoechst 33342 (5 µg/mL) was used to stain cell nuclei. Negative controls were performed by omitting the incubation with the primary antibody. Imaging was performed by confocal laser scanning microscopy using a TCS SPE-II system (Leica Microsystems GmbH, Wetzlar, Germany) attached to an inverted semi-automated DMI4000 microscope (Leica) at 40 x magnification. Five random fields of view in the center of the membrane were imaged for each animal and, at least, 350 cells per animal were classified; the percentage of ciliated cells was determined.

Transepithelial electrical resistance (TEER)

TEER measurements were performed using a Millicell ERS-2 Volt-ohmmeter (Merck Millipore, Darmstadt, Germany). Before measurement, 500 µL of 3D culture medium was added in the apical compartment of the day 27 3D culture and cells were placed back into the incubator for 15 min. Electrodes were equilibrated and sterilized according to the manufacturer's recommendations. The TEER value of a transwell without cells was utilized as a blank value. To determine the sample resistance, the blank value was subtracted from the total resistance of

the sample and the TEER value ($\Omega.cm^2$) was calculated by multiplying the sample resistance with the area of the transwell membrane (1.12 cm^2).

Oocyte collection and in vitro maturation (IVM)

Bovine ovaries were collected from a local abattoir and transported to the laboratory within 2 h after dissection. The ovaries were washed in physiological saline solution (0.9 % w/v NaCl) and held in physiological saline solution containing 100 U/mLpenicillin and 100 µg/mL streptomycin at a temperature of 30°C. The fluid and cumulus oocyte complexes (COCs) were aspirated from follicles with a diameter ranging from 2 to 8 mm and collected into a 50 mL conical tube using a 19-gauge needle and a vacuum pump[31]. COCs with a minimum of three layers of intact cumulus cells were selected and first washed in HEPES-buffered M199 (Gibco BRL, Paisley, UK) before being washed and cultured in maturation medium (M199 supplemented with 0.02 IU/mL follicle-stimulating hormone (Sioux Biochemical Inc., Sioux Center, IA)), 0.02 IU/mL luteinizing hormone (Sioux Biochemical Inc.), 7.71 µg/mL cysteamine, 10 ng/mL epidermal growth factor in 0.1% (w/v) fatty acid-free bovine serum albumin (BSA) and 100 U/mL penicillin and 100 µg/mL streptomycin. Selected COCs were cultured in four-well culture plates (Nunc A/S, Roskilde, Denmark) containing maturation medium. The oocytes were matured in groups of 50 COCs in 500 µL maturation medium and incubated in a humidified atmosphere of 5% CO_2-in-air for 24 h at 38.5°C.

Sperm preparation for in vitro fertilization (IVF)

Frozen sperm was thawed and prepared as described before[31]. Briefly, sperm 250-µL straws were thawed at 37°C for 30 s and washed by centrifugation at 700 x g for 30 min through a discontinuous Percoll gradient (GE Healthcare, USA) at 27°C. The supernatant was removed and the pellet resuspended in fertilization medium (modified Tyrode's medium supplemented with 25 mM sodium bicarbonate, 22 mM lactate, 1 mM pyruvate, and 6 mg/mL fatty acid–free BSA; the medium containing 100 U/mL penicillin and 100 µg/mL streptomycin).-

In vitro fertilization (IVF) and culture (IVC) using 3D cultured BOECs

Fertilization medium and culture media (synthetic oviductal medium; SOF medium) were conditioned for 24 h with routinely detoxified PIC100 structures, and compared to control media that have not been exposed to PIC100 structures. At day 28 of BOEC culture the basolateral 3D medium was replaced by fertilization medium (conditioned and not conditioned) and a total of 50 *in vitro* matured COCs were added to the apical compartment (with 500 µL of fertilization medium not conditioned, but supplemented with 10 µg/ml heparin, 20 µM d-penicillamine, 10 µM hypotaurine, and 1 µM epinephrine) of each of the 3D culture transwells (n=8 transwells; 35-50 COCs per insert). Sperm was also added to a final concentration of 10^6 sperm cells/mL.

After 20-22 h of co-incubation under a humidified atmosphere of 5% CO_2-in-air at 38.5°C, cumulus cells were removed by pipetting, the presumptive zygotes were cultured in the apical compartment (with 500 µL of SOF medium not conditioned; 35-50 zygotes per insert) and the basolateral fertilization medium (conditioned and not conditioned) was replaced by SOF medium (conditioned and not conditioned). The embryos were cultured for eight days under a humidified atmosphere of 5% CO_2 and 5% O_2 at 38.5°C. At day 5 post-fertilization all embryos were transferred to fresh SOF medium.

Similar IVF and IVC procedures were performed in transwell without BOECs as a control group. Three replicates for both control and 3D culture groups (with conditioned and not conditioned medium) were performed. A total of 380 COCs in conditioned medium group and 396 COCs in control non-conditioned medium group were fertilized and further cultured in the same conditioned versus non-conditioned media in the 3D culture transwell, respectively. In parallel a total of 376 COCs were fertilized in conditioned medium group and 380 COCs in non-conditioned medium group and their further embryo development was followed in the absence of 3D cultured BOECs.

In vitro fertilization (IVF) and culture (IVC) using PDMS, PS, E-Shell200 and E-Shell300 polymer structures

Mature COCs were distributed in groups of 35-50 in four-well culture plates (Nunc A/S, Roskilde, Denmark) with 500 µL of fertilization medium supplemented with 10 µg/mL heparin, 20 µM d-penicillamine, 10 µM hypotaurine, and 1 µM epinephrine. Polymer structures of PS, PDMS, E-Shell200 and E-Shell300 were separately added to individual fertilization wells while control wells did not include any polymer structure. After 20-22 h of co-incubation under a humidified atmosphere of 5% CO_2-in-air at 38.5°C, cumulus cells were removed by pipetting and the presumptive zygotes were cultured in groups of 50 in four-well culture plates with 500 µL of SOF medium, with or without respective polymer structures. The embryos were cultured for eight days under a humidified atmosphere of 5% CO_2 and 5% O_2 at 38.5°C.

Three replicates for both control and all polymer structure groups were performed (total number of COCs used were 604 for control and 152, 150, 150 and 148 for PDMS, PS, E-Shell200 and E-Shell300 polymers, respectively).

Scoring of embryo developmental competence

Two days post-fertilization (dpf), the number of cleaved embryos was scored under a reversed light microscope, using a 20x objective (Olympus Nederland BV, The Netherlands). At eight dpf the number of expanded blastocysts was determined.

Collection of leachates from the plastics for toxicology assays

Cell culture medium and ultrapure water (Milli-Q water; Millipore, Darmstadt, Germany) were conditioned for 24 h with routinely detoxified PIC100, E-Shell200, E-Shell300, PDMS and PS structures under a humidified atmosphere of 5% CO_2 and 5% O_2 at 38.5°C. A ratio of 2.5 mL of media/water per cm^2 of polymer structure was used. As a control 2.5 mL milliQ water or cell culture medium was subjected to the same procedure as negative control. The resulting polymer conditioned MilliQ water or media and their negative controls were kept at -20°C until use.

Cell-based ER-mediated bioassay

For the estrogen receptor assay culture media with eventual leachates from the polymers was used for evaluating their possible effects on the estrogen receptor (ER) activation on the BG1Luc4E2 cell line, as described previously[32]. This recombinant human ovarian carcinoma (BG-1) cell line is stably transfected with an estrogen receptor element (ERE) and a luciferase transporter gene[33]. The cells were plated in luminescence 96-wells plates at a cell density of $0.4x10^5$ cells/well. After 24 h, the cells were exposed to the conditioned media or medium containing estradiol as positive control. Thereafter, the cells were washed with warm PBS and subsequently lysed with 20 µL lysis buffer (Promega, Leiden, Netherlands) per well. After 30 min, luminescence was measured with a luminometer (Lumistar OPTIMA, BMG Labtech, Ortenberg Germany), after adding 100 µL of a luciferine buffer solution composed of 470 µM luciferin (Promega, Leiden, Netherlands) as well as 530 µM ATP (Roche Diagnostics, Leiden, Nederland B.V.) in MiliQ at a pH of 7.8.

MS analysis for identification of leaked compounds from the plastics

MilliQ water (negative control) and MilliQ water exposed to plastic materials were processed for MALDI-MS detection of eventual leachates from the plastics. To this end the samples were first dried under vacuum and the resulting dried powders were subsequently solubilized in 20 µL of a 1:1 methanol:tetrahydrofuran mixture. For each analysis, 0.5 µL of this solution was mixed with 0.5 µL of dihydrobenzoic acid matrix in solution at 10 mg/mL in methanol with 0.1% of formic acid, and this mixture was deposited on a MALDI polished steel target, and let dry and crystallize. MALDI-MS analysis was performed on a Voyager-DE™ PRO Biospectrometry Workstation (Applied Biosystems) controlled by Voyager Control Panel Software (Foster City, CA, USA). Analyses were conducted in positive linear mode using a nitrogen laser (337 nm) for ionization and using Data Explorer 4.0 software from Applied Biosystems.

A more precise measurement of the components present in the samples exposed to the polymer materials was done by direct injection (5 µL per minute) into a high precision electrospray ionization mass spectrometer (ESI-MS) (Orbitrap Fusion™, Tribrid™ from Thermo Scientific, Waltham, Massachussetts, USA). ESI-MS analyses were conducted at 3.5 kV in the positive mode at an ionization temperature of 100°C in the m/z range of 150-4000 *m/z* allowing to determine *m/z* values with a precision of 0.001 m/z. For quantitation of the 177.06 and

223.10 m/z peaks di-ethyl phthalate (Sigma-Aldrich Chemie GmbH, Steinheim, Germany) was solubilized first 1:100 (v/v) in distilled ethanol and subsequently further to a concentration series of 10^{-3} – 10^{-12} M in MilliQ water. This series were injected into the ESI-MS; the 1 µM diethyl-phthalate sample was used to check whether this fragmented similarly to the 223.10 peak from the expose samples. (See supplemental figure 1 for reference mass spectrogram).

Data analysis

Data were analyzed using IBM SPSS Statistics (version 24). A Shapiro-Wilk test was performed and all groups were normally distributed. Differences between groups were examined using independent samples t-tests ($p<0.05$).

Results and Discussion

Toxicological screening of bioengineered materials is of great importance before one can safely use such materials for medical and biological applications. This is even more relevant when using miniaturized and microfluidic systems, in which the surface–to-volume ratio is increased and the distance between the polymer surface and cells is minimized[20,28,34,35]. These properties cause a dramatic increase in the exposure of the biological entity to bioengineered materials including possible toxic component(s), when compared to classical cell culture systems (in culture flasks or petri dishes). In this study, polymer structures produced from PIC100, E-Shell200, E-Shell300, PDMS and PS were tested in a bovine embryo development bioassay. The plastic materials were chosen either because they are commonly used for bioengineering purposes or because they were shown to improve bovine *in vitro* fertilization[17].

PIC100 inhibits blastocyst formation

We observed that using medium conditioned with PIC100 3D-printed structures, the cleavage rate had a 7-fold reduction and the blastocyst formation was completely blocked, when compared to non-conditioned medium ($p<0.05$; Figure 1). Interestingly, this negative effect was less pronounced but still significant when embryos were produced in transwell devices with BOEC monolayers that were fed, on their basolateral side, with PIC100-conditioned medium, when compared to basolateral feeding with non-conditioned medium ($p<0.05$; Figure 1). Thus the confluent BOEC monolayer partly acted as a protective layer, preventing the diffusion of toxic compound(s) leaked from the PIC100 material into the apical compartment, where the oocyte is fertilized, followed by cell cleavages and further embryo development.

PIC100 is an inexpensive material used for 3D stereolithographic printing. Its exact compo-

sition is not mentioned in the product information sheet by the manufacturer, but the safety data sheet indicates that it contains photoinitiator, methacrylate and acrylate monomers. The PIC100 polymerized material was first subjected to an extensive and stringent washing using solvents (ethanol and isopropanol) and additional light-curing. Indeed this washing of PIC100 material resulted in unaffected oviductal epithelial cell growth, confluency and differentiation (Table 1, Figure 2)[17]. In contrast, this extensive cleaning of PIC100 did not prevent inhibition of embryo development (Figure 1). Similarly, post-curing methods using extensive solvent washes were previously reported to only bring limited improvement on zebrafish embryo survival, when a Visijet Crystal polymer was used for fabricating 3D-printed devices[20]. More intensive washing of PIC100 using solvents resulted in cracking and loss of its 3D morphology and of the specific features originally required for cell cultures (such as perfusion required for the oviduct-on-a-chip system[17]).

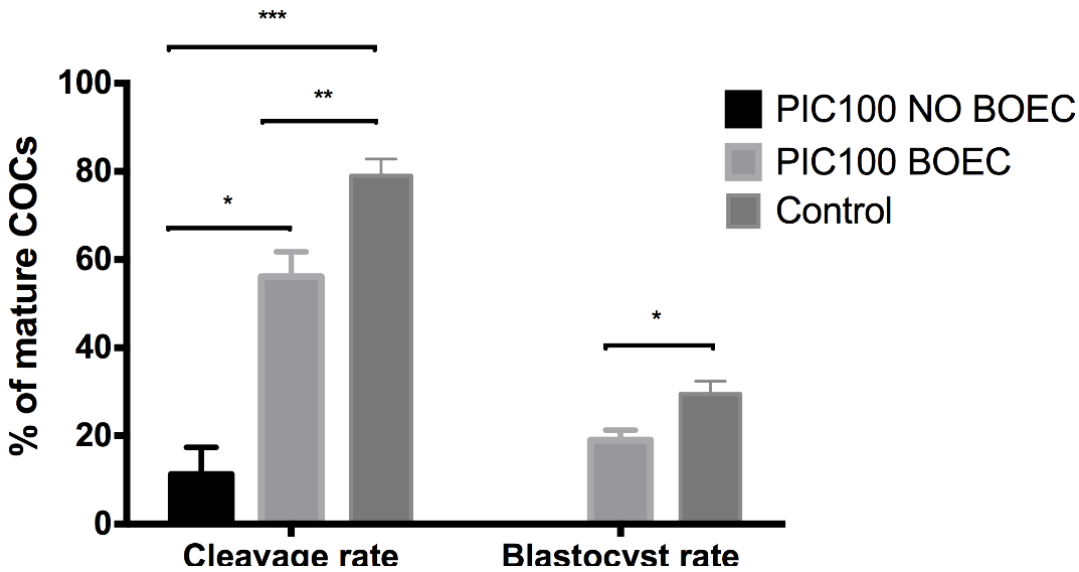

Figure 1. Cleavage and blastocyst rates are shown as percentage of cleaved embryos and blastocysts, respectively, of the total mature cumulus oocyte complexes (COCs) used for *in vitro* fertilization (IVF). IVF and *in vitro* culture (IVC) were performed using medium conditioned with PIC100 material in absence or presence of a bovine oviductal epithelial cell culture (PIC100 NO BOEC and PIC100 BOEC, respectively). Standard IVF and IVC were also performed without conditioned medium (Control). The cleavage rate was reduced for both PIC100 BOEC and PIC100 NO BOEC compared to the control group ($p<0.05$). A reduction in blastocyst rate was observed for PIC100 BOEC, compared to the control group ($p<0.05$) and blastocyst formation was completely blocked in PIC100 NO BOEC. Different symbols indicate statistically significant differences ($p<0.05$).

Table 1. Transepithelial electrical resistance (TEER) measurements and ciliation rate of bovine oviductal epithelial cells (BOECs) cultured in Transwell and originating from six animals, used in this study. TEER measurements were obtained at day 27 of air-liquid interface culture and data are presented as mean TEER ± standard deviation. Ciliation is determined as the percentage of cells positive to acetylated alpha-tubulin (ciliated cell) from the total cells counted.

Animal	TEER (mean ± SD Ω*cm²)	Ciliation (% of total cells counted)
1	534±25	23.3
2	546±37	26.2
3	523±56	25.4
4	782±63	24.3
5	631±47	23.6
6	578±34	24.7

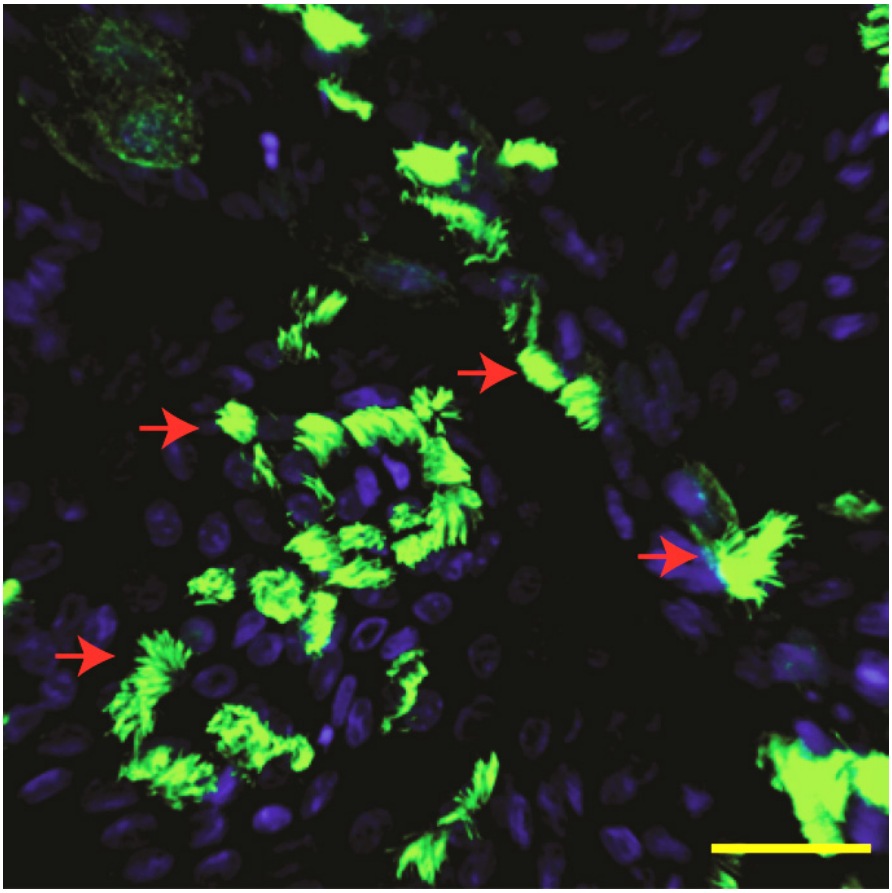

Figure 2. Immunofluorescence image of bovine oviductal epithelial cells (BOECs) cultured under 3D conditions in transwells at day 27 of air-liquid interface. Note the presence of ciliated (acetylated alpha-tubulin positive cells, green; red arrows) and non-ciliated cells (acetylated alpha-tubulin negative cells), nuclei were counter-stained using HOECHST33342 (blue). Scale bar = 25 µm.

Interestingly, the early stage embryos are not directly exposed to toxic compounds at the same concentrations as found in the blood plasma. Actually, under *in vivo* conditions, toxic components originating from the circulation need to transpass the oviductal epithelium before they can elicit effects in the lumen of the oviduct and on the developing embryo. Likewise, we demonstrated that the confluent BOEC monolayer partly protected the early embryo from the toxic components released from PIC100, probably by limiting the diffusion of these components into the apical compartment of the transwell devices, where embryos were located.

3D-printed E-Shell200 and E-Shell300 polymers also have a negative impact on embryo development

As an alternative to PIC100 we designed and stereolithographically printed 3D structures based on E-Shell200 and E-Shell300 materials. Both materials were reported to be biocompatible according to ISO 10993 by the manufacturer. Indeed, these two materials did not affect IVF and the first two cleavages of embryos (2-4 cell stages), but a reduction of 1.8 and 1.7-fold was observed in the blastocyst formation for E-Shell200 and E-Shell300, respectively ($p<0.05$; Figure 3). In contrast to the stated biocompatibility according to the international standard ISO 10993, both E-Shell200 and E-Shell300 had a negative impact on embryo development, though they were less harmful than PIC100 (Figures 1 & 3).

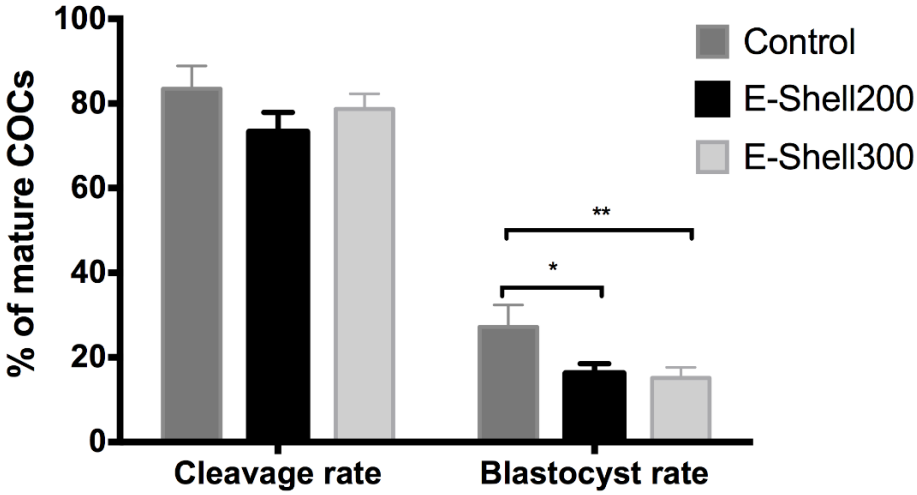

Figure 3. Cleavage and blastocyst rates are shown as percentage of cleaved embryos and blastocysts, respectively, of the total mature cumulus oocyte complexes (COCs) used for *in vitro* fertilization (IVF). IVF and *in vitro* culture (IVC) were performed in the presence of E-Shell200 or E-Shell300 polymer structures (E-Shell200 and E-Shell300, respectively). Standard IVF and IVC were also performed without polymer structures (Control). No difference was found in cleavage rates ($p>0.05$). A reduction in the blastocyst rates was observed for both E-Shell200 and E-Shell300 when compared to the control group ($p<0.05$).

Post-curing of E-Shell200 and E-Shell300 structures did not enhance the blastocyst rates when compared to no post-curing (16.2 and 15.1% *vs*. 14.3 and 15.4%, respectively; $p>0.05$). These results indicate that neither E-Shell200 nor E-Shell300 is a suitable starting material for creating bioengineered devices for embryo production and development.

Bioengineered PS and PDMS structures did not affect embryo development

The most commonly used polymer material for the production of microfluidic circuits and for lab-on-a-chip applications is poly(dimethylsiloxane) (PDMS)[37,38]. PDMS is an elastomer, which is widely used in academic research for rapid prototyping of microfluidic devices and organ-on-a-chip platforms[1,39]. Previous works have reported that PDMS is not toxic for embryo *in vitro* culture[28,29,40]. Here, the biocompatibility of PDMS structures was also tested for bovine embryo development (Figure 4). Indeed, no difference in cleavage and blastocyst rates were observed when IVF and IVC were performed in the presence of PDMS structures, compared to control conditions (no PDMS structure) ($p>0.05$). Hence, PDMS is a suitable alternative material for bioengineering devices for embryo production.

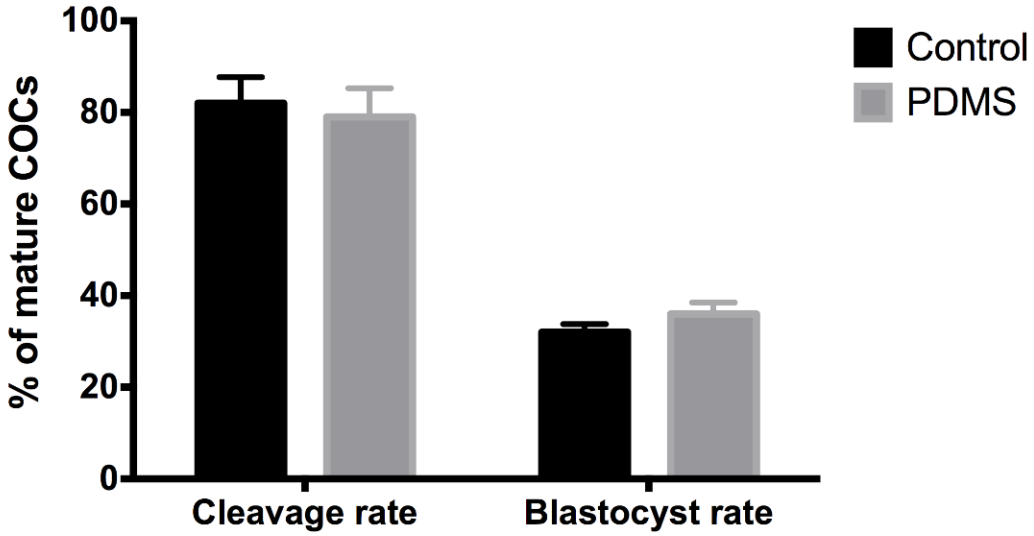

Figure 4. Cleavage and blastocyst rates are shown as percentage of cleaved embryos and blastocysts, respectively, of the total mature cumulus oocyte complexes (COCs) used for *in vitro* fertilization (IVF). IVF and *in vitro* culture (IVC) were performed in the presence of PDMS polymer structures (PDMS). Standard IVF and IVC were performed without PDMS structure (Control). No difference on cleavage neither blastocyst rate was observed ($p>0.05$).

Polystyrene (PS) is a hydrophobic thermoplastic polymer that is widely available at low costs[41], and most of the culture dishes used for IVP and cell culture are made from it. Therefore, we also evaluated the biocompatibility of PS structures with respect to embryo development. As shown in Figure 5, no adverse effects were observed neither on cleavage nor on blastocyst rates when IVF and IVC were performed in the presence or absence of PS structures ($p>0.05$). These results demonstrate that PS is another promising candidate for fabricating bioengineered devices for embryo production. Overall, the cleavage and blastocyst rates obtained in the presence of both PDMS and PS materials illustrate their suitability for use in

advanced manufacturing for the delivery of *in vitro* culture platforms.

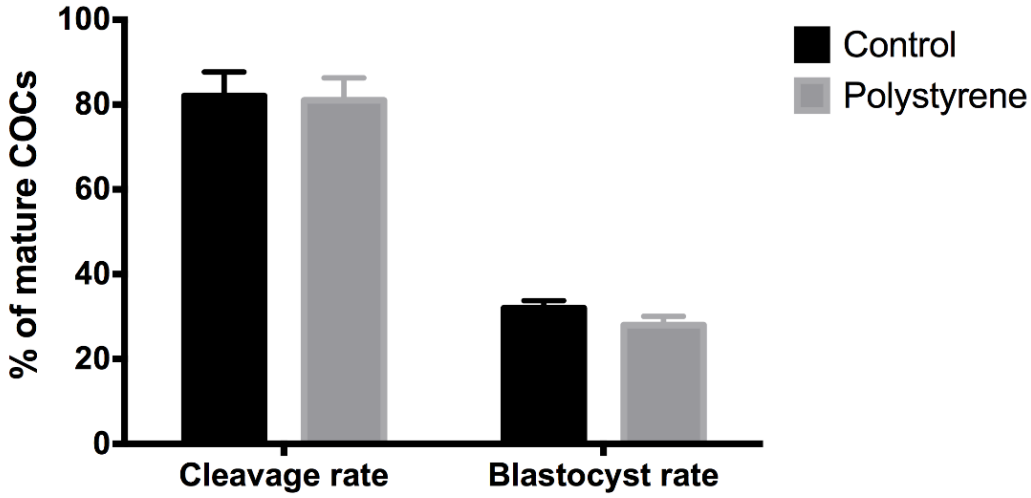

Figure 5. Cleavage and blastocyst rates are shown as percentage of cleaved embryos and blastocysts, respectively, of the total mature cumulus oocyte complexes (COCs) used for *in vitro* fertilization (IVF). IVF and *in vitro* culture (IVC) were performed in the presence of polystyrene polymer structures (PS). Standard IVF and IVC were performed without polystyrene structure (Control). No difference in cleavage and blastocyst rates was observed ($p>0.05$).

PS is the only bioengineered polymer that does not increase estrogen-dependent luciferase intensity

Considering that embryogenesis is strongly influenced by the hormonal environment and that polymers have been shown to leach hormonally active compounds[42–44], we tested whether the polymers considered in this work would release components that could activate the estrogen receptor (ER) using a cell based ER reporter gene assay[33,45]. The media were conditioned with polymer structures for 24 h and the luciferase assay indicated an increase in estrogen-dependent response after conditioning with PIC100, E-Shell-200, E-Shell300 and PDMS, while PS did not elicit any activation effects (Figure 6). It is worth noticing that the ER reporter assay is more sensitive than the blastocyst rate assay as PDMS did activate the ER response while it did not inhibit blastocyst formation. These results would suggest that the adverse effects on blastocyst rate caused by the leaked components from the 3D polymers do not necessarily have to interfere in the tested estrogen-dependent route.

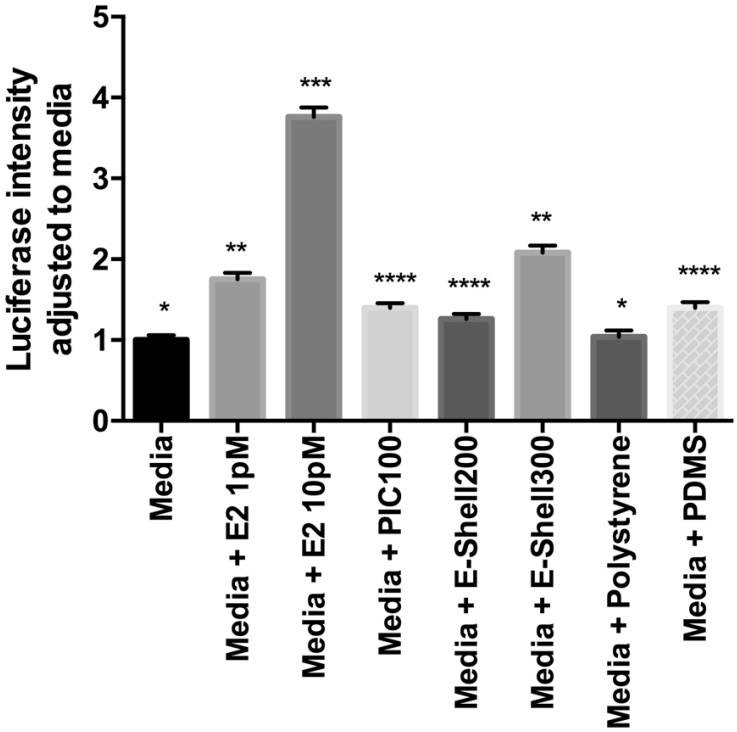

Figure 6. BG1ERE bioassay to detect ER-dependent luciferase increase by media conditioned with PIC100, E-Shell-200, E-Shell300, PS or PDMS or without any coditioning. An increase in the luciferase intensity is found for PIC100, E-Shell-200, E-Shell300 and PDMS. 1 pM and 10 pM estrogen (E2) supplementation was used to check the responsiveness of the cells in the assay. Different symbols indicate statistically significant differences ($p<0.05$).

Poly-ethylene glycol oligomers are released from the bioengineered PIC100 and E-Shell200 structures

One limitation in our study is the restricted information about the exact composition of the polymers. Polymers are versatile long chain organic molecules composed of covalently bound repeating units (monomers) linked to form a common backbone[46]. Normally, the polymer is constituted by chains of different lengths, since it is difficult to produce multiple polymer chains with identical lengths and its molecular weight (MW) is reported as an average value[46]. Importantly, unreacted monomers and short polymers can leak into the culture medium, which could lead to adverse intervention in physiological processes[46].

We hypothesized that oligomers could leak out of the bioengineered polymers to contribute to the toxic effects observed on bovine embryos. Through the use of Matrix Assisted Laser Desorption/Ionization- Mass Spectrometry (MALDI-MS) we observed that PIC100 and E-Shell200 released poly-ethylene glycol (PEG) oligomers after 24 h of conditioning in water (Figure 7), while the other tested materials (E-Shell300, PS and PDMS) did not release any PEG oligomers in the conditioned water. These results are in good agreement with Oskui et al., who detected using gas chromatography-mass spectrometry

leakage of at least three different chemical species from stereolithographic 3D-printed devices[21].

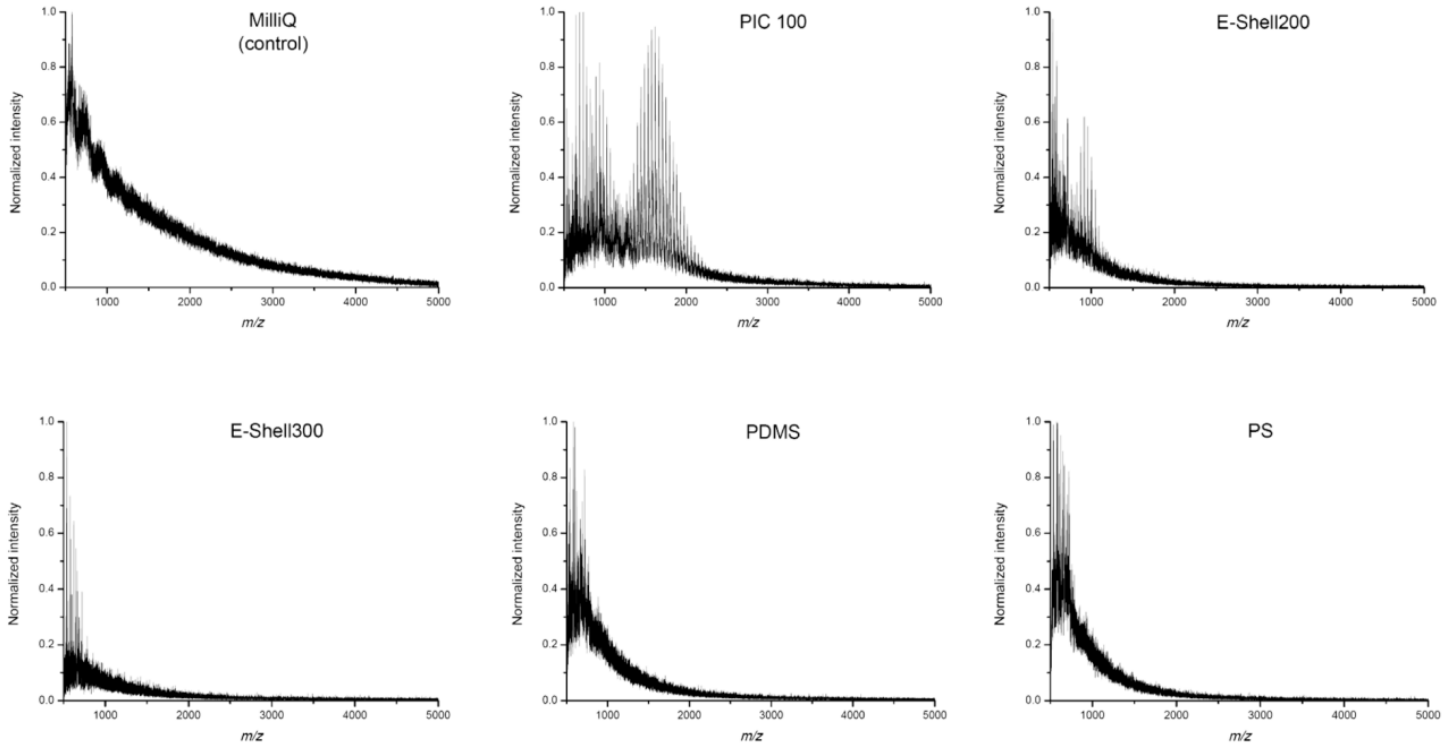

Figure 7. MALDI analysis of the leachate samples: MilliQ water only and milliQ water conditioned by PIC100, E-Shell200, E-Shell 300, PDMS and PS. Massifs of peaks spaced by 44 *m/z* were indicative for the release of diverse polyethylene glycols into MilliQ water

Identification of diethyl-phthalate as major component leaking from the plastics using high resolution ESI-MS

To further identify low molecular weight leaked components, which cannot be detected by MALDI-MS, the same samples (non-plastic but sham incubated MilliQ water; negative control) as well as MilliQ water incubated with PIC-100, E-shell200, E-shell300, PDMS or PS) were also analyzed by high resolution ESI-MS. The control MilliQ water contained trace amounts of a compound with an *m/z* value of 304.25 (Figure 8), which corresponds to a molecular formula $C_{16}H_{33}NO_4$ (with the assumption that the molecule is composed only of C, H, O, N with a C/H ratio between 1 and 3) for the non-ionized molecule. This molecule can originate from any material the sample has being in contact with: for instance, from MilliQ anion exchange resins or from pipette tips, tubes, bottles in which water was stored or handled with. It should be noted that the MilliQ water was -like immediately after tapping- before use of extreme purity (conductivity of MilliQ water was in each case >18 MΩ/cm^2). Since this peak at *m/z* 304.25 was present on all spectra, we decided to use it as an internal calibration to quantify the relative amount of released diethyl-phthalate (Table 2). As depicted in Figure 8, two peaks at *m/z* 223.10 and 177.06 were also detected in all water samples exposed to polymer materials. These peaks correspond respectively to a protonated diethyl-phthalate compound having a molecular formula of $C_{12}H_{24}O_4$ (theoretical *m/z* 223.0965) and a stable fragment of this compound formed by loss of ethanol (C10H9O3, theoretical *m/z* 177.0546), for which the fragmentation mechanism is provided in Figure 8. Based on this information, the diethyl-phthalate was successfully identified (see metabolite chart at https://metlin.scripps.edu/showChart.php?molid=69854&h=240&collE=20&Imode=p&etype=insilico). In addition we have injected a sample of 1 µM diethyl-phthalate into the ESI-MS and found an identical $[M+H]^+$ and fragment ion peak with identical fragmentation efficiency (see supplemental file 1). Next to this, for some of the materials (PIC100 and E-Shell200) oligomers of poly-ethylene glycol were found. As for the MALDI analysis, massifs of peaks spaced by 44 m/z were found, which is a characteristic signature of poly-ethylene glycol. In MS/MS spectra of individual poly-ethylene glycol peaks again such series with 44 *m/z* differences were found (data not shown). For the PIC-100 material, a second massif of peaks was detected in a lower *m/z* range, with a spacing of 22 *m/z*, corresponding to doubly charged poly-ethylene oligomers. These polymer peak series were also found with MALDI-MS analysis but their mass ranges differed to the ESI-MS analysis. In the MALDI-MS spectra, the ethylene glycol containing oligomers are found at higher *m/z* values (compare Figures 7 and 8). This result is expected as the sensitivity for different classes of compounds is very different when using ESI and MALDI, for which the ionization processes are totally different. Furthermore, the use of different analyzers - time-of-flight (TOF) for MALDI *vs*. Orbitrap for ESI - contributes to this difference, as a TOF analyzer is better adapted to higher *m/z* values. As summarized in Table 2, the relative amounts of diethyl-phthalate leaked from the polymer materials into the MilliQ water were in good agreement with the level of toxicity detected using the conditiond media for the different polymer materials (see Figures 1, 3-5).

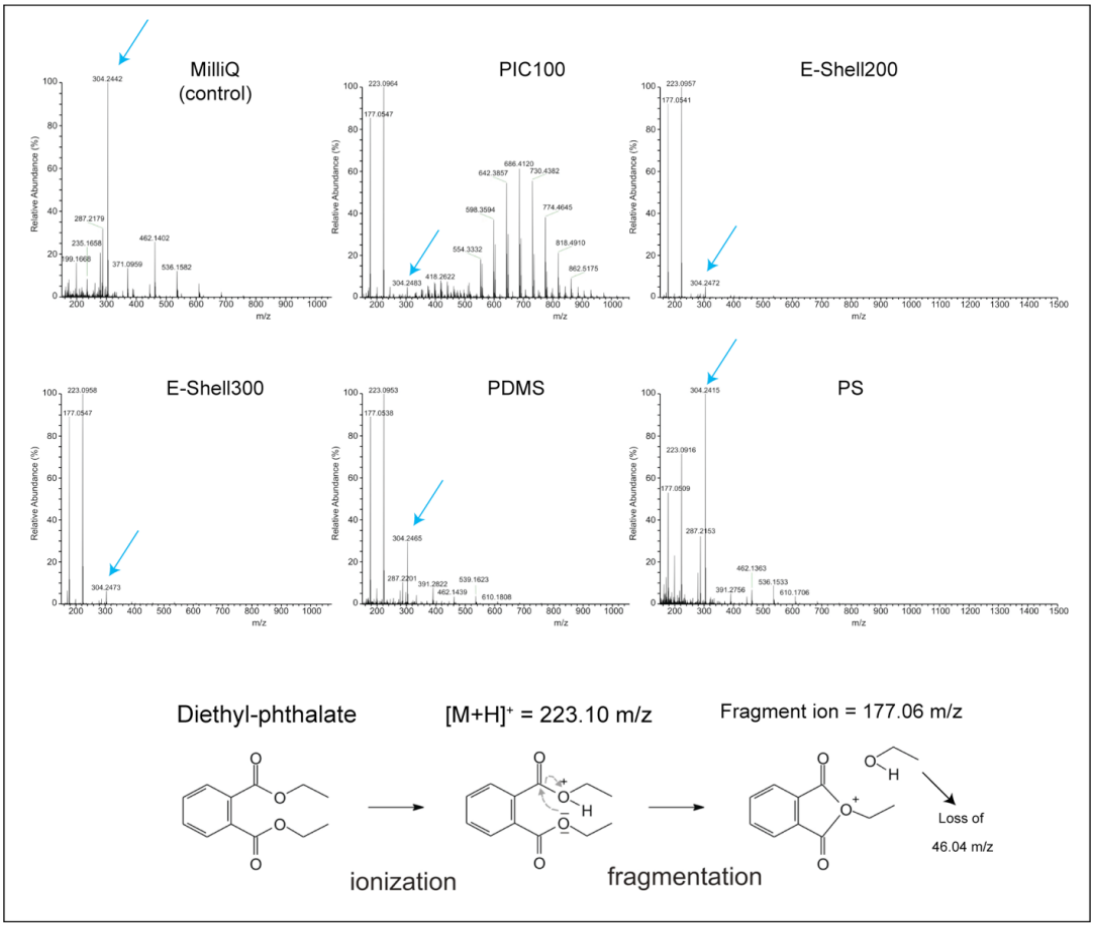

Figure 8. High resolution ESI-MS analysis of MilliQ water and MilliQ water conditioned with PIC100, E-Shell200, E-Shell300, PDMS or PS. The peaks at *m/z* 223.096 and 177.058 correspond to the positive mother ion and a fragment ion of diethyl-phthalate (see bottom panel for formation principle of fragment ion). The higher molecular weight peaks (*m/z* 500-1000) represent massifs of peaks spaced by 44 *m/z* were found, which is a characteristic signature of polyethylene glycol of polyethylene glycol. Blue arrows represent the reference peak at *m/z* 304.24 found in all samples and used here for quantification purposes.

The absolute amounts of released diethyl-phthalate from PIC-100 to distilled water, in 24 h time, was 78 nM while for other plastics the release was much lower (Table 2). It should be noted that IVF media contain diverse ions, metabolites and albumin and these components will influence the efficiency of uptake of diethyl-phthalates, which may, therefore, be different in such fluid environment when compared to the leached water. Additionally, the cells in the IVF condition can also take up and metabolize diethyl-phthalates. Regardless of such interfering influences, the noted concentration of diethyl-phthalate into water (78 nM), is above reported reproductive toxic levels of phthalates and their metabolites (10-23 nM [47,48]). Phthalates have long ago been established to have toxic effects on mammalian reproduction in which diethyl-phthalate was amongst the most toxic species when exposed to rats[49] (for a recent review on toxic effects of phthalates on female reproduction see Rattan et al., 2017[50]). Note that the amount of diethyl-phthalate released from the other plastics was considerably lower than 1 nM which can explain the reduced effects of E-Shell200 and E-Shell300 on embryo development when compared to PIC100. Likewise, these results may indicate that the 2-4 cell stage embryos are more susceptible to this leached component when compared to the oviduct cell as well as the fertilization itself. The other component released from only PIC100 and E-Shell200 is poly-ethylene glycol, adverse effects of its metabolites on embryo development was also described before[51,52].

Table 2. Relative amount of diethyl-phthalate and its fragment ion present in each MilliQ sample conditioned with one polymer material compared to the control MilliQ sample without any conditioning.

Substance	Diethyl-phthalate ion events**	Concentration of released diethyl-phthalate
MilliQ water*	0.023	38.00 fM
PIC100	47,109.500	78.00 nM
EShell200	381.100	0.63 nM
EShell300	21.200	35.00 pM
PDMS	5.440	9.00 pM
PS	1.180	1.95 pM

*MilliQ water was sham handled exactly as the MilliQ water used for plastic conditioning but without adding a polymer for leachate testing.
** diethyl-phthalate ion events (223.10 and 177.06 *m/z*) relative to 100 ion counts of the MilliQ ion (304.247 *m/z*).

A key-finding of this study is that the notion of material biocompatibility is different for specific applications. In line with this, Williams (2014) stated: “there is no such a thing as biocompatible material”[53]. The developing bovine embryo was shown to be much more sensitive to its environment and for toxic components released from 3D-printed materials when compared to epithelial cells and gametes. It was also demonstrated that the tested polymers leaked

a toxic diethyl-phthalate compound in solution. It has been reported before that phthalates (plasticizers) can have an adverse influence on biological activities; their toxic effect on bovine embryo production has also been reported[48,54] and they are known to have effects on steroid production[48], which indeed was very reliable covered in the cell based ER reporter gene assay. Altogether, our results revealed that the fertilized bovine oocyte is extremely sensitive to compounds leaking from 3D-printed polymer materials, such as phthalates, which may inhibit early embryogenesis. Our studies also revealed that only after performing a dedicated set of toxicity screening tests one can make a reliable prediction on the biocompatibility of 3D-printed bioengineered polymers for biological applications in general - and more specific as demonstrated here - for embryo production.

Acknowledgements

This research is part of the research focus theme Life Sciences of Utrecht University, experiments were performed in the research group Fertility and Reproduction and confocal imaging was performed at the Centre for Cell Imaging, both on the Faculty of Veterinary Medicine of the same university. The ESI mass spectrometry measurements were carried out in the Lipidomics Facility of the Faculty of Veterinary Medicine at Utrecht University.

Authors contributions

S.L.G., P.F.C. and J.M. provided the polymer structures. M.A.M.M.F., T.A.E.S., P.L.A.M.V., B.M.G. and H.H.W.H. designed the experiments and prepared the manuscript. M.A.M.M.F. performed all the experiments and analyzed the data. S.L.G and F.B performed the MALDI-TOF MS analysis, J.F.B. performed the high resolution ESI-MS analysis and identified the diethyl-phthalate $[M+H]^+$ ion and its stable positive fragment ion. M.D. performed the luciferase assay, and all authors reviewed the manuscript.

Competing interests

The authors do not have competing interests.

References

1. Huh, D., Hamilton, G. A. & Ingber, D. E. From 3D cell culture to organs-on-chips. *Trends Cell Biol.* **21,** 745–754 (2011).
2. Kane, B. J., Zinner, M. J., Yarmush, M. L. & Toner, M. Liver-specific functional studies in a microfluidic array of primary mammalian hepatocytes. *Anal. Chem.* **78,** 4291–4298 (2006).
3. Allen, J. W., Khetani, S. R. & Bhatia, S. N. In vitro zonation and toxicity in a hepatocyte bioreactor. *Toxicol. Sci.* **84,** 110–119 (2005).
4. Carraro, A. *et al.* In vitro analysis of a hepatic device with intrinsic microvascu-

lar-based channels. *Biomed. Microdevices* **10,** 795–805 (2008).
5. Huh, D. *et al.* Acoustically detectable cellular-level lung injury induced by fluid mechanical stresses in microfluidic airway systems. *Proc. Natl. Acad. Sci. U. S. A.* **104,** 18886–18891 (2007).
6. Hagiwara, M., Peng, F. & Ho, C.-M. In vitro reconstruction of branched tubular structures from lung epithelial cells in high cell concentration gradient environment. *Sci. Rep.* **5,** 8054 (2015).
7. Jang, K.-J. *et al.* Fluid-shear-stress-induced translocation of aquaporin-2 and reorganization of actin cytoskeleton in renal tubular epithelial cells. *Integr. Biol* **3,** 134–141 (2011).
8. Jang, K.-J. & Suh, K.-Y. A multi-layer microfluidic device for efficient culture and analysis of renal tubular cells. *Lab Chip* **10,** 36–42 (2010).
9. Costello, C. M. *et al.* Synthetic small intestinal scaffolds for improved studies of intestinal differentiation. *Biotechnol. Bioeng.* **111,** 1222–1232 (2014).
10. Imura, Y., Asano, Y., Sato, K. & Yoshimura, E. A microfluidic system to evaluate intestinal absorption. *Anal. Sci.* **25,** 1403–7 (2009).
11. Kimura, H., Yamamoto, T., Sakai, H., Sakai, Y. & Fujii, T. An integrated microfluidic system for long-term perfusion culture and on-line monitoring of intestinal tissue models. *Lab Chip* **8,** 741–6 (2008).
12. You, L. *et al.* Osteocytes as mechanosensors in the inhibition of bone resorption due to mechanical loading. *Bone* **42,** 172–179 (2008).
13. Song, J. W. *et al.* Microfluidic endothelium for studying the intravascular adhesion of metastatic breast cancer cells. *PLoS One* **4,** (2009).
14. Torisawa, Y.-S. *et al.* Microfluidic platform for chemotaxis in gradients formed by CXCL12 source-sink cells. *Integr. Biol. (Camb).* **2,** 680–686 (2010).
15. Puleo, C. M., McIntosh Ambrose, W., Takezawa, T., Elisseeff, J. & Wang, T.-H. Integration and application of vitrified collagen in multilayered microfluidic devices for corneal microtissue culture. *Lab Chip* **9,** 3221–3227 (2009).
16. Chung, S. *et al.* Cell migration into scaffolds under co-culture conditions in a microfluidic platform. *Lab Chip* **9,** 269–275 (2009).
17. Ferraz, M. A. M. M. *et al.* Improved bovine embryo production in an oviduct-on-a-chip system: Prevention of poly-spermic fertilization and parthenogenic activation. *Lab Chip* (2017). doi:10.1039/C6LC01566B
18. Xiao, S. *et al.* A microfluidic culture model of the human reproductive tract and 28-day menstrual cycle. *Nat. Commun.* **8,** 14584 (2017).
19. Laronda, M. *et al.* A bioprosthetic ovary created using 3D printed microporous scaffolds restores ovarian function in sterilized mice. *Nat. Commun.* **8,** 1–10 (2017).
20. Macdonald, N. P. *et al.* Assessment of biocompatibility of 3D printed photopolymers using zebrafish embryo toxicity assays. *Lab Chip* **16,** 291–7 (2016).
21. Oskui, S. M. *et al.* Assessing and Reducing the Toxicity of 3D-Printed Parts. *Environ. Sci. Technol. Lett.* **3,** 1–6 (2016).
22. El-Sherry, T. M., Elsayed, M., Abdelhafez, H. K. & Abdelgawad, M. Characterization of rheotaxis of bull sperm using microfluidics. *Integr. Biol.* **6,** 1111–1121 (2014).
23. Scherr, T. *et al.* Microfluidics and numerical simulation as methods for standardization of zebrafish sperm cell activation. *Biomed. Microdevices* **17,** 1–10 (2015).
24. Angione, S. L., Oulhen, N., Brayboy, L. M., Tripathi, A. & Wessel, G. M. Simple perfusion apparatus for manipulation, tracking, and study of oocytes and embryos. *Fertil. Steril.* **103,** 281–290 (2015).
25. Suarez, S. S. & Wu, M. Microfluidic devices for the study of sperm migration. *Mol. Hum. Reprod.* (2016). doi:10.1093/molehr/gaw039
26. Lai, D., Takayama, S. & Smith, G. D. Recent microfluidic devices for studying gamete and embryo biomechanics. *J. Biomech.* **48,** 1671–1678 (2015).
27. Kim, M. S., Bae, C. Y., Wee, G., Han, Y. M. & Park, J. K. A microfluidic in vitro cul-

tivation system for mechanical stimulation of bovine embryos. *Electrophoresis* **30,** 3276–3282 (2009).
28. Esteves, T. C. *et al.* A microfluidic system supports single mouse embryo culture leading to full-term development. *RSC Adv.* **3,** 26451 (2013).
29. Kieslinger, D. C. *et al.* In?vitro development of donated frozen-thawed human embryos in a prototype static microfluidic device: a randomized controlled trial. *Fertil. Steril.* **103,** 680–686.e2 (2015).
30. Fleming, T. P. The Embryo and Its Future. *Biol. Reprod.* **71,** 1046–1054 (2004).
31. Van Tol, H. T. A. A., Van Eerdenburg, F. J. C. M. C. M., Colenbrander, B. & Roelen, B. A. J. J. Enhancement of Bovine oocyte maturation by leptin is accompanied by an upregulation in mRNA expression of leptin receptor isoforms in cumulus cells. *Mol. Reprod. Dev.* **75,** 578–587 (2008).
32. van Duursen, M. B. M., Smeets, E. E. J. W., Rijk, J. C. W., Nijmeijer, S. M. & van den Berg, M. Phytoestrogens in menopausal supplements induce ER-dependent cell proliferation and overcome breast cancer treatment in an in vitro breast cancer model. *Toxicol. Appl. Pharmacol.* **269,** 132–140 (2013).
33. Rogers, J. M. & Denison, M. S. Recombinant cell bioassays for endocrine disruptors: development of a stably transfected human ovarian cell line for the detection of estrogenic and anti-estrogenic chemicals. *In Vitr. Mol. Toxicol.* **13,** 67–82 (2000).
34. Huh, D. *et al.* Microfabrication of human organs-on-chips. *Nat. Protoc.* **8,** 2135–57 (2013).
35. Wolbers, F. *et al.* Viability study of HL60 cells in contact with commonly used microchip materials. *Electrophoresis* **27,** 5073–5080 (2006).
36. Lo, C.-M., Keese, C. R. & Giaever, I. Cell–Substrate Contact: Another Factor May Influence Transepithelial Electrical Resistance of Cell Layers Cultured on Permeable Filters. *Exp. Cell Res.* **250,** 576–580 (1999).
37. Bhattacharjee, N., Urrios, A., Kang, S. & Folch, A. The upcoming 3D-printing revolution in microfluidics. *Lab Chip* **16,** 1720–1742 (2016).
38. Hinton, T. J., Hudson, A., Pusch, K., Lee, A. & Feinberg, A. W. 3D Printing PDMS Elastomer in a Hydrophilic Support Bath via Freeform Reversible Embedding. *ACS Biomater. Sci. Eng.* acsbiomaterials.6b00170 (2016). doi:10.1021/acsbiomaterials.6b00170
39. Bhatia, S. N. & Ingber, D. E. Microfluidic organs-on-chips. *Nat. Biotechnol.* **32,** 760–772 (2014).
40. Raty, S. *et al.* Embryonic development in the mouse is enhanced via microchannel culture. *Lab Chip* **4,** 186 (2004).
41. Sameenoi, Y., Nongkai, P. N., Nouanthavong, S., Henry, C. S. & Nacapricha, D. One-step polymer screen-printing for microfluidic paper-based analytical device (μPAD) fabrication. *Analyst* **139,** 6580–6588 (2014).
42. Choi, B.-I., Harvey, A. J. & Green, M. P. Bisphenol A affects early bovine embryo development and metabolism that is negated by an oestrogen receptor inhibitor. *Sci. Rep.* **6,** 29318 (2016).
43. Pocar, P., Perazzoli, F., Luciano, A. M. & Gandolfi, F. In vitro reproductive toxicity of polychlorinated biphenyls: Effects on oocyte maturation and developmental competence in cattle. *Mol. Reprod. Dev.* **58,** 411–416 (2001).
44. Sone, K. *et al.* Effects of 17β-estradiol, nonylphenol, and bisphenol-A on developing Xenopus laevis embryos. *Gen. Comp. Endocrinol.* **138,** 228–236 (2004).
45. Ahn, K. C. *et al.* In Vitro Biologic Activities of the Antimicrobials Triclocarban, Its Analogs, and Triclosan in Bioassay Screens: Receptor-Based Bioassay Screens. *Environ. Health Perspect.* **116,** 1203–1210 (2008).
46. Binyamin, G., Shafi, B. M. & Mery, C. M. Biomaterials: A primer for surgeons. *Semin. Pediatr. Surg.* **15,** 276–283 (2006).
47. Du, Y.-Y. *et al.* Follicular fluid and urinary concentrations of phthalate metabolites

among infertile women and associations with in vitro fertilization parameters. *Reprod. Toxicol.* **61,** 142–50 (2016).
48. Kalo, D. & Roth, Z. Low level of mono(2-ethylhexyl) phthalate reduces oocyte developmental competence in association with impaired gene expression. *Toxicology* **377,** 38–48 (2017).
49. Singh, A. R., Lawrence, W. H. & Autian, J. Teratogenicity of phthalate esters in rats. *J. Pharm. Sci.* **61,** 51–5 (1972).
50. Rattan, S. *et al.* Exposure to endocrine disruptors during adulthood: consequences for female fertility. *J. Endocrinol.* **233,** R109–R129 (2017).
51. Klug, S., Merker, H. J. & Jäckh, R. Effects of ethylene glycol and metabolites on in vitro development of rat embryos during organogenesis. *Toxicol. In Vitro* **15,** 635–42 (2001).
52. Carney, E. W., Tornesi, B., Markham, D. A., Rasoulpour, R. J. & Moore, N. Species-specificity of ethylene glycol-induced developmental toxicity: toxicokinetic and whole embryo culture studies in the rabbit. *Birth Defects Res. B. Dev. Reprod. Toxicol.* **83,** 573–81 (2008).
53. Williams, D. F. There is no such thing as a biocompatible material. *Biomaterials* **35,** 10009–10014 (2014).
54. Kalo, D. *et al.* Carryover Effects of Acute DEHP Exposure on Ovarian Function and Oocyte Developmental Competence in Lactating Cows. *PLoS One* **10,** e0130896 (2015).

Supplementary file 1

Reference mass spectrum of diethyl-phthalate (1 µM end concentration). Diethyl-phthalate was first solubilized 1:50 in distilled ethanol and subsequently diluted 1:1 in MilliQ water and further diluted to the end concentration in MilliQ water. This solution was injected directly into the ESI mass spectrometer as described in the materials and methods. The exclusive presence of the $[M+H]^+$ peak (223.10 m/z) and the fragment ion (177.06 m/z) as well as the relative abundance of both correspond to those measured in Figure 8. The satellite peaks on the right are C^{13} isotope peaks (224.10 and 178.06 m/z respectively). Note that we have made a series of dilutions of diethyl-phthalate in MilliQ water (10^{-3} to 10^{-13} M) and with this titration curve we have quantified the amount of released diethyl-phthalate from the diverse plastics as is indicated in Table 2.

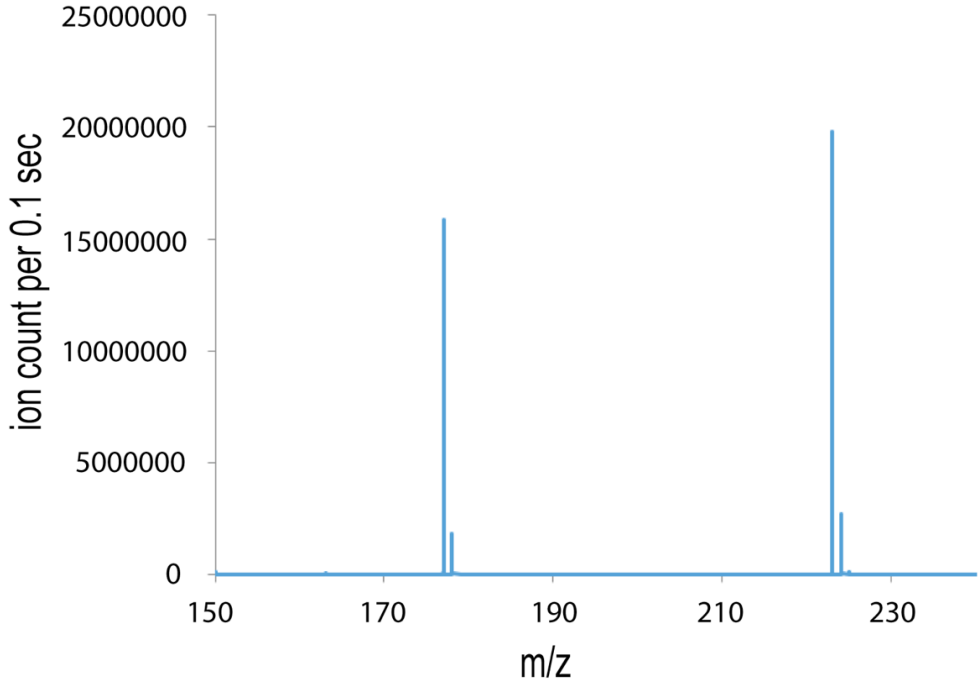

Chapter 5

An oviduct-on-a-chip provides an enhanced in vitro environment for zygote (epi)genome reprogramming

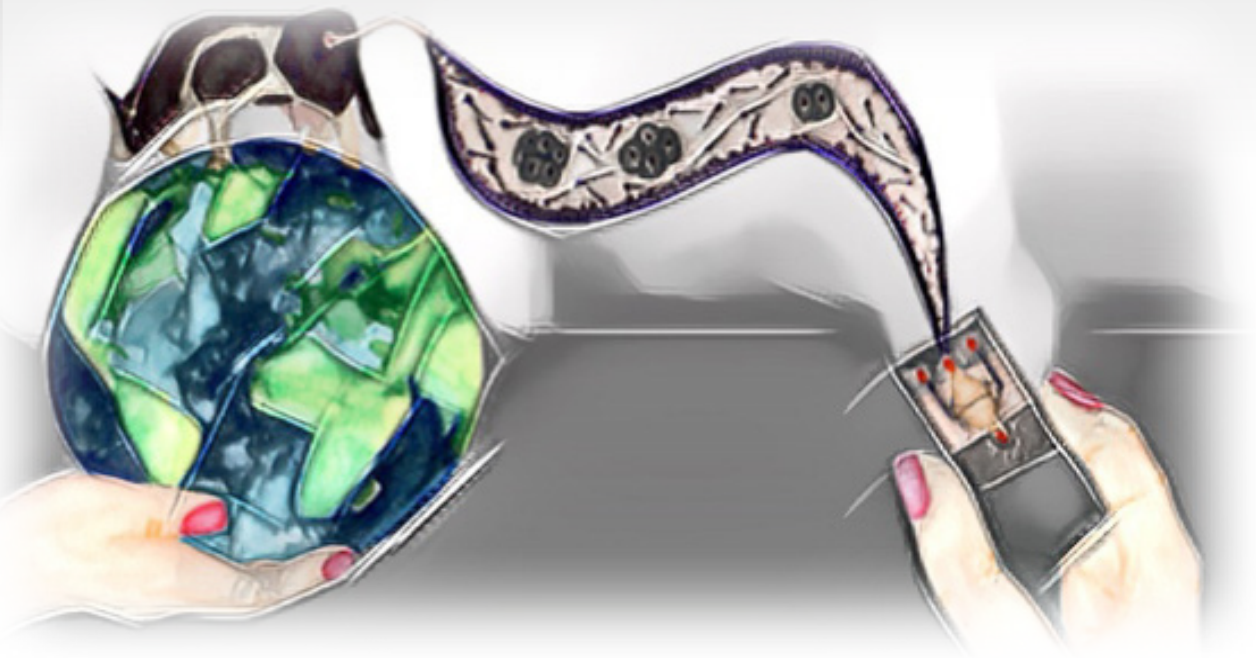

***Marcia A.M.M Ferraz**, Hoon Suk Rho, Daiane Hemerich, Heiko H.W. Henning, Helena T.A. van Tol, Michael Hölker, Urban Besenfelder, Michal Mokry, Peter L.A.M. Vos, Tom A.E. Stout, Séverine Le Gac and Bart M. Gadella.* An oviduct-on-a-chip provides an enhanced *in vitro* environment for zygote (epi) genome reprogramming. Submitted.

Abstract

Worldwide more than 5 million children have been conceived using assisted reproductive technologies (ART). Most of the research in the field of ART has focused on increasing the likelihood of an ongoing pregnancy or live birth, whereas the long-term impact on the health of the resulting child has been relatively neglected. Recent studies using animal models have highlighted the effects of *in vitro* embryo culture on subsequent offspring development and health. *In vivo*, the oviduct hosts a period in which the early embryo undergoes almost complete reprogramming of its (epi)genome in preparation for the reacquisition of epigenetic marks. In this context, we have developed an oviduct-on-a-chip platform to better investigate the effects of the oviduct epithelium on mechanisms related to embryonic epigenetic and genetic reprogramming. The oviduct-on-a-chip device was found to support more physiological (*in vivo*-like) embryonic (epi)genetic reprogramming than conventional IVF. This platform will be instrumental in identifying and investigating factors critical to fertilization and pre-implantation development, to eventually improve the quality and (epi)genetic integrity of IVF embryos.

Introduction

In vitro embryo production (IVP) in mammals involves a dramatic change in the micro-environment to which the early embryo is exposed and, despite considerable improvements in the success of assisted reproductive technologies (ART), IVP systems are still far from physiological. That these conditions are suboptimal is evidenced by substantial differences between embryo production in vitro and in vivo; depending on species, the former is associated with lower blastocyst per oocyte yields, reduced developmental competence, altered gene expression patterns, changes in epigenetic reprogramming and a reduced likelihood of successful pregnancy[1–12]. In vivo, the oviduct hosts a period in which the early embryo undergoes almost complete reprogramming of its (epi)genome in preparation for the reacquisition of epigenetic marks in specific cell populations as they progress through differentiation [3,13,14]. This period of epigenetic reprogramming has proven to be extremely sensitive to changes in environmental conditions, such as compromised maternal health or an unhealthy diet[15]. Epigenetic reprogramming can also be disturbed by the conditions imposed by IVP, such as culture medium components, light, temperature and oxygen tension[3,5,6,16]. Many of the epigenetic effects associated with in vitro embryo production can be detected during the pre-implantation period[5,17,18]. Other effects only become apparent during later fetal or even post-natal development, and these include unbalanced fetal-placental development, abnormal fetal growth, abnormal metabolic responses or predilection to 'lifestyle' related diseases in neonatal or adult life[1,3,19,20].

Improvements in IVP, not only in terms of numbers of embryos produced, time to pregnancy and likelihood of live birth, but more specifically in terms of embryo quality and 'normality' are

essential to safeguard the health of future generations of in vitro fertilization (IVF) offspring. In this light, it is somewhat surprising that the influence of the oviduct on mammalian embryo development has not been thoroughly investigated to guide the refinement of ART procedures[4]. We hypothesized that by mimicking an oviductal environment in vitro, the processes of fertilization and early embryo development would more closely resemble the physiological situation. In turn, our approach would assist discovery of key-factors that can be applied to optimize IVF and IVP. To this end, we designed a microfluidic 'oviduct-on-a-chip platform' which permitted the production of bovine zygotes with a transcriptome and global methylation pattern resembling in vivo produced zygotes but dissimilar to conventional IVP zygotes.

Results

Oviduct-on-a-chip design.

Bovine oviduct epithelial cells (BOECs) rapidly lose their polarization and differentiation in 2D static culture[21–23]. To maintain *in vivo*-like morphology (a cuboidal to columnar pseudostratified epithelium with ciliated and secretory cells[24–26]) and function, alternative 3D culture methods have been described, e.g., tusing air-liquid interfaces[27–29], organoids[30], suspensions[24] and perfusion and/or microfluidic cultures[31–33]. Microfluidic technologies can considerably enhance cell culture conditions[34]. First, microfluidics provides exquisite spatial and temporal control of the cell's microenvironment, and proper design may allow faithful recreation of *in vivo*-like conditions. Microfluidics also allows dynamic culture, with continuous or pulsatile perfusion, and the creation of time-dependent gradients of specific bioactive components. The volumes of fluids used in a microfluidic platform are in the low nanoliter range, which drastically reduces operating costs when expensive culture media or components are required. Thanks to a high level of integration, multiple biological processes can be implemented in a single device and experiments and processes run in parallel allowing high-throughput operation[33]. Finally, liquid handling can be automated, and complex protocols programmed[34].

We developed a microfluidic device containing two independent, perfusable 370 µm deep compartments separated by a porous membrane. On top of the porous membrane, a confluent oviduct epithelial cell layer was grown (apical side of the oviduct-on-a-chip), while the basolateral compartment was used to mimic the circulating hormone changes that occur during the peri-ovulation period. The two compartments were designed as rectangles (2,800 µm wide x 3,000 µm long) to ensure uniform shear stress across the entire epithelial layer under perfusion (5 µl/h). Importantly, the apical compartment contained pillars to trap oocytes and/or embryos on top of the monolayer. This design permitted the continuous apical perfusion of the oviduct epithelial cell layer, which is required to maintain its functional differentiation, throughout the period of IVF and IVP (Fig. 1). A point considered essential in the design of the oviduct-on-a-chip was the total thickness of the apical compartment of the device,

which was not higher than 2 mm to allow live imaging of the epithelial cells, gametes and embryos inside the chip (Supplementary movie 1). Devices were successfully manufactured from poly(dimethylsiloxane) (PDMS), a fairly inexpensive, transparent, gas-permeable, water-impermeable, copyright-free and rapidly prototyped elastomeric material[35]. PDMS has previously been successfully utilized to fabricate *in vitro* embryo culture systems[12,31,34,36,37].

BOEC morphology, differentiation and responses to hormones perfused via the basolateral medium.

BOECs attached to and proliferated over the entire apical compartment of the microfluidic device, forming a tight cell monolayer (Supplementary fig. 1 and supplementary movie 2). Moreover, some areas exhibited villus-like structures that resembled mucosal folding of the oviduct *in vivo* (Supplementary fig. 1). After addition to the apical culture chamber, sperm cells were found to attach to both ciliated and non-ciliated epithelial cells (Supplementary fig. 1). A total of three different pools of epithelial cells, and 18 microfluidic devices per pool, were used to investigate: (1) cell confluence via both trans-epithelial electrical resistance (TEER) measurements and an apparent permeability assay (Papp); (2) cell morphology, ciliation and oviductal glycoprotein 1 (OVGP1) expression by immunofluorescence; (3) changes in the transcriptome under different hormonal conditions by RNA sequencing (Cel-seq II). All measurements were compared for BOECs cultured under three different conditions; no hormonal stimulation, luteal phase simulation and pre-ovulatory phase simulation via the basolateral compartment of the platform (n=6 devices per condition and pool). Supplementary figure 2a summarizes the times and hormone treatments for each group; the hormone treatments were based on the progesterone and estrogen concentrations measured in the oviduct of cows at different stages of the estrous cycle[38].

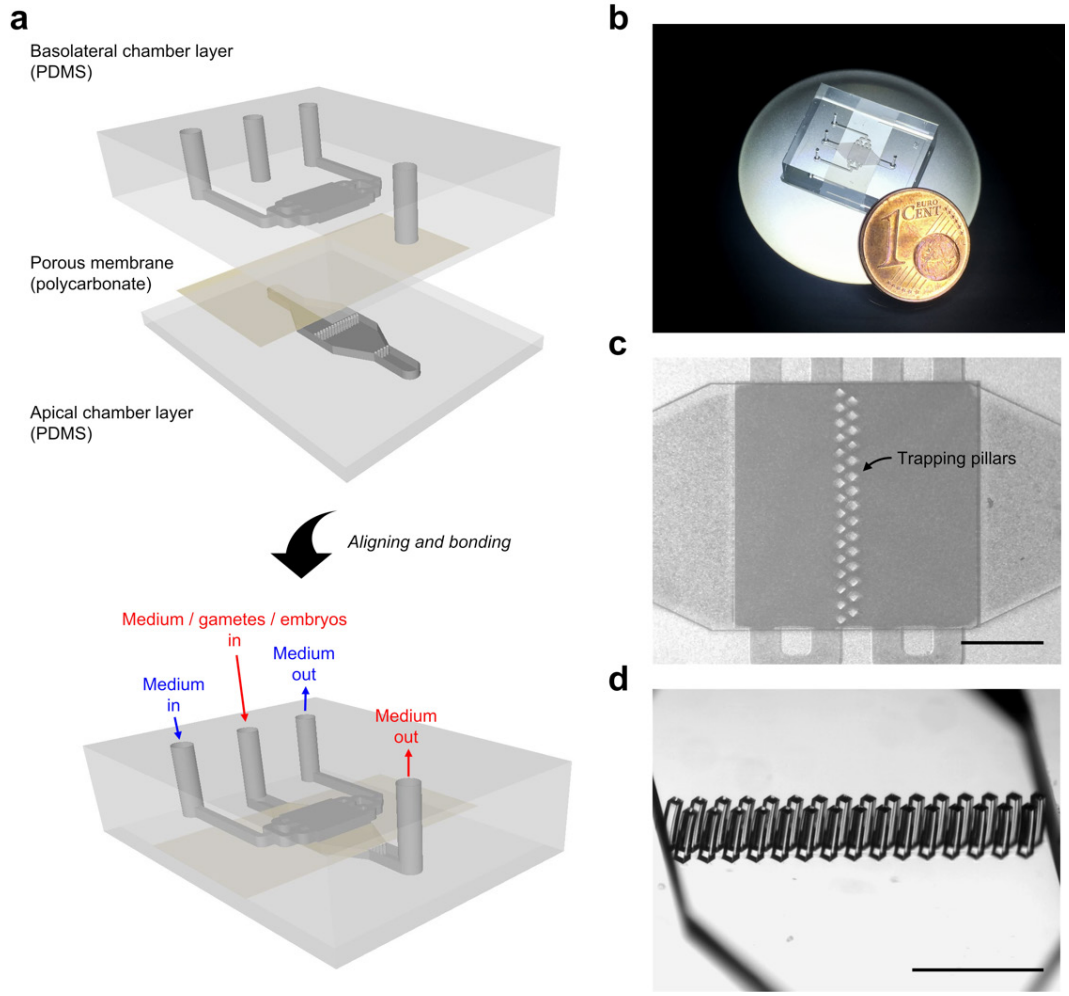

Figure 1: Oviduct-on-a-chip platform - design and fabrication. (a) Schematic drawing of the apical and basolateral chambers that are assembled with a porous polycarbonate membrane between them. (b) Picture of an assembled PDMS device. (c) Microscopic picture of the assembled PDMS device, focusing on the apical culture chamber that contains the trapping pillars. (d) Stereomicroscopic picture of the trapping pillars (W 103 µm X L 103 µm X H 380 µm, spacing = 40 µm). Scale bars = 1 mm.

TEER measurement is a non-invasive way to assess the confluence and integrity of oviduct epithelial monolayers cultured on a porous substrate[39]. Indeed, TEER measurements are influenced by the expression of specific tight junction proteins, reflecting physical properties of the epithelium[40]. For the oviduct-on-a-chip, the average TEER values of three replicates were: 150.44 ± 7.14 (n=16), 186.00 ± 22.20 (n=18) and 204.61 ± 84.50 (n=18) Ω*cm^2 for no hormone, the luteal and pre-ovulatory phases, respectively (Supplementary fig. 2b). The TEER value for the luteal phase was higher than for no hormone ($p<0.0001$), but no statistical difference was observed between no hormone and pre-ovulatory phase simulation, or between the luteal and pre-ovulatory groups ($p=0.17$ and $p=0.81$, respectively). The TEER measurements

confirmed the formation of a robust epithelial barrier, that also restricted the passage of both, fluorescent dextran nanoparticles (4.4 kDa) and fluorescein dye (0.4 kDa), between the basolateral and apical compartments (Supplementary fig. 2c), mimicking the barrier function of the oviduct epithelium *in vivo*. Hormone stimulation did not influence the permeability to the fluorescent dyes (0.4k Da: p=0.616; p=0.681 and p=0.994. 4.4k Da: p=0.894; p=0.536 and p=0.809; for no hormone *vs*. luteal phase, no hormone *vs*. pre-ovulatory phase and luteal *vs*. pre-ovulatory phases, respectively). The tight, confluent BOEC monolayers formed in the perfused oviduct-on-a-chip exhibited similar morphology to *in vivo* oviduct epithelium and, under estrogenic stimulation, produced the major oviductal glycoprotein OVGP1 (Fig. 2a). As previously described for a porcine oviductal epithelium[28], stimulation with estrogens to mimic the pre-ovulatory phase increased the height of cultured BOECs ($p<0.0001$ for all groups comparisons; Fig. 2b). Furthermore, hormone stimulation enhanced the number of ciliated cells compared to no added hormones, with no significant difference between luteal and pre-ovulatory phase simulation (p=0.014; p=0.002 and p=0.172; for no hormone *vs*. luteal phase, no hormone *vs*. pre-ovulatory phase and luteal *vs*. pre-ovulatory phase, respectively; Fig. 2c). Additionally, as described previously for porcine, human and canine oviduct[28,33,41], the pre-ovulatory phase (high estrogen) enhanced OVGP1 expression compared to control or luteal phase conditions (p=0.829; p=0.002 and $p<0.0001$; for no hormone *vs*. luteal phase, no hormone *vs*. pre-ovulatory phase and luteal *vs*. pre-ovulatory phase, respectively, Fig. 2d).

To evaluate the effects of steroid hormone treatment (luteal and pre-ovulatory phase simulation) on transcriptional activity in the epithelial cells, we performed RNA sequencing (RNA-seq). A total of 14,383 genes were detected by Cel-seq II, with no significant difference (fold change 1/ False discovery rate <1%) between no hormone stimulation (CNH) and the simulated luteal phase (CP). By contrast, 183 transcripts were up-regulated and 140 were down-regulated in the pre-ovulatory phase (CE) compared to the CP. Functional gene ontology (GO) clustering of upregulated genes into “molecular and biological processes” indicated an increase in genes related to ciliogenesis and cilia movement in the pre-ovulatory phase (Fig. 3a). Progesterone has previously been reported to inhibit oviduct epithelial cell cilia beating in man, mouse, guinea pig and cow[42–45]. The pre-ovulatory phase also showed increased expression of transcripts related to the immune response (Fig. 3a) similar to what has previously been described *in vivo*[46]. The oviductal epithelium must presumably protect itself from any pathogens that may accompany spermatozoa and seminal fluids. The ovarian steroid hormone-dependent change in immune responsiveness is likely a physiologically important process activated during the pre-ovulatory phase, when spermatozoal contact is expected.

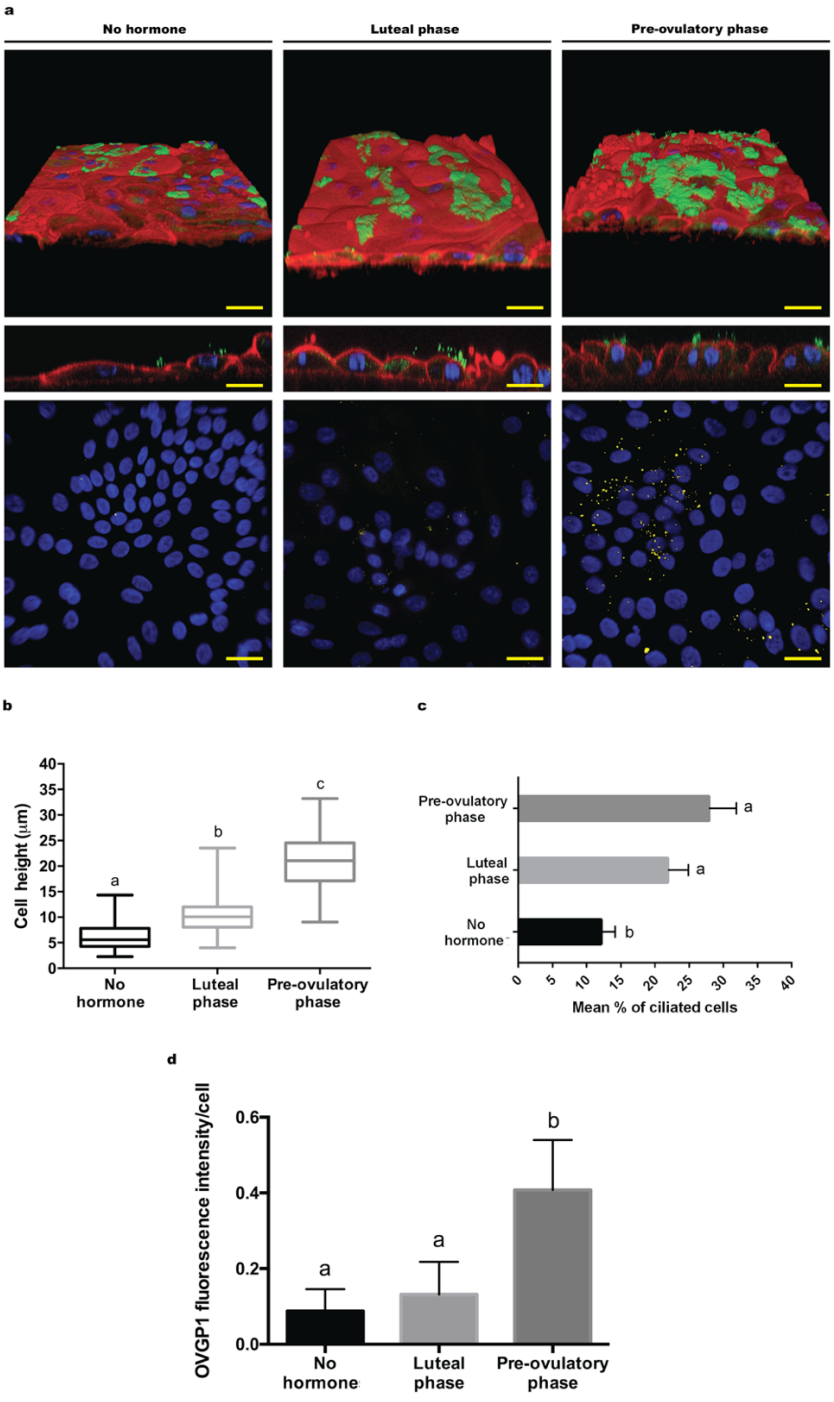

Figure 2: Effects of hormone stimulation of 3D cultured BOECs on cell height, ciliation and oviductal glycoprotein 1 (OVGP1) expression under control, and simulated luteal and pre-ovulatory phases. (a) Top and middle figures: 3D reconstruction of confocal immunofluorescent (IF) images for cilia (acetylated alpha-tubulin, green), nuclei (HOECHST 33342, blue) and actin filaments (phalloidin, red); bottom figures: IF for nuclei (blue) and OVGP1 (yellow). (b) Quantification of cell height in the different groups ($F=697.51$, $p<0.0001$). (c) Mean percentage of ciliated cells for each group ($F=20.415$, $p=0.002$). (d) Quantification of OVGP1 expression adjusted for cell number ($F=12.52$, $p<0.0001$). Different letters indicate statistically significant differences ($p<0.05$). Scale bars represent 10 µm.

Other up-regulated GO pathways in the pre-ovulatory phase include; inflammatory response, regulation of protein activation cascade, regulation of protein processing and maturation, retinoid metabolic process and regulation of endocytosis (Fig. 3a). The luteal-phase epithelium was characterized by increased cell-cell junction organization, response to growth factors, antioxidant activity, lipid biosynthetic and metabolic processes, response to oxidative stress, epithelial cell proliferation and regulation of chemotaxis (Fig. 3b; see supplementary data 1 for a complete list of GO pathways differentially regulated between the pre-ovulatory and luteal phases).

BOECs cultured in the oviduct-on-a-chip, independent of hormone stimulation, expressed genes related to sperm-oviduct adhesion[47] (FUCA1, ANXA1, ANXA2, ANXA4 and ANXA5), COC-oviduct interaction[48] (MUC20, SPP1, PDGC, CSTA), fertilization[48,49] (HEXDC, HEXIM1, HYAL2, GLB1, HSPA9, HSPA8, HSP90AB1,RPS6, CD46, CD9, MFGE8, ADAM9 and NTS) and embryo development[48,50] (C3, IGF2, TGFB2 and TGFB3). Together, the expression of these genes in the oviduct-on-a-chip supports the conclusion that the platform permits the *in vitro* culture of a functional bovine oviduct epithelium that responds appropriately to ovarian steroid hormones.

The oviduct-on-a-chip supports in vitro fertilization and embryo development.

Using *in vitro* matured (IVM) oocytes, *in vitro* fertilization (IVF) was performed either in a 4-well dish (*in vitro* embryos - VT) or inside a microfluidic device containing a confluent layer of differentiated BOECs (*on chip* embryos - CH, Supplementary video 3). Ten devices (from the three different animal pools) were used for on chip fertilization and culture. In the oviduct-on-a-chip device, both cleavage and blastocyst formation were observed. However, neither cleavage (56.0 *vs.*84.4%, $p = 0.0021$) nor blastocyst formation (9.8 *vs.* 29.8%, $p = 0.0045$) was as successful on chip as in an optimized *in vitro* embryo production protocol. This reduced success can in part be explained by the fact that nearly half of the mature oocytes/embryos (103 out of 230) were able to 'escape' through the pillars and were subsequently either lost during perfusion or became trapped between the pillars, which resulted in developmental arrest (Supplementary fig. 3). Another factor that influences embryo development is shear stress. Previous studies have shown that high shear stresses can impair mouse embryo development[51] through the activation of stress-activated protein kinase-mediated apoptosis, and that early stage embryos (8-16 cells) are more sensitive to shear stress than blastocysts[51]. In our experiments, the average shear stress exerted on the embryos was 0.70±0.46 dyne/cm^2. However, embryos trapped between pillars and other lines of embryos, were exposed to a maximum shear stress of 2.06 dyne/cm^2 (Supplementary fig. 4), which is higher than the values shown to have a negative impact on mouse embryos (1.2 dyne/cm^2).

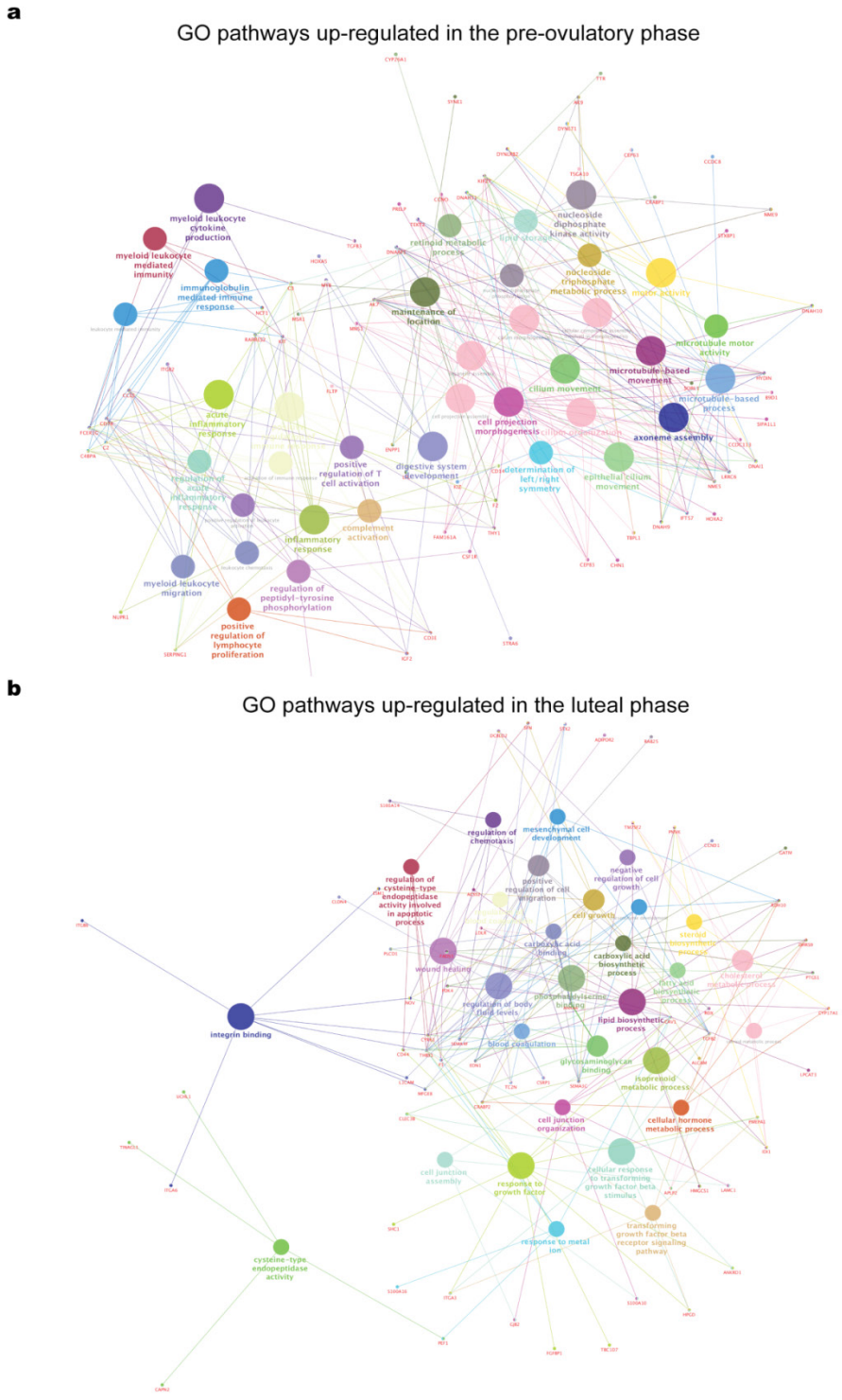

Figure 3. Functionally grouped gene ontology (GO) terms for up or down-regulated gene expression in simulated pre-ovulatory and luteal phases. The CytoScape plugin ClueGO was used to group the genes into functional GO terms of “molecular processes” and “biological processes”. (a) Up-regulated GO pathways in the pre-ovulatory phase; and (b) up-regulated GO pathways in the luteal phase.

Global methylation levels of on chip zygotes are similar to those of in vivo *zygotes.*

The global methylation patterns of 30 *in vitro (VT)*, 30 *on chip (CH)* and 30 *in vivo (VV)* zygotes were analyzed using fluorescent 5mC staining, with the fluorescence intensity being normalized to that of a general DNA stain (propidium iodide: PI). Zygotes were analyzed independent on their developmental stage. We found that nuclear intensity of 5mC of *VT* was 3.2-times higher than in *VV* (p=0.004) and 2.1-times higher than in *CH* zygotes (p=0.021). Interestingly, the global methylation staining intensity did not differ between *VV* and *CH* zygotes (p=0.929). These results collectively suggest that the interaction between the gametes and/or zygotes with the epithelium in the oviduct-on-a-chip platform overcomes the changes to the demethylation process that results during standard *in vitro* culture. Similar failure of pronucleus demethylation during ARTs has been reported for porcine zygotes, where the effect was most marked after conventional IVF and slightly less pronounced after parthenogenetic activation or somatic cell nuclear transfer[18]. Likewise, partial recovery of the methylation levels at the blastocyst stage was observed in pig embryos cultured in the presence of female reproductive tract fluids (oviductal and uterine fluids)[52].

IVF induced alterations to the zygotic transcriptome are ameliorated by the oviduct-on-a-chip.

Here, we used Cel-seq II to compare the transcriptome of individual bovine zygotes produced under different conditions: *in vivo (VV), in vitro (VT)* and on chip *(CH)* (n = 10 zygotes for each group). A total of 18,258 transcripts were detected, of which 14,042 were common to *VV*, *VT* and *CH* zygotes. A principal component analysis (PCA) revealed two distinct clusters of zygotes: Group 1 (G1) contained all *VT*, two *VV* and five *CH* zygotes; and Group 2 (G2) comprised eight *VV* and five *CH* zygotes (Fig. 5). In G1, 3,063 transcripts were up-regulated and 3,507 down-regulated compared to G2 (see Supplementary data 2 for all differentially expressed genes). From the down-regulated transcripts, four important GO pathways were identified: initiation of transcription, initiation of translation, (de)methylation and (de) acetylation (Fig. 5c-e and Supplementary fig. 5-7). This indicates that zygotes in G1 have a delayed minor embryonic transcriptome activation compared to zygotes in G2. Likewise, the oviduct epithelium plays an important role in regulating embryo development, since all zygotes that were not in contact with oviduct epithelial cells (*VT* zygotes) were in the delayed group whereas 80% of *VV* zygotes were in G2.

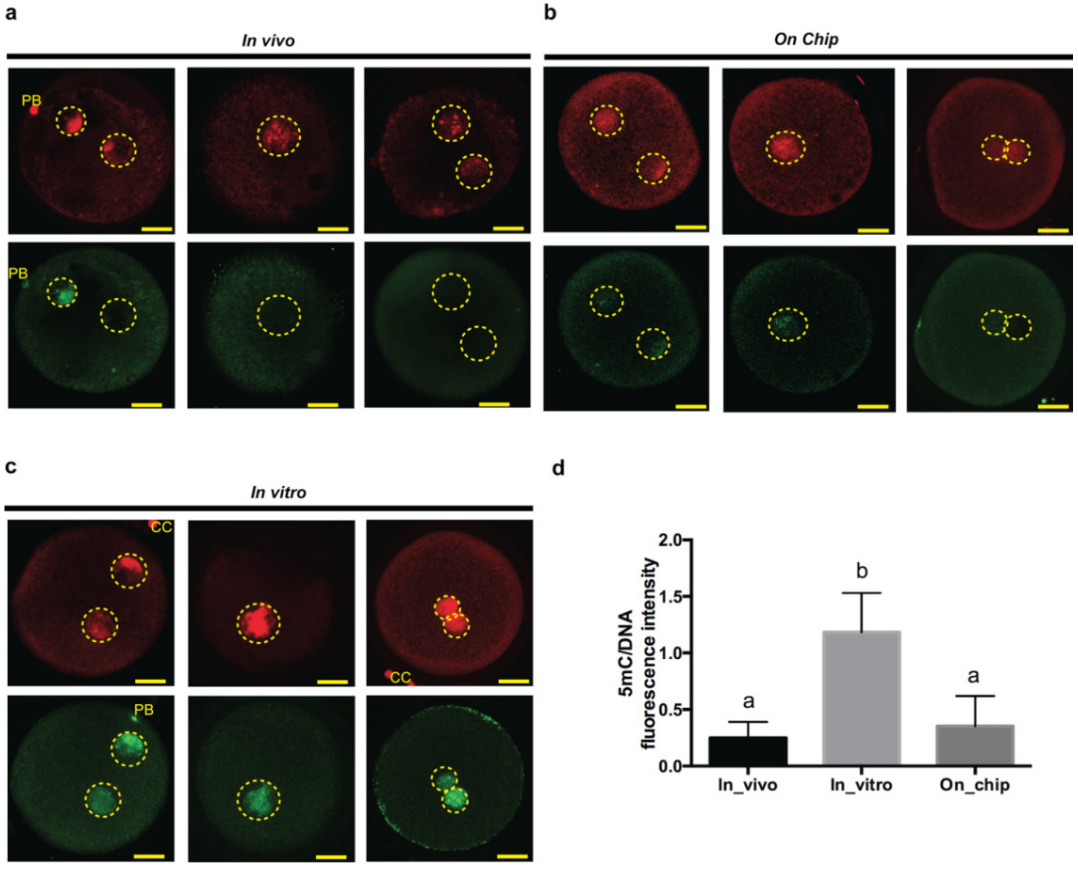

Figure 4. In vivo *(a), On chip (b) and* In vitro *(c) zygotes; indirect immunofluorescent staining for global methylation (5mC, green) and DNA (propidium iodide, red) in the pronuclei. (d) Quantification of 5mC staining in zygotes at three developmental stages: (i) prior to syngamy (corresponding to PN stages 2-5; 1C-PN); (ii) during syngamy (1C-Sy); and (iii) immediately after syngamy, but before the first cleavage division (pre-2C). 5mC fluorescence intensity was normalized using total DNA fluorescence (n=30 for* in vivo*, n=30 for in vitro and n=30 for on chip zygotes; F=7.921, p=0.002). Different letters indicate statistical differences between the groups (p<0.05). Scale bars = 25 um*

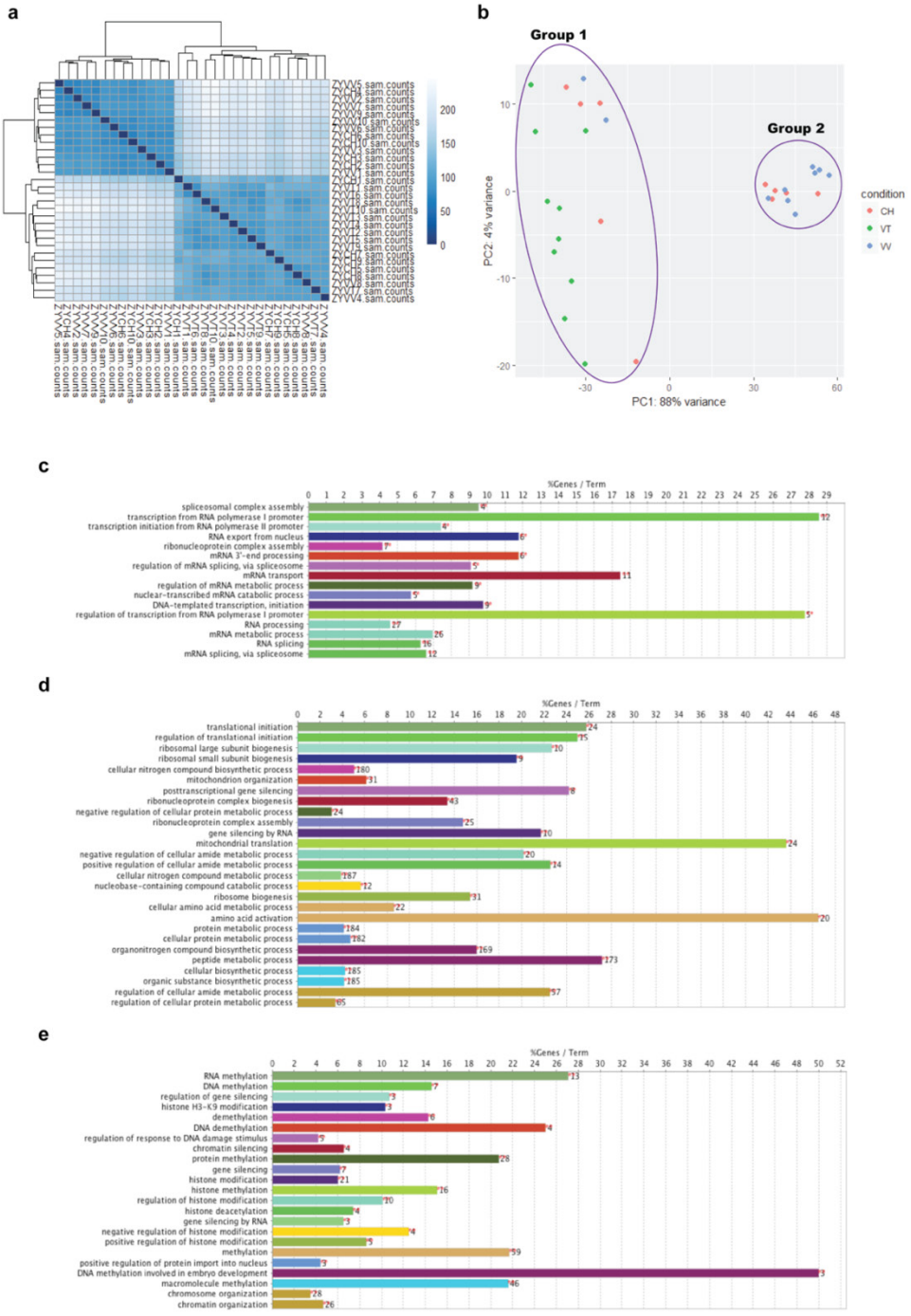

Figure 5. Comparison of the transcriptomes identified by Cel-seq for *in vivo (VV)*, *in vitro (VT)* and on chip *(CH)* zygotes. (a) Heat map comparing all zygotes. (b) Principal component analysis (PCA) of the transcriptomes for *in vivo* (*VV*, blue), *in vitro* (*VT*, green) and on chip *(CH, red)* zygotes; PC1 and PC2 represent the top two dimensions of the differentially expressed genes among the zygote groups. Note, from (a) and (b), the division between two main clustering groups, Groups 1 and 2 in (b). (c-e) Functionally grouped gene ontology (GO) terms for genes up-regulated in Group 1 compared to Group 2. The CytoScape plugin ClueGO was used to group the genes into functional GO terms of "biological processes". (c) Up-regulated GO terms related to transcription pathways; (d) Up-regulated GO terms related to translation pathways and (e) Up-regulated GO terms related to (de)methylation and (de)acetylation pathways.

The oviduct-on-a-chip platform rescued the gene expression pattern of half of the analyzed zygotes. By contrast, the other half of the *CH* zygotes clustered with the G1 delayed zygote group, which included all *VT* zygotes and also 20% of the *VV* zygotes. One possible explanation for the presence of *CH* and *VV* zygotes in the delayed G1 group is that oocyte penetration and/or activation was not simultaneous. We used transvaginal endoscope-guided oviduct flushing to collect *VV* zygotes 43-47.5 h post insemination (hpi; 19-23.5 h post presumed ovulation), while *VT* and *CH* zygotes were collected 20-22 h after incubation with sperm cells. Although embryos were collected at similar times after sperm-oocyte encounter, we were not able to distinguish different pronuclear stages of the zygotes collected (bovine zygotes have dark cytoplasm, which prevents assessment of the pronuclei by normal light microscopy as performed in mouse and human zygotes). Therefore, zygotes were selected purely on the basis of two extruded polar bodies, which may have allowed for asynchrony to affect zygote stage.

Discussion

"ART in humans is a multibillion-dollar industry, full of eager patients and a contradictory scientific literature full of vague concerns"[53]. As a consequence, the majority of ART research has focused on improving the chances of producing a baby, but has neglected the potential long-term impact of ART on the health of the newborns[53]. In mice and other animal models, the possible effects of ART on offspring development and health have been investigated (for review see Feuer & Rinaudo, 2016[54]). However, mouse data is of limited utility to human embryogenesis because of large differences in gene expression patterns and genome sequences. Indeed for these aspects, human embryos are more similar to bovine embryos[55]. Bovine and human preimplantation embryos have also been reported to be similar in terms of biochemical and intrinsic paternal and maternal regulatory (imprinting) processes[56]. Along with the ethical issues of experimenting on human embryos, all these reasons justify the use of bovine oocytes/embryos as a model for human embryogenesis.

In a previous study, we demonstrated benefits of the oviductal environment to support fertilization[31]. However, our first oviduct-on-a-chip platform did not allow perfusion during embryo culture. Additionally, the material used to produce the original devices released toxic compounds, which adversely affected the developing embryos (Ferraz et al, submitted). Therefore, we developed a novel platform that promoted epithelial cell growth and differentiation under perfusion, and that allowed live imaging and embryo production. The oviduct-on-a-chip device was produced using PDMS, a plastic that did not compromise embryo development (Ferraz et al., submitted). BOECs grown in the oviduct-on-a-chip responded to steroid hormone simulation of the luteal and pre-ovulatory phases. Transcriptome changes similar to the *in vivo* luteal phase were observed after progesterone treatment, and included reduced expression of genes involved in ciliary activity, and increases in those involved in tight junction formation and transmembrane signaling receptor activity. By contrast, a high

estrogen environment increased expression of genes related to the immune response, regulation of protein processing, maturation and cell projection morphogenesis[46]. These results collectively demonstrate that the oviduct-on-a-chip allowed BOEC growth and differentiation similarly to that observed *in vivo.* Furthermore, the BOEC monolayer exhibited villus-like structures that resembled natural oviduct folding[25]. The oviduct-on-a-chip supported fertilization and embryo development up to the blastocyst stage, although blastocyst production rates were not as high as for optimized IVP protocols. We conclude that the chip could be further improved by: (1) minor changes to its to ensure that COCs/embryos are retained during perfusion; (2) mimicking the steroid hormone environment of the peri-conception period; and (3) analyzing and optimizing flow rates and shear stress to better protect developing on chip embryos.

Although reduced cleavage and blastocyst formation rates were observed, on chip (*CH*) zygotes were more similar to *in vivo* (*VV*) zygotes than to conventional *in vitro* (*VT*) zygotes in terms of their global DNA methylation levels and transcriptome. Interestingly, *VV* and *CH* zygotes exhibited lower global DNA methylation than *VT* zygotes, which is presumably related to the higher expression of genes involved in demethylation (TET1, TDG, TRIM28, KDM6A, APEX1 and DDX5) in 80% of the *VV* and 50% of the *CH* zygotes (G2). This lower methylation level seems to be essential for the minor embryonic genome activation, since an up-regulation of genes related to transcription and translation initiation was apparent in G2 compared to G1 zygotes. Moreover, when we compared our data with genes described to be first expressed at the 4, 8, 16-cell or blastocyst stages of *IVP* bovine embryo development[57], 24% of the 220 genes reported to be detected at only one of these stages, were up-regulated in the G2 zygotes. This suggests that standard IVP conditions delay zygote transcriptome activation, but that the delay can be ameliorated using our oviduct-on-a-chip platform. Overall, our results highlight the importance of a more *in vivo*-like environment when studying pathways related to normal fertilization and embryo development *in vitro*. This is especially relevant when the use of *in vivo* embryos is not an option for ethical reasons. The addition of oviductal and uterine fluids to culture medium was recently described to 'improve' blastocyst gene expression and DNA methylation patterns in porcine embryos[52]. However, the reported recovery of *in vivo* characteristics was only partial whereas our oviduct-on-a-chip yielded 50% of zygotes with no discernible difference in gene expression pattern to *VV* zygotes. It is therefore possible that not only oviduct epithelial secretions, but also direct contact with the epithelial cells influences the embryonic transcriptome and epigenome. In support of this theory, the apposition of blastocysts to endometrial cells, but not contact with endometrial secretions, was able to initiate trophectoderm differentiation in mouse embryos[58].

In conclusion, we have designed a new tool for investigating early maternal-gamete/embryo interaction in which we can produce zygotes that closely resemble *in vivo* zygotes. Using this state-of-the-art oviduct-on-a-chip platform, we expect to increase our overall understanding of gamete interaction, fertilization and early embryo development, by more faithfully mimicking the *in vivo* environment. In contrast to previously described microfluidic models[33], we used

cell rather than tissue culture, which has several advantages. First, the apical and basolateral compartments were completely separated, which allows distinct collection of secreted factors from, or introduction of exogenous factors to, the apical (luminal) and basolateral (blood circulation) compartments. Permitting both culture conditioning and the introduction of estrous cycle changes that creates an even more *in vivo*-like environment, which is of interest when testing or developing new IVP supplements or when performing toxicological assays. Second, gene-editing of the BOECs is conceivable using this approach, for instance to investigate the effects of specific oviductal factors on gametes or embryos. This would help reduce the need for animal experimentation and, in particular, mouse knockout models.

Beyond its use for refining ART, the oviduct-on-a-chip platform could find other exciting applications. Since it permits live imaging for tracking cell migration and/or specific molecular pathways, it opens new avenues for interrogating pathways associated with tubal derived ovarian cancers and thereby for the identification of biomarkers for the early diagnosis of this lethal disease. Ultimately, the oviduct-on-a-chip platform could facilitate development of patient-derived *in vitro* cancer models which could be extremely valuable for personalized medicine purposes.

Methods

Chemicals.

Unless stated otherwise, all chemicals were obtained from Sigma Chemical Co. (St. Louis, MO) and were of the highest available purity.

Design and fabrication of the oviduct-on-a-chip.

The microfluidic devices (Figure 1) were fabricated using soft lithography[59]. Uncured PDMS mixture (GE RTV-615, Permacol B.V., Ede, The Netherlands; prepolymer:curing agent = 7:1) was poured on 4'-silicon wafers with 380 µm thick patterns of SU-8 100 (MicroChemicals GmbH, Ulm, Germany) and cured for 60 min at 80°C. The apical and basolateral compartments were peeled off the mold, and holes for inlets and outlets were made using a 25-gauge punch (Syneo Co., Angleton, TX, USA). A 10-µm thick porous polycarbonate membrane (TRAKETCH® PC10, pore size: 0.4 µm, pore density: 100 X 10^6/cm^2, SABEU GmbH & Co. KG) was sandwiched between the aligned apical and basolateral layers and bonded using PDMS mortar[60]. Before use with cells, the chambers were sterilized for 1 h in 70% ethanol, washed three-times for 30 min each in phosphate-buffered saline (PBS; 163.9 mM Na^+, 140.3 mM Cl^-, 8.7 mM HPO_4^{3-}, 1.8 mM $H_2PO_4^-$, pH 7.4; Braun, Melsungen, Germany) and washed overnight in HEPES buffered Medium 199 (Gibco BRL, Paisley, U.K.)

supplemented with 100 U/mL penicillin and 100 µg/mL streptomycin (Gibco BRL, Paisley, U.K.). The porous membrane was finally coated with a matrigel solution (3 µg/mL in DMEM/F12; Corning, USA) at 37°C for 2 h.

Computational fluid dynamics and shear stress simulation.

Computation of the flow and shear stresses in the apical compartment was performed using the CFD mode of the commercial finite element code COMSOL Multiphysics 4.4 (COMSOL Inc., MA, USA). To simulate velocity within the microfluidic channel, the "Steady Flow" module was used with liquid set to water and a flow rate of 5 µL/h. The shear stress (Ʈ) within the fluid channel is related to the volume flow rate (*Q*), the fluid viscosity (η), and the channel dimensions (height *h* and width *w*) as follows:

$$\tau = 12\left(\frac{Q\,\eta}{h^2 w}\right)$$

Isolation of oviduct cells and cell culture.

Cow oviducts were collected from a local abattoir immediately after slaughter and transported to the laboratory on ice, within two hours. The oviducts were dissected free of surrounding tissue and washed three times in cold PBS supplemented with 100 U/mL penicillin and 100 µg/mL streptomycin. BOECs were isolated by squeezing the oviductal contents out of the ampullary end of the oviducts, and collected in HEPES buffered Medium 199 supplemented with 100 U/mL penicillin and 100 µg/mL streptomycin. The cells were washed twice by centrifuging for 500 x g for 5 min at 25°C in HEPES buffered Medium 199 supplemented with 100 U/mL penicillin and 100 µg/mL streptomycin. The cells were then cultured for 24 h in HEPES buffered Medium 199 supplemented with 100 U/mL penicillin, 100 µg/mL streptomycin and 10% fetal calf serum (FCS; Bovogen Biologicals, Melbourne, Australia). During these 24 h, the cells formed floating vesicles with outward facing, actively beating cilia. These vesicles were collected, centrifuged at 500 x g for 5 min at 25°C, suspended in DMEM/Ham's F12 medium (DMEM/F-12 Glutamax I, Gibco BRL, Paisley, U.K.) supplemented with 5 µg/mL insulin, 5 µg/mL transferrin, 10 ng/mL epidermal growth factor, 50 nM trans-retinoic acid, 10 mM glutathione, 100 µg/mL gentamycin, and 2.5 mg/mL amphotericin B (chip culture medium, adapted from Ferraz et al.[31]), and pipetted up and down several times to mechanically separate the cells. Next, cells from 3 different donor animals were mixed and seeded into the apical compartments of the oviduct-on-a-chip devices at a concentration of 10 x 10^6 cells/mL (17.8 x 10^6 cells/cm^2) and allowed to attach and reach confluence during 4 days

under static conditions. The culture medium in the basolateral compartment was manually replaced twice a day during the first 4 days during which the device was kept in a humidified atmosphere of 5% CO_2 and 7% O_2 at 38.5°C. Once the cells had reached confluence (4 days after seeding), both the basolateral and apical compartments were maintained under constant flow perfusion (5 µL/h) using a Programmable Aladdin Syringe Pump (WPI, Germany), in a humidified atmosphere of 5% CO_2, 7% O_2 and 38.5°C.

Hormonal stimulation.

Cultures were stimulated periodically with exogenous progesterone (P4) and estradiol 17β (E2) via the basolateral medium. The concentrations of E2 and P4 were based on *in vivo* oviductal fluid concentrations reported for cows[38]. From the day they were seeded into the chips (day 0), BOECs were cultured under one of three different conditions: (1) a control with no hormone stimulation in which the basolateral channel was perfused with chip culture medium plus 1% ethanol for 14 days; (2) a simulated luteal phase in which the basolateral channel was perfused with chip culture medium supplemented with 100 ng/mL P4 and 75 pg/mL E2 for 14 days; and (3) a simulated pre-ovulatory phase in which the basolateral channel was perfused with chip culture medium supplemented with 100 ng/mL P4 and 75 pg/mL E2 for 11 days followed by 10 ng/mL P4 and 300 pg/mL E2 for 3 days (Supplementary fig. 2).

Paracellular tracer flux assay.

For permeability measurements, 8 µL of a dextran–TRITC (4 kDa) or Fluorescein disodium salt (0.4 kDa) solution in culture medium (48 µg/mL) was perfused through the apical channel on day 14 of culture, while unsupplemented culture medium was perfused through the basolateral compartment. Two hours later, the fluorescence intensity was measured in the medium recovered from the basolateral chamber of individual devices. An empty device without any BOECs served as a control. The fluorescence intensity was measured using a BMG Clariostar fluorimeter (Ortenberg, Germany). The apparent permeability *Papp* (µg*cm^2/h) was calculated using the following formula:

$$Papp = (Q/t)/(\frac{1}{A})$$

Where *Q*/*t* is the steady-state flux (µg/mL*h^{-1}) and *A* the total area of diffusion (cm^2).

Trans-epithelial electrical resistance (TEER).

TEER measurements were performed as described previously[61] on day 14 of culture. Briefly, two Ag/AgCl wire electrodes (World Precision Instruments, Germany) were sterilized for 10 min in 70% ethanol and connected to a digital volt-ohm meter (Millicell, USA) using alligator clips. The microfluidic devices were filled with HEPES buffered Medium 199 supplemented with 100 U/mL penicillin and 100 µg/mL streptomycin injected into the apical and basolateral compartments through silicone tubing connected to the inlet ports. Electrodes were inserted into each compartment (one via the apical and one via the basolateral inlet tubing). After 1 min of stabilization, the electrical resistance was recorded. The electrical resistance of a blank device (without cells) was measured in parallel. To obtain the TEER (in $\Omega*cm^2$), the blank value was subtracted from the total resistance of the sample, and the final unit area resistance ($\Omega*cm^2$) was calculated by multiplying the sample resistance by the effective area of porous membrane onto which the cells are grown (0.09 cm^2).

Cell ciliation and morphology.

At day 14 of culture, two oviduct-on-a-chip devices were fixed per pool (3 pools, n = 6 devices per condition) to assess cilia formation and the morphology of epithelial cells using immunofluorescent staining as described previously[31]. Briefly, chips were fixed in 4% paraformaldehyde for 30 min, and permeabilized for 30 min using 0.5 % Triton-X100 in PBS. Non-specific binding was blocked by incubation for 1 h in PBS containing 5% normal goat serum at room temperature. The chips were then incubated overnight at 4°C with rabbit anti-acetylated α-tubulin (1:100, Abcam, Cambridge, UK) and mouse anti-OVGP1 (1:50; Santa Cruz Biotechnology, Santa Cruz, CA) primary antibodies. Next, the chips were washed and incubated with an Alexa 488 conjugated goat anti-rabbit antibody and an Alexa 647 conjugated goat anti-mouse antibody (1:100; Santa Cruz Biotechnology, Santa Cruz, CA) for 1 h. Hoechst 33342 (5 µg/mL) was used to stain cell nuclei and phalloidin conjugated to Alexa 568 (1:100) was used to stain actin filaments. For imaging, laser scanning confocal microscopy using a TCS SPE-II system (Leica Microsystems GmbH, Wetzlar, Germany) attached to an inverted semi-automated DMI4000 microscope (Leica) with a 40x NA 1.25 objective was used. 3D images of the cell monolayers were re-constructed from 0.2 µm Z-stacks using ImageJ software (National Institutes of Health, Bethesda, MD, USA) to evaluate cell morphology, ciliation and OVGP1 expression. A total of six randomly selected areas were imaged per device. For OVGP1 quantification, images were analyzed by evaluating fluorescence intensity for OVGP1 and DNA in each area using ImageJ software. After maximum projection reconstruction of Z-stacks, the fluorescence intensity of each channel was measured and adjusted for cytoplasmic background. The average intensity of fluorescence for OVGP1 was then normalized by dividing the OVGP1 intensity by Hoechst 33342 fluorescence to normalize for DNA content.

Live cell imaging.

After 14 days of culture, the oviduct-on-a-chip platform was incubated with MitoTracker Red labeled sperm, as described previously[31], and stained with Hoechst 33342 (5 µg/mL) in the chip culture medium for 30 min. Live cell imaging was performed by laser scanning confocal microscopy using a 20 x NA 1.25 objective.

Oocyte collection and in vitro maturation (IVM).

Bovine ovaries were collected from a local abattoir and transported to the laboratory within 2 h. The ovaries were washed in physiological saline (0.9% w/v NaCl) and held in physiological saline containing 100 U/mL penicillin and 100 µg/mL streptomycin at 30°C. Follicular fluid and cumulus oocyte complexes (COCs) were aspirated from follicles with a diameter of 2 to 8 mm and collected into 50 mL conical tubes using a 19-gauge needle and a vacuum pump[62]. COCs with a minimum of three layers of intact cumulus cells were selected and washed first in HEPES-buffered M199 (Gibco BRL, Paisley, U.K.) before being washed and cultured in maturation medium (M199 supplemented with 0.02 IU/mL follicle-stimulating hormone [Sioux Biochemical Inc., Sioux Center, IA], 10% FCS, 100 U/mL penicillin and 100 µg/mL streptomycin) in four-well culture plates (Nunc A/S, Roskilde, Denmark). Groups of 50 COCs in 500 µL maturation medium were incubated in a humidified atmosphere of 5% CO_2-in-air for 24 h at 38.5°C.

Sperm preparation for in vitro fertilization (IVF).

Frozen spermatozoa were thawed and prepared as described previously[62]. Briefly, 250 µL straws were thawed at 37°C for 30 s and the spermatozoa washed by centrifugation at 700 x g for 30 min through a discontinuous Percoll gradient (GE Healthcare, USA) at 27°C. The supernatant was removed and the pellet suspended in fertilization medium (modified Tyrode's medium supplemented with 25 mM sodium bicarbonate, 22 mM lactate, 1 mM pyruvate, 6 mg/mL fatty acid–free BSA containing 100 U/mL penicillin and 100 µg/mL streptomycin).

In vitro fertilization (IVF), in vitro culture (IVC), zygote and blastocyst collection.

At day 11 of BOEC culture, the apical medium was replaced by fertilization medium (supplemented with 10 µg/mL heparin, 20 µM d-penicillamine, 10 µM hypotaurine, and 1 µM epinephrine) and a total of 27 *in vitro* matured COCs were added to the apical compartment of each chip (n=20 devices); sperm was then added at a final concentration of $1x10^6$ sperm cells/mL. The chips were maintained under perfusion (5 µL/h flow: fertilization medium in the apical compartment and chip culture medium in the basolateral compartment). After 20-22 h of co-incubation under a humidified atmosphere of 5% CO_2 and 7% O_2 at 38.5°C, the presumptive zygotes (on chip zygotes) were collected from the apical compartment, cumulus cells were

removed by pipetting, and the zygotes were either fixed in 4% paraformaldehyde for 30 min at room temperature (n=30) or frozen for RNA extraction (n=10). Likewise, for conventional IVF, *in vitro* matured COCs were distributed into groups of 35-50 in four-well culture plates (Nunc A/S, Roskilde, Denmark) with 500 µL of fertilization medium supplemented with 10 µg/mL heparin, 20 µM d-penicillamine, 10 µM hypotaurine, and 1 µM epinephrine, and spermatozoa were added at a final concentration of $1x10^6$ sperm cells/mL (normal IVF). After 20-22 h of co-incubation under a humidified atmosphere containing 5% CO_2 and 20% O_2 at 38.5°C, cumulus cells were removed by pipetting and the presumptive zygotes (*in vitro* zygotes) were fixed (n=30) and/or frozen (n=10) as described above.

Remaining zygotes were placed back into the apical compartment of the microfluidic chips and cultured under 5 µL/h flow, with synthetic oviductal medium (SOF medium) in the apical and chip culture medium in the basolateral compartment in a humidified atmosphere of 5% CO_2 and 7% O_2 at 38.5°C. At days 5 and 8, embryos were scored respectively for cleavage or development to the blastocyst stage. For conventional IVP, following denudation presumptive zygotes were distributed in groups of 35-50 in four-well culture plates with 500 µL of SOF medium. The embryos were cultured in a humidified atmosphere of 5% CO_2 and 5% O_2 at 38.5°C. At day 5 post-fertilization all cleaved embryos were transferred to fresh SOF medium. At day 8, blastocysts (*in vitro* blastocysts) were counted and harvested.

Animal preparation for embryo collection.

Eight Simmental heifers aged between 15 and 20 months and weighing between 380 and 500 kg were used in this study. All experimental animals were handled according to German animal experimentation laws and kept under identical farm conditions within the same herd. Pre-synchronization of animals was performed by i.m. administration of 500 µg Cloprostenol (a PGF2α analogue, Estrumate ®; Essex Tierarznei, Munich, Germany) twice with an 11 day interval. Two days after each of PGF2α treatment, animals received 20 µg of GnRH (Receptal ®; Intervet, Boxmeer, the Netherlands) by i.m. administration. Twelve days after the last GnRH injection, heifers received the first of eight consecutive FSH-injections over 4 days in decreasing doses (in total 400 mg of FSH equivalent according to body weight; Stimufol ®, University of Liege, Belgium). Two PGF2α treatments were performed 60 and 72 h after the initial FSH injection. The first of a total of three artificial inseminations within a 12-h interval was performed 48h after the first PGF2α injection. Finally, 60 h after the first PGF2α application, coincident with the second insemination, ovulation was induced by administration of 10 mg of GnRH.

Collection of in vivo *zygote stage embryos.*

Zygotes were collected 19-23.5 h after expected ovulation. Flushing was accomplished as

described previously[63]. Briefly, after restraining the cow, inducing epidural anesthesia with 5 mL of a 2% lidocaine solution (Xylanest ®, Richter Pharma, Wels, Austria) and disinfecting the vulva (Octenisept, Schülke/Mayer, Vienna, Austria), a trocar set consisting of a metal tube (12.5 mm x 52 cm, Storz, Vienna, Austria) and an atraumatic mandrin was placed caudodorsal to the fornix vagina. The mandrin was replaced by a sharp trocar, and the trocar set was inserted through the vaginal wall into the peritoneal cavity. The trocar was replaced by a shaft bearing the endoscope (5.5 mm forward Hopkins endoscope; Storz) and the transfer system. The site was illuminated using a fiberoptic cold light (250W, Storz) and visualized with a camera (Telecam PAL-Endovision, Storz) connected to a monitor. The flushing system consisted of a 20-mL syringe connected to a perfusor tube (No. 08272514; Braun, Melsungen, Germany) and a metal tube (14 cm × 2.5 mm) with numerous lateral holes covered by a silicone tube. After the metal tube had been inserted via the infundibulum into the ampulla, careful management of the flushing pressure allowed the balanced adjustment of tubal sealing to avoid medium reflux. Oviducts were flushed with 50 mL flushing medium (phosphate-buffered saline supplemented with 1% fetal calf serum). Flushing medium (50 mL) was forced through the uterotubal junction into the uterine horn and from there was collected via a uterus flushing catheter (CH15, Wörrlein, Ansbach, Germany) into an embryo filter (Emcon filter, No. 04135; Immuno Systems Inc., Spring Valley, WI, USA).

Immunofluorescence for global methylation.

Immunofluorescent staining for 5-methylcytosine (5mC) was performed in zygotes at different pronuclear stages. Fixed zygotes were permeabilized by incubation for 30 min in 1% Triton-X100 in PBS, followed by denaturation with 3 M HCl for 30 min, which was then neutralized using 100 mM Tris-HCl buffer (pH 8.5) for 15 min. Non-specific binding was blocked by incubating the permeabilized zygotes for 1 h in PBS containing 5% normal goat serum (NGS). The zygotes were then incubated overnight at 4^{o}C with a mouse anti-5mC primary antibody (1:100 dilution with PBS + 5% NGS + 0.1% Triton-X100; Eurogentec, BI-ME-CY-0100). Next, the zygotes were washed three times in PBS-polyvinylpyrrolidone (PVP, 3 mg/mL; 10 min each) and incubated with an Alexa 488 conjugated goat anti-mouse antibody (1:100, Santa Cruz Biotechnology, Santa Cruz, CA) for 1 h. Zygotes were then incubated with propidium iodide (PI; 25 µg/mL) for 30 min to counterstain the DNA. Negative controls were produced by omitting incubation with the primary antibody. Analysis was performed by laser scanning confocal microscopy with a 40x NA 1.25 objective. Z-stacks of 1 µm of both pronuclei were obtained. Images were analyzed by evaluating the fluorescence intensity for 5mC and DNA in each pronucleus using ImageJ software (National Institutes of Health, Bethesda, MD, USA). After maximum projection reconstruction of Z-stacks, the fluorescence intensity of each channel was measured by manually outlining each pronucleus and adjusted for cytoplasmic background. The average intensity of 5mC fluorescence was then adjusted by dividing by PI fluorescence to normalize the 5mC intensity for DNA content.

RNA extraction.

Cells were collected from the chips by perfusing with 200 µL of kit lysis buffer for 2 min (RNEasy Micro RNA extraction kit; Qiagen GmbH, Hilden, Germany)**.** Total RNA was isolated from single zygotes, or from the cells collected from the devices using the RNEasy Micro RNA extraction kit; Qiagen GmbH, Hilden, Germany), and treated with RNAse-free DNAse I (Qiagen GmbH, Hilden, Germany) to remove genomic DNA, following the manufacturer's instructions.

Cel-seq II primer design.

The reverse transcription primer was designed with an anchored polyT, a 6 bp unique barcode, a 6 bp UMI (unique molecular identifier), the 5' Illumina adapter and a T7 promoter. The barcodes were designed such that each pair was different by at least two nucleotides, so that a single sequencing error would not produce the wrong barcode (adapted from Hashimshony et al., 2012[64]).

Linear mRNA amplification.

RNA extracted from single zygotes was precipitated with isopropanol and the pellet was used for the reverse-transcription (RT) reaction. RT was performed with 5 ng of primer per reaction. A total of 0.2 µL of the primer mixed with 1 µL of water or 1 µL of a 1:1,000,000 dilution of the ERCC spike-in kit (a total of 1.2 µL) was added directly to the Eppendorf tube in which the RNA was precipitated, and incubated at 65°C for 5 min (with the lid of the thermal cycler heated to 65°C). The sample was spun to the bottom of the tube mid incubation. After the second-strand synthesis, samples were pooled and cleaned on a single column before proceeding to the IVT (Ambion AM1334) reaction for 13 h. The solution was treated with EXO-SAP to remove the primers and the RNA was fragmented (one-fifth volume of 200 mM Tris-acetate [pH 8.1], 500 mM KOAc, 150 mM MgOAc added) for 3 min at 94°C. The reaction was stopped by placing the sample on ice and adding one-tenth volume of 0.5 M EDTA, followed by RNA cleanup. The RNA quality and yield were analyzed using a Bioanalyzer (Agilent).

Library construction and Cel-seq II.

RT reaction was performed using SuperScript II, following the manufacturer's protocol (Invitrogen). A total of 14 cycles of PCR was performed using Phusion® High-Fidelity PCR Master Mix with HF Buffer (NEB, MA, USA) and an elongation time of 30 s. PCR products were cleaned twice with AMPure XP beads (Beckman Coulter, Woerden, Netherlands). Li-

braries were sequenced on the Illumina Nextseq500 platform; a high output paired end run of 2x 75bp was performed.

Cel-seq II data analysis.

Differentially expressed genes were identified using the Deseq2 (v1.10.1) package[65]. Genes with low counts (whose sum of all counts across samples included in the analysis was < 10) were removed. The p-value was determined by Wald statistics. An adjusted p-value to correct for multiple testing was calculated using the Benjamini-Hochberg method. Differentially expressed genes (DEGs) were filtered by fold change (lfcThreshold=1) and a false discovery rate (FDR) less than 1% (alpha = 0.1). Biological functions of differentially regulated gene sets were identified using ToppGene Suite tool ToppFun (default setting: FDR correction, p-value cutoff of 0.05 and gene limit set of $1 \leq n \leq 2000$[66]).

Functional GO Clustering.

The Cytoscape 3.5.1 plugin ClueGO[67] was used to functionally group the up- and down-regulated genes by GO terms “biological processes” and “cellular components” using the *Bos taurus* genome. The evidence was set to “Inferred by Curator (IC),” and the statistical test was set to a right-sided hypergeometrical test with a Bonferroni (step down) and a κ score of 0.7-0.9. The GO term restriction levels were set to 3–8, with a minimum of three genes or 5% genes in each GO term, and the function “GO Term fusion” was selected.

Data analysis.

The data were analyzed using IBM SPSS Statistics (version 24). A Shapiro-Wilk test was performed, and all data proved to be normally distributed. Mean and standard deviations are provided in graphs; differences between groups were examined by ANOVA followed by a post-hoc Tukey test with a confidence interval of 95%.

References

1. Nelissen, E. C. M. *et al.* Altered gene expression in human placentas after IVF/ICSI. *Hum. Reprod.* **29,** 2821–31 (2014).
2. Lonergan, P., Fair, T., Corcoran, D. & Evans, a. C. O. Effect of culture environment on gene expression and developmental characteristics in IVF-derived embryos. *Theriogenology* **65,** 137–152 (2006).
3. Ventura-Juncá, P. *et al.* In vitro fertilization (IVF) in mammals: epigenetic and developmental alterations. Scientific and bioethical implications for IVF in humans. *Biol.*

Res. **48,** 68 (2015).
4. Ménézo, Y., Guérin, P. & Elder, K. The oviduct: A neglected organ due for re-assessment in IVF. *Reprod. Biomed. Online* **30,** 233–240 (2015).
5. Santos, F. *et al.* Evaluation of epigenetic marks in human embryos derived from IVF and ICSI. *Hum. Reprod.* **25,** 2387–2395 (2010).
6. Li, T. *et al.* IVF results in de novo DNA methylation and histone methylation at an Igf2-H19 imprinting epigenetic switch. *Mol. Hum. Reprod.* **11,** 631–640 (2005).
7. Räty, M. *et al.* In vitro maturation supplements affect developmental competence of bovine cumulus-oocyte complexes and embryo quality after vitrification. *Cryobiology* (2011). doi:10.1016/j.cryobiol.2011.09.134
8. Cao, Z. *et al.* Dynamic reprogramming of 5-hydroxymethylcytosine during early porcine embryogenesis. *Theriogenology* **81,** 496–508 (2014).
9. Schnorr, J. A., Muasher, S. J. & Jones, H. W. Evaluation of the clinical efficacy of embryo cryopreservation. *Mol.Cell Endocrinol.* **169,** 85–89 (2000).
10. Thompson, J. G., Kind, K. L., Roberts, C. T., Robertson, S. A. & Al, E. Epigenetic risks related to assisted reproductive technologies: Short-and long-term consequences for the health of children conceived through assisted reproduction. *Hum. Reprod.* **17,** 2783–2786 (2002).
11. Huntriss, J. D. & Picton, H. M. Epigenetic consequences of assisted reproduction and infertility on the human preimplantation embryo. *Hum. Fertil. (Camb).* **11,** 85–94 (2008).
12. Schwarzer, C. *et al.* ART culture conditions change the probability of mouse embryo gestation through defined cellular and molecular responses. *Hum. Reprod.* **27,** 2627–40 (2012).
13. Fraser, R. & Lin, C. J. Epigenetic reprogramming of the zygote in mice and men: On your marks, get set, go! *Reproduction* **152,** R211–R222 (2016).
14. Feil, R. Epigenetic asymmetry in the zygote and mammalian development. *Int. J. Dev. Biol.* **53,** 191–201 (2009).
15. Salilew-Wondim, D., Tesfaye, D., Hoelker, M. & Schellander, K. Embryo transcriptome response to environmental factors: Implication for its survival under suboptimal conditions. *Anim. Reprod. Sci.* **149,** 30–38 (2014).
16. Gaspar, R. C. *et al.* Oxygen tension affects histone remodeling of invitro-produced embryos in a bovine model. *Theriogenology* **83,** 1408–1415 (2015).
17. Maalouf, W. E., Alberio, R. & Campbell, K. H. S. Differential acetylation of histone H4 lysine during development of in vitro fertilized, cloned and parthenogenetically activated bovine embryos. *Epigenetics* **3,** 199–209 (2008).
18. Deshmukh, R. S. *et al.* DNA methylation in porcine preimplantation embryos developed in vivo and produced by in vitro fertilization, parthenogenetic activation and somatic cell nuclear transfer. *Epigenetics* **6,** 177–187 (2011).
19. Young, L. E. *et al.* Epigenetic change in IGF2R is associated with fetal overgrowth after sheep embryo culture. *Nat. Genet.* **27,** 153–154 (2001).
20. DeBaun, M. R., Niemitz, E. L. & Feinberg, A. P. Association of in vitro fertilization with Beckwith-Wiedemann syndrome and epigenetic alterations of LIT1 and H19. *Am. J. Hum. Genet.* **72,** 156–60 (2003).
21. Betsha, S. *et al.* Sperm binding properties and secretory activity of the bovine oviduct immediately before and after ovulation. *Mol. Reprod. Dev.* **80,** 315–333 (2013).
22. Sostaric, E. *et al.* Sperm binding properties and secretory activity of the bovine oviduct immediately before and after ovulation. *Mol. Reprod. Dev.* **75,** 60–74 (2008).
23. Ferraz, M. A. M. M., Henning, H. H. W., Stout, T. A. E., Vos, P. L. A. M. & Gadella, B. M. Designing 3-Dimensional In Vitro Oviduct Culture Systems to Study Mammalian Fertilization and Embryo Production. *Ann. Biomed. Eng.* (2016). doi:10.1007/s10439-016-1760-x
24. Nelis, H. *et al.* Equine oviduct explant culture: a basic model to decipher embryo–ma-

ternal communication. *Reproduction, Fertility and Development* **26,** 954–966 (2014).
25. Steinhauer, N., Boos, A. & Günzel-Apel, A. R. Morphological changes and proliferative activity in the oviductal epithelium during hormonally defined stages of the oestrous cycle in the bitch. *Reprod. Domest. Anim.* **39,** 110–119 (2004).
26. Yaniz, J. L., Lopez-Gatius, F. & Hunter, R. H. F. Scanning electron microscopic study of the functional anatomy of the porcine oviductal mucosa. *Anat. Histol. Embryol.* **35,** 28–34 (2006).
27. Chen, S., Einspanier, R. & Schoen, J. Long-term culture of primary porcine oviduct epithelial cells: Validation of a comprehensive invitro model for reproductive science. *Theriogenology* **80,** 862–869 (2013).
28. Chen, S., Einspanier, R. & Schoen, J. In vitro mimicking of estrous cycle stages in porcine oviduct epithelium cells: estradiol and progesterone regulate differentiation, gene expression, and cellular function. *Biol. Reprod.* **89,** 54 (2013).
29. Gualtieri, R. *et al.* Bovine oviductal monolayers cultured under three-dimension conditions secrete factors able to release spermatozoa adhering to the tubal reservoir in vitro. *Theriogenology* **79,** 429–435 (2013).
30. Kessler, M. *et al.* The Notch and Wnt pathways regulate stemness and differentiation in human fallopian tube organoids. *Nat. Commun.* **6,** 8989 (2015).
31. Ferraz, M. A. M. M. *et al.* Improved bovine embryo production in an oviduct-on-a-chip system: Prevention of poly-spermic fertilization and parthenogenic activation. *Lab Chip* (2017). doi:10.1039/C6LC01566B
32. Reischl, J. *et al.* Factors affecting proliferation and dedifferentiation of primary bovine oviduct epithelial cells in vitro. *Cell Tissue Res.* **296,** 371–383 (1999).
33. Xiao, S. *et al.* A microfluidic culture model of the human reproductive tract and 28-day menstrual cycle. *Nat. Commun.* **8,** 14584 (2017).
34. Le Gac, S. & Nordhoff, V. Microfluidics for mammalian embryo culture and selection: where do we stand now? *Mol. Hum. Reprod.* (2016). doi:10.1093/molehr/gaw061
35. Duffy, D. C., McDonald, J. C., Schueller, O. J. A. & Whitesides, G. M. Rapid prototyping of microfluidic systems in poly(dimethylsiloxane). *Anal. Chem.* **70,** 4974–4984 (1998).
36. Esteves, T. C. *et al.* A microfluidic system supports single mouse embryo culture leading to full-term development. *RSC Adv.* **3,** 26451 (2013).
37. Lai, D., Takayama, S. & Smith, G. D. Recent microfluidic devices for studying gamete and embryo biomechanics. *J. Biomech.* **48,** 1671–1678 (2015).
38. Lamy, J. *et al.* Steroid hormones in bovine oviductal fluid during the estrous cycle. *Theriogenology* **86,** 1409–1420 (2015).
39. Chen, S., Einspanier, R. & Schoen, J. Transepithelial electrical resistance (TEER): a functional parameter to monitor the quality of oviduct epithelial cells cultured on filter supports. *Histochem. Cell Biol.* (2015). doi:10.1007/s00418-015-1351-1
40. Lo, C.-M., Keese, C. R. & Giaever, I. Cell–Substrate Contact: Another Factor May Influence Transepithelial Electrical Resistance of Cell Layers Cultured on Permeable Filters. *Exp. Cell Res.* **250,** 576–580 (1999).
41. Saint-Dizier, M. *et al.* OVGP1 is expressed in the canine oviduct at the time and place of oocyte maturation and fertilization. *Mol. Reprod. Dev.* **81,** 972–982 (2014).
42. Lyons, R. a., Saridogan, E. & Djahanbakhch, O. The effect of ovarian follicular fluid and peritoneal fluid on Fallopian tube ciliary beat frequency. *Hum. Reprod.* **21,** 52–56 (2006).
43. Nakahari, T. *et al.* The regulation of ciliary beat frequency by ovarian steroids in the guinea pig Fallopian tube: interactions between oestradiol and progesterone. *Biomed. Res.* **32,** 321–8 (2011).
44. Bylander, A. *et al.* Rapid effects of progesterone on ciliary beat frequency in the mouse fallopian tube. *Reprod. Biol. Endocrinol.* **8,** 48 (2010).
45. Mahmood, T., Saridogan, E., Smutna, S., Habib, A. M. & Djahanbakhch, O. The effect

of ovarian steroids on epithelial ciliary beat frequency in the human Fallopian tube. *Hum. Reprod.* **13,** 2991–4 (1998).
46. Cerny, K. L., Garrett, E., Walton, A. J., Anderson, L. H. & Bridges, P. J. A transcriptomal analysis of bovine oviductal epithelial cells collected during the follicular phase versus the luteal phase of the estrous cycle. *Reprod. Biol. Endocrinol.* **13,** 84 (2015).
47. Talevi, R. & Gualtieri, R. Molecules involved in sperm-oviduct adhesion and release. *Theriogenology* **73,** 796–801 (2010).
48. Coy, P., García-Vázquez, F. a., Visconti, P. E. & Avilés, M. Roles of the oviduct in mammalian fertilization. *Reproduction* **144,** 649–660 (2012).
49. Almiñana, C. *et al.* Oviduct extracellular vesicles protein content and their role during oviduct–embryo cross-talk. *Reproduction* **154,** 153–168 (2017).
50. García, E. V. *et al.* Bovine embryo-oviduct interaction in vitro reveals an early cross talk mediated by BMP signaling. *Reproduction* **153,** 631–643 (2017).
51. Y, X. *et al.* Shear Stress Induces Preimplantation Embryo Death That Is Delayed by the Zona Pellucida and Associated with Stress-Activated Protein Kinase-Mediated Apoptosis. *Biol. Reprod.* **75,** 45–55 (2006).
52. Canovas, S. *et al.* DNA methylation and gene expression changes derived from assisted reproductive technologies can be decreased by reproductive fluids. *Elife* **6,** 1–24 (2017).
53. Servick, K. Unsettled questions trail IVF's success. *Science (80-.).* **345,** 744–746 (2014).
54. Feuer, S. & Rinaudo, P. From Embryos to Adults: A DOHaD Perspective on In Vitro Fertilization and Other Assisted Reproductive Technologies. *Healthcare* **4,** 51 (2016).
55. Jiang, Z. *et al.* Transcriptional profiles of bovine in vivo pre-implantation development. *BMC Genomics* **15,** 756 (2014).
56. Ménézo, Y. J. & Hérubel, F. Mouse and bovine models for human IVF. *Reprod. Biomed. Online* **4,** 170–175 (2002).
57. Graf, A. *et al.* Fine mapping of genome activation in bovine embryos by RNA sequencing. *Proc. Natl. Acad. Sci. U. S. A.* **111,** 4139–4144 (2014).
58. Ruane, P. T. *et al.* Apposition to endometrial epithelial cells activates mouse blastocysts for implantation. *MHR Basic Sci. Reprod. Med.* 1–11 (2017). doi:10.1093/molehr/gax043
59. Xia, Y. & Whitesides, G. M. SOFT LITHOGRAPHY. *Annu. Rev. Mater. Sci.* **28,** 153–184 (1998).
60. Chueh, B. *et al.* Leakage-free bonding of porous membranes into layered microfluidic array systems. *Anal. Chem.* **79,** 3504–8 (2007).
61. Huh, D. *et al.* Microfabrication of human organs-on-chips. *Nat. Protoc.* **8,** 2135–57 (2013).
62. Van Tol, H. T. A. A., Van Eerdenburg, F. J. C. M. C. M., Colenbrander, B. & Roelen, B. A. J. J. Enhancement of Bovine oocyte maturation by leptin is accompanied by an upregulation in mRNA expression of leptin receptor isoforms in cumulus cells. *Mol. Reprod. Dev.* **75,** 578–587 (2008).
63. Besenfelder, U., Havlicek, V., Mösslacher, G. & Brem, G. Collection of tubal stage bovine embryos by means of endoscopy a technique report. *Theriogenology* **55,** 837–845 (2001).
64. Hashimshony, T., Wagner, F., Sher, N. & Yanai, I. CEL-Seq: Single-Cell RNA-Seq by Multiplexed Linear Amplification. *Cell Rep.* **2,** 666–673 (2012).
65. Love, M. I., Huber, W. & Anders, S. Moderated estimation of fold change and dispersion for RNA-seq data with DESeq2. *Genome Biol.* **15,** 550 (2014).
66. Chen, J., Bardes, E. E., Aronow, B. J. & Jegga, A. G. ToppGene Suite for gene list enrichment analysis and candidate gene prioritization. *Nucleic Acids Res.* **37,** W305-11 (2009).
67. Bindea, G. *et al.* ClueGO: a Cytoscape plug-in to decipher functionally grouped gene

ontology and pathway annotation networks. *Bioinformatics* **25,** 1091–3 (2009).

Acknowledgements

The authors would like to thank Dr. Eugene Y. Kathruka for his help with live imaging of the chips, Nuno F. Pinheiro for his help in modeling chips for flow rate and shear stress calculations and Juliette Delahaye for her help in designing the microfluidic devices.

Author contributions statement

MAMMF designed and performed all experiments and wrote the manuscript. SLG and HR designed and produced the microfluidics devices and reviewed the manuscript. HvT performed *in vitro* fertilization experiments and reviewed the manuscript. MH and UB performed *in vivo* collection of embryos and reviewed the manuscript. DH and MM performed RNAseq data analysis. BMG, HHWH, TAES, PLAMV, supervised MAMMF, designed experiments and reviewed the manuscript.

Supplementary file 1.

We used two Aladdin Syringe Pumps (WPI, Germany) to deliver solutions into the microfluidic devices. Solutions were transferred into 1 ml plastic syringes (BD Biosciences, Breda, The Netherlands) and Tygon® microbore tubing (0.020” ID x 0.060” OD, Cole-Parmer, Schiedam, The Netherlands) was connected using EFD Precision tips (23 gauge, EFD Nordson, Maastricht, The Netherlands). The other end of the tubing was connected to inlets on the microfluidic device using stainless steel pins (23 gauge, New England Small Tube Co., Litchfield, NH, USA) as shown below.

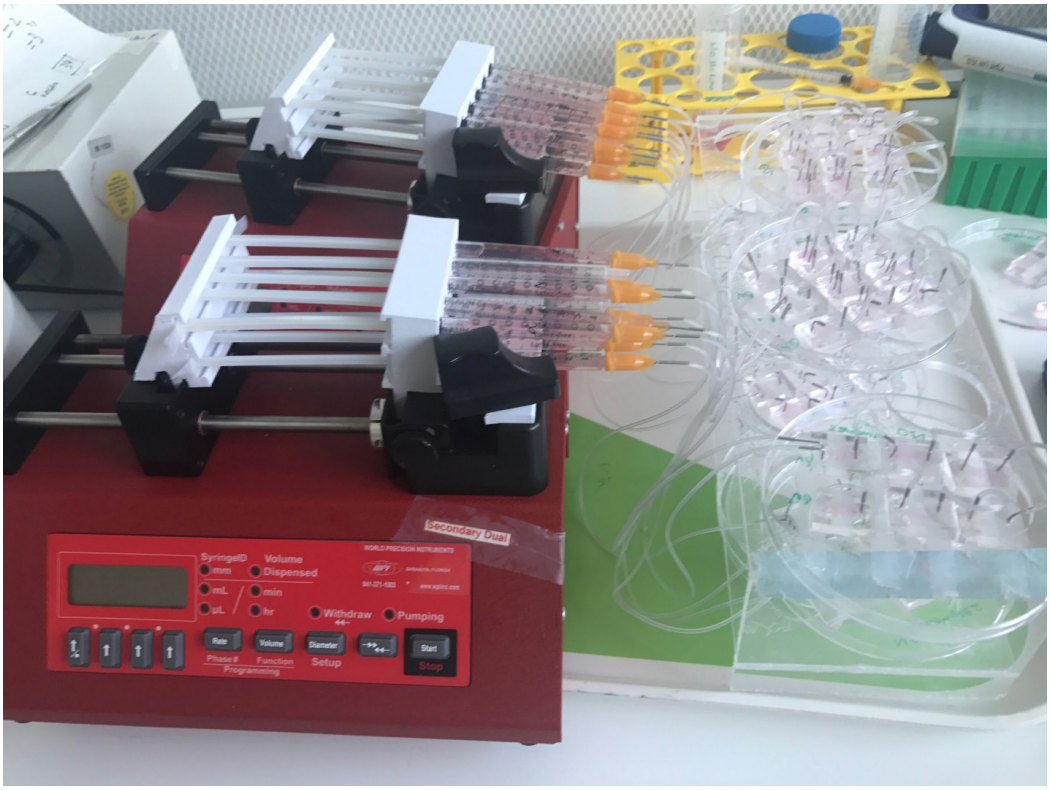

Supplementary figures.

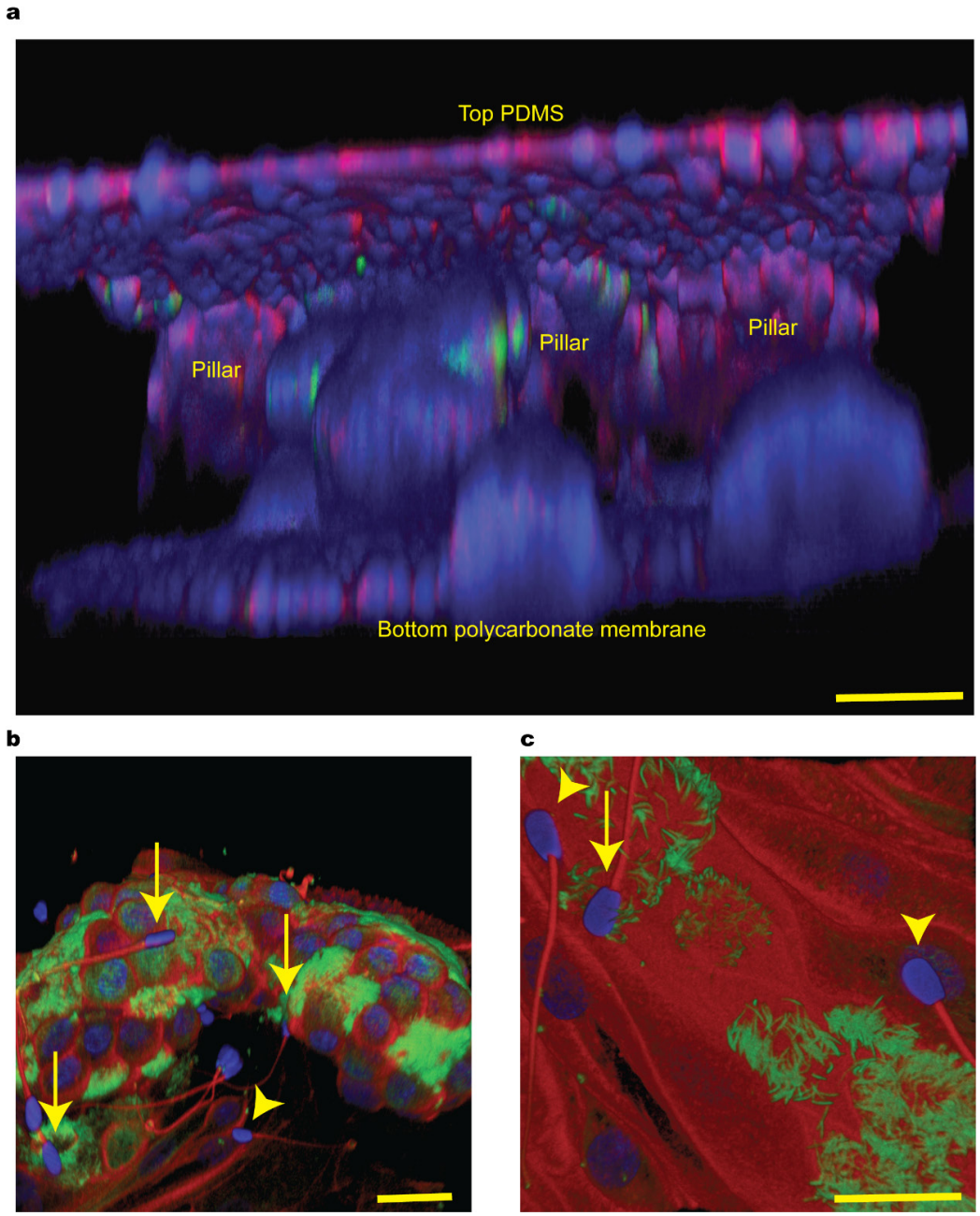

Supplementary figure 1: 3D reconstruction of confocal immunofluorescence (IF) images for cilia (acetylated alpha-tubulin, green), nuclei (HOECHST33342, blue) and actin filaments (phalloidin, red) with and without sperm cells. (a) 3D reconstruction of part of the apical chamber, showing that BOECs grew on the overlying PDMS, on the trapping pillars and on the underlying polycarbonate membrane. Note the formation of villus-like structures, mimicking oviduct mucosal folding. (b) Closer look at a villus-like structure with attached sperm cells. Sperm cells were bound to ciliated (arrows) and non-ciliated cells (arrow heads). (c) Closer look at sperm-epithelium binding: sperm cells were bound to ciliated (arrows) and non-ciliated cells (arrow heads). Scale Bars = 50 µm (a) and 10 µm (b and c).

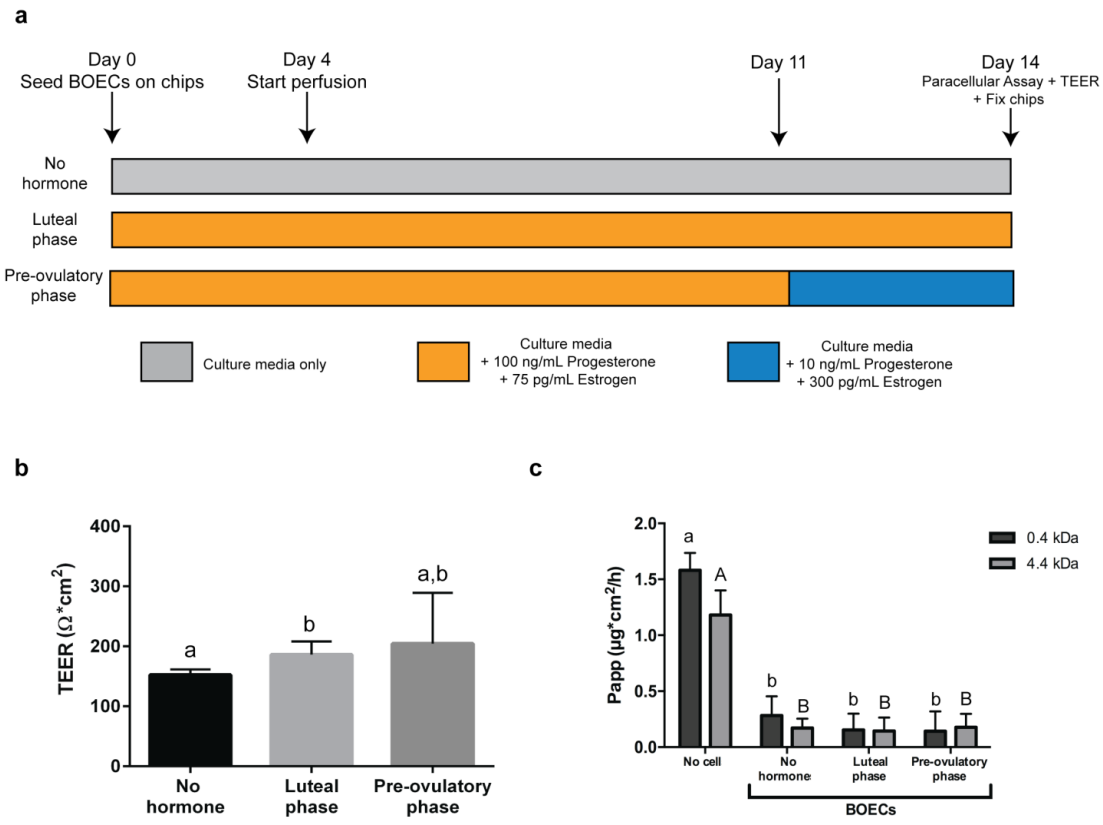

Supplementary figure 2: Hormonal stimulation experimental design and effects on the trans-epithelial electrical resistance (TEER) and Paracellular permeability (Papp). (a) Experimental design for mimicking the luteal and pre-ovulatory phases. (b) TEER measurements in the microfluidic devices under the three conditions; values were adjusted for the resistance found in an empty device ($F=14.503$, $p<000.1$). (c) Apparent permeability (Papp) of 0.4 and 4.4 kDa fluorescent markers in devices without cells (no cell) or in the presence of bovine oviductal epithelial cells (BOECs) under the three experimental conditions ($F=0.537$, $p=0.590$ and $F=0.583$, $p=0.564$ for 0.4 and 4.4 kDa, respectively). Different letters indicate statistically significant differences ($p<0.05$).

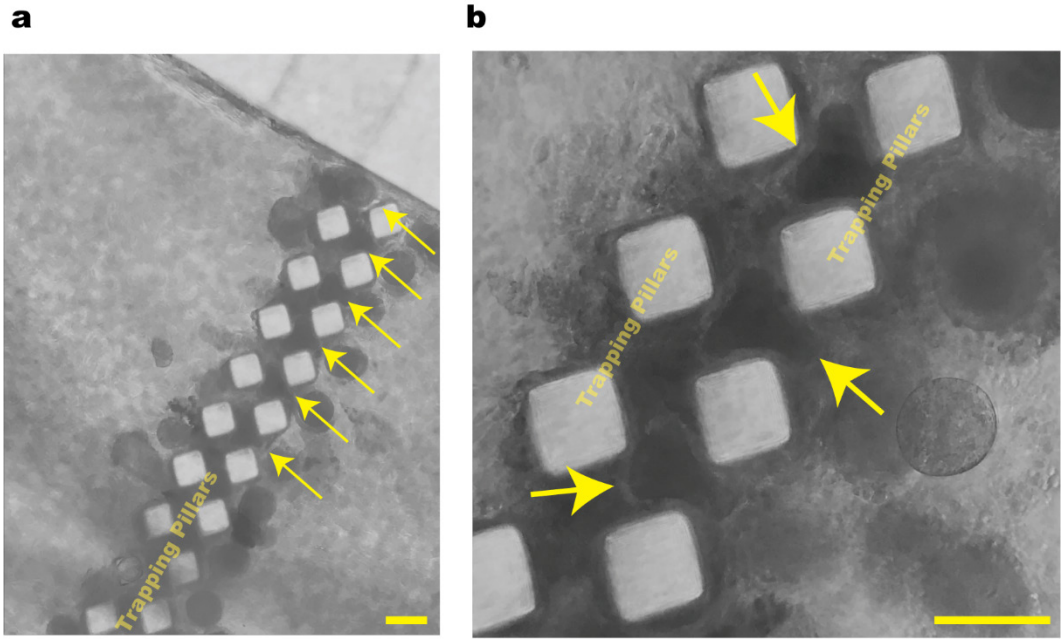

Supplementary figure 3: Phase-contrast images of cumulus-oocyte-complexes (COCs) inside the oviduct-on-a-chip. Note the COCs trapped (arrows) between the trapping pillars in (a) and (b). Scale bars = 100 µm.

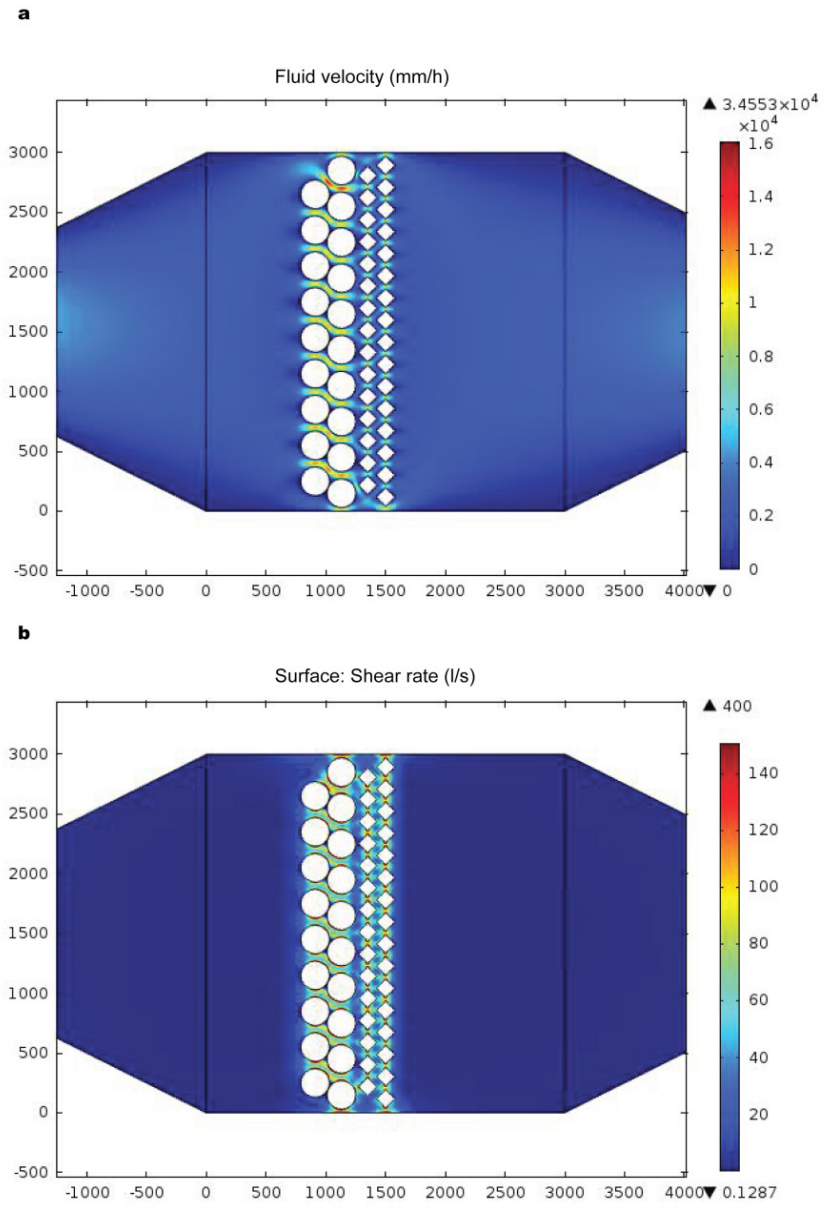

Supplementary figure 4: Modulation of the flow and shear rate inside the oviduct-on-a-chip. In (a) notice the evenly distributed flow, that is direct and increases between pillars and "COCs/embryos" (white circles), mimicking IVF simultaneous with perfusion of the apical compartment. In (b) simulation of shear rate, note that embryos between the pillars and other embryos experience a higher shear rate.

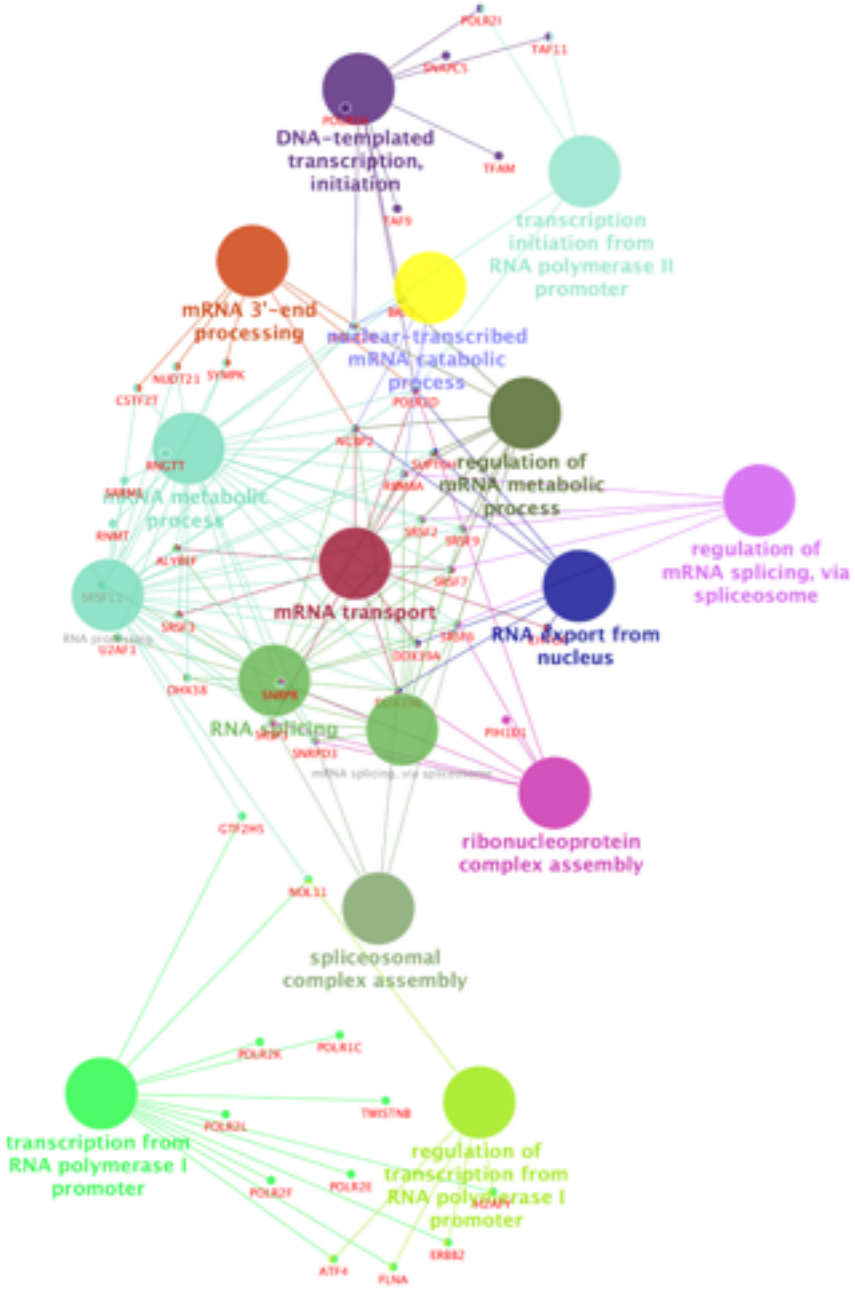

Supplementary figure 5: Functionally grouped gene ontology (GO) terms for genes up-regulated in G2 zygotes. The CytoScape plugin ClueGO was used to group the genes into functional GO terms of “molecular processes” and “biological processes” using genes related to transcription.

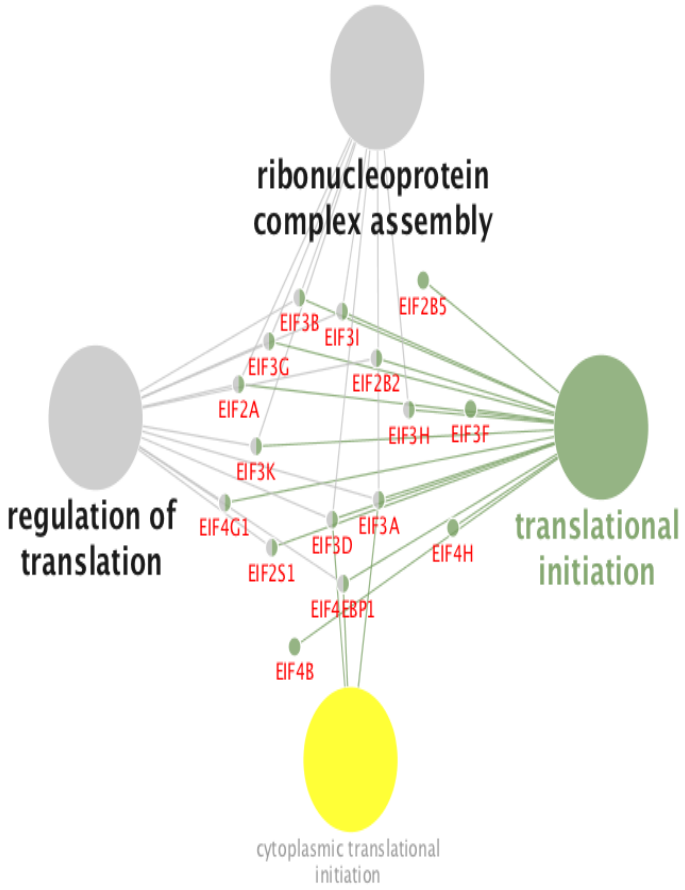

Supplementary figure 6: Functionally grouped gene ontology (GO) terms for genes up-regulated in G2 zygotes. The CytoScape plugin ClueGO was used to group the genes into functional GO terms of "molecular processes" and "biological processes" using genes related to translation initiation.

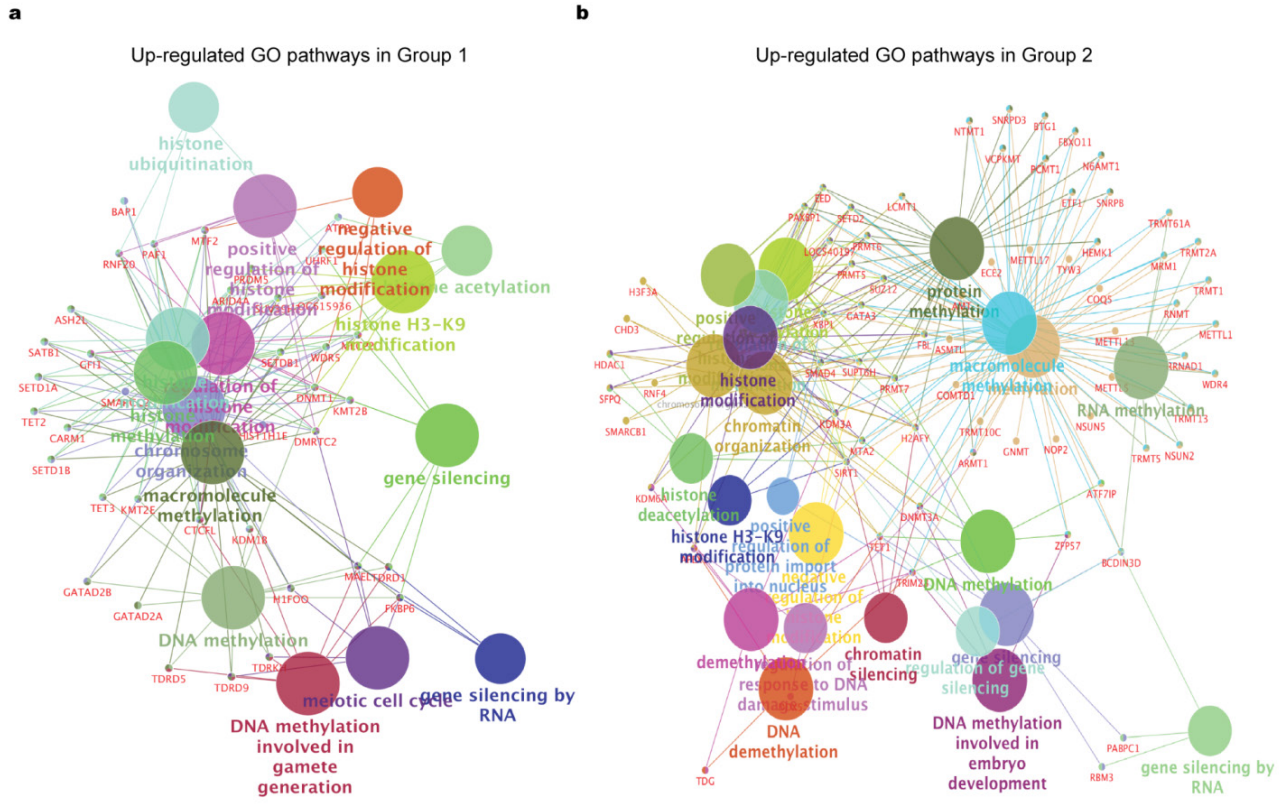

Supplementary figure 7: Functionally grouped gene ontology (GO) terms for genes up-regulated in G1 and G2 zygotes. The CytoScape plugin ClueGO was used to group the genes into functional GO terms of “molecular processes” and “biological processes” using genes related to (de)methylation and (de)acetylation. In (a) up-regulated GO pathways in G1 zygotes; in (b) up-regulated GO pathways in G2 zygotes.

Supplementary movies.

Scan the QR code or access the link.

Supplementary movie 1.

https://drive.google.com/file/d/0B5NUOD2zMReOSHN5WXEyaEZjX3M/view?usp=sharing

Supplementary movie 2.

https://drive.google.com/file/d/0B5NUOD2zMReOMG10S29jbFFscnM/view?usp=sharing

Supplementary movie 3.

https://drive.google.com/file/d/0B5NUOD2zMReOYVp2c1lEZ2hnMGM/view?usp=sharing

Supplementary data.

Scan the QR code or access the link.

Supplementary data 1.

https://drive.google.com/file/d/0B5NUOD2zMReORjFtTGlOSWZZMnM/view?usp=sharing

Supplementary data 2.

https://drive.google.com/file/d/0B5NUOD2zMReOc0NBOFptZ1MwZlU/view?usp=sharing

Chapter 6
Summarizing discussion

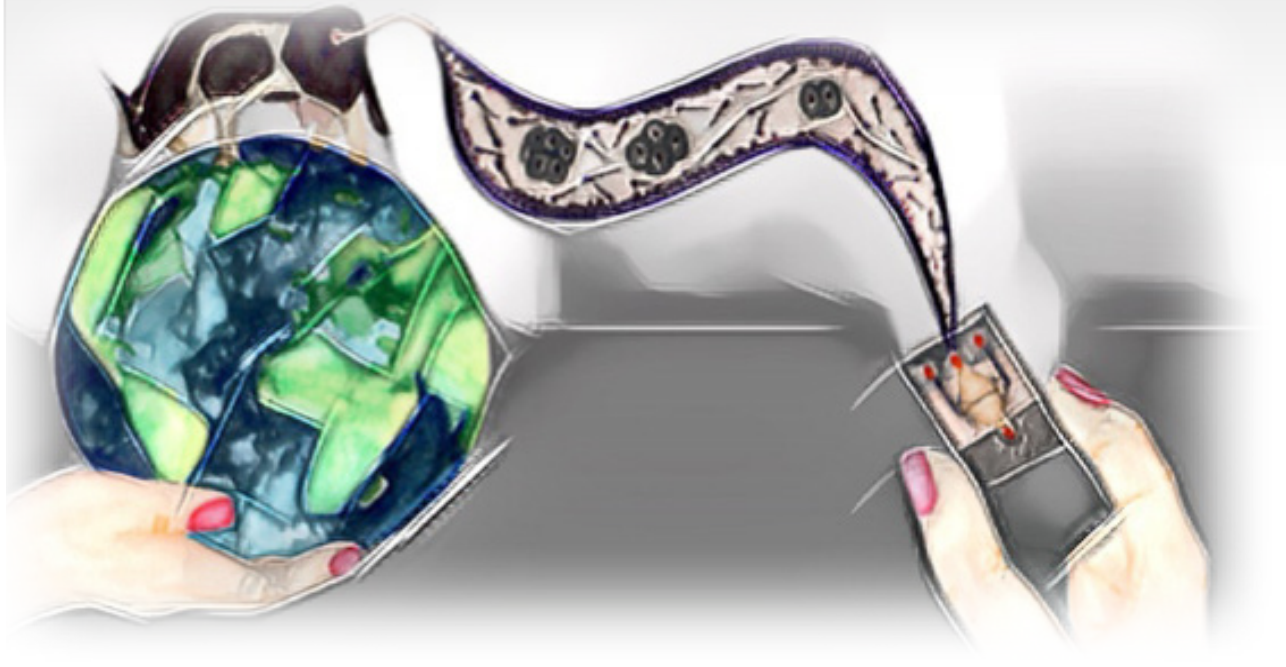

When we first drafted the general outline for this thesis in 2013, reliable techniques for mimicking the *in vitro* environment in which fertilization and early embryo development take place (the oviduct) were not available. Growing *in* vitro organs from cells, although first described in the late 1990s, was in its infancy and the two main techniques used to culture bovine oviductal cells were: (1) 2D culture in petri dishes[1] and (2) 3D culture using porous membrane ('transwell') inserts[2]. From the time that the first 3D-printer was invented in 1984, various attempts to use this technology to create *in vitro* organs were made, with the first live cells incorporated into 3D-printing in 2003[3]. Motivated by the growing use of 3D-printing to customize cell culture approaches, we decided to use this technology to create our first oviduct-on-a-chip prototype (chapter 3). Meanwhile, the use of microfluidics was also increasing in the organs-on-a-chip field and, mindful of the role of circulating steroid hormones in preparing the oviduct for its various roles in fertilization and embryo development, we incorporated this technology into our second oviduct-on-a-chip prototype (chapter 5). The need for an *in vitro* oviduct and the advantages and disadvantages of each prototype are discussed in the chapters presented in this thesis and summarized here. A timeline of important events that directly or indirectly made the developments in this thesis possible or tangible, including the novel contributions, is detailed in figure 1.

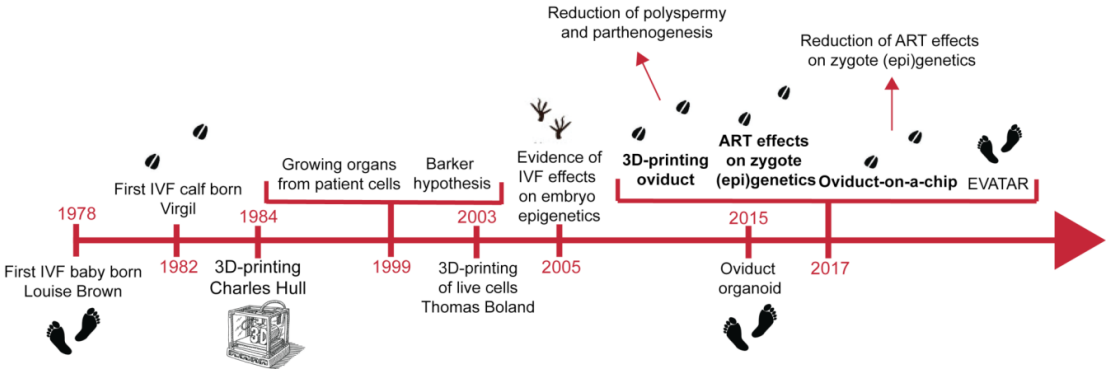

Figure 1. Timeline of events debated in the present thesis; starting with the first baby born after IVF (1978), proceeding through the invention of 3D-printers (1984) and the growth of organs *in vitro* (1999) up to the creation of our new oviduct-on-a-chip (2017).

Effects of ART on embryo development

Since the first IVF baby was born in 1978 (and the first IVF calf in 1982) improvement of *in vitro* embryo production systems for mammals has been an important goal. IVP imposes a dramatic change in the environment in which the early embryo develops, and the *in vitro* culture systems used to support this development are still far from physiological. For many years, the oviduct was considered as little more than a conduit to the uterus for the gametes and the embryo[4]. However, much more than a simple passage way, the oviduct forms the specific and specialized niche in which mammalian fertilization takes place, and the oviductal lumen creates the physiological microenvironment required for gamete interaction and early embryo development[5–9]. Moreover, the oviduct is host to the period in which the early embryo undergoes complete reprogramming of its (epi)genome in preparation for the reacquisition of epigenetic

marks as differentiation proceeds[10–12]. This period of epigenetic reprogramming is exquisitely vulnerable to changes in environmental conditions, such as compromised maternal health or an unhealthy diet. Likewise, ART related factors introduced, such as culture medium composition, light, temperature and oxygen tension, probably also affect the epigenetic programming of early developing embryos[11,13–19].

In this respect, in chapter 2 we demonstrated that conventional IVM and IVF markedly alter the dynamics of DNA (de)methylation and the expression of genes related to DNA (de)methylation in bovine zygotes. We were not, however, able to determine whether the observed differences are due primarily to IVM or also to the IVF procedure *per se*. It is generally believed that, at the zygote stage, control of embryo development depends primarily on maternal (oocyte) mRNA transcripts since embryonic transcription (genome activation) doesn't begin until between the 4-8 cell stages in bovine *in vivo* embryos[20] and between the 8-16 cell stages in bovine *in vitro* embryos[21]. However, a minor embryonic genome activation event has also been described to take place at *in vivo* the 2 cell stage[20]. When we provided an improved *ex vivo* oviductal environment, using an oviduct-on-a-chip culture system, we were able to restore 'normal' (i.e. *in vivo* like) global DNA methylation levels and partially recover changes to the transcriptome caused by *in vitro* culture, even though the zygotes were derived from IVM oocytes (chapter 5). These results lead us to propose that the oviduct-on-a-chip environment is able to overcome the changes to the oocyte arising during IVM and enable an appropriate minor embryonic genome activation event to occur at the zygote stage (chapter 5). The fact that *in vivo* zygotes underwent more profound DNA demethylation suggests a more effective re-establishment of the totipotent state, enabling enhanced potential for widespread genome activation. The perturbed demethylation of *in vitro* produced bovine zygotes may contribute to suboptimal embryo development and embryo quality following conventional bovine IVP. It is anticipated that a similar delayed/inhibited DNA demethylation of the male pronucleus also occurs during IVF in other mammalian species, including man. However, to prove this hypothesis demethylation of 5mC in the male pronucleus after IVF in the target species should first be compared to that in zygotes that developed *in vivo* or in an *in vivo*-like environment, such as an oviduct-on-a-chip.

Important points to take into consideration before creating organs-on-a-chip

Toxicological screening of bioengineered materials is essential before one can safely use such materials for medical and biological applications. This is even more relevant when using miniaturized and microfluidic systems, in which the surface–to-volume ratio is increased, and the distance between the polymer surface and cells is minimized[22–25]. These properties lead to a dramatic increase in the exposure of the biological entity to the bioengineered materials, including possible toxic component(s), when compared to classical cell culture systems (in culture flasks or petri dishes). As described in chapter 4, three out of five tested polymer

structures (PIC100, E-Shell200 and E-Shell300) impaired embryo development, whereas PDMS and PS had no measureable negative effect. A key-finding of chapter 4 is that the notion of material 'biocompatibility' is very much dependent on the specific applications. The developing bovine embryo was shown to be much more sensitive to its environment, and the toxic components released from 3D-printed materials, than epithelial cells or gametes. We also demonstrated that the tested polymers leaked a toxic diethyl-phthalate compound into solution. It has previously been reported that phthalates (plasticizers) can adversely influence biological processes; their toxic effects on bovine embryo production has also been reported previously,[26,27] and they are known to have effects on steroid production[26], as was confirmed by the cell-based ER reporter gene assay in chapter 4. Overall, our results revealed that the fertilized bovine oocyte is extremely sensitive to compounds leaking from 3D-printed polymer materials, such as phthalates, which may inhibit early embryogenesis. Our studies also demonstrate that , only after performing a dedicated set of toxicity screening tests, can one reliably predict the biocompatibility of 3D-printed bioengineered polymers for biological applications.

Improvements to ART are possible using an oviduct-on-a-chip

In chapter 3, we designed and successfully 3D-printed an oviduct-on-a-chip model using a stereo-lithographic technique. Bovine oviduct epithelial cells (BOECs) cultured in the 3D-printed device regained and maintained their ciliated and cuboidal to columnar pseudostratified epithelium for a period of at least 6 weeks, with a mixed population of ciliated and non-ciliated secretory cells comparable to that in the *in vivo* oviduct epithelium. The functionality of our oviduct-on-a-chip system was tested using a bio-monitoring assay in which sperm penetration of the oocyte was scored. In this system, the oviduct cells in culture conditioned the apical medium, which in turn supported physiological sperm-oocyte interaction and fertilization, and completely abolished polyspermic fertilization and parthenogenetic activation of oocytes; all in the absence of added sperm activating factors. A reduction of polyspermy was reported previously in an IVF system that incorporated BOECs cultured on porous membrane inserts[28]. Moreover, the concept that conditioning the apical medium using BOECs in the 3D system is responsible for preventing polyspermy, is in line with previously described inhibitory effects of oviduct fluid on polyspermic fertilization in cows and pigs[29,30]. Other studies have also reported beneficial effects of oviduct fluid and/or oviductal proteins on sperm motility, the acrosome reaction and bull fertility [7,28,31–37], and on oocyte and embryo development and quality[5,30,38–44]. Since our first oviduct-on-a-chip prototype was found to release components toxic to developing embryos (chapter 4), we identified a non-toxic material (PDMS) to create an improved oviduct-on-a-chip (chapter 5). BOECs grown in the new oviduct-on-a-chip (chapter 5) were responsive to steroid hormone stimulation, mimicking the luteal- and pre-ovulatory phases, with changes in the transcriptome similar to those described to occur *in vivo*, *e.g.*, reduced ciliary activity and increased tight junction and transmembrane signaling receptor activity un-

der progesterone dominance, and increased immune responsiveness, regulation of protein processing and maturation, and cell projection morphogenesis under estrogen dominance[45]. Moreover, the improved oviduct-on-a-chip supported not only fertilization, but also embryo development up to the blastocyst stage. However, partially due to the loss of a subpopulation of fertilized oocytes through the pillars of the microfluidic device the net amount of blastocyst development in our chip was lower when compared to optimized conventional IVP protocols. In the future our model can be further improved by: (1) minor changes in the design so that the 'trapping structures' completely retain the COCs/embryos during perfusion; (2) simulating the steroid hormone changes of the peri-conception period in the basal compartment; and (3) analyzing the effect of different flow rates, and consequently shear stress levels, on the developing embryo. On the other hand, while lower embryo development was observed, the zygotes resulting from on chip (*CH*) culture were more similar to their *in vivo* counterparts (*VV*) than to conventional *in vitro* (*VT*) zygotes, in terms of their global DNA methylation level and transcriptome. Interestingly, *VV* and *CH* zygotes exhibited lower global DNA methylation levels than *VT* zygotes, which is presumably a factor of the up-regulation of genes related to DNA demethylation in 80% of the *VV* and 50% of the *CH* zygotes (G2). This reduced level of DNA methylation seems to be essential to the minor embryonic genome activation event, since an up-regulation of genes related to transcription and translation initiation was observed in G2 zygotes. In addition, when comparing our data with genes described to be first expressed at the 4-, 8-, 16-cell or blastocyst stages of *IVP* bovine embryos[21], 24% of the 220 genes that were only detected in one of these stages were already detected and up-regulated in the G2 zygotes, suggesting that standard IVP conditions delay zygote minor transcriptome activation, but that the delay can be partially ameliorated using our oviduct-on-a-chip platform. Finally, our results highlight the importance of using a more *in vivo*-like environment to study pathways related to normal fertilization and embryo development *in vitro*, especially when using *in vivo* embryos is not a viable option for ethical reasons.

Future perspectives and uses of the oviduct-on-a-chip

By using the innovative oviduct-on-a-chip approach (described in chapter 5), we expect to shed light on mechanisms and pathways that will increase our overall understanding of how gametes interact, and how fertilization and early embryo development are regulated. This bio-mimicked model for studying oviductal function may also lead to a reduction of the need for, and thereby reduced suffering of, experimental animals. Moreover, the oviduct-on-a-chip model allows both collection from and introduction of secreted factors into the luminal (the mimicked oviduct tubal side) compartment. Similarly, it allows collection from or introduction of factors into the basolateral (the mimicked blood circulation side) compartment. Both culture conditioning itself and introduction of estrous cycle like hormone changes will allow further refinement of the *in vivo*-like environment. Future studies should then provide novel insight into processes and molecules relevant to oocyte maturation, fertilization and embryo develop-

ment. Additionally, this bio-mimicked system may transpire to be a useful platform to test and develop new drugs and perform toxicological assays.

Finally, the oviduct-on-a-chip can offer important insights relevant to human *in vitro* embryo production (a species with many interesting reproductive similarities to the cow). For wildlife species, this knowledge may also be beneficial to advancing *in vitro* culture and fertilization systems, without the need for extensive species-specific IVM and IVF protocol development, for embryo production to assist genetic management and conservation of valuable species.

In addition to its use for ART improvement, this oviduct-on-a-chip will allow live imaging to trace cell migration and/or follow molecular events and may become a useful tool for advancing general understanding of pathways associated with tubal derived ovarian cancers and enabling the study of tubal cell migration processes. Moreover, the oviduct-on-a-chip model can give new insights into molecules and processes involved in the development of tubal cancers, and may be applicable to studies on techniques for early diagnosis of this lethal disease. Ultimately, our oviduct-on-a-chip platform may help in the development of patient-derived *in vitro* cancer models that could, in turn, be instrumental for personalized medicine purposes.

References

1. Schoen, J., Bondzio, a., Topp, K. & Einspanier, R. Establishment and characterization of an adherent pure epithelial cell line derived from the bovine oviduct. *Theriogenology* **69,** 536–545 (2008).
2. Gualtieri, R. *et al.* Bovine oviductal monolayers cultured under three-dimension conditions secrete factors able to release spermatozoa adhering to the tubal reservoir in vitro. *Theriogenology* **79,** 429–435 (2013).
3. Boland, T., Wilson, W. C. & Xu, T. Ink-jet printing of viable cells. (2006).
4. Ménézo, Y., Guérin, P. & Elder, K. The oviduct: A neglected organ due for re-assessment in IVF. *Reprod. Biomed. Online* **30,** 233–240 (2015).
5. Lloyd, R. E. *et al.* Effects of oviductal fluid on the development, quality, and gene expression of porcine blastocysts produced in vitro. *Reproduction* **137,** 679–687 (2009).
6. Coy, P., García-Vázquez, F. a., Visconti, P. E. & Avilés, M. Roles of the oviduct in mammalian fertilization. *Reproduction* **144,** 649–660 (2012).
7. Killian, G. Physiology and endocrinology symposium: Evidence that oviduct secretions influence sperm function: A retrospective view for livestock. *J. Anim. Sci.* **89,** 1315–1322 (2011).
8. Zhang, B. R., Larsson, B., Lundeheim, N. & Rodriguez-Martinez, H. Sperm characteristics and zona pellucida binding in relation to field fertility of frozen-thawed semen from dairy AI bulls. *Int. J. Androl.* **21,** 207–16 (1998).
9. Suarez, S. S. Mammalian sperm interactions with the female reproductive tract. *Cell Tissue Res.* **363,** 185–194 (2016).
10. Fraser, R. & Lin, C. J. Epigenetic reprogramming of the zygote in mice and men: On your marks, get set, go! *Reproduction* **152,** R211–R222 (2016).
11. Ventura-Juncá, P. *et al.* In vitro fertilization (IVF) in mammals: epigenetic and developmental alterations. Scientific and bioethical implications for IVF in humans. *Biol. Res.* **48,** 68 (2015).
12. Feil, R. Epigenetic asymmetry in the zygote and mammalian development. *Int. J. Dev. Biol.* **53,** 191–201 (2009).
13. Thompson, J. G., Kind, K. L., Roberts, C. T., Robertson, S. A. & Al, E. Epigenetic

risks related to assisted reproductive technologies: Short-and long-term consequences for the health of children conceived through assisted reproduction. *Hum. Reprod.* **17,** 2783–2786 (2002).
14. Huntriss, J. D. & Picton, H. M. Epigenetic consequences of assisted reproduction and infertility on the human preimplantation embryo. *Hum. Fertil. (Camb).* **11,** 85–94 (2008).
15. El Hajj, N. & Haaf, T. Epigenetic disturbances in in vitro cultured gametes and embryos: Implications for human assisted reproduction. *Fertil. Steril.* **99,** 632–641 (2013).
16. Young, L. E. *et al.* Epigenetic change in IGF2R is associated with fetal overgrowth after sheep embryo culture. *Nat. Genet.* **27,** 153–154 (2001).
17. DeBaun, M. R., Niemitz, E. L. & Feinberg, A. P. Association of in vitro fertilization with Beckwith-Wiedemann syndrome and epigenetic alterations of LIT1 and H19. *Am. J. Hum. Genet.* **72,** 156–60 (2003).
18. Li, T. *et al.* IVF results in de novo DNA methylation and histone methylation at an Igf2-H19 imprinting epigenetic switch. *Mol. Hum. Reprod.* **11,** 631–640 (2005).
19. Gaspar, R. C. *et al.* Oxygen tension affects histone remodeling of invitro-produced embryos in a bovine model. *Theriogenology* **83,** 1408–1415 (2015).
20. Jiang, Z. *et al.* Transcriptional profiles of bovine in vivo pre-implantation development. *BMC Genomics* **15,** 756 (2014).
21. Graf, A. *et al.* Fine mapping of genome activation in bovine embryos by RNA sequencing. *Proc. Natl. Acad. Sci. U. S. A.* **111,** 4139–4144 (2014).
22. Macdonald, N. P. *et al.* Assessment of biocompatibility of 3D printed photopolymers using zebrafish embryo toxicity assays. *Lab Chip* **16,** 291–7 (2016).
23. Esteves, T. C. *et al.* A microfluidic system supports single mouse embryo culture leading to full-term development. *RSC Adv.* **3,** 26451 (2013).
24. Huh, D. *et al.* Microfabrication of human organs-on-chips. *Nat. Protoc.* **8,** 2135–57 (2013).
25. Wolbers, F. *et al.* Viability study of HL60 cells in contact with commonly used microchip materials. *Electrophoresis* **27,** 5073–5080 (2006).
26. Kalo, D. & Roth, Z. Low level of mono(2-ethylhexyl) phthalate reduces oocyte developmental competence in association with impaired gene expression. *Toxicology* **377,** 38–48 (2017).
27. Kalo, D. *et al.* Carryover Effects of Acute DEHP Exposure on Ovarian Function and Oocyte Developmental Competence in Lactating Cows. *PLoS One* **10,** e0130896 (2015).
28. Pollard, J. W. *et al.* Fertilizing capacity of bovine sperm may be maintained by binding of oviductal epithelial cells. *Biol. Reprod.* **44,** 102–107 (1991).
29. Coy, P. & Avilés, M. What controls polyspermy in mammals, the oviduct or the oocyte? *Biol. Rev.* **85,** 593–605 (2010).
30. Mondéjar, I., Martínez-Martínez, I., Avilés, M. & Coy, P. Identification of potential oviductal factors responsible for zona pellucida hardening and monospermy during fertilization in mammals. *Biol. Reprod.* **89,** 67 (2013).
31. Topper, E. K., Killian, G. J., Way, a, Engel, B. & Woelders, H. Influence of capacitation and fluids from the male and female genital tract on the zona binding ability of bull spermatozoa. *J. Reprod. Fertil.* **115,** 175–183 (1999).
32. Rodríguez, C., Killian, G., Rodríguez, C. & Killian, G. Identification of ampullary and isthmic oviductal fluid proteins that associate with the bovine sperm membrane. *Anim. Reprod. Sci.* **54,** 1–12 (1998).
33. Killian, G. J. Evidence for the role of oviduct secretions in sperm function, fertilization and embryo development. *Anim. Reprod. Sci.* **82–83,** 141–153 (2004).
34. Erikson, D. W., Way, A. L., Bertolla, R. P., Chapman, D. A. & Killian, G. J. Influence of osteopontin , casein and oviductal fluid on bovine sperm capacitation. *Anim. Reprod.* **4,** 103–112 (2007).

35. Taitzoglou, I. a., Kokoli, A. N. & Killian, G. J. Modifications of surface carbohydrates on bovine spermatozoa mediated by oviductal fluid: A flow cytometric study using lectins. *Int. J. Androl.* **30,** 108–114 (2007).
36. Dejonge, C. J. *et al.* The Acrosome Reaction-Inducing Effect of Human Follicular and Oviductal Fluid. *J. Androl.* **141,** 359–365 (1993).
37. King, R. S., Anderson, S. H. & Killian, G. J. Effect of Bovine Oviductal Estrus-Associated Protein on the Ability of Sperm to Capacitate and Fertilize Oocytes. *J. Androl.* **15,** 468–478 (1994).
38. Besenfelder, U., Havlicek, V. & Brem, G. Role of the oviduct in early embryo development. *Reprod. Domest. Anim.* **47,** 156–163 (2012).
39. Monaco, E. *et al.* Effect of osteopontin (OPN) on in vitro embryo development in cattle. *Theriogenology* **71,** 450–457 (2009).
40. Kölle, S., Reese, S. & Kummer, W. New aspects of gamete transport, fertilization, and embryonic development in the oviduct gained by means of live cell imaging. *Theriogenology* **73,** 786–795 (2010).
41. Zaccagnini, G., Maione, B., Lorenzini, R. & Spadafora, C. Increased production of mouse embryos in in vitro fertilization by preincubating sperm cells with the nuclease inhibitor aurintricarboxylic acid. *Biol. Reprod.* **59,** 1549–53 (1998).
42. Lopera-Vásquez, R. *et al.* Extracellular Vesicles from BOEC in In Vitro Embryo Development and Quality. *PLoS One* **11,** e0148083 (2016).
43. Maillo, V. *et al.* Oviduct-Embryo Interactions in Cattle: Two-Way Traffic or a One-Way Street? *Biol. Reprod.* **92,** 144–144 (2015).
44. Sanches, B. V. *et al.* Comparison of Synthetic Oviductal Fluid and G1/G2 Medium under Low-1 Oxygen Atmosphere on Embryo Production and Pregnancy Rates in Nelore (Bos indicus) Cattle. *Reprod. Domest. Anim.* **48,** 7–9 (2013).
45. Cerny, K. L., Garrett, E., Walton, A. J., Anderson, L. H. & Bridges, P. J. A transcriptomal analysis of bovine oviductal epithelial cells collected during the follicular phase versus the luteal phase of the estrous cycle. *Reprod. Biol. Endocrinol.* **13,** 84 (2015).

Chapter 7
Nederlandse Samenvatting

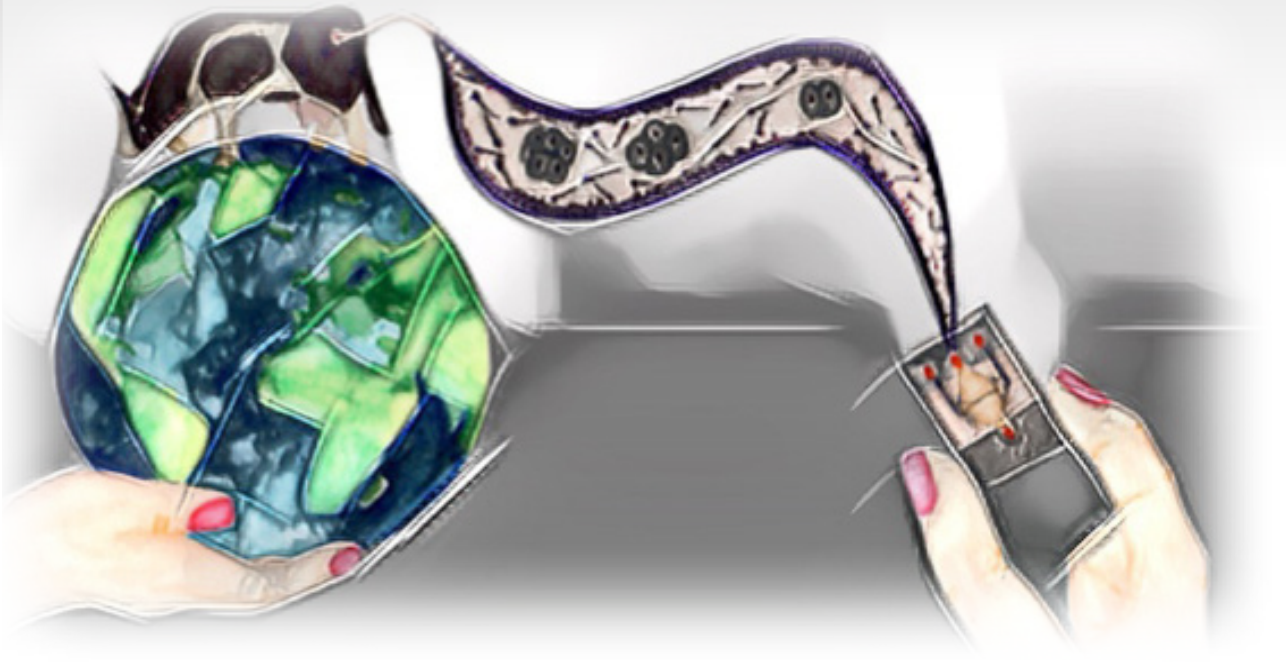

Gedurende de periode, waarin tijdens de differentiatie van het jonge embryo de complete herprogrammering van het (epi)genoom wordt voltooid in de voorbereiding op het verwerven van het epigenetische eindpunt, bevindt het embryo zich in de eileider van het voortplantingsapparaat. In deze periode is de omgeving van de eileider extreem gevoelig voor veranderende omgevingsinvloeden zoals de toestand van de gezondheid van de moeder of de blootstelling aan onvoldoende en/of ongezonde voeding. Daarnaast kunnen aan de kunstmatige voortplantingstechnieken gerelateerde factoren, zoals de compositie van de toegepaste kweekmedia maar ook bijv. licht, temperatuur en zuurstofspanning, mogelijke effecten hebben op het proces van de epigenetische (re)programmering van de jonge embryo's.

In hoofdstuk 2 van dit proefschrift wordt aangetoond dat bij de conventionele IVM (*in vitro* rijping van de eicel) en IVF (*in vitro* bevruchting van de eicel) kweek-procedures het proces van de DNA (de)methylering en de expressie van genen die hierbij zijn betrokken nadrukkelijk beïnvloed kunnen worden. Hierbij kon niet worden vastgesteld of de waargenomen veranderingen primair werden veroorzaakt door alleen het IVM proces of dat ook de IVF procedure zelf van invloed was.

Algemeen wordt geaccepteerd dat bij de koe vanaf het zygote stadium de regulatie van de eerste celdelingen tijdens de ontwikkeling primair afhankelijk is van de maternale mRNA transcriptie factoren (opgeslagen in de eicel); de activering van de embryonale transcriptie van het genoom ('major' genoom activatie) start niet eerder dan het 4-8 cellige stadium van de ontwikkeling bij *in vivo* embryo's en rond het 8-16 cellige stadium bij *in vitro* gekweekte embryo's. Naast de 'major' genoom activering vindt er tijdens het 2-cellige stadium bij *in vivo* embryo's ook een 'minor' embryonale genoom activering plaats.

In hoofdstuk 3 wordt het succes van de ontwikkeling van het 3D geprinte eileider-op-de-chip model beschreven waarbij gebruik is gemaakt van een stereo-lithografische techniek. Eileiderepitheelcellen (afkomstig van het rund) die tijdens een periode van minstens zes weken werden gekweekt op dit 3D chip model vormden een laag van kubisch tot kolomvormig, pseudo-gelaagd epitheel bestaande uit een gemengde populatie van secretiecellen met en zonder trilharen, vergelijkbaar met *in vivo* eileiderepitheel. In dit systeem conditioneerden de eileiderepitheelcellen het apicale medium in de chip in die mate dat de fysiologische processen van sperma-eicel interactie en de bevruchting normaal verliepen, dus zónder dat er sprake was van een bevruchting met meer dan een spermacel (polyspermie) dan wel een parthenogenetische activering van de eicellen.

Vanaf het moment dat werd vastgesteld (hoofdstuk 4) dat ons eerste 3D prototype van de chip componenten bevatte en uitscheidde in het kweekmedium die toxisch werden bevonden voor jonge embryo's (diethyl-phthalaat en polyethyleen-glycolen), is er door ons een verbeterde versie van het eileider-op-de-chip model ontwikkeld door gebruik te maken van een materiaal met bewezen, niet-toxisch eigenschappen: het polydimethylsiloxane (PDMS; hoofdstuk 5).

Eileiderepitheelcellen die gekweekt werden en groeiden op het nieuwe chipsysteem (hoofdstuk 5) bleken gevoelig te zijn voor hormonale, in dit geval steroïden, stimulatie. Hiermee

konden de luteale (progesteron) en pre-ovulatoire (oestrogenen) fasen van de oestrische cyclus bij het rund worden nagebootst (Hoofdstuk 5). Door het aangepaste en verbeterde eileider-op-de-chip kweeksysteem werd niet alleen de bevruchting van de eicel ondersteund, maar kon ook de ontwikkeling van de verkregen zygoten na een geslaagde bevruchting tot het blastocyststadium van de vroeg-embryonale ontwikkeling worden gerealiseerd. Bij zygoten gekweekt in dit nieuwe 3D kweeksysteem (*CH*) kon worden aangetoond dat zowel het 'global' DNA methyleringsniveau en als ook het transcriptoom beter vergelijkbaar waren met de *in vivo* (*VV*) dan met de *in vitro* (*VT*), conventioneel, gekweekte zygoten. Bovendien is het interessant om te vermelden dat de *VV* en *CH* zygoten een significant lager 'global' DNA methyleringsniveau toonden dan de *VT* zygoten, een factor die mogelijk een rol vervult bij de up-regulatie van genen die betrokken zijn bij de DNA methylering van respectievelijk 80% *VV* en 50% *CH* zygoten (G2 stadium). Deze gereduceerde mate van DNA methylering lijkt essentieel te zijn voor het 'minor' embryonale genoom activeringsproces waarbij een up-regulatie van genen die betrokken zijn bij de initiatie van de transcriptie en translatie processen in G2 zygoten werd waargenomen. Bij de aanname dat het kweken van *in vitro* embryo's onder standaard (traditionele) IVP condities tot een vertraging leidt van het 'minor' transcriptoom activatie proces van de zygote, kan worden geconcludeerd uit dit proefschrift dat in het door ons ontwikkelde eileider-op-de-chip platform deze vertraging voor een groot deel kan worden gereduceerd.

De bevindingen in dit proefschrift tonen het belang van de toepassing van een *in vitro* embryo (lab-op-de-chip) kweeksysteem dat de *in vivo* omgeving en condities van de eileider gecontroleerd nabootst om de normale, fysiologische processen van bevruchting en de vroeg-embryonale ontwikkeling *in vitro* nauwkeurig te kunnen bestuderen. Het kweeksysteem is zodanig ontwikkeld dat het mogelijk is om deze processen onder een speciaal toegeruste microscoop 'real time' te kunnen vervolgen. De lab-op-de-chip kweeksystemen zijn speciaal van belang voor het onderzoek waarbij de toepassing van *in vivo* embryo's voor onderzoeksdoeleinden op ethische gronden en wetgeving wordt belemmerd. Tot slot, kan dit kweeksysteem in de toekomst worden ingezet als middel om embryoproductie te verbeteren ten behoeve van de intensieve dierfokkerij, maar ook bij het opzetten van een embryo bio-bank voor de bescherming van zeldzame huisdierrassen, of bedreigde (zoog)-diersoorten.

Acknowledgements

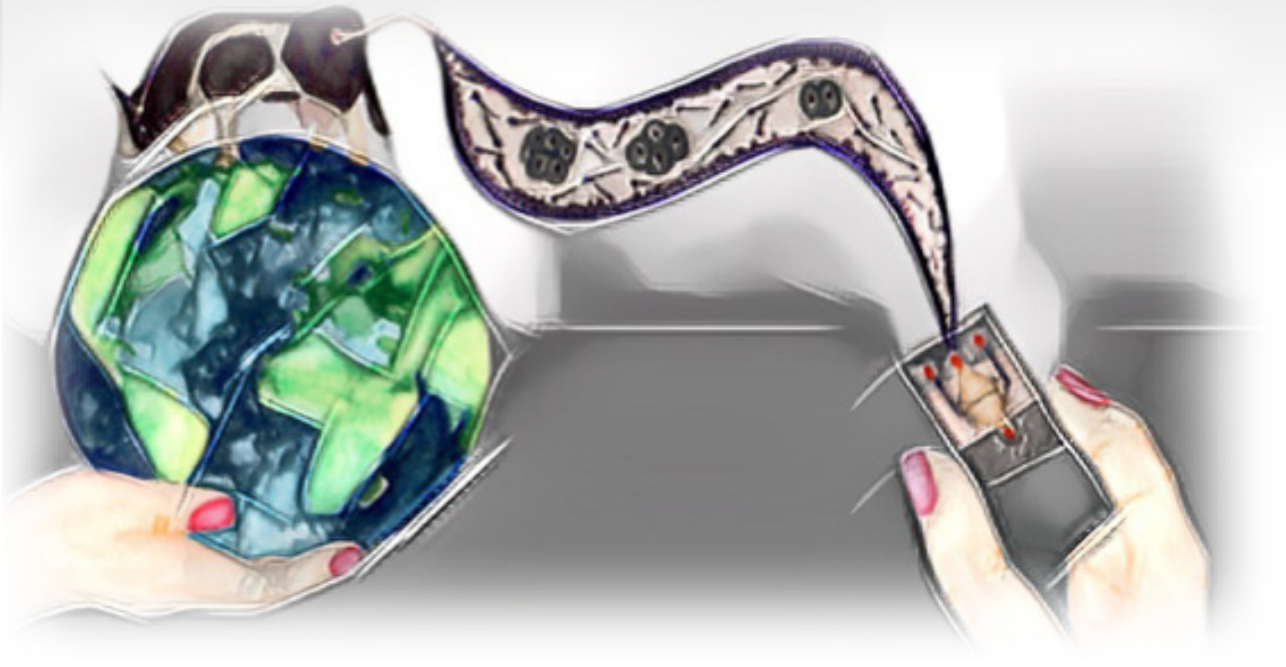

Primeiramente eu agradeço a meus pais, Eduardo e Marcia, a meu irmão Eduardo, e a meu gordinho Marvin, por todo o apoio, carinho e suporte que me deram. Por sempre acreditarem em meus sonhos, estarem ao meu lado e me ajudarem a conquistar meus objetivos. Sem vocês eu não estaria onde estou. Também agradeço aos meus avós, Nelson, Angelina a Adelina, por serem uma grande inspiração em minha vida, por me ensinarem a ser forte, persistente e generosa. Também agradeço a toda minha família, em especial a minha paraninfa Renata, por nossos inúmeros facetimes que muitas vezes me fizeram chorar de tanto rir nesses dias holandeses cinzentos… Amo vocês!

I want to thank my promoter Tom Stout, for being a great mentor and for guiding me through my PhD. You were always bringing me back to reality and making me a better scientist! To my daily supervisor Peter Vos, for all great input and help, it was great being your student! A special thank you to Bart Gadella, my other daily supervisor, you were more than only a supervisor, you were always there for me, for professional and personal matters. Bart, you were an inspiration and it was great sharing conferences and beers with you! Although we were more efficient being in two different continents, I wouldn't have succeeded in my thesis without you,. It was great being your student and I learnt a lot from you. I also want to thank Heiko Henning, my paranimf, for always being there for me, for all the countless hours we spent working on this project, and for helping me to be more organized and focused.

I special thanks to every single mentor that was part of my professional life in the past 10 years: Mayra Assumpção, Peter Ryan, Jean Feugang, Teresa Mogas, Roser Morató and Marc Yeste you all made me love science and showed me how to be a better researcher.

Thank you Ferry Melchels, Pedro Costa and Jos Malda, for the great collaboration on the oviductal biofabrication. Séverine le Gac and Hoon Rho, for all the knowledge on microfluidics and for preparing me all the microfluidics chips. Thank you Richard, Rob and Ester from the CCI, for all the help and shared knowledge on imaging. Now my colleagues from the lab: Eric, Christine, Elly, Arend, Mabel, Claudia, Marta, Marilena, Bo, Mahdi, Bas, Hilde and Bernard, thank you for all the moments and knowledge shared, it was great working with each one of you and I learnt a lot from you. A special thank to you Leni, for all your input, help and shared knowledge!

Also a big thanks to those that were more than a colleague: Karen, Charlotte, Minjie, Anne and Kaatje, it was great to have you girls around, and to share not only moments at work, but also meals, festivals, conferences and drinks; life was much easier having you girls around!

Thank you to my Spanish friends: Manu, Rayner, Davi, Nuria, Xime, Juanmi and Tony, you guys were part of my success and made my life happier.

Last, but not least, to my Brazilian "family" in Dutch land: Vinicius, Gudrun, Tom, Zori, Daniel, Karola, Rafael and Camila for all great moments we spent together the past 4 years, for the delicious dinners, barbecues and drinks shared. Vocês vão deixar saudades!

Curriculum vitae

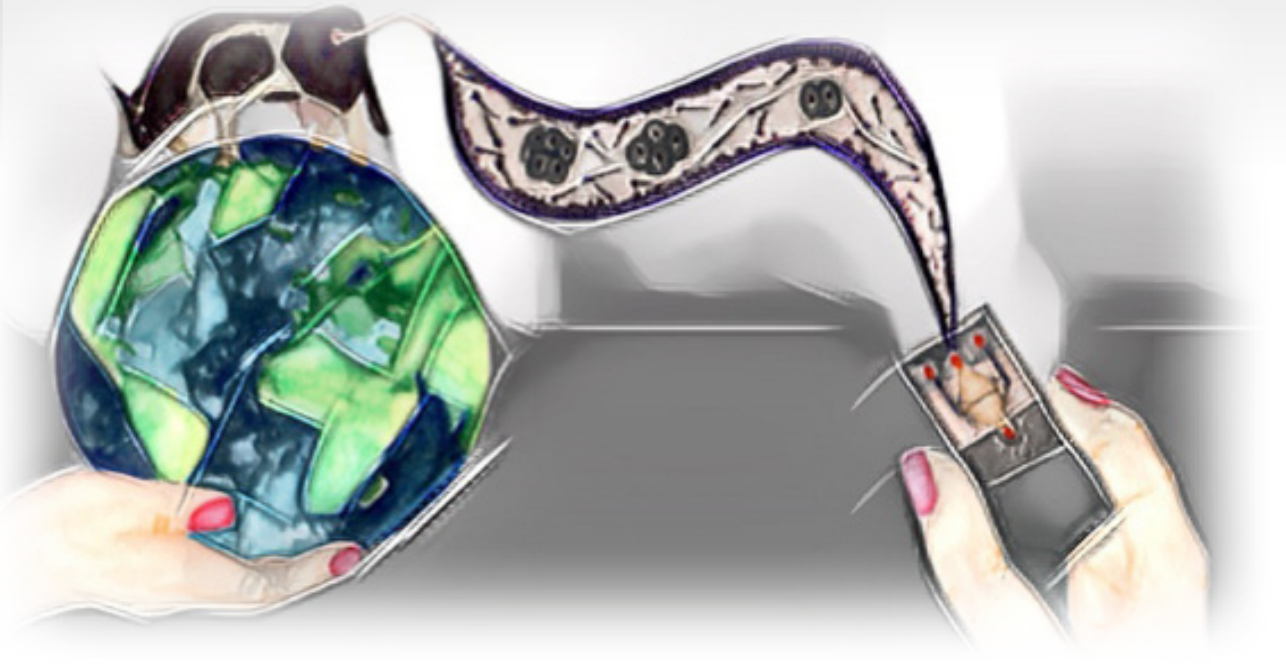

Marcia de Almeida Monteiro Melo Ferraz was born on February 11th 1986 in Poá, São Paulo, Brazil. She finished her secondary education in the Objetivo School in Suzano, São Paulo, Brazil. In 2005 she started to study Veterinary Medicine at the University of São Paulo and graduated as a DVM in December 2010. During her DVM studies she performed internships at Royal Veterinary College, London, UK in 2008 and at Mississippi State University, MS, USA in 2010. In 2011 she started a master in Animal Breeding and Biotechnology of Reproduction at the Autonomous University of Barcelona, in Barcelona, Spain. Which she graduated *cum maxima laude* in June 2013. In September 2013 she started a PhD track at the Department of Farm Animal Health of the Faculty of Veterinary Medicine, Utrecht University and it resulted in the present thesis.

List of Publications

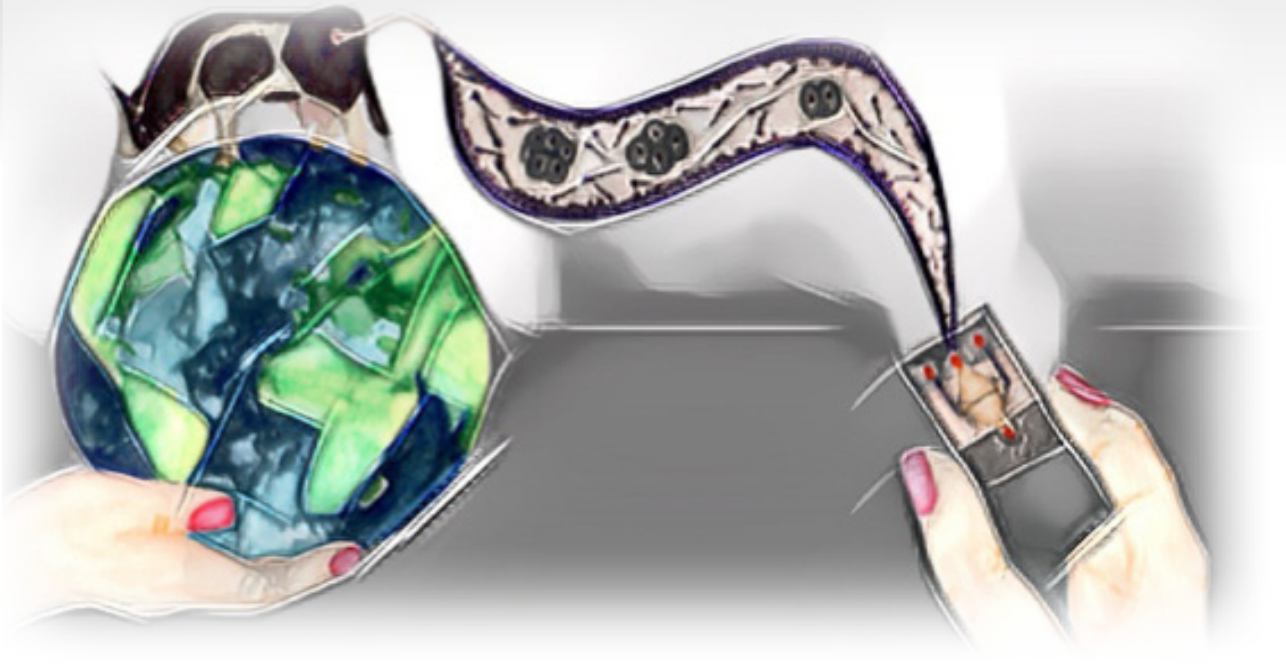

Peer reviewed articles

Ferraz, M.A.M.M.; Rho, H.S.; Hemerich, D.; Henning, H.H.W.; van Tol, H.; Hölker, M.; Besenfelder, U.; Mokry, M.; P.L.A.M., Stout, T.A.E.; Le Gac, S.; Gadella, B.M. An oviduct-on-a-chip provides an enhanced *in vitro* environment for zygote (epi)genome reprogramming. Submitted.

Ferraz, M.A.M.M. ; Henning, H.H.W.; Malda, J.; Costa, P.F.; Rho, H.; Le Gac, S.; P.L.A.M., Stout, T.A.E.; Gadella, B.M. 3D-engineered polymers: their potential health and environmental risks. Submitted.

Ferraz, M.A.M.M. ; Henning, H.H.W.; van Tol, H.; Hölker, M.; Besenfelder, U.; P.L.A.M., Stout, T.A.E.; Gadella, B.M. In vitro produced bovine zygotes exhibit aberrant global (de)methylation dynamics. Submitted.

FERRAZ, M.A.M.M. ; Henning, H.H.W.; Costa, P.F.; Malda, J.; Vos, P.L.A.M., Stout, T.A.E.; Gadella, B.M. Improved bovine embryo production in an oviduct-on-a-chip system: Prevention of poly-spermic fertilization and parthenogenic activation. Lab on a chip. 2017, 17, 905 – 916.

FERRAZ, M.A.M.M. ; Henning, H.H.W.; Stout, T.A.E.; Vos, P.L.A.M., Gadella, B.M. 3-dimensional in vitro oviduct culture designing for studying mammalian fertilization and producing embryos. Ann Biomed Eng (2016). doi:10.1007/s10439-016-1760-x

Gadella B.M. and **Ferraz M.A**. A Review of New Technologies that may Become Useful for in vitro Production of Boar Sperm. Reprod Domest Anim. 2015 Jul; 50 Suppl 2:61-70. doi: 10.1111/rda.12571.

Arcarons N., Morató R., Spricigo J.F., **Ferraz M.A.,** Mogas T. Spindle configuration and developmental competence of in vitro-matured bovine oocytes exposed to NaCl or sucrose prior to Cryotop vitrification. Reprod Fertil Dev. 2015 Apr 22. doi: 10.1071/RD14516.

FERRAZ, M.A.M.M. ; MORATÓ, R. ; YESTE, M. ; ARCARONS, N. ; PENA, A.I. ; TAMARGO, C. ; HIDALGO, C.O. ; MUIÑO, R. ; MOGAS, T. Evaluation of sperm subpopulation structure in relation to in vitro sperm-oocyte interaction of frozen-thawed semen from Holstein bulls. Theriogenology, v. 81, p. 1067-1072, 2014.

FERRAZ, M. A. M. M.; SIMÕES, R.; MILAZZOTTO, M. P.; VISINTIN, J. A.; ASSUMPÇÃO, M. E. O. A. Gene expression profile of Protamines and Transition Nuclear Proteins in bovine testis. Brazilian Journal of Veterinary Research and Animal Science 08/2013; 50(4):316-322, 2014.

FERRAZ, M. A. M. M. ; MORENO, L. Z. ; MORICONE, P. R. ; BRUNO, D. G. ; MARTINS, S. M. M. K. ; MORETTI, A. S. Embrionary and foetal loss in swines. Porkworld magazine, São Paulo, p. 36-40, 01 mar. 2007.

Abstracts

Ferraz, M.A.M.M. ; Henning, H.H.W.; Vos, van Tol, H.; Hölker, M.; Besenfelder, U.; Rho, H.; Le Gac, S.; P.L.A.M., Stout, T.A.E.; Gadella, B.M. Oviduct-on-a-Chip: Creating a Niche to Support Physiological Epigenetic Reprogramming During Bovine In Vitro Embryo Production. Gordon Conference on Fertilization and Activation of Development. New Hampshire, USA, 2017.

Ferraz, M.A.M.M. ; Henning, H.H.W.; Vos, van Tol, H.; Hölker, M.; Besenfelder, U.; Rho, H.;

Le Gac, S.; P.L.A.M., Stout, T.A.E.; Gadella, B.M. Oviduct-on-a-Chip: Creating a Niche to Support Physiological Epigenetic Reprogramming During Bovine In Vitro Embryo Production. 50th Annual meeting of the Society for the Study of Reproduction. Washington DC, USA, 2017.

Henning, H.H.W.; **Ferraz, M.A.M.M.**; Vos, P.L.A.M., Stout, T.A.E.; Gadella, B.M. Differentiating equine oviduct epithelial cells into monolayers of ciliated and non-ciliated cells; developing a new in vitro oviduct model. 18th International Congress on Animal Reproduction. Tours, France.

FERRAZ, M.A.M.M.; Henning, H.H.W.; Van Dorenmalen, K.M.A.; Vos, P.L.A.M., Stout, T.A.E.; Malda, j.; Costa, P.F.; Gadella, B.M Use of transwell cell culture and 3d-printing technology to develop an in vitro oviduct model to study bovine fertilization. World Biomaterial Conference 2016. Montreal, Canada.

Henning, H.H.W.; **Ferraz, M.A.M.M.**; Vos, P.L.A.M., Stout, T.A.E.; Gadella, B.M. Isolating equine oviduct epithelial cells. 49th Annual Conference on Physiology & Pathology of Reproduction and 41st Joint Conference of Veterinary and Human Reproductive Medicine. Leipzig, Germany.

Ferraz, M.A.M.M.; Henning, H.H.W.; Van Dorenmalen, K.M.A.; Vos, P.L.A.M., Stout, T.A.E.; Malda, j.; Costa, P.F.; Gadella, B.M. Use of transwell cell culture and 3D printing technology to develop an in vitro bovine oviduct. 42nd IETS Annual Meeting 2016. Kentucky, USA.

Ferraz, M.A.M.M.; Henning, H.H.W.; Vos, P.L.A.M., Stout, T.A.E.; Gadella, B.M. Creating a 3D culture system to study bovine oviduct physiology. 48th Annual meeting of the Society for the Study of Reproduction 2015. San Juan, Puerto Rico.

Ferraz, M.A.M.M.; Morató, R.; Yeste, M.; Arcarons, N.; Pena, A.I.; Tamargo, C.; Hidalgo, C.O.; Muiño, R.; Mogas, T. Existence of a relationship between sperm zona-binding ability and motile sperm subpopulations structure in post-thawed ejaculates from Holstein bulls. Reproduction in Domestic Animals 09/2013; 48(1):77.

Ferraz, M.A.M.M.; Simões, R.; Milazzoto, M.P.; Visintin, J.A.; Assumpção, M.E.O.A. Gene expression profile of Protamine and Transition Nuclear Proteins in bovine testis. 39th Annual Conference of IETS. 2013. Hannover, Germany.

Feugang, J.M.; **Ferraz, M.A.M.M.**; Rodriguez-Muñoz, J.C.; Willard, S. T.; Ryan, P. L. Comparative assessment of boar spermatozoa having different cryopreservation potential. ADSA-ASAS Joint annual meeting. 2011, New Orleans –USA.

Ferraz M.A.M.M.; Simões, R.; Visintin, J.A.; Assumpção, M.E.O.A. Bovine sperm protamination gene expression profile. XVIII International Symposium of Scientific Initiation of the University of São Paulo – SIICUSP. 2010, Piracicaba - Brazil.

Ferraz, M. A. M. M.; Wathes, D. C.; Cheng, Z. Evaluation of the production of PGE and PGF in non-pregnant ewe endometrial cells treated with polyunsaturated fatty acids. In: XVIII Scientific Week Benjamin Eurico Malucelli, 2009, São Paulo - Brazil.

Oral Presentations

Ferraz, M.A.M.M. Creating an oviduct-on-a-chip. Centre for species survival, Smithsonian National Zoo. Front Royal, USA, 2017.

Ferraz, M.A.M.M. ; Henning, H.H.W.; Vos, van Tol, H.; Hölker, M.; Besenfelder, U.; Rho, H.; Le Gac, S.; P.L.A.M., Stout, T.A.E.; Gadella, B.M. Oviduct-on-a-Chip: Creating a Niche to

Support Physiological Epigenetic Reprogramming During Bovine In Vitro Embryo Production. 50th Annual meeting of the Society for the Study of Reproduction. Washington DC, USA, 2017.

Ferraz, M.A.M.M. 3D printing a bovine oviduct. 2016 Summer School on Biofabrication and 3D printing. Utrecht Medical Center, Utrecht, The Netherlands.

Ferraz, M.A.M.M. ; Henning, H.H.W.; Vos, P.L.A.M., Stout, T.A.E.; Gadella, B.M. Three-dimensional bovine oviduct cell cultures promote sperm activation and monospermic in vitro fertilization. 18th International Congress on Animal Reproduction. Tours, France, 2016.

Ferraz, M.A.M.M. ; Henning, H.H.W.; Vos, P.L.A.M., Stout, T.A.E.; Gadella, B.M. Bovine embryo production is very sensitive to toxins released from 3-D printed acrylate chambers. Student Competition of the Annual Conference of the European Embryo Transfer Association 2016. Barcelona, Spain.

Ferraz, M.A.M.M. ; Henning, H.H.W.; Van Dorenmalen, K.M.A.; Vos, P.L.A.M., Stout, T.A.E.; Malda, j.; Costa, P.F.; Gadella, B.M. Use of transwell cell culture and 3-D printing technology to develop an in vitro bovine oviduct. 42nd Annual meeting of the International Embryo Technology Society, Louisville, Kentucky, USA, 2016.

Ferraz, M.A.M.M. ; Henning, H.H.W.; Van Dorenmalen, K.M.A.; Vos, P.L.A.M., Stout, T.A.E.; Malda, j.; Costa, P.F.; Gadella, B.M. Use of transwell cell culture and 3-D printing technology to develop an in vitro bovine oviduct. Veterinary Science Day 2015. Utrecht, The Netherlands.

Ferraz, M.A.M.M. ; Henning, H.H.W.; Van Dorenmalen, K.M.A.; Vos, P.L.A.M., Stout, T.A.E.; Malda, j.; Costa, P.F.; Gadella, B.M. A novel 3-D culture system to study bovine oviduct physiology, gamete interaction and early embryo development. Student Competition of the Annual Conference of the European Embryo Transfer Association 2015. Ghent, Belgium.

Henning, H.H.W.; **Ferraz, M.A.M.M.**; Van Dorenmalen, K.M.A.; Vos, P.L.A.M., Stout, T.A.E.; Malda, j.; Melchels, F.P.W.; Gadella, B.M. Developing an in vitro oviduct model: Post-printing treatment of tubular transwell constructs influences oviduct epithelial cell survival. Biofabrication Conference 2015. Utrecht, The Netherlands.

Ferraz, M.A.M.M.; Simões, R.; Milazzoto, M.P.; Visintin, J.A.; Assumpção, M.E.O.A. Bovine sperm protamination gene expression profile. III International Symposium on Animal Biology of Reproduction. 2010, São Pedro - Brazil.

Ferraz M.A.M.M.; Simões, R.; Visintin, J.A.; Assumpção, M.E.O.A. Bovine sperm protamination gene expression profile. II Symposium of the Department of Animal Reproduction, School of Veterinary Medicine and Animal Science, University of São Paulo. 2010, Pirassununga - Brazil.